Diversity and ecophysiology of the conjugating green algae (Zygnematophyceae), with special reference to their photoprotective strategies

I n a u g u r a l – D i s s e r t a t i o n

zur

Erlangung des Doktorgrades

der Mathematisch-Naturwissenschaftlichen Fakultät

der Universität zu Köln

vorgelegt von

Anna Busch

aus Bad Kreuznach

2024

Abstract

The conjugating green algae (Zygnematophyceae) inhabit a wide range of freshwater fed systems worldwide – including lakes, rivers, ephemeral ponds and moorlands. Some species even thrive in extreme habitats, for example, on terrestrial surfaces or glacial ice. Zygnematophytes have a rather simple cellular organization and have been traditionally divided into three morphologically defined groups: the *placoderm desmids* (semi-symmetrical unicells with ornamented cell walls), the *saccoderm desmids* (rod-shaped unicells with smooth cell walls), and the filamentous forms (also with smooth cell walls). Surprisingly, the Zygnematophyceae were found to be the closest relatives of land plants (Embryophyta) – despite their rather simple organization. Since this discovery, the number of studies on zygnematophytes has increased rapidly, and they are now very popular study objects for understanding the evolution of land plants. And yet, the evolutionary relationships between major zygnematophyte groups are unclear and the zygnematophyte taxonomy is outdated. In particular, the saccoderm desmids are under-studied and consist of only a few polyphyletic genera, for example *Mesotaenium* and *Cylindrocystis*. Interestingly, these algae colonize various extreme habitats and have been reported to accumulate colorful specialized compounds, whose inducing factors, biological function and chemical identity remain largely unknown.

During this doctoral study, saccoderm desmids were isolated from freshwater and terrestrial habitats, resulting in axenic laboratory cultures. Based on these cultures, the cell morphology as well as vegetative and sexual processes were studied with different microscopy techniques. In addition, established marker genes (*rbc*L and 18S rRNA) were used to localize the new strains in the tree of zygnematophytes by molecular phylogenetics. Furthermore, available datasets from 46 taxonomically diverse zygnematophytes were used to infer a multigene phylogeny (326 nuclear loci) of the Zygnematophyceae in a collaborative effort. To study the colorful specialized compounds, species of the two genera *Ancylonema* (with vacuolar pigments) and *Serritaenia* (with extracellular pigments) were subjected to light and nutrient experiments as well as to analytical methods. Additionally, comparative transcriptomics was employed to investigate the cellular responses of the selected zygnematophyte *Serritaenia testaceovaginata* to ultraviolet radiation.

The morphological studies combined with the single-gene phylogenies revealed twelve distinct lineages of *Mesotaenium*-like algae, including four new lineages. This allowed the introduction of a provisional nomenclature to facilitate communication and highlight the diversity of these morphologically plain zygnematophytes. The well-resolved phylogenomic tree provided a clear separation of major zygnematophycean lineages and a basis for the establishment of a new five-order system for these algae. Furthermore, a new species of the genus *Ancylonema*, *A. palustre* sp. nov., was discovered and described. It is the first known mesophilic relative (from moorlands) of common glacier algae. The well growing, axenic cultures of *A. palustre* enabled the full reconstruction of vegetative and sexual reproductive processes as well as the experimental induction of reddish, vacuolar compounds. Another major contribution was the rediscovery of saccoderm desmids, here assigned to the new genus

Serritaenia (formerly *Mesotaenium*), which produce pigmented extracellular mucilage. Experimental work on *Serritaenia testaceovaginata* provided the evidence for a sunscreening function of the pigmented mucilage. This included the specific induction by ultraviolet B radiation, a broad absorbance with a maximum in the ultraviolet B waveband, and a perfect cellular localization for shielding. The comparative RNA-seq analysis of *S. testaceovaginata* revealed a plant-like UVB perception system and specialized metabolite pathways (shikimate and phenylpropanoid biosynthesis) that were regulated during pigment production. Furthermore, several extracellular oxidative enzymes, which are known to act on phenolic compounds, as well as ATP-binding cassette transporters, which are known to transport phenolics across membranes, were highly upregulated in *S. testaceovaginata* upon UVB exposure. Together with the chemical properties of the pigmented mucilage, these results suggest a polyphenolic nature of *Serritaenia's* sunscreen compound.

Overall, this thesis presents perspectives for studying and understanding the diversity and cellular adaptations of the saccoderm desmids from high-light habitats. In particular, the novel sunscreen strategy of *Serritaenia* is discussed in a broader context and compared to known sunscreen compounds from plants, cyanobacteria and fungi. Finally, the potential of combining biodiversity research and functional characterization of non-model organisms is discussed.

Kurzzusammenfassung

Die Jochalgen (Zygnematophyceae) besiedeln weltweit eine Vielzahl von Süßwassersystemen, darunter Seen, Flüsse, ephemere Gewässer und Moore. Einige Arten leben sogar in Extremhabitaten, beispielsweise auf terrestrischen Oberflächen oder Gletschereis. Die Organisation der Jochalgen ist relativ einfach und sie wurden traditionell in drei Gruppen eingeteilt: Placoderme einzellige Formen (spiegelsymmetrische Algen mit ornamentierten Zellwänden), saccoderme einzellige Formen (stäbchenförmige Algen mit glatten Zellwänden) und filamentöse Formen (mit glatten Zellwänden). Trotz ihrer eher einfachen Organisation, erwiesen sich die Jochalgen als die nächsten Verwandten der Landpflanzen (Embryophyta). Seitdem hat die Forschung an Jochalgen rasant zugenommen und heute sind sie beliebte Studienobjekte für das Verständnis der Landpflanzenevolution. Die evolutionären Beziehungen zwischen den größeren Jochalgengruppen ist aktuell jedoch weitgehend ungeklärt und die Taxonomie ist veraltet. Besonders die saccodermen Formen sind schlecht untersucht und bestehen nur aus wenigen polyphyletischen Gattungen, zum Beispiel *Mesotaenium* und *Cylindrocystis*. Interessanterweise, besiedeln die saccodermen Formen eine Reihe extremer Lebensräume, in welchen sie farbige Substanzen akkumulieren. Die Induktion, biologische Funktion und chemische Identität dieser Substanzen sind noch weitestgehend unbekannt.

Im Rahmen dieser Doktorarbeit wurden saccoderme Jochalgen aus aquatischen und terrestrischen Habitaten isoliert. Mittels bestimmter Aufreinigungsmethoden wurden aus diesen Zellen axenische Kulturen für Laboruntersuchungen etabliert. Sowohl die Zellmorphologie als auch vegetative und sexuelle Prozesse wurden mithilfe verschiedener Mikroskopietechniken untersucht. Um die neuen Stämme phylogenetisch einzuordnen, wurden etablierte Markergene (*rbcL* und 18S rRNA) verwendet. In einer kollaborativen Arbeit, wurden zudem verfügbare Datensätze von 46 taxonomisch diversen Jochalgen verwendet und eine Multigen-Phylogenie (326 Gene) der Jochalgen berechnet. Außerdem wurden die nichtphotosynthetischen Pigmente der beiden Gattungen *Ancylonema* (mit vakuolären Pigmenten) und *Serritaenia* (mit extrazellulären Pigmenten) mittels Licht- und Nährstoffexperimenten induziert und mit analytischen Methoden untersucht. Mit vergleichender Transkriptomik wurden zudem die zellulären Reaktionen der ausgewählten Jochalge *Serritaenia testaceovaginata* auf Ultraviolett-Strahlung studiert.

Die morphologischen Studien kombiniert mit den Einzelgen-Phylogenien zeigten zwölf verschiedene Linien *Mesotaenium*-ähnlicher Algen, darunter vier neue Linien. Dies ermöglichte die Einführung einer vorläufigen Nomenklatur, welche die Kommunikation erleichtert und die Vielfalt dieser morphologisch einfachen Jochalgen gebührend reflektiert. Die Multigen-Phylogenie ermöglichte die Etablierung eines neuen Systems aus fünf Ordnungen für die Jochalgen. Des Weiteren wurde eine neue Art der Gattung *Ancylonema*, *A. palustre* sp. nov., entdeckt und beschrieben. Es ist der erste bekannte mesophile Verwandte (aus Moorgebieten) der ansonsten ausschließlich auf Eis lebenden *Ancylonema*-Arten. Die gut wachsenden, axenischen Kulturen von *A. palustre* ermöglichten die Rekonstruktion vegetativer und sexueller Fortpflanzungsprozesse sowie die experimentelle Induktion

rötlicher, vakuolärer Substanzen. Ein weiterer wesentlicher Beitrag war die Wiederentdeckung von Jochalgen, die hier der neuen Gattung *Serritaenia* (früher *Mesotaenium*) zugeordnet werden und pigmentierten, extrazellulären Schleim produzieren. Die experimentellen Arbeiten an *Serritaenia testaceovaginata* lieferten den Nachweis, dass der pigmentierte Schleim den Algenzellen als Sonnenschutz dient. Dies beinhaltete die spezifische Induktion durch Ultraviolett-B-Strahlung, eine breite Absorption mit einem Maximum im Ultraviolett-B-Bereich sowie eine perfekte zelluläre Lokalisation zur Abschirmung. Die vergleichende Transkriptomstudie von *S. testaceovaginata* zeigte die Präsenz eines pflanzenähnlichen Rezeptorsystems für Ultraviolett-B-Strahlung sowie spezieller Stoffwechselwege (Shikimat- und Phenylpropanoid-Biosynthese), die während der Pigmentproduktion reguliert werden. Weiterhin wurde eine Hochregulierung von ABC-Transportern, welche phenolische Substanzen durch Membranen transportieren können, festgestellt. Ähnliche Reaktionen wurden auch von mehreren extrazellulären, oxidativen Enzymen beobachtet, die phenolische Substanzen umsetzen könnten. In Kombination mit den chemischen Eigenschaften des pigmentierten Schleims, deuten diese Ergebnisse auf eine polyphenolische Natur des Sonnenschutzpigments von *Serritaenia* hin.

Die vorliegende Arbeit weist Perspektiven auf, wie in Zukunft die Diversität und die zellulären Anpassungen der saccodermen Jochalgen aus sonnenexponierten Lebensräumen besser untersucht und verstanden werden können. Insbesondere die neuartige Sonnenschutzstrategie von *Serritaenia* wird in einem breiteren Kontext diskutiert und mit bekannten Sonnenschutzsubstanzen aus Pflanzen, Cyanobakterien und Pilzen verglichen. In der Schlussbetrachtung wird das Potenzial der Kombination von Biodiversitätsforschung und funktioneller Charakterisierung von Nicht-Modellorganismen erörtert.

Table of contents

- The green lineage: Spotlight on the algal relatives of land plants

- Zygnematophytes and their adaptations to terrestrial stressors

- Aims of this thesis

- Scientific contributions

Introduction

The green lineage: Spotlight on the algal relatives of land plants

Green algae have an interesting evolutionary position. They are part of the Archaeplastida and derive from a primary endosymbiosis (Bhattacharya & Medlin, 1998; Irisarri et al., 2022). During this event, a heterotrophic eukaryote took up a cyanobacterium, which developed into a semiautonomous organelle, the chloroplast. It led to the emergence of phototrophic eukaryotes, which performed oxygenic photosynthesis and eventually resulted in the green algae, the red algae, and the glaucophytes (Bhattacharya & Medlin, 1995; Cavalier-Smith, 2000; McFadden & van Dooren, 2004). Within the green algae, there is an early divergence of two clades, the two divisions Chlorophyta and Streptophyta (**Fig. 1**; Bierenbroodspot et al., 2024; Leliaert et al., 2012; Lemieux et al., 2007). The Streptophyta include green algae from freshwater and terrestrial habitats as well as the land plants (Embryophyta) (Becker & Marin, 2009; Bierenbroodspot et al., 2024). Most subgroups of the Streptophyta are not particularly diverse, but the land plants are a notable exception with ~ 450,000 species (Leliaert et al., 2012; Pimm & Joppa, 2015). Besides the land plants, six different groups of algae belong to the Streptophyta, namely the Charophyceae, Coleochaetophyceae, Klebsormidiophyceae, Chlorokybophyceae, Mesostigmatophyceae and Zygnematophyceae (Irisarri et al., 2021; Wodniok et al., 2011). As the streptophyte green algae form a paraphyletic group from which land plants evolved, they are important for understanding the transition from algae to plants.
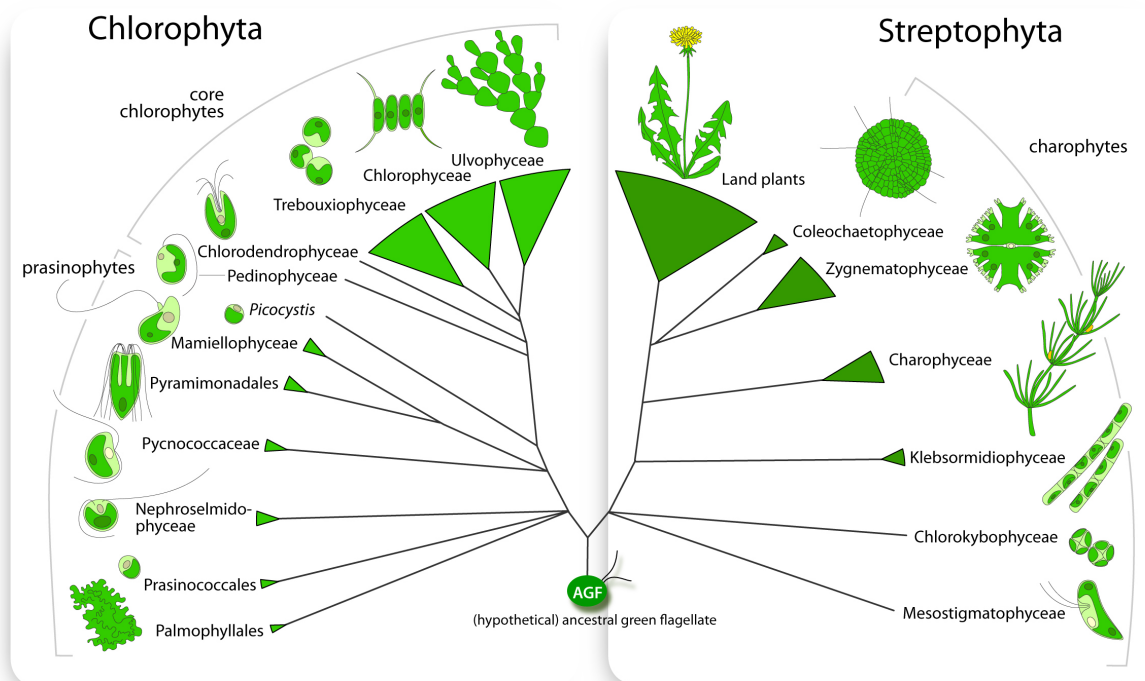
Modified from Leliaert et al., Crit. Rev. Plant Sci. 31:1-46 (2012)
updated 25 Oct 2013

Fig. 1: Schematic phylogeny of the green algae depicting major forms of organization. Note that the shown relationship of the Zygnematophyceae and plants does not reflect the current state of knowledge (see main text); figure kindly provided by Frederik Leliaert (Meise Botanic Garden, Belgium).

The exact topology of the streptophyte tree was unclear for a long time, and the question of the closest relative of land plants was unresolved (Hall et al., 2008; Lemieux et al., 2007; Turmel et al., 2006). Early hypotheses were based on the concept that morphological complexity increases in evolutionary derived groups. Therefore, the Charophyceae and Coleochaetophyceae, which form relatively complex, multicellular thalli, were favored as the closest relatives of land plants (Graham et al., 2000; Karol et al., 2001; Kranz et al., 1995). However, early multigene phylogenies suggested that the Zygnematophyceae are the closest relatives to the embryophytes (Timme et al., 2012; Wodniok et al., 2011). More recently, this was confirmed by several phylogenomic analyses (Cheng et al., 2019; Gitzendanner et al., 2018; Irisarri et al., 2021). The Zygnematophyceae have a rather simple cell morphology with vegetative non-flagellated unicells or filaments. Unlike other streptophyte green algae, they lack centrioles and flagellated stages, and are characterized by a special mode of sexual reproduction known as conjugation (Hall & McCourt, 2017; Tsuchikane & Sekimoto, 2019). During conjugation the contents of two vegetative haploid cells are transformed into amoeboid gametes, which fuse to form a resistant diploid zygospore (Permann, et al., 2022; Pickett-Heaps & Fowke, 1971; Sekimoto, 2000). Due to their special mode of genetic recombination, the Zygnematophyceae are also referred to as "conjugating green algae". Overall, the Zygnematophyceae are morphologically very different from the land plants and it was proposed that these algae underwent a secondary reduction during evolution (De Vries & Archibald, 2018; Delwiche & Cooper, 2015; Wickett et al., 2014). However, despite their simple growth form, zygnematophytes exhibit a great ecological diversity. Many species grow benthic, some planktonic and some have a terrestrial lifestyle (Hall & McCourt, 2017). Some species from the genera *Mougeotia* and *Spirogyra* can be considered nuisance algae which form pond scum in eutrophic waters (McKernan & Juliano, 2001; Zohary et al., 2019). However, many unicellular species are key organisms for peatlands (Neustupa et al., 2023), and some thrive in extreme habitats, for example on glacial ice (Remias et al., 2009). The glacier algae of the genus *Ancylonema* can form blooms on the ice surfaces in alpine and polar regions, and thereby contribute to increased glacial melting rates (Di Mauro et al., 2020; Lutz et al., 2014).

The zygnematophytes have a long taxonomic history. They have been studied since the 19th century and comprise likely more than 4,000 described species (de Bary, 1858; Hall & McCourt, 2017; Kützing, 1843). Traditionally, the class was divided into two orders, based primarily on differences in cell wall structure: The Zygnematales, unicells and filaments characterized by smooth, non-ornamented cell walls, and the Desmidiales, unicells with cell wall pores and a rather complex cell wall. The Desmidiales, also known as "placoderm desmids", are also characterized by two symmetrical cell halves (semicells) that are connected by a narrow bridge (isthmus) (Gerrath, 1993; Gontcharov, 2008; Mix, 1972). In contrast, the unicellular representatives of the Zygnematales, have a rather simple cell morphology (mainly rod-shaped) and are referred to as "saccoderm desmids" (**Fig. 2**; Gerrath, 1993; Gontcharov, 2008; Kadlubowska, 1984; Prescott, 1972). Molecular phylogenetics revealed that the Desmidiales are indeed a monophyletic group, while the Zygnematales are paraphyletic (Besendahl &

Bhattacharya, 1999; Gontcharov et al., 2003, 2004; McCourt et al., 2000). As in many other protist groups, the exclusive use of morphological characters proved to be unsuitable for drawing evolutionary conclusions in the Zygnematophyceae (Gontcharov & Melkonian, 2008, 2011; Hall et al., 2008; Schiwitza & Nitsche, 2021; Zhao et al., 2016). The phylogenetic analyses were mainly based on nuclear rRNA genes, the mitochondrial *cox3* (subunit III of the cytochrome c oxidase) gene and the chloroplast *rbcL* (large subunit of the ribulose-bisphosphate carboxylase) gene. Based on these marker genes it was, however, not possible to resolve the deep nodes of the zygnematophycean tree. **Hence, the true relationships between major zygnematophycean groups are still unresolved.**
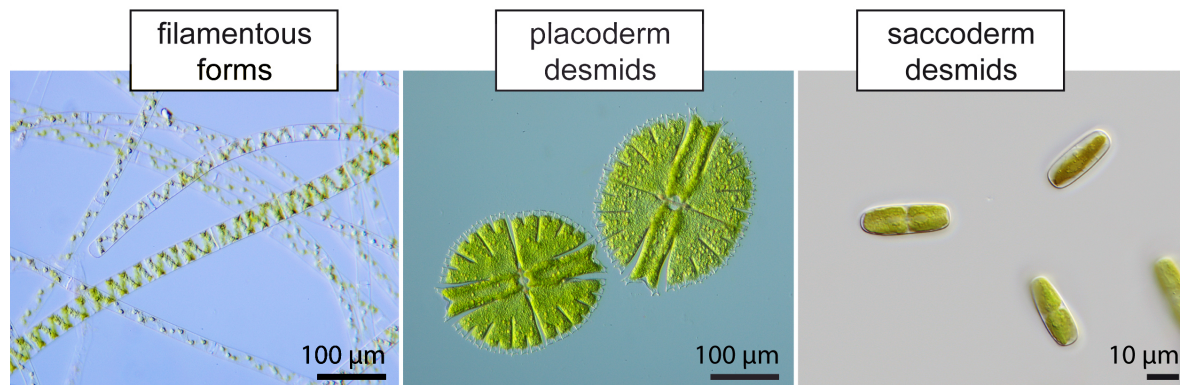

Fig. 2: Three morphologically defined groups of the Zygnematophyceae; from Busch & Hess, 2022b, modified.

The definition of species in the Zygnematophyceae is another prevailing problem. For example, the members of certain genera of placoderm desmids (e.g. *Cosmarium*, *Micrasterias*) have distinct genetic sequences, but show only minor morphological differences. This makes it difficult to define taxonomic units on the basis of morphology, a problem called pseudocryptic diversity (Gontcharov & Melkonian, 2008; Nemjová et al., 2011). Furthermore, some other zygnematophyte species show phenotypic plasticity. This is the expression of specific cellular characteristics in a species, depending on environmental conditions (Chia et al., 2015; Neustupa et al., 2008). This had exactly the opposite effect and led to the description of redundant species names (Kouwets, 2008). The saccoderm desmids are particularly affected by these circumstances. Their plain morphology and the difficulties in distinguishing species and genera have led to numerous unverified synonyms and misclassifications. These algae currently consist of only a few poorly defined and polyphyletic genera, for example *Mesotaenium* and *Cylindrocystis* (Gontcharov, 2008; Gontcharov et al., 2003). **Hence, the taxonomy of the phylogenetically diverse saccoderm desmids is still confusing and their true diversity remains unrecognized.**

The Zygenmatophyceae are the closest algal relatives of land plants and important subjects to study evolutionary transitions (Gitzendanner et al., 2018; Wodniok et al., 2011). Land plants evolved around 500 million years ago and led to a dramatic change of life on earth (Benton et al., 2022; Morris et al., 2018). The colonization of the terrestrial habitat by plants, a process known as "terrestrialization", could only be achieved through a successful adaptation to certain abiotic stress factors (also referred to as stressors). In terrestrial habitats, organisms can be exposed to prolonged drought, extreme temperature

fluctuations (including freezing) and increased solar radiation. It is assumed that the ecophysiological adaptations of the first land plants included osmoregulation and osmoprotection, desiccation and frost tolerance as well as heat resistance (Dadras et al., 2023; Delaux et al., 2012; Jiao et al., 2020; Nishiyama et al., 2018; Rensing et al., 2008). Some authors even suggest that the ancestors of streptophyte green algae were pre-adapted to a life on land in terms of their cellular and metabolic properties (Becker & Marin, 2009). To learn more about how the common ancestor of land plants and zygnematophytes coped with terrestrial stress factors, it is interesting to compare the cellular toolbox of these algae with that of land plants. This way, it is possible to identify characteristics that are exclusive to land plants and those that were probably already present in the algal ancestor. So far, only relatively few zygnematophyte species (e.g. from the genera *Mesotaenium*, *Mougeotia*, *Penium, Spirogloea*, *Zygnema*) have been subjected to in-depth genomic or transcriptomic analyses (Cheng et al., 2019; Dadras et al., 2023; Feng et al., 2024; Fürst-Jansen et al., 2021; Jiao et al., 2020; Rieseberg et al., 2023). These analyses revealed adaptations, which were previously thought to be specific to plants. Some examples are specific stress responses (de Vries et al., 2020; Holzinger et al., 2014), homologues of phytohormone receptors (de Vries et al., 2018; Sun et al., 2019), and key enzymes of the phenylpropanoid pathway (de Vries et al., 2017). Interesting insights were further gained from the genome of the saccoderm desmid *Spirogloea muscicola*. It revealed an expansion of certain genes (GRAS and PYR/PYL/RCAR), which are known to increase the resistance to biotic and abiotic stressors in land plants. These genes were likely gained via horizontal gene transfer from soil bacteria (Cheng et al., 2019). However, the genomic analyses also reveal significant taxon-specific differences, which reflects the vast diversity of the zygnematophytes and their lifestyles (Rieseberg et al., 2023). **To understand how the algal progenitor of land plants adapted to terrestrial conditions, we need to learn more about terrestrial zygnematophytes and how they cope with abiotic stressors.**

Zygnematophytes and their adaptations to terrestrial stressors

Algae that live in terrestrial habitats derive from different eukaryotic supergroups. This includes members of the chlorophyte and streptophyte green algae (Rindi et al., 2009) as well as xanthophytes (Rybalka et al., 2020), eustigmatophytes (Neustupa & Némcová, 2001), euglenophytes (Ashley et al., 1985), cryptophytes (Paulsen et al., 1992), dinophytes (Kutovaya et al., 2012) and bacillariophytes (Foets et al., 2021). Furthermore, numerous cyanobacterial genera can be found in terrestrial habitats (Gaysina et al., 2018). Terrestrial algae are specialists and require specific environmental conditions to survive and grow. Under suitable conditions terrestrial algae can form blooms that are visible to the naked eye as colorful biofilms (e.g. green, brown, red). Such biofilms can be composed of a single or several algal species (Baumann et al., 2018; Liu et al., 2012; Williamson et al., 2018). In multi-species biofilms, it has been shown that different taxa occupy well-defined areas depending on their competitive strength and ecophysiological preferences (Jung et al., 2019; Oren et al., 1995). The dominant algal groups on land belong to the cyanobacteria and green algae (Broady, 1979; Büdel et al., 2016; Leliaert

et al., 2012; Lin et al., 2013; Rybalka et al., 2023). Most of the terrestrial green algae stem from to the Chlorophyta, including the common photobionts of lichens (Honegger, 2009). In fact, chlorophytes and the widespread streptophyte genus *Klebsormidium* are among the best studied terrestrial green algae, as they can be easily isolated and cultivated (Hodač et al., 2012, 2016; Mikhailyuk et al., 2008, 2015). In contrast, terrestrial zygnematophytes are underexplored and there is no recent literature on their diversity and identification. This might be due to the fact that these algae are very sticky and difficult to isolate. Furthermore, some of them have very low growth rates and are easily overgrown by chlorophyte green algae. And yet, zygnematophytes colonize various terrestrial surfaces, including tree bark, deadwood, bare soil, various types of rock as well as bryophytes (de Bary, 1858; Fucikova et al., 2008; Pichrtová et al., 2016). In these habitats, the algal cells are attached to the substrate and can be exposed to long periods of drought. Additionally, zygnematophytes colonize other extreme habitats, that may not be strictly terrestrial, but are dominated by terrestrial stressors. For example, on glacier surfaces, water is abundant, but the algal cells are exposed to freezing temperatures and high levels of solar radiation (Procházková et al., 2021; Remias et al., 2012). Furthermore, shallow and temporary bodies of water, such as puddles, are colonized by certain zygnematophyte species. Such water bodies can dry up or have semi-moist margins (Aigner et al., 2013; Pichrtová et al., 2016).

All of these habitats present a "high-stress" environment for microalgae. There are three primary stressors to consider: desiccation, extreme temperature fluctuations and high solar radiation (Karsten et al., 2007; Karsten & Holzinger, 2014; Permann et al., 2022). All of these conditions can lead to cell damage, which can be fatal if no protection is in place. Drought leads to a loss of membrane fluidity, the disintegration of organelles and the irreversible aggregation of macromolecules (i.e. proteins, nucleic acids, membrane lipoproteins) (Holzinger & Karsten, 2013; Lüttge et al., 2011). In addition, reactive oxygen species (ROS) are generated, in particular, when cells dehydrate in the light. In this situation, photosynthetic pigments are excited, but the energy cannot pass the photosynthetic electron transport chain due to damaged proteins (Rothschild & Mancinelli, 2001; Smirnoff, 1993). The resulting ROS can damage DNA, cause conformational changes in proteins, and lead to lipid peroxidation (Halliwell, 1987; Kranner & Birtić, 2005). The diversity of cellular damage demonstrates, that terrestrial algae must have evolved strategies to cope with dry conditions. In zygnematophytes, most research on adaptive strategies has been done on a few filamentous representatives, for example polar and alpine *Zygnema* species. Adaptive strategies against drought can be classified into two groups, namely those that prolong periods of hydration and those that alter the cells to survive dehydration. One strategy, which prolongs the period of hydration is the production of extracellular mucilage. Under dry conditions, *Zygnema* filaments have been shown to form massive mucilaginous sheaths, that protect the alga from excessive water loss (Fuller, 2013; Pichrtová, 2015; Pichrtová et al., 2014). In fact, zygnematophytes in general are well known for their ability to produce large amounts of extracellular mucilage (Domozych & Domozych, 2008). This mucilage can be complex in composition, with polysaccharides being the major component and may also contain uronic acid and proteins (Kiemle et al., 2007). The extracellular

mucilage of *Zygnema circumcarinatum,* for example, contains arabinogalactan proteins, which have been demonstrated to facilitate cell-cell and cell-surface adhesion (Palacio-López et al., 2019). Another mechanism to prolong periods of hydration, is the synthesis and accumulation of organic osmolytes such as sugars and sugar alcohols. These substances can lower the osmotic potential within the cell and thereby prevent excessive water loss (Holzinger & Karsten, 2013; Nagao et al., 2008). In *Zygnema* sucrose-synthesizing enzymes are upregulated during desiccation, and the analysis of osmolytes from alpine *Zygnema* samples revealed that sucrose is the dominant substance (Hawes, 1990; Rippin et al., 2017). Mechanisms that enable cells to survive dehydration include modifications to the plasma membrane and cell wall to maintain fluidity and flexibility. Zygnematophytes of the genera *Penium* and *Zygnema* modify their plasma membrane and cell wall composition in response to water scarcity (Domozych et al., 2021; Herburger et al., 2019). In one *Zygnema* species, for example, the pectic substance homogalacturonan accumulates during desiccation and increases desiccation resistance (Herburger et al., 2019). Moreover, a variety of cellular repair proteins are upregulated upon dehydration to counteract cell damage. These include DNA repair proteins, ROS scavenging enzymes, chaperones, and aquaporins that facilitate water flux across the plasma membrane (Rieseberg et al., 2023; Rippin et al., 2017).

Extreme temperatures can lead to heat denaturation of biomolecules, on one hand, and to structural destruction by ice crystals, on the other (Lepock et al., 1993; Tan et al., 2021). At high temperatures, the fluidity of membranes can increase to a lethal level, chlorophyll degrades (at 70-80 °C) (Lípová et al., 2010), and proteins (>40°C) (Lepock et al., 1993) and nucleic acids (>85°C) (Rice & Doty, 1957) denature. In response to a rapid short-term increase in temperature, the two filamentous zygnematophytes *Mougeotia* and *Spirogyra*, show upregulation of heat shock proteins and aquaporins, remodeling of the photosynthetic apparatus, and a change in amino acid metabolism. However, each species showed its own, individual gene expression profile, which suggests species-specific differences (de Vries et al., 2020). At cool temperatures, membrane fluidity decreases and the rate of metabolic reactions slows down. This also leads to slower repair processes (Queiroz et al., 1998; Roos & Vincent, 1998). Exposure to sub-zero temperatures damages the plasma membrane, in particular (Steponkus & Lynch, 1989). Antarctic *Zygnema* species have been shown to survive repeated freeze-thaw cycles with very fast recovery rates (Hawes, 1990; Pichrtová et al., 2016), indicating that psychrophilic zygnematophytes must have cellular mechanisms to survive freezing temperatures. Currently, the research on the adaptations of zygnematophytes to extreme temperatures is limited, and the underlying mechanisms are not yet fully understood. However, a very recent study suggests that the psychrophilic zygnematophyte *Ancylonema nordenskioeldii* may be protected from freeze-thaw injury by an ice-binding protein (Procházková et al., 2024).

Sunlight is essential for algae to carry out photosynthesis, grow and reproduce. However, extreme solar radiation interferes with biological processes. High levels of PAR (photosynthetically active radiation: 400-700 nm) result in damage of the photosynthetic apparatus (Franklin & Forster

1997) and ultraviolet radiation (UV) can damage a variety of biomolecules. Ultraviolet A radiation (UVA, 315-380 nm) causes the formation of ROS and ultraviolet B radiation (UVB, 280-315 nm) damages DNA and proteins directly. UVB leads to the dimerization of pyrimidine bases in DNA and destroys tryptophan residues in proteins (Hargreaves et al., 2007; Pattison & Davies, 2006; Vincent & Neale, 2000). In terrestrial algae, UV- and light-absorbing specialized compounds (also referred to as secondary pigments) protect the cells from strong solar radiation. One example is the secondary carotenoid astaxanthin, which is accumulated by a number of chlorophyte green algae in sun-exposed habitats and acts as a photoprotective agent (Bidigare et al., 1993; Gao & Garcia-Pichel, 2011; Lemoine & Schoefs, 2010). Common and well-studied UV-screening compounds are the colorless mycosporine-like amino acids (MAAs) found in various algal groups, including certain chlorophyte and streptophyte green algae (Garcia-Pichel & Castenholz, 1993; Hartmann et al., 2020; Kitzing & Karsten, 2015). In Zygnematophyceae, however, no MAAs could be detected (Aigner et al., 2013; Remias et al., 2012). Instead, there are indications of colorless, phenolic compounds with presumed screening ability in the cytoplasm of some *Zygnema* species (Holzinger et al., 2018; Pichrtová et al., 2013). Furthermore, reddish, water-soluble compounds have been described in the vacuoles of several zygnematophytes from glacial and alpine environments (**Fig. 3**; Barcytė et al., 2020; Garduño-Solórzano et al., 2021; Nedbalová & Sklenár, 2008; Remias et al., 2012; Stancheva et al., 2014). The vacuolar reddish pigments of the ice-inhabiting alga *Ancylonema alaskanum* were isolated from natural material and identified as a glycosylated purpurogallin derivative by nuclear magnetic resonance spectroscopy. The isolated compound absorbed visible light as well as ultraviolet radiation, suggesting a role in photoprotection (Remias et al., 2012). However, the cultivation of zygnematophytes from extreme habitats is challenging – if possible at all – (Remias & Procházková, 2023), which makes experimental studies on the formation of these vacuolar compounds difficult. The extracellular mucilage of zygnematophytes has been suggested to have a role in sun protection as well (Lütz et al., 1997). Moreover, there are sporadic reports of pigmented extracellular mucilage in certain *Mesotaenium* species (de Bary, 1858; Fucikova et al., 2008). However, we currently lack any understanding of their formation, identity and biological function.

Fig. 3: Habitat and cell morphology of ice-inhabiting *Ancylonema* species: *A. alaskanum* (upper right) and *A. nordenskioeldii* (lower right); from Busch & Hess, 2022b, modified, original images were kindly provided by Daniel Remias. Scale bars: 10 μm.

Although many zygnematophyte species inhabit sun-exposed habitats, their photoprotective strategies remain poorly understood. Sunscreening compounds which are known from other algae (e.g.

MAAs, secondary carotenoids) do not seem to play a major role. **Zygnematophytes accumulate poorly known specialized compounds, which might represent novel biological sunscreens. As zygnematophytes are the closest relatives of land plants, there is a high interest in learning more about these photoprotective strategies.**

Aims of this thesis

The principal objective of this thesis is to investigate the phylogeny, morphological traits, life histories and cellular adaptations of saccoderm desmids traditionally ascribed to the polyphyletic genus *Mesotaenium*. The results will facilitate our understanding of the diversity of these poorly studied life forms, paving the way for their taxonomic revision. This will also provide a more detailed account of zygnematophyte diversity in general. Special emphasis is placed on species from sun-exposed habitats and their cellular responses to UV radiation, a dominant terrestrial stressor. Specifically, I pose the following questions:

1) **Are there major undiscovered zygnematophyte lineages in terrestrial habitats, and how do they differ in terms of their morphology and cellular adaptations?**

2) **Which environmental factors induce the colorful specialized compounds found in zygnematophytes, and what is the biological function of these substances?**

3) **What is the metabolic origin of zygnematophycean secondary pigments, and how is their biosynthesis triggered on a molecular level?**

To address these questions, freshwater and terrestrial habitats were sampled and screened for saccoderm desmids. The found algae were isolated and axenic cultures were established. In addition, available strains of saccoderm desmids were ordered from public culture collections and purified. The resulting cultures were studied concerning their cell morphology as well as vegetative and sexual reproduction. By using established marker genes (*rbc*L and 18S rRNA), the studied strains were phylogenetically placed in the tree of zygnematophytes and their evolutionary history reconstructed.

Light and nutrient limitation experiments were performed to induce and study the colored specialized compounds found in the two genera *Ancylonema* and *Serritaenia*. Controlled laboratory experiments and analytical techniques such as microspectrophotometry were used to determine the physicochemical and physiological properties of the specialized compounds and the algal cells.

Based on the established laboratory setup, a comparative RNA-seq analysis was performed to investigate the response of a selected terrestrial zygnematophyte (*S. testaceovaginata*) to UV radiation. To functionally annotate gene sequences, the sequence data was compared with database entries from plants, especially the model plant *Arabidopsis thaliana*. These comparisons were also used to draw evolutionary conclusions. In addition, I was involved in a collaborative study, in which we used multigene phylogenies to resolve the deep branches of the zygnematophyte tree, creating the framework for future taxonomic advancements.

Scientific contributions

Chapter I: Sunscreen mucilage: a photoprotective adaptation found in terrestrial green algae (Zygnematophyceae)

<u>Short summary</u>: In this study, we describe and analyze an extracellular sunscreen in a new genus of zygnematophyte green algae. A similar phenomenon was only known from cyanobacteria and is unique within the zygnematophytes. The study provides evidence for a sunscreening function, namely the induction based on UVB radiation, a broad absorbance with a maximum in the UVB portion, and a perfect localization for shielding (outside of the cell). We establish the new zygnematophyte genus *Serritaenia* and reveal a so far hidden diversity within the genus.

<u>Author contribution</u>: The author of this doctoral thesis took natural samples, isolated single cells from natural material, established axenic cultures, and performed laboratory experiments (except micro-spectrophotometry: done by external facility). Data analysis, manuscript writing and figure design were performed by the author. Results and preliminary manuscript versions were discussed with the last author (S. Hess). A part of the sampling and laboratory experiments was done during the author's master thesis, while the analysis of the data and the preparation of the manuscript were done during the doctoral studies.

<u>Publication</u>: Busch A., Hess S. (2022): Sunscreen mucilage: a photoprotective adaptation found in terrestrial green alga (Zygnematophyceae). *European Journal of Phycology* 57: 107-124. https://doi.org/10.1080/09670262.2021.1898677

Chapter II: Comparative transcriptomics elucidates the cellular responses of an aeroterrestrial zygnematophyte to UV radiation

<u>Short summary:</u> Using comparative transcriptomics, the cellular reaction of an aeroterrestrial zygnematophyte (*Serritaenia testaceovaginata*) to UV radiation was studied. While the cellular reactions of land plants to UV radiation have been studied very well, it is the first study of this kind on their closest algal relatives, the Zygnematophyceae. Our results reveal a plant-like UVB perception system in zygnematophyte green algae and point to a phenolic origin of *Serritaenia*'s sunscreen compound, whose synthesis might be extracellular and oxidative. Comparing our results with the vast information on land plants, it appears that the reaction of zygnematophyte green algae towards UV radiation is similar to land plants in terms of photosynthesis, DNA repair, ROS scavenging and light perception. The specialized (=secondary) metabolite pathway, however, does not seem to correspond exactly to that of land plants and probably harbors other enzymes and pathways, which await future characterization.

Author contribution: The author of this doctoral thesis co-designed the study and performed laboratory experiments. The author independently performed bioinformatic analyses after an introduction to comparative transcriptomics by one of the co-authors (J. Gerbracht). Data interpretation, manuscript writing and figure design were performed by the author. Results and preliminary manuscript versions were discussed with the co-authors U. Höcker, K. Davies and S. Hess. The whole study was performed during the doctoral studies.

Publication: Busch A., Gerbracht J. V., Davies K., Hoecker U., Hess S. (2024). Comparative transcriptomics elucidates the cellular responses of an aeroterrestrial zygnematophyte to UV radiation. *Journal of Experimental Botany:* erae131. https://doi.org/10.1093/jxb/erae131

Chapter III: A diverse group of underappreciated zygnematophytes deserves in-depth exploration

Short summary: Unicellular zygnematophytes with a rather simple cell morphology, traditionally referred to as "saccoderm desmids", have a broad geographic distribution and are ecologically diverse. However, these life forms are understudied and harbor several polyphyletic genera. To study these organisms in more detail, diverse freshwater and terrestrial habitats were sampled, interesting candidates were isolated and axenic cultures were established. The study highlights the morphological, genetic and ecophysiological diversity of *Mesotaenium*-like zygnematophytes, and reveals twelve genetically distinct lineages, four of which have not been recognized before. The different lineages vary in their cell morphology, growth form and lifestyle. Furthermore, the study indicates that a significant proportion of these algae colonize terrestrial surfaces and display intriguing cellular adaptations to their natural habitat, including the production of colored specialized compounds.

Author contribution: The author of this doctoral thesis took natural samples, isolated single cells from natural material, established axenic cultures, and performed laboratory experiments. Data analysis, manuscript writing and figure design were performed by the author. Results and preliminary manuscript versions were discussed with the last author (S. Hess). Some of the data on algal strains were collected during the author's master thesis. Data analysis and manuscript writing was done during the doctoral studies.

Publication: Busch A., Hess S. (2022): A diverse group of underappreciated zygnematophytes deserves in-depth exploration. *Applied Phycology* 3: 306-323. https://doi.org/10.1080/26388081.2022.2081819

Chapter IV: A mesophilic relative of common glacier algae, *Ancylonema palustre* sp. nov., provides insights into the induction of vacuolar pigments in zygnematophytes

Short summary: The zygnematophyte green algae of the genus *Ancylonema* colonize glacier surfaces in many different areas on the planet. In their natural habitat, the cells display a phenolic, intracellular pigment of reddish color, whose induction and biological function is unknown. These algae are true psychrophiles, which impairs research on this group, as they depend on low temperatures and are difficult to cultivate. In our study, we describe a mesophilic *Ancylonema* species, *A. palustre* sp. nov., which shows unique autecological and photophysiological characteristics. We studied its vegetative and sexual processes and identified nutrient limiting conditions to induce zygospore formation, providing the first detailed account of sexual processes in the genus *Ancylonema*. Moreover, we found that nutrient limiting conditions combined with UVB radiation result in the production of the reddish, vacuolar pigment, which supports a function in photoprotection.

Author contribution: The author of this doctoral thesis co-designed the study. The laboratory experiments (except pulse amplitude modulation fluorometry: done by D. Remias and L. Prochazkova) and data analysis were conducted by the author and E. Slominski (bachelor student co-supervised by the author). Manuscript writing and figure design were performed by the author. Results and preliminary manuscript versions were discussed with the co-authors: D. Remias, L. Prochazkova, S. Hess. The whole study was performed during the doctoral studies.

Manuscript under review: Busch A., Slominski E., Remias D., Procházková L., Hess S. A mesophilic relative of common glacier algae, *Ancylonema palustre* sp. nov., provides insights into the induction of vacuolar pigments in zygnematophytes. *Environmental Microbiology* (under review).

Chapter V: A phylogenomically informed five-order system for the closest relatives of land plants

Short summary: Due to their interesting phylogenetic position, the Zygnematophyceae have attracted increasing attention in recent years. The internal zygnematophyte phylogeny, however, is largely unknown. We conducted a phylogenomic analysis (326 nuclear loci) for 46 taxonomically diverse zygnematophytes. Moreover, we studied a filamentous green alga representing *Mougeotiopsis calospora* PALLA, which was described 120 years ago, but never subjected to molecular analyses. We found, that *M. calospora* lacks discernible pyrenoids and that it branches with unicellular species. It represents another zygnematophycean lineage with filamentous growth, which was not known before. Furthermore, we propose a new five-order system for the Zygnematophyceae based on our well-supported phylogenomic tree and provide evidence for five independent origins of true filamentous growth within the Zygnematophyceae.

<u>Author contribution:</u> The study was designed by S. Hess and J. de Vries. The author of this doctoral thesis established the axenic culture of *Mougeotiopsis calospora*, studied the strain with conventional light microscopy and confocal laser scanning microscopy, and interpreted the data in a taxonomic context. Furthermore, the author provided the morphological description of *M. calospora* and the Figure 1A-E for the manuscript, and reviewed the latter before submission. This work was done during the doctoral studies.

<u>Publication:</u> Hess S., Williams,S. K., Busch A., Irisarri I., Delwiche,C. F., de Vries S., Darienko T., Roger A. J., Archibald J. M., Buschmann,H., von Schwartzenberg,K., de Vries J. (2022): A phylogenomically informed five-order system for the closest relatives of land plants. *Current Biology* 32: 4473-4482. https://doi.org/10.1016/j.cub.2022.08.022

Sunscreen mucilage: a photoprotective adaptation found in terrestrial green algae (Zygnematophyceae)

Published in the European Journal of Phycology

Chapter I

British Phycological Society
Understanding and using algae

Taylor & Francis
Taylor & Francis Group

OPEN ACCESS   Check for updates

Sunscreen mucilage: a photoprotective adaptation found in terrestrial green algae (Zygnematophyceae)

Anna Busch and Sebastian Hess

Institute for Zoology, University of Cologne, Zülpicher Str. 47b D-50674 Cologne, Germany

ABSTRACT
Terrestrial microalgae evolved a variety of photoprotective strategies enabling a life on land. This includes the production of sunscreen compounds, which shield cells from excess radiation. Here, we report a new genus of conjugating green algae, *Serritaenia* gen. nov., whose members produce extracellular mucilage with a striking pigmentation. This phenomenon is very unusual for eukaryotic algae and poses cell biological and functional questions. So far, extracellular sunscreen pigments are exclusively known from cyanobacteria, while eukaryotic algae typically contain intracellular sunscreens. We demonstrate that pigmented mucilage in *Serritaenia* spp. can be induced by experimental exposure to UVB in an intensity-dependent manner, and that it strongly absorbs deleterious wavebands. Microscopic details of UVR-treated cells suggest that the directional secretion of pigmented mucilage is responsible for the defined and well-oriented pigment layers observed in natural material. Even though the chemical nature of the pigment remains to be elucidated, several pieces of evidence suggest that the 'sunscreen mucilage' of *Serritaenia* represents an elaborate photoprotective adaptation, unprecedented in eukaryotic algae.

Introduction

Microalgae from diverse evolutionary lineages have a terrestrial lifestyle and colonize natural as well as anthropogenic surfaces on land (Fritsch, 1922; Hoffmann, 1989; Rindi & Guiry, 2004; Karsten et al., 2007; Ettl & Gärtner, 2014). Compared with their aquatic relatives, terrestrial microalgae face increased levels of solar radiation, which is considered a major stress factor (Rozema et al., 2002; Wynn-Williams & Edwards, 2002; Karsten, 2008; Kitzing & Karsten, 2015). In particular, the ultraviolet radiation (UVR) of sunlight is harmful: ultraviolet A (UVA, 315–400 nm) causes the formation of free radicals and reactive oxygen species, while ultraviolet B (UVB, 280–315 nm) can damage DNA and proteins directly (Vincent & Neale, 2000; Pattison & Davies, 2006; Hargreaves et al., 2007). There are a number of cellular and physiological features of terrestrial microalgae that are expected to have a photoprotective function. This includes non-photochemical quenching, self-shading (exposed cell layers protect underlying cells), and the production of sunscreen compounds, which strongly absorb harmful wavebands (Karsten, 2008; Gao & Garcia-Pichel, 2011; Karsten & Holzinger, 2014). Algal sunscreen compounds are chemically diverse and can be found in eukaryotic as well as prokaryotic microalgae. They comprise mycosporine-like amino acids (MAAs, e.g. in the cytoplasm of chlorophytes, streptophytes,

rhodophytes, dinoflagellates and cyanobacteria; Garcia-Pichel & Castenholz, 1993; Karsten et al., 1998; Jeffrey et al., 1999; Řezanka et al., 2004; Hotter et al., 2018; Hartmann et al., 2020), secondary carotenoids (e.g. in extraplastidic lipid droplets of chlorophytes; Bidigare et al., 1993; Remias & Lütz, 2007), and the non-photosynthetic pigments scytonemin and gloeocapsin in the extracellular mucilage of cyanobacteria (Garcia-Pichel & Castenholz, 1991; Storme et al., 2015). Whereas the colourless MAAs absorb only UVR, 'sunscreen pigments' such as carotenoids, scytonemin and gloeocapsin show broader absorbance spectra (including visible light) that lead to their colourful appearance. Some algal sun-screen pigments still require a chemical and physiological characterization, and it is not always certain that they represent a single compound (e.g. gloeocapsin).

Here, we report unicellular 'conjugating green algae' (Zygnematophyceae, Streptophyta), traditionally lumped in the polyphyletic genus *Mesotaenium* Nägeli, that can form mass developments in terrestrial habitats and display a striking pigmentation of their extracellular mucilage. The Zygnematophyceae are the likely sister clade to land plants (Wodniok et al., 2011; Timme et al., 2012; Wickett et al., 2014), and their adaptations to the terrestrial environment have gained much attention in recent years (Gitzendanner et al., 2018; de Vries et al., 2018; Cheng et al., 2019; Philippe et al., 2020). Although

several species live on land, this group of algae seems to lack the well-known sunscreen compounds mentioned above (Remias *et al.*, 2012*a*; Aigner *et al.*, 2013). Instead, there are accounts of reddish pigments in the vacuoles of some representatives (Nedbalová & Sklenár, 2008; Holzinger *et al.*, 2010; Remias *et al.*, 2012*a*, *b*; Garduño-Solórzano *et al.*, 2020) and of colourless, phenolic compounds (Pichrtová *et al.*, 2013; Holzinger *et al.*, 2018), both of which absorb UVR and presumably have photoprotective roles.

The colourful, mucilaginous capsules studied here differ fundamentally from these intracellular compounds and are unusual for eukaryotic microalgae in general. Instead, a similar phenomenon is known from terrestrial cyanobacteria, which accumulate extracellular sheath pigments (e.g. scytonemin) in response to UVR (Garcia-Pichel & Castenholz, 1991; Garcia-Pichel *et al.*, 1992; Ehling-Schulz *et al.*, 1997). This resemblance found across two domains of life raises the question of whether the extracellular pigmentation of the Zygnematophyceae reported here serves as a sunscreen as well. So far, pigmented mucilage in *Mesotaenium* species was only sporadically reported (de Bary, 1858; Fučíková *et al.*, 2008), and we lack any understanding of its formation and biological function.

During this study we sampled unicellular Zygnematophyceae with extracellular pigmentation from several sites in Europe and North America and explored their diversity with molecular and morphological methods. Based on these data, we introduce the new genus *Serritaenia* gen. nov. for this widespread and distinctive group of unicellular Zygnematophyceae, taking a step towards an unambiguous taxonomy of evolutionarily interesting green algae. Using bacteria-free laboratory cultures of *Serritaenia* established in this study, we successfully induced pigmented mucilage with artificial UVR, determined its spectral properties, and studied its formation. We present several pieces of evidence that the pigmented capsules of *Serritaenia* represent an elaborate photoprotective adaptation.

Materials and methods

Sampling, isolation and maintenance of algae

Algal material was collected at several sites in Western Germany and in the Great Smoky mountains (North Carolina, USA) listed in Supplementary table S1. Blackish crusts (dry) or gelatinous masses (wet) on bryophytes and from rock surfaces were transferred to the lab, if necessary rehydrated with distilled water and stored at 4–15°C in dim light (14/10 h light/dark cycle, PAR 3–15 µmol photons m^{-2} s^{-1}). To determine pH values of substrates (plant litter, bryophytes) from our main study site (Wohlsberg, Wiehl, Germany), seven samples were mixed with 100 ml distilled water each,

incubated for a few hours and then measured with a SevenEasy™ pH meter (Mettler-Toledo GmbH, Germany). Algal samples were photo-documented (for details see below), then diluted with distilled water and ultrasonicated on ice (max. 10 s) with the ultrasonicator XL-2000 (Misonix Inc., New York, USA) to liberate cells from the mucilage. Resulting cell suspensions were sprayed with pressurized air onto agar plates with solidified culture medium Waris-H (with 1.5% agar; McFadden & Melkonian, 1986) and incubated at 16°C and dim light until bacterial colonies appeared. Bacteria-free algal cells from these plates were transferred into liquid growth medium Waris-H and grown at 16°C under a 14/10 h light/dark cycle with a photon fluence rate of 30 µmol photons m^{-2} s^{-1} (PAR), giving rise to the clonal and axenic cultures used in this study. For long-term maintenance of cultures, about 2 ml of a running culture was transferred to fresh medium every 2 months. Algal strains are available through the corresponding author and the 'Central Collection of Algal Cultures' (CCAC; https://www.uni-due.de/biology/ccac/).

Light microscopy and confocal laser scanning microscopy (CLSM)

Regular brightfield microscopy and photo-documentation of experimental cultures were done with the Zeiss Axiovert 200M inverted microscope equipped with the Zeiss AxoCam ICc5 camera. For high-resolution imaging, the Zeiss IM35 inverted microscope equipped with the objective lenses Plan 40×/0.65 and Planapochromat 63×/1.4 (Carl Zeiss, DE), electronic flash, and the digital single lens reflex camera Canon EOS 6D were used. Colour balance and contrast of light micrographs were adjusted with Photoshop CS4 (Adobe Inc., California, USA). Confocal laser scanning microscopy was done with a Zeiss LSM 710 and the Zen software (Carl Zeiss, DE). Algal cells from actively growing cultures were collected by centrifugation (3000 *g*, 5 min), mixed with 0.1% Calcofluor White (CFW) in distilled water and used for conventional preparations sealed with Vaseline to prevent evaporation. The plastid morphology was visualized using chlorophyll autofluorescence (excitation: 458 nm; emission: 651–707 nm) and the algal cell wall by cellulose-bound Calcofluor White (excitation: 405 nm; emission: 410–502 nm). Z-stacks were recorded with a step size of 0.42 µm and processed with the software ZEN lite (Carl Zeiss, DE) and the image processing package Fiji (Schindelin *et al.*, 2012).

DNA sequencing, alignment and molecular phylogenetics

Algal material from 2 ml of an axenic culture was collected by centrifugation (5000 *g*, 5 min), resuspended

in sterile water, and lysed by ultrasonication on ice (5 × 5 s) with the ultrasonicator XL-2000 (Misonix Inc., New York, USA). Insoluble debris was pelleted by centrifugation (5000 g, 1 min) and the supernatant was used as template for PCR (details below). For the morphotype GSM.5.thick, which did not grow under our culture conditions, single colonies were isolated from the natural sample, photo-documented and crushed with a sterile coverslip to liberate DNA. The coverslip was then removed, the cell debris diluted with 10 µl sterile water, supplemented with 10 µl PCR-buffer (10×), heated at 95°C for 5 min and then used as template for PCR. The chloroplast encoded gene for the RuBisCO large subunit (rbcL) was amplified by a semi-nested PCR with the primers MaGo1F, MaGo2F and MaGo3R (Gontcharov et al., 2004) and Invitrogen Taq DNA Polymerase (Thermo Fisher Scientific, Massachusetts, USA), using the following protocol: Initial denaturation (3 min at 94°C), then 34 cycles of denaturation (45 s at 94°C), annealing (1 min at 47°C), and extension (2 min at 72°C), then final extension (5 min at 72°C). PCR products were subjected to commercial Sanger sequencing at the McGill University and Génome Québec Innovation Centre (Montreal, Canada) with the primers MaGo2F and MaGo3R. The rbcL gene sequences were assembled from the two overlapping partial reads using the program AlignIR™ 2.0 (LI-COR Biosciences, Nebraska, USA) and manually added to a comprehensive alignment of zygnematophycean sequences (plus sequences of streptophyte outgroup taxa) with the alignment editor SeaView 4.5.4 (Galtier et al., 1996; Gouy et al., 2010). The generated rbcL gene sequences have been deposited in GenBank under the accession numbers MW159369– MW159377 (see also Supplementary table S1). After pre-analyses with varying taxon sampling, a refined dataset with 43 zygnematophycean rbcL gene sequences (including all codon positions) was subjected to phylogenetic inference with Neighbour-joining (NJ), Maximum-parsimony (MP) and Maximum-likelihood (ML) methods using MEGA software version X (Kumar et al., 2018). NJ (distances computed with the Maximum composite likelihood method) and MP (with the Subtree-pruning-regrafting (SPR) algorithm) were done with the 'complete deletion option' resulting in 1033 remaining sites. The ML analysis was done with full alignment (1211 sites) using the GTR+I+G model (discrete Gamma distribution; 5 categories). To assess support of the branches, we performed 1000 bootstrap repetitions for every analysis and added the resulting values to the NJ topology shown in the results.

UV-PAR exposure experiments

Algae used for UV-PAR exposure experiments (strains GSM.5.thin and OBE.1) were grown under 'PAR only' conditions as detailed above to a sufficient density,

mixed with fresh culture medium Waris-H (ratio 1:1), dispensed in six-well multi-titre plates or 60 mm Petri dishes (both Fischer, Germany), and then exposed to the experimental conditions with varying UV-PAR intensities (14/10 h light/dark cycle) but stable temperature of 16°C (in triplicate). During these experiments treated algae were analysed with respect to extracellular pigmentation, presence/absence of mucilage, colony formation, and the number of dead cells. To test for the effects of different UV-PAR intensities on the algae, cells were exposed to the Arcadia D3+ Reptile Lamp T5 with 12% UVB (Arcadia, UK) in five irradiance settings adjusted by distance to the lamp (see Results for details), and observed and photo-documented over 14 days (7 days for replicates). The effect of specific wavebands on the production of extracellular pigment was assessed with algal material exposed to optimal UV-PAR intensities for pigment production (as determined before) but covered by optical filters that block UVB (longpass filter WG-320, Schott, Germany) or total UVR (longpass filter GG-385, Schott, Germany; 6 mm polycarbonate sheets Makrolon®, Covestro AG, Germany). Transmission spectra of used filters and consumables were recorded with the Epoch Microplate Spectrophotometer (BioTek Instruments Inc., Vermont, USA) and are shown in the results. In two further experiments, cells of strain GSM.5.thin were exposed to UVB from (1) the UVB Broadband TL fluorescent tube lamp, and (2) the UVB Narrowband TL fluorescent tube lamp, respectively (both 20W, Philips, the Netherlands). The UVB treatments of 0.8–3 W m^{-2} were for 4 h per day and supplemented with 30–100 µmol photons m^{-2} s^{-1} PAR (14 h per day from SunLike LEDs, 5000 K, Seoul Semiconductor, Korea). To study the effects of high 'PAR only' intensities on the algae, cells were exposed to a 25 W SunLike high-power LED (5000 K; Seoul Semiconductor, Korea) with photon fluence rates of 200, 300, 400, 600, 700 and 1000 µmol photons m^{-2} s^{-1} and a 14/10 h light/dark cycle and observed for 7 days. PAR intensities were measured with the MQ-500 Full-Spectrum Quantum Sensor (Apogee Instruments Inc., Utah, USA), UVA and UVB intensities with the digital UV radiometers Solarmeter® Model 4.2 and Solarmeter® Model 6.2, respectively (both Solar Light Company Inc., Pennsylvania, USA).

Microspectrophotometry

The absorbance spectra of pigmented and non-pigmented mucilage of $S.$ $testaceovaginata$ (strain GSM.5.thin) from the light experiments detailed above (UV-PAR and PAR only) were recorded with a CRAIC QDI 2010 UV-VIS-NIR Microspectrophotometer (CRAIC Technologies Inc., California, USA) in transmission mode at the NanoScale Fabrication and Characterization Facility at the University of Pittsburgh, USA. Algal cells were analysed in conventional wet

mounts with UV-transparent quartz glass coverslips and microscope slides (both Ted Pella Inc., California, USA). Using a 36× mirror objective (numerical aperture 0.5), the absorbance of defined areas (15 × 15 μm) was sampled over 200–1600 nm in sub-nanometer intervals. We made 54 measurements of pigmented mucilage and 15 measurements of non-pigmented mucilage. Each measurement contained 25 averaged sample scans. The absorbance spectra obtained from the regions outside of the colonies (only culture medium) served as reference. Digital micrographs of the analysed specimens documenting the sampling area were taken with the DFK 41AF02 colour industrial camera (The Imaging Source Europe GmbH, Germany).

Pigment extraction attempts

Cells of *S. testaceovaginata* (strain GSM.5.thin) with strongly pigmented mucilage (induced under UVR as detailed above) were concentrated by centrifugation (3000 *g*, 8 min), washed with distilled water, collected by centrifugation (10 000 *g*, 5 min), frozen in liquid nitrogen, and lyophilized with the Christ Alpha 1-4 LSC freeze-dryer (Christ, Germany). Freeze-dried cells were suspended in acetone, methanol, acidic methanol (with 0.5% concentrated HCl = 0.05 N), diethyl ether, trichloromethane, *n*-hexane, respectively, and incubated at room temperature for at least 72 h. Cells and their mucilage were then examined for pigment loss under the Motic AE2000 inverted microscope (Motic Deutschland GmbH, Germany).

Results and Discussion

Serritaenia *species with pigmented mucilage colonize various terrestrial substrates*

In several forests of Western Germany (listed in Supplementary table S1) we observed macroscopic, gelatinous crusts composed of unicellular conjugating green algae, which resembled *Mesotaenium braunii* de Bary (and similar species) and are here described as *Serritaenia* spp. (taxonomic details below). The forests comprise spruce monocultures (*Picea*) and deciduous trees (e.g. *Fagus, Quercus, Betula*), and harbour a prominent bryophyte flora (Fig. 1) due to the warm 'oceanic' climate (Cfb after Köppen-Geiger) and significant rainfall (www.climate-data.org). At several sites in the studied areas, the algae formed mass developments, which appeared as dry, black crusts during summer, covering decomposing tree logs, tree bark, plant litter and bryophytes (Fig. 2). Pleurocarpous and acrocarpous mosses, and leafy liverworts have been found heavily colonized by the algae, and, in some instances, entire plants appeared black due to the algal biofilm (Fig. 3).

We assume that such algal mass developments have unrecognized, detrimental effects on bryophytes, similar to those of well-known fungal infections (Fenton, 1983; Davey & Currah, 2006; Tamura *et al.*, 2019; Rosa *et al.*, 2020).

As revealed by hydrated material, the crusts were either formed by homogeneous populations of *Serritaenia* species, or by more complex assemblages comprising other gelatinous algae as well (e.g. chlorophytes resembling *Coccomyxa*). Even if macroscopic crusts were absent, seemingly unaffected bryophyte plants were frequently found colonized by such algae, e.g. in the form of microscopic colonies on the leaflets (Figs 4, 5). These colonies represented nearly spherical, gelatinous clusters of cells, each cell bounded by a mucilaginous capsule. As indicated by the hierarchical mucilage layers surrounding subgroups of cells, the *Serritaenia* colonies emerged from serial cell divisions and secretion of copious mucilage. In algae from all study sites, we observed a striking pigmentation of extracellular mucilage, ranging from blackish-violet to red-brown (Figs 5–9). The strength of pigmentation varied from a diffuse tint to intensely pigmented zones. Interestingly, the pigment distribution was not homogeneous, and we frequently observed a prominent, unilateral pigmentation of the mucilaginous capsules (Figs 6–8). Furthermore, a single natural sample could contain algal mucilage of different colour (Figs 6, 7) as well as pigmented cells of different sizes (Fig. 9), indicating a yet unrecognized diversity of Zygnematophyceae with extracellular pigmentation.

We also sampled the type locality of *Mesotaenium testaceovaginatum*, a species reported to have brick-red mucilage (Fučíková *et al.*, 2008). This alga was described from the 'wet walls' in the Great Smoky Mountains National Park (North Carolina, USA), a vertical, exposed rock surface with acidic water, harbouring a diversity of prokaryotic and eukaryotic microalgae (Fig. 10; Furey *et al.*, 2007; Lowe *et al.*, 2007). We found red-brown biofilm (Fig. 11), which, surprisingly, contained two *Mesotaenium*-like algae with reddish mucilage (morphotypes 'GSM.5.thin' and 'GSM.5.thick'; here assigned to *Serritaenia*). Both formed irregular, mucilaginous colonies, but differed consistently in cell diameter (15 vs. 20 μm) and the strength of extracellular pigmentation (Figs 12, 13). There might be physiological differences as well, as we were not able to cultivate GSM.5.thick (several attempts), while GSM.5.thin grew well under our culture conditions. The original description of *M. testaceovaginatum* was probably based on cells of both morphotypes (see Supplementary text for details) and requires an emendation (see below).

In fact, all species of the ill-defined genus *Mesotaenium* that match the studied algae were described on a purely morphological basis (Kützing,
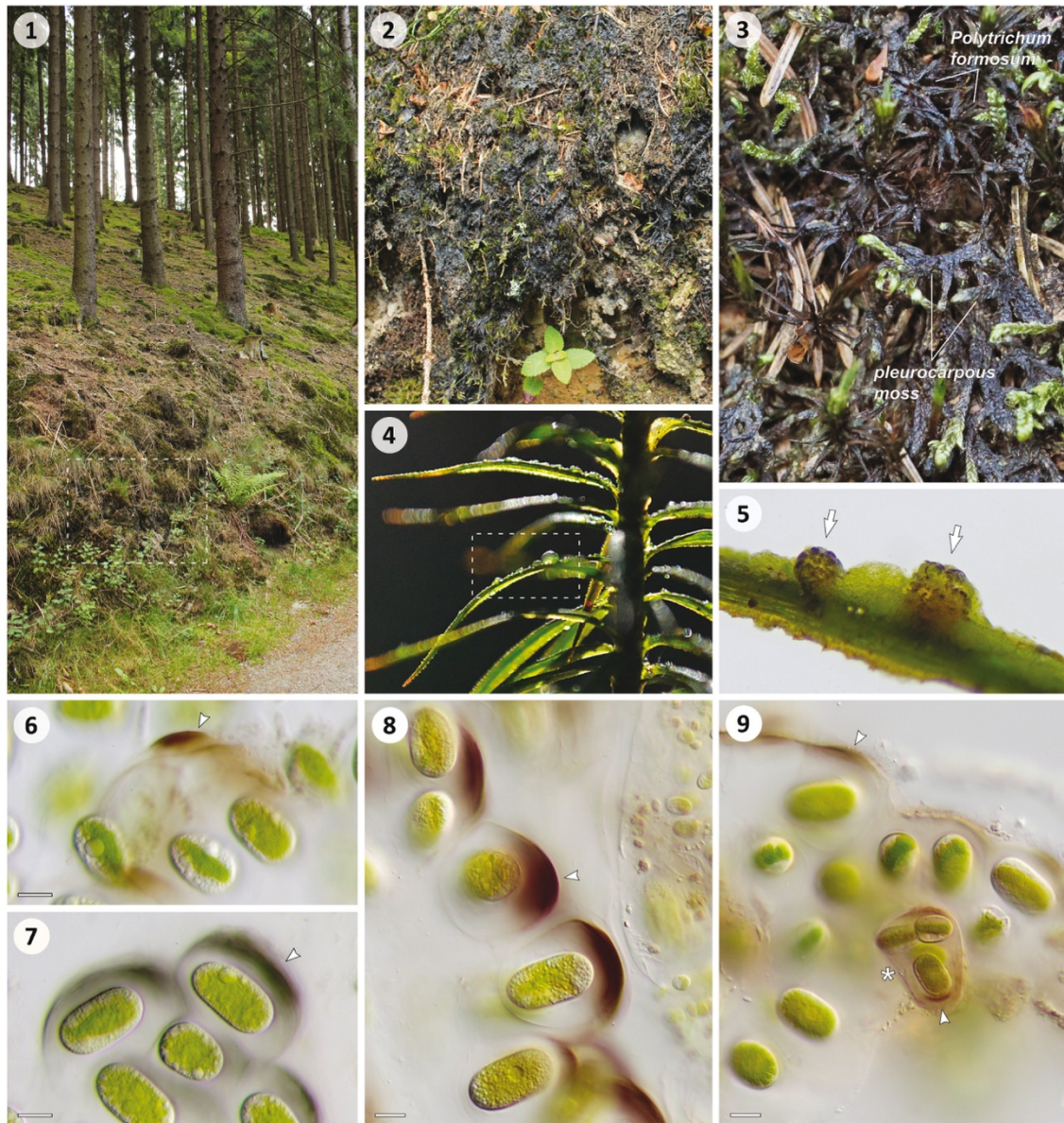
Figs 1–9. Habitat of *Serritaenia* species in western Germany, macroscopic appearance and microscopic details of natural material. **Fig. 1**. Exposed slope in spruce monoculture (Wiehl, DE) with black crusts formed by *Serritaenia* sp. (dashed square). **Fig. 2**. Close-up of dry crusts covering dead plant litter and bryophytes. **Fig. 3**. Pleurocarpous and acrocarpous mosses covered by black algal crusts. **Fig. 4**. Hydrated algal colonies (dashed square) on the leaflets of *Polytrichum formosum*. **Fig. 5**. *Serritaenia* colonies with brown pigmentation (arrows) next to other gelatinous green algae (Chlorophyta) on a leaflet of *Polytrichum formosum*. **Figs. 6, 7**. *Serritaenia* cells with extracellular pigmentation of different colour (arrowheads) found in the same sample (Wiehl, DE). **Fig. 8**. *Serritaenia* sp. (Bad Kreuznach, DE) showing intense, unilateral pigmentation of the mucilaginous capsules (arrowhead). **Fig. 9**. Small-celled *Serritaenia* species (asterisk) co-occurring with a large-celled species (Wiehl, DE). Both species exhibit zones of brown mucilage (arrowheads). Scale bars: 10 μm.

1845; de Bary, 1858; Fučíková *et al.*, 2008) (see Supplementary text for details). Hence, there is no information about the true diversity of these microalgae and their relationships. Specifically, the variation observed in natural populations (cell size, mucilage colour) poses the question of whether the different colours found in the extracellular mucilage of the studied algae are caused by species-specific compounds, or are a result of varying environmental conditions.

Serritaenia *comprises genetically diverse microalgae with subtle morphological differences*

We subjected natural material and cultivated *Serritaenia* strains to genetic and morphological analyses (listed in
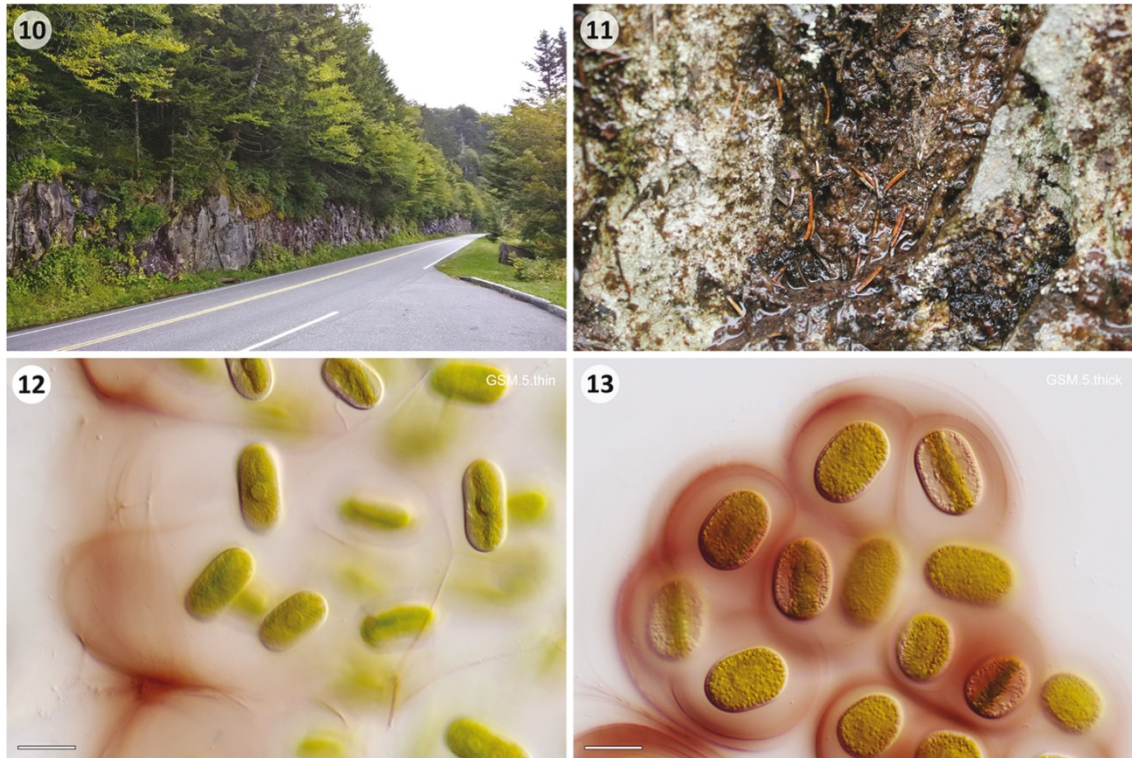
Figs 10–13. 'Wet walls' near Clingmans Dome in the Great Smoky Mountains National Park (North Carolina, USA) and the two *Serritaenia* morphotypes found in this habitat. **Fig. 10.** Sampling area at 'wet walls' (left side). **Fig.11.** Red-brown biofilm on rock surface containing various microalgae, including two *Serritaenia* morphotypes. **Fig. 12.** Cells of morphotype GSM.5.thin loosely arranged in copious, reddish mucilage. **Fig. 13.** Colony of morphotype GSM.5.thick with well-defined, intensely pigmented capsules. Note the difference in cell width to cells shown in (12). Scale bars: 20 μm.

Supplementary table S1). The *rbc*L gene sequences generated from nine cultures and three individual colonies of the *Serritaenia* morphotype GSM.5.thick (picked from samples) were analysed in the framework of the Zygnematophyceae with phylogenetic methods. As known from previous studies (McCourt *et al.*, 2000; Gontcharov *et al.*, 2004), the molecular phylogeny based on the *rbc*L gene was not able to resolve the deeper branching patterns within the conjugating green algae but resolved genus-level clades. We recovered six distinct lineages with unicellular Zygnematophyceae currently assigned to the genus *Mesotaenium* (Supplementary fig. S1), exemplifying once more that the structurally simple, yet diverse 'saccoderm desmids' (traditionally *Mesotaeniaceae*) are still heavily understudied (Gontcharov *et al.*, 2004; Gontcharov & Melkonian, 2010). However, these phylogenetically diverse life forms show clear cell morphological differences (Gontcharov, 2008) and, recently, gained importance for evolutionary inferences (Bonnot *et al.*, 2019; Cheng *et al.*, 2019; Liang *et al.*, 2019; Xu *et al.*, 2019; Philippe *et al.*, 2020), so that a taxonomic revision of these algae is desirable.

The *Serritaenia* strains formed a well-supported clade with considerable genetic distance from other Zygnematophyceae (Fig. 14). It was most closely related to

strain SAG 12.97 that was previously referred to as 'Mesotaenium endlicherianum' (Gontcharov *et al.*, 2003, 2004; Gontcharov, 2008; Matasci *et al.*, 2014; Cheng *et al.*, 2019), but does not meet the original description of that species (already noticed by Gontcharov *et al.*, 2003). The *Serritaenia* clade displayed a so far undetected genetic diversity comprising eight genotypes falling into three subclades (Fig. 14). The members of different subclades showed a divergence of 2–7% in the *rbc*L gene, which compares to interspecific distances found in many other algal and embryophyte genera (Chase *et al.*, 2005; Newmaster *et al.*, 2006; Hall *et al.*, 2010). The three sequences derived from individual colonies of *Serritaenia* morphotype GSM.5.thick (natural material) were identical, but differed clearly from that of strain GSM.5.thin (in 13 nucleotides). This aligns well with the observed phenotypic and physiological differences between the two *Serritaenia* morphotypes, and suggests that they represent different biological entities.

In terms of morphology, the studied *Serritaenia* strains displayed a set of common cellular details, which – in combination – are characteristic for these algae. During interphase, cells of all strains were cylindrical, i.e. with parallel sides, and exhibited roundish (not truncated) cell poles (Fig. 15). Each cell contained a single plate-like chloroplast situated in the cell's centre, not
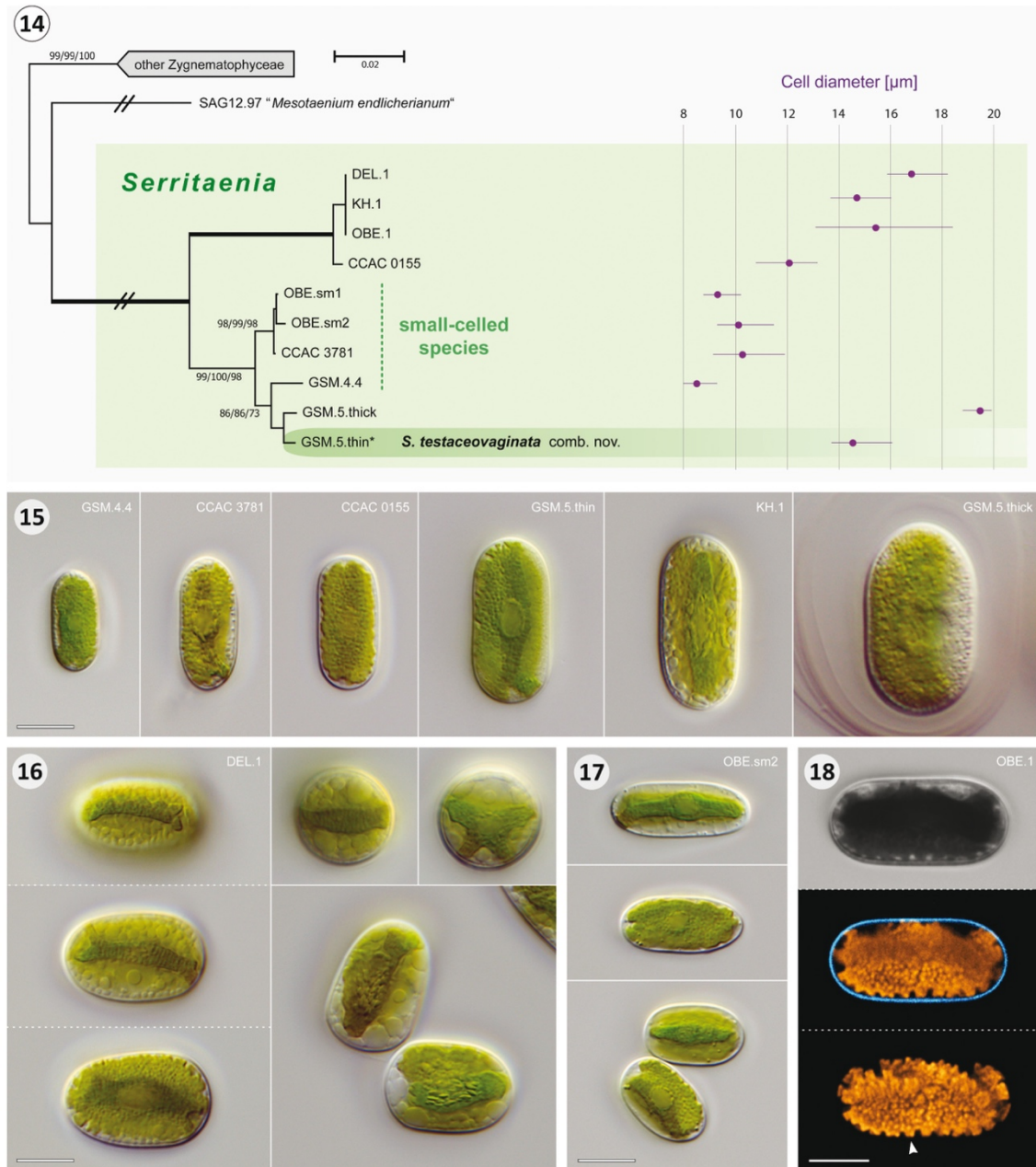
Figs 14–18. Phylogeny of the genus *Serritaenia* and cellular details of representative strains. **Fig. 14.** Unrooted Neighbour-joining phylogeny of 43 zygnematophycean *rbc*L gene sequences (partially collapsed) displaying the genetic diversity of the genus *Serritaenia*. Support values are shown on the respective branches (NJ/ML/MP) when > 50%, and branches with maximum support (100/100/100) are bold. The scale bar represents 0.02 nucleotide substitution per site and branches marked with '//' were reduced in length to 40%. The cell width of the strains is shown on the right side of the diagram (purple dots = mean, purple lines = size range; n = 20). The asterisk indicates the sequence of the type species. **Fig. 15.** Cell morphology of six *Serritaenia* strains illustrating the variability of the genus. **Fig. 16.** Large-celled *Serritaenia* species (strain DEL.1) in side view (left, focal series), top view (two top right micrographs) and shortly after cell division (bottom right). **Fig. 17.** Cells of a small-celled representative (strain OBE.sm2) in side view. Bottom micrograph displays cells shortly after division. **Fig. 18.** CLSM data of a large-celled *Serritaenia* strain (OBE.1) revealing the complexity of the chloroplast and its serrated edges (arrowhead). The middle image displays a section through the cell in two channels (orange = chlorophyll autofluorescence; cyan = Calcofluor White fluorescence), the bottom image shows a 3D-model of the chloroplast. Scale bars in micrographs: 10 μm.

parietal (Figs 16, 17). The chloroplast extended for the length of the entire cell and, depending on its orientation to the observer, could create two typical appearances, 'top view' and 'profile view' (compare the top two cells in Fig. 17). Under laboratory conditions, in particular, the chloroplasts of all studied strains frequently exhibited one

or more additional ridges, giving the chloroplast a more complex morphology (Figs 16, 17). *Serritaenia* chloroplasts were always characterized by serrate or crenate edges (Figs 16–18) and a single circular or elliptical pyrenoid in the chloroplast centre (Figs 15–17). Each cell contained a rather inconspicuous nucleus with a central nucleolus, displaced towards the cell wall, while the chloroplast occupied the cell's centre (Figs 16, 17). Furthermore, the somewhat asymmetric daughter cells resulting from cell division showed an 'angled' arrangement (Figs 16, 17) that differed from the patterns found in many other unicellular Zygnematophyceae (including strain SAG 12.97). Taken together, the studied algae differ fundamentally from the type species of the genus *Mesotaenium* (*M. endlicherianum* Nägeli, see Supplementary text for details), and form a morphologically coherent clade, well-separated from other saccoderm desmids.

To assess the phenotypic diversity within the *Serritaenia* clade, we performed a comparative morphological analysis with cells of axenic cultures grown under controlled abiotic conditions (16°C, medium Waris-H, 30 µmol photons m^{-2} s^{-1} PAR). In fact, there are reports of phenotypic plasticity in some unicellular Zygnematophyceae (Brook, 1981; Neustupa et al., 2008; Černá & Neustupa, 2010), and we also found some variability concerning the presence of additional chloroplast ridges and the abundance of colourless globules in *Serritaenia*, especially in natural material. The cell width, however, was rather constant within strains, and turned out to be a clear distinguishing character for some *Serritaenia* genotypes recognized in our *rbc*L phylogeny (Fig. 14). This is in line with recent findings about cell width stability in genotypes of the structurally similar saccoderm desmid *Cylindrocystis* (Barcytė et al., 2020). Interestingly, the strains DEL.1 and KH.1 with identical *rbc*L gene sequences showed marked differences in cell width as well (Fig. 14), which might point to some hidden diversity, not resolved by the *rbc*L gene. Delimitation of biological entities in the Zygnematophyceae remains difficult and integrative species-level taxonomy is still in an early stage (Kouwets, 2008; Neustupa et al., 2011; Stastny et al., 2013; Schagerl & Zwirn, 2015). We conclude that a fine-grained taxonomy of *Serritaenia* species should be ideally based on more variable genetic markers, and on extended sampling in nature. Hence, we refrain from introducing new species at this point, but establish new combinations for former *Mesotaenium* species: *Serritaenia braunii* comb. nov. and *Serritaenia testaceovaginata* comb. nov. (see below). *S. testaceovaginata* is defined as the type species of the new genus and assigned to a specific genotype (strain GSM.5.thin; Fig. 14). This genotype was sampled at the type locality of *M. testaceovaginatum* and closely matches the original description of the latter (see Supplementary text for details). As the

other members of the *Serritaenia* clade are genetically more diverse than expected, we postpone the decision about the reference strain for *S. braunii* until original material of *M. braunii* de Bary or new samples from its type locality are analysed. Due to the excellent description of *M. braunii* by de Bary (1858) there is no doubt that this species belongs to *Serritaenia* (compare Supplementary fig. S2 and our micrographs), warranting a new combination. Contrary to the information found in several monographs (e.g. Lenzenweger, 2003; Coesel & Meesters, 2007; Brook & Williamson, 2010; Ettl & Gärtner, 2014), *M. braunii* should not be treated as a heterotypic synonym of *Mesotaenium macrococcum* (first described as *Palmogloea macrococca* Kütz.). Unpublished observations on the holotype of *P. macrococca* (Germany: Oberharz, nearby Auerhahn, 1845, coll. Kütz., L.3940277 (L)) revealed that this species more resembles *M. braunii* var. *minus* de Bary in size. However, an in-depth (ideally genetic) analysis of respective type material is required before these names can be considered for certain *Serritaenia* strains. This also applies to *Palmogloea macrococca* var. *nigrescens* C.Cramer, while *M. macrococcum* var. *lagerheimii* Willi Krieg. and *M. macrococcum* var. *truncatum* (West & G.S.West) Willi Krieg. can be excluded due to gross morphological differences from *Serritaenia* (see Supplementary text for further details on relevant taxa). Based on our taxonomic assessment and the phylogenetic results, we here make a start on revising the genus-level taxonomy of *Mesotaenium*-like algae and introduce the genus *Serritaenia* gen. nov. with two new combinations.

Serritaenia A.Busch & S.Hess, gen. nov.

Description

Cells cylindrical, with rounded or slightly pointed apices and smooth cell wall. Chloroplast axial, extending for entire length of cell, plate-like or more complex due to additional ridges, typically with serrate, dentate or crenate edges, exhibiting a single, central pyrenoid. Nucleus displaced towards cell wall (never central), with distinct nucleolus. Cytoplasm colourless, with varying numbers of opaque globules, sometimes obscuring chloroplast details. Cells form colonies with confluent mucilage or well-defined, sometimes lamellated capsules. Mucilage colourless or pigmented (reddish, brown, blackish or violet). Arrangement of daughter cells shortly after cell division angled, never chain-like.
TYPE (here designated): *S. testaceovaginata* (Fučíková et al.) A.Busch & S.Hess, comb. nov.
ETYMOLOGY: The generic name *Serritaenia* is derived from Latin *serra, -ae*, f. [saw] and *taenia, -ae* f. [band], referring to the chloroplast morphology.
PhycoBank ID: http://phycobank.org/102647.

Serritaenia testaceovaginata (Fučíková *et al.*)
A.Busch & S.Hess, comb. nov.

≡ *Mesotaenium testaceovaginatum* Fučíková, J.D.Hall, J.R.Johans & R.L.Lowe. *Bibliotheca Phycologica*, 113: 31, Pl. VI, figs 6, 26–28. 2008 (basionym).

Emended Description: Cells with characters of the genus, on average about 14–15 μm wide, 18–30 μm long. Nucleus 5–7 μm, nucleolus about 2 μm. Pyrenoid circular to slightly elliptic, 4–5 × 3–4 μm. LECTOTYPE (here designated): [icon!] Fučíková *et al.*, *Bibliotheca Phycologica*, 113: pl. VI, fig. 6. 2008; oml trf. (reproduced in Supplementary fig. S3). EPITYPE (here designated): Permanent slide with fixed material of strain GSM.5.thin deposited in *Herbarium Berolinense* (Botanic Garden and Botanical Museum Berlin), accession B 40 0001077, locality: 'Wet walls' on the way to Clingmans Dome, Great Smoky Mountains, North Carolina, USA; 13 September 2017, leg. A. Busch and S. Hess.

Notes: The holotype (fixed sample) was lost and likely contained more than one taxon. We select a here cited illustration, as part of the original material published along with the original description as lectotype. In addition, we designate an epitype that supports the lectotype and is associated with DNA sequence data. REFERENCE SEQUENCE: MW159377 (*rbc*L gene sequence of strain GSM.5.thin).

PhycoBank ID: http://phycobank.org/102650.

Serritaenia braunii (de Bary) **A.Busch & S.Hess, comb. nov.**

≡ *Mesotaenium braunii* de Bary, *Unters. Conjugaten*: 74. 1858 (basionym).

TYPE: Schwarzwald (Black Forest, Germany)

PhycoBank Id: http://phycobank.org/102648.

UVB induces extracellular pigmentation in Serritaenia

All *Serritaenia* strains lost their extracellular pigmentation under our standard culturing conditions with PAR at about 30 μmol photons m^{-2} s^{-1}. Treatment of our experimental strain GSM.5.thin (*S. testaceovaginata*) with the SunLike high-power LED (5000 K, 25 W, see Fig. 19 for spectrum) at 200, 300, 400, 600, 700, and 1000 μmol photons m^{-2} s^{-1} for 7 days, still resulted in healthy, dividing cells but no extracellular pigmentation. Exposure of the algae to the Arcadia D3+ fluorescent tube lamp, which emits PAR, UVA and UVB (see Fig. 19 for spectrum), caused clear cellular reactions depending on the five irradiance settings used (Fig. 20). Over 14 days under settings 1–3, cells remained in colonies, showed growth, and formed purple mucilage, which was already visible 3–5 days after starting the experiment. The extracellular pigmentation correlated with the applied irradiance and was especially pronounced under settings 2 and 3 (Fig. 20). Algal colonies treated with higher intensities (settings 4 and 5) disintegrated and the cells bleached, demonstrating the deleterious effect of the applied UVR (this never happened with PAR only). After 14 days of exposure, more than 40% of the cells were dead and bleached under setting 4, more than 95% under setting 5.

To identify the waveband of the Arcadia D3+ fluorescent tube lamp which induces pigment formation, we used longpass filters that block UVB and total UVR, respectively (see Fig. 21 for transmission spectra). Colonies of *S. testaceovaginata* (strain GSM.5.thin) exposed to conditions optimal for pigment production (setting 3) but covered by filters blocking total UVR (SCHOTT GG-385, Makrolon® polycarbonate) did not show any sign of extracellular pigmentation after 7 days, while the control (without filter) contained colonies with strongly pigmented mucilage (Fig. 22). Algal colonies covered by a filter that reduces the UVB irradiance to 0–20% (SCHOTT WG-320) resulted only in very few slightly pigmented colonies; the vast majority of colonies still displayed colourless mucilage (Fig. 22). We then treated the same algal strain with the Philips UVB 'Broadband' and 'Narrowband' fluorescent tube lamps at different intensities (see Rizzini *et al.*, 2011 for spectra), and confirmed the pigment-inducing effect of UVB in our experiments. In the case of both light sources, pigmentation was clearly visible in a range of 1.5–3 W m^{-2} UVB after 2 weeks of treatment.

We have to acknowledge that light experiments in the laboratory are highly artificial, since the spectral power distribution of the used lamps clearly differs from sunlight. Therefore, it cannot be excluded that other wavebands at higher intensities, or light with other spectral ratios can trigger similar reactions in the algae. However, UVB is already known to induce the production of screening compounds, especially MAAs, in diverse microalgae (Ehling-Schulz *et al.*, 1997; Portwich & Garcia-Pichel, 2000; Sinha *et al.*, 2001, 2003*a*, *b*; Gröniger & Häder, 2002; Klisch & Häder, 2002), and it is probably of special relevance for *Serritaenia* as well. There are indications of UVB-photoreceptors in cyanobacteria and eukaryotic algae, but the molecular basis of UV perception in these life forms remains largely unknown (Portwich & Garcia-Pichel, 2000; Kräbs *et al.*, 2002; Singh *et al.*, 2010). In land plants and chlorophyte green algae, UVB is perceived by the UVR8 photoreceptor and induces photoprotective mechanisms (Rizzini *et al.*, 2011; Allorent *et al.*, 2016; Clayton *et al.*, 2018). Homologues of UVR8 were also identified in transcriptome data of several Zygnematophyceae including *Serritaenia* sp. (strain CCAC 0155, formerly referred to as '*Mesotaenium braunii*'), but not yet

10 A. BUSCH S. HESS
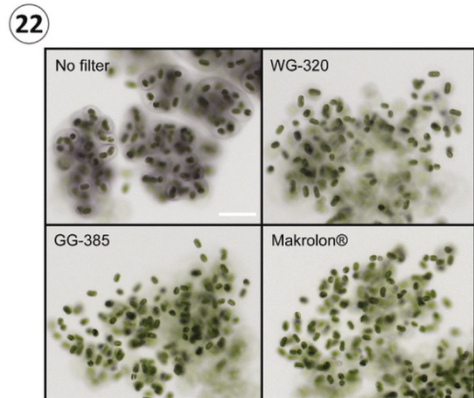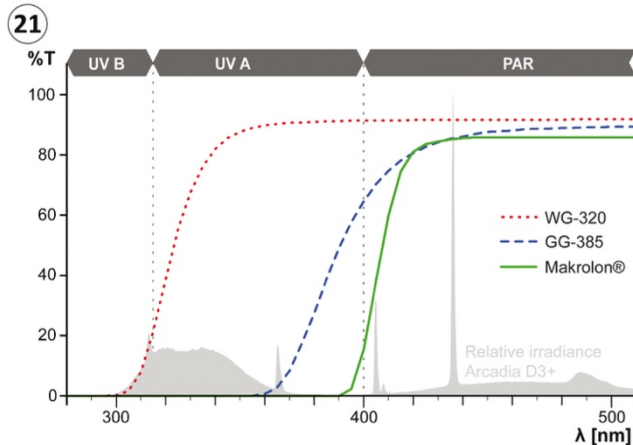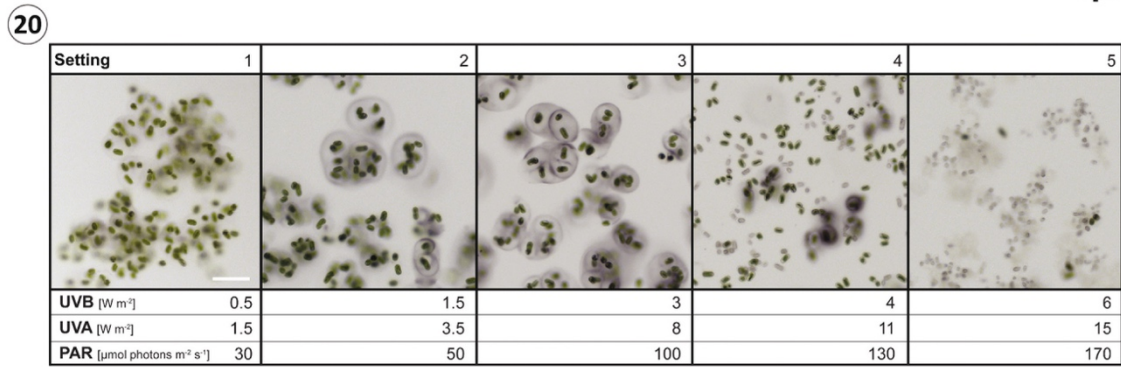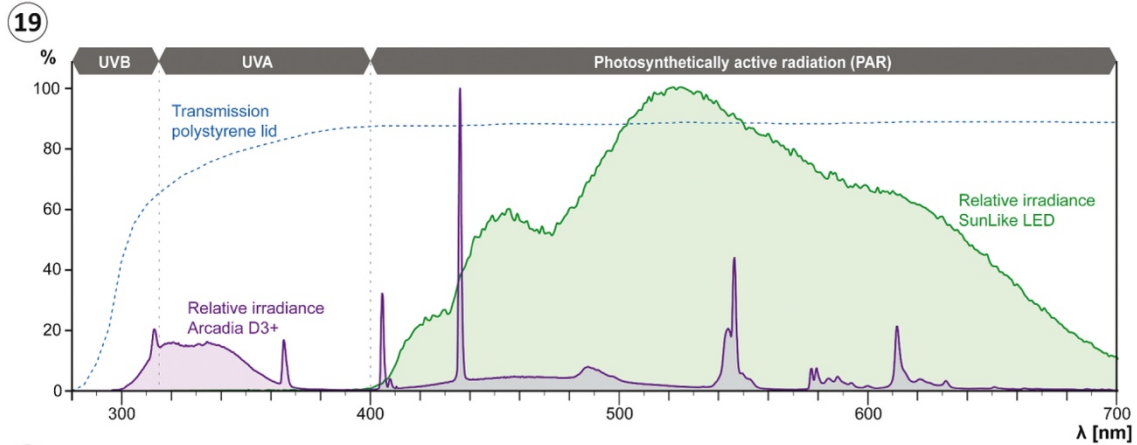
Figs 19–22. Effect of irradiance and light quality on the production of extracellular pigmentation in *Serritaenia testaceovaginata* (strain GSM.5.thin). **Fig. 19.** Relative spectral power distribution of the Arcadia D3+ fluorescent tube lamp (violet) and the SunLike LED (green), and relative transmittance of the polystyrene lids of the used multiwell plates (dashed blue line). **Fig. 20.** Brightfield images of *Serritaenia* cells after 14 days of exposure to the Arcadia D3+ lamp under five different irradiance settings (1–5). Algal colonies under settings 2 and 3 exhibit marked extracellular pigmentation. **Fig. 21.** Relative transmittance of the applied longpass filters (lines), and relative spectral power distribution of the used lamp (light grey). **Fig. 22.** Brightfield images of *Serritaenia* cells after 7 days of exposure to the Arcadia D3+ lamp (setting 3 in (20)), but covered by different longpass filters. A control sample without longpass filter is shown as well ('No filter'). Scale bars: 100 µm.

functionally characterized (Han *et al.*, 2019). It thus remains an open question whether the induction of *Serritaenia's* extracellular pigment is based on such a photoreceptor or on other effects of UVB (e.g. cell damage). In any case, *Serritaenia* with its pronounced reaction to short-wavelength UVR might be a valuable laboratory model for future experimentation.

Pigmented mucilage absorbs deleterious radiation and can change colour

So far, we did not succeed in extracting the pigment from the mucilage using a number of solvents and acidic hydrolysis (see Methods for details), which is not unusual considering the diversity of difficult-to-dissolve, wall-bound pigments in plants, especially bryophytes (Mårtensson & Nilsson, 1974; Hooijmaijers & Gould, 2007). Hence, we used microspectrophotometry to determine the absorbance spectra of pigmented mucilage *in vivo*, enabling a direct assessment of the shielding effect. Transmission data of pigmented mucilage from *S. testaceovaginata* (strain GSM.5.thin) revealed absorbance over the entire UV-PAR spectrum (n = 54) compared with non-pigmented mucilage (n = 15; Figs 23, 24). As illustrated by three representative measurements (sample 1–3), the absorbance spectra showed a consistent pattern with two maxima at ~300 nm and ~580 nm (Fig. 23; see Supplementary figs S2–S4 for all spectra recorded). The absolute maximum was always at 290–320 nm, corresponding to UVB and far UVA, the most harmful wavebands of terrestrial sunlight. In this spectral range the pigmented mucilage from
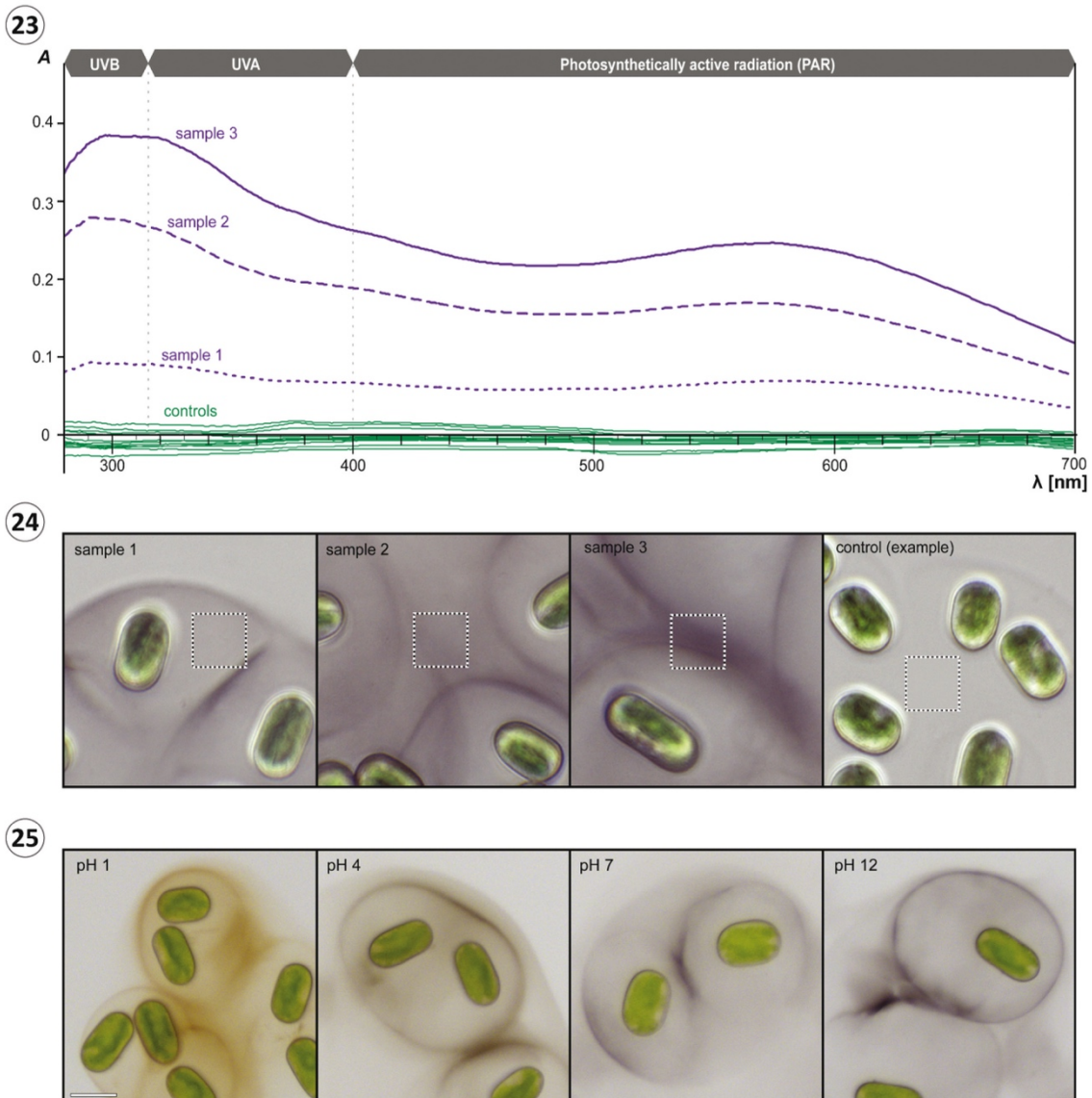
Figs 23–25. UV-VIS absorbance of pigmented and non-pigmented mucilage of *Serritaenia testaceovaginata* (strain GSM.5.thin), microscopic appearance of the sampled spots, and pH-dependent colour changes of pigmented mucilage. **Fig. 23.** Absorbance spectra of pigmented mucilage (violet lines; samples 1–3) and non-pigmented mucilage (green lines, 15 samples) determined by microspectrophotometry. **Fig. 24.** Brightfield micrographs displaying the spots (dashed squares, 15×15 µm) analysed for samples 1–3 shown in (23) as well as a representative sampling spot in non-pigmented mucilage. **Fig. 25.** Colour of pigmented mucilage of *S. testaceovaginata* (strain GSM.5.thin) at different pH values. Scale bar: 20 µm.

12   A. BUSCH S. HESS

experimental cultures blocked up to 60% of incoming radiation, representing UVB-screening factors comparable to those estimated for other algal sunscreens, e.g. scytonemin and MAAs of cyanobacteria (Garcia-Pichel & Castenholz, 1993). Differences in overall absorbance between the individual sampling spots clearly correlated with the degree of pigmentation visible in the corresponding light micrographs (Fig. 24). At this point, we cannot exclude the possibility that *Serritaenia* secretes more than one compound into the mucilage and that the observed spectra are a sum thereof. Some cyanobacteria of the genus *Nostoc*, for example, accumulate two complementary sunscreens (scytonemin and oligosaccharide-linked MAAs) in their extracellular glycan sheath, thereby extending the spectral range of photoprotection (Böhm *et al.*, 1995; Ferroni *et al.*, 2010). The observed correlation of UVR absorbance and visible pigmentation (also apparent from the spectral curves), however, lets us assume that the intensely coloured capsules of *Serritaenia* cells found in nature provide an effective broadband-screening including the UV waveband.

Interestingly, the pigmented mucilage of *S. testaceovaginata* (strain GSM.5.thin) formed under experimental conditions always showed a violet-blue colour, while this species was found with reddish mucilage in nature

(compare Figs 12 and 24). Experimental changes of the pH value of the medium resulted in reversible colour changes of the pigmented mucilage, from violet-blue under alkaline and neutral conditions to black and reddish-brown under acidic conditions (Fig. 25). These colour changes can explain the reddish-brown tones frequently observed in mucilage from natural material. Both the 'wet walls' in the Great Smoky Mountains as well as the substrates (bryophytes, plant litter) at our main study site (Wohlsberg, Wiehl, Germany) showed acidic reactions, pH 4.4 (Furey *et al.*, 2007) and pH 4.3–4.8 (n = 7), respectively. We assume that different *Serritaenia* species produce the same compound, which can show different colours depending on the chemical conditions of the substrate. Consequently, mucilage colour seems to be a trait of poor taxonomic value (which applies to gloeocapsin-containing cyanobacteria as well) and should not be used for species descriptions as done for *Mesotaenium testaceovaginatum* (Fučíková *et al.*, 2008).

How do the pigmented capsules form?

With very few exceptions such as the MAAs deposited in the silica frustules of planktonic diatoms (Ingalls *et al.*, 2010), most (putative) sunscreen compounds from
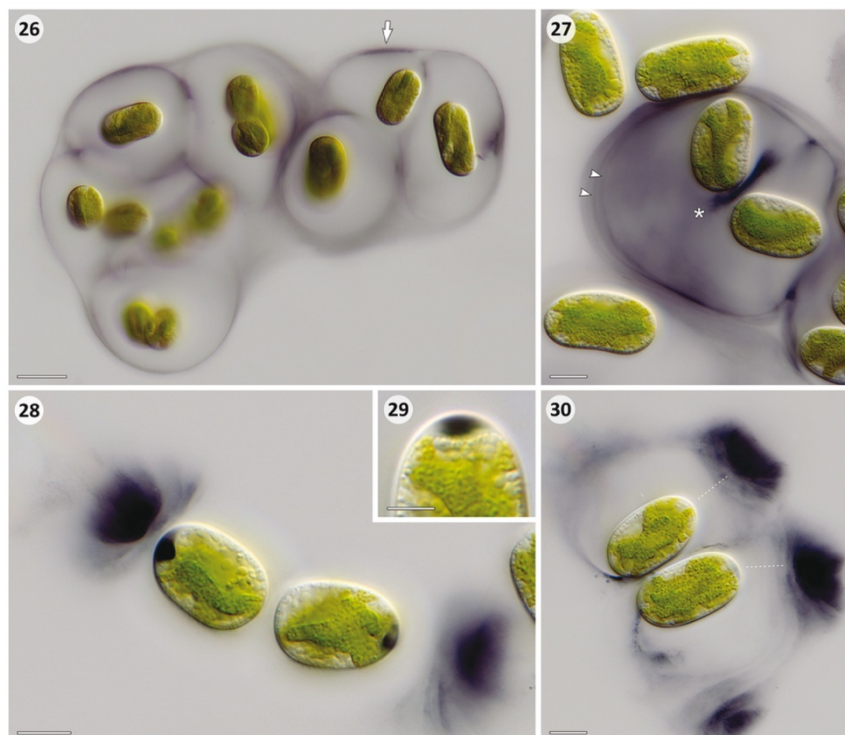
Figs 26–30. Microscopic details of extracellular pigmentation in *Serritaenia* species induced under setting 3 for 14 days. **Fig. 26**. Colony of *S. testaceovaginata* (strain GSM.5.thin) with pigmentation in outermost layer of the mucilaginous capsules (arrow). **Fig. 27**. Cells of *Serritaenia* sp. (strain OBE.1) exhibiting several pigment layers (arrowheads) and a pigment accumulation between recently divided cells (asterisk). **Fig. 28**. Dark, polar inclusions in the cells of *Serritaenia* sp. (strain OBE.1) associated with zones of intensely pigmented mucilage. **Fig. 29**. Detail of lens-like pigment inclusion at the cell pole of *Serritaenia* sp. (strain OBE.1). **Fig. 30**. Two cells of *Serritaenia* sp. (strain OBE.1) surrounded by mucilaginous capsules with intensely pigmented zones. The assumed trajectory of secretion is indicated by dashed lines. Scale bars: Fig. 26, 20 μm; Figs 27, 28, 30, 10 μm; Fig. 29, 5 μm.

eukaryotic microalgae have an intracellular localization. They can accumulate in the cytoplasm (e.g. MAAs; Garcia-Pichel & Castenholz, 1993), in vacuoles (e.g. purpurogallin-derivatives; Remias *et al.*, 2012*a*), or in lipid droplets (e.g. carotenoids; Bidigare *et al.*, 1993). Since some of these substances might be involved in physiological processes as well (carotenoids, MAAs), their primary role as sunscreen is not always established. The *Serritaenia* pigment, instead, is often found in distant layers of extracellular mucilage, which is an ideal localization for effective shielding of the entire cell, including the cell periphery and plasma membrane. Furthermore, *Serritaenia* capsules from nature showed a striking unilateral pigmentation (Fig. 8), suggesting a directed ('economic') deposition of a sunscreen. Based on our microscopic data from experimentally treated cells, we can infer some aspects of the formation of pigmented capsules by *Serritaenia*. Two strains from distinct subclades, GSM.5.thin and OBE.1, produced pigmented mucilage upon exposure to moderate UV-PAR intensities (setting 3, Fig. 20), but showed different patterns of mucilage secretion. In strain GSM.5.thin the outermost regions of the mucilaginous capsules exhibited an intense pigmentation, often forming a thin, discrete pigment layer (Fig. 26). The pigmentation in these layers was not always evenly distributed and occasionally concentrated in zones of increased density (Fig. 26, arrow), reminiscent of the unilateral pigmentation observed in natural material. Strain OBE.1 frequently produced several nested pigmented layers within the capsules (Fig. 27, arrowheads) as well as pigmentation at the site of cell division and between recently divided cells (Fig. 27, asterisk). Furthermore, cells of this strain exhibited dark, lens-like inclusions at the cell poles, situated between the plasma membrane and the cell wall (Figs 28, 29). These inclusions were often associated with confined zones of intensely pigmented mucilage located well outside the cells (Fig. 28). In some instances, it became clear that these pigmented zones are in fact part of otherwise colourless or faintly pigmented, extracellular capsules (Fig. 30). We assume that the lens-like inclusions correspond to secreted mucilage, which normally travels through the cellulosic mesh work of the wall, but – under the experimental conditions – accumulated underneath the wall (maybe due to a sudden overreaction of the cell). It is well known from other Zygnematophyceae (e.g. *Closterium, Micrasterias, Netrium, Penium*) that gel-like exopolymers such as pectic substances are secreted through the existing cell wall after fusion of secretory vesicles with the plasma membrane (Oertel *et al.*, 2004; Eder & Lütz-Meindl, 2010; Domozych *et al.*, 2014). We conclude that the colourful capsules of *Serritaenia* are likely formed by the secretion of pigmented exopolymers, and not by the release of pigments into existing capsules. This idea is supported by the radial pigment gradients and hierarchical pigment layers often found in natural material. These layers can

be easily explained by the initial deposition of pigmented mucilage followed by the secretion of (less-pigmented) mucilage that pushes the pigmented layer apart from the cell. Furthermore, the pigmented inclusions found at the cell poles in experimental material demonstrate that the secretion of pigmented mucilage can be local. We therefore assume that *Serritaenia* cells in the natural habitat (i.e. when the colonies are stuck to a substrate in a fixed position) are able to form well-oriented 'sunshades' by the directed secretion of pigmented mucilage.

Several pieces of evidence support a role as a sunscreen

Sunscreen compounds of microbes and plants are expected to meet a number of criteria which are relevant to their function (Cockell & Knowland, 1999; Gao & Garcia-Pichel, 2011). This includes (1) a sensible (cellular) localization for effective shielding of sensitive structures, (2) the effective absorption of deleterious radiation, especially UVR and (3) the synthesis of the compound in response to elevated levels of deleterious radiation, or during life history stages which typically experience such conditions. Our microscopic and experimental data demonstrate that these criteria are met by the pigmented capsules of *Serritaenia* species. Ideally, there is also experimental evidence for resistance to harmful doses of respective wavebands gained by the accumulation of the compound. Indeed, we occasionally observed strongly pigmented colonies surviving the adverse conditions in our experiments (Fig. 20, setting 4), but could not undoubtedly prove the role of the pigmentation. In poorly known non-model organisms such as *Serritaenia* clear evidence for a cause-effect relationship is difficult to obtain, since the cells can potentially react in several unknown ways at the same time; e.g. on a physiological level or with repair mechanisms (Garcia-Pichel *et al.*, 1993; Cockell & Knowland, 1999). However, some additional evidence for effective UV-screening by the pigmented *Serritaenia* capsules comes from the observed correlation of the strength of pigmentation and the applied UVB irradiance, pointing to self-regulatory pigment accumulation: Higher intensities of UVR require higher concentrations of the extracellular sunscreen compound to attenuate below the response threshold of the cell. An important requirement for this self-regulative effect is that the action spectrum of sunscreen synthesis aligns with the absorbance spectrum of the sunscreen to some extent, as is known from some MAAs and scytonemin (Ehling-Schulz *et al.*, 1997; Cockell & Knowland, 1999). Indeed, the pigment-inducing waveband in *Serritaenia* matches the main absorbance peak of pigmented mucilage very well (both in the UVB/far UVA range). Self-regulatory pigment production could also explain the hierarchical pigment layers frequently found in larger *Serritaenia* colonies from natural populations. Repeated

cell division and capsule formation during colony growth likely results in stretching of the outer mucilage, thereby reducing the thickness (= optical path length) and absorbance of the outer pigment layer. Due to the diminished screening effect (and increased UV-exposure), the cells are triggered to form additional, interior pigment layers to restore full photoprotection. Taken together, the pigmented capsules of *Serritaenia* strongly absorb deleterious short-wavelength radiation and can be induced by the same stressor. The extracellular pigment is deposited in a sunshade-like pattern, ideal to shield entire cells from excess radiation, but unlikely to play additional physiological roles (as for example known from intracellular screening compounds such as carotenoids). All this points to a primary function in photoprotection.

In addition, the secretion of light-absorbing mucilage as a strategy aligns very well with the ecology of the studied algae. *Serritaenia* species are found predominantly in terrestrial habitats, where they are exposed to a large range of environmental conditions, including freezing temperatures, drought, heat and increased solar radiation. The high concentrations of the extracellular pigment observed in field material suggest that the extracellular mucilage of *Serritaenia* not only extends the active phases of this alga by its water-holding capacity, but also represents an effective 'broadband' sunscreen. The pigmented mucilage shields the entire cells in the active (hydrated) and inactive (desiccated) state. This might be of particular relevance during summer, when the *Serritaenia* cells survive in desiccated crusts and lack the ability to react on the cellular level (e.g. with non-photochemical quenching or repair mechanisms).

Serritaenia's *sunscreen mucilage in an evolutionary context*

Among eukaryotic microalgae, members of the new genus *Serritaenia* stand out by their ability to form heavily pigmented extracellular mucilage. This phenomenon differs drastically from the photoprotective strategies already known from other Zygnematophyceae, e.g. the reddish, water-soluble pigments found in the vacuoles of representatives from alpine and glacier environments (Remias *et al.*, 2012a, b; Aigner *et al.*, 2013; Herburger *et al.*, 2016; Garduño-Solórzano *et al.*, 2020). It seems that members of different zygnematophycean lineages that colonize high-light habitats evolved different solutions for the same problem, demonstrating once more that these algae are exciting candidates for studying terrestrialization processes in a comparative way.

A stunning analogy to *Serritaenia*'s sunscreen capsules, however, can be found in the world of prokaryotes. Terrestrial cyanobacteria of the *Chroococcales* form extracellular capsules with reddish layers containing gloeocapsin, a pigment which (similar to scytonemin) is believed to act as an extracellular UV-screen (Storme *et al.*, 2015). The pigmented, extracellular capsules of *Serritaenia* and *Chroococcales* display a remarkable resemblance regarding the pattern of pigment deposition, and we assume that similar evolutionary pressures resulted in the evolution of very similar photoprotective adaptations. These adaptations, however, must be based on a very different cell biological background, and represent a prime example for convergent evolution across two domains of life.

The closest potential homologies to *Serritaenia*'s sunscreen mucilage might be found among the colourful cell walls of plants (e.g. various bryophytes) and their algal relatives. Topologically, cell walls correspond to the same cellular compartment as secreted mucilage, namely the extracellular space (apoplast). The cell walls of Zygnematophyceae are typically colourless, but some representatives of the genera *Spirogyra, Zygnema* and *Zygnemopsis* form zygospores with blue, brown or reddish spore walls (Stancheva *et al.*, 2012, 2013; Pichrtová *et al.*, 2018; Takano *et al.*, 2019). Although there are no physicochemical data about these zygospore pigments, a photoprotective role in these propagules of aquatic Zygnematophyceae is not unlikely. In future, modern molecular and analytical techniques (e.g. transcriptomics and metabolomics) applied to non-model organisms like *Serritaenia* and relatives might provide deeper insights into the physiology and evolution of photoprotective strategies found in the 'green lineage' of life.

Supplementary information

The following supplementary material is accessible via the Supplementary Content tab on the article's online page at http://dx.doi.org/10.1080/09670262.2021.1898677
Supplementary table S1. Studied *Serritaenia* strains and associated data (sampling sites and accession numbers of the Central Collection of Algal Cultures (CCAC) and *rbc*L gene sequences).
Supplementary fig. S1. Unrooted Neighbour-joining phylogeny of 43 zygnematophycean *rbc*L gene sequences displaying the polyphyly of *Mesotaenium* (red) and the position of the new genus *Serritaenia* (green). Support values are shown on the respective branches (NJ/ML). Branches with maximum support (100/100) are in bold. The scale bar represents 0.02 nucleotide substitution per site.
Supplementary figs S2 and S3. Illustrations published with the original descriptions of *Mesotaenium braunii* (S2: A, 1-8), *M. braunii* var. *minus* (S2: A, 9-11) and *M. testaceovaginatum* (S3). The illustration of *M. testaceovaginatum* (S3) is designated as lectotype for this species.
Supplementary figs S4–S6. Microspectrophotometric measurements taken from the mucilage of *Serritaenia testaceovaginata* (strain GSM.5.thin) over a spectral range of 200–1600 nm. S4 and S5 display absorbance spectra of mucilage with varying degree of pigmentation from two independent wet mounts with 21 and 33 measurements, respectively. S6 displays 15 absorbance measurements of non-pigmented mucilage for comparison.
Supplementary text. Rationale for the new genus *Serritaenia* and taxonomy of its members.

Author contributions

SH conceived the study. AB and SH designed and performed the experiments, analysed and interpreted the data, and wrote the manuscript.

ORCID

Anna Busch http://orcid.org/0000-0002-5377-7150
Sebastian Hess http://orcid.org/0000-0003-1262-8201

References

Aigner, S., Remias, D., Karsten, U. & Holzinger, A. (2013). Unusual phenolic compounds contribute to ecophysiological performance in the purple-colored green alga *Zygogonium ericetorum* (Zygnematophyceae, Streptophyta) from a high-alpine habitat. *Journal of Phycology*, 49: 648–660.

Allorent, G., Lefebvre-Legendre, L., Chappuis, R., Kuntz, M., Truong, T.B., Niyogi, K.K., Ulm, R. & Goldschmidt-Clermont, M. (2016). UV-B photoreceptor-mediated protection of the photosynthetic machinery in *Chlamydomonas reinhardtii*. *Proceedings of the National Academy of Sciences USA*, 113: 14864–14869.

Barcytė, D., Pilátová, J., Mojzeš, P. & Nedbalová, L. (2020). The arctic *Cylindrocystis* (Zygnematophyceae, Streptophyta) green algae are genetically and morphologically diverse and exhibit effective accumulation of polyphosphate. *Journal of Phycology*, 56: 217–232.

de Bary, A. (1858). Untersuchungen über die Familie der Conjugaten (Zygnemeen und Desmidieen): Ein Beitrag zur physiologischen und beschreibenden Botanik. Förstnersche Buchhandlung, Leipzig.

Bidigare, R.R., Ondrusek, M.E., Kennicutt, M.C., Iturriaga, R., Harvey, H.R., Hoham, R.W. & Macko, S. A. (1993). Evidence for a photoprotective function for secondary carotenoids of snow algae. *Journal of Phycology*, 29: 427–434.

Böhm, G.A., Pfleiderer, W., Böger, P. & Scherer, S. (1995). Structure of a novel oligosaccharide-mycosporine-amino acid ultraviolet A/B sunscreen pigment from the terrestrial cyanobacterium *Nostoc commune*. *Journal of Biological Chemistry*, 270: 8536–8539.

Bonnot, C., Hetherington, A.J., Champion, C., Breuninger, H., Kelly, S. & Dolan, L. (2019). Neofunctionalisation of basic helix–loop–helix proteins occurred when embryophytes colonised the land. *New Phytologist*, 223: 993–1008.

Brook, A.J. (1981). *The Biology of Desmids*. University of California Press, Berkeley, CA.

Brook, A.J. & Williamson, D.B. (2010). *A Monograph on some British Desmids*. The Ray Society, London.

Černá, K. & Neustupa, J. (2010). The pH-related morphological variations of two acidophilic species of Desmidiales (Viridiplantae) isolated from a lowland peat bog, Czech Republic. *Aquatic Ecology*, 44: 409–419.

Chase, M.W., Salamin, N., Wilkinson, M., Dunwell, J.M., Kesanakurthi, R.P., Haidar, N. & Savolainen, V. (2005). Land plants and DNA barcodes: short-term and long-term goals. *Philosophical Transactions of the Royal Society B: Biological Sciences*, 360: 1889–1895.

Cheng, S., Xian, W., Fu, Y., Marin, B., Keller, J., Wu, T., Sun, W., Li, X., Xu, Y., Zhang, Y., Wittek, S., Reder, T., Günther, G., Gontcharov, A., Wang, S., Li, L., Liu, X., Wang, J., Yang, H., Xu, X., Delaux, P.-M., Melkonian, B., Wong, G.K.-S. & Melkonian, M. (2019). Genomes of subaerial Zygnematophyceae provide insights into land plant evolution. *Cell*, 179: 1057–1067.

Clayton, W.A., Albert, N.W., Thrimawithana, A.H., McGhie, T.K., Deroles, S.C., Schwinn, K.E., Warren, B. A., McLachlan, A.R.G., Bowman, J.L., Jordan, B.R. & Davies, K.M. (2018). UVR8-mediated induction of flavonoid biosynthesis for UVB tolerance is conserved between the liverwort *Marchantia polymorpha* and flowering plants. *The Plant Journal*, 96: 503–517.

Cockell, C.S. & Knowland, J. (1999). Ultraviolet radiation screening compounds. *Biological Reviews*, 74: 311–345.

Coesel, P.F.M. & Meesters, K.J. (2007). *Desmids of the Lowlands: Mesotaeniaceae and Desmidiaceae of the European Lowlands*. KNNV Publishing, Zeist.

Davey, M.L. & Currah, R.S. (2006). Interactions between mosses (Bryophyta) and fungi. *Canadian Journal of Botany*, 84: 1509–1519.

Domozych, D.S., Sørensen, I., Popper, Z.A., Ochs, J., Andreas, A., Fangel, J.U., Pielach, A., Sacks, C., Brechka, H., Ruisi-Besares, P., Willats, W.G.T. & Rose, J.K.C. (2014). Pectin metabolism and assembly in the cell wall of the charophyte green alga *Penium margaritaceum*. *Plant Physiology*, 165: 105–118.

Eder, M. & Lütz-Meindl, U. (2010). Analyses and localization of pectin-like carbohydrates in cell wall and mucilage of the green alga *Netrium digitus*. *Protoplasma*, 243: 25–38.

Ehling-Schulz, M., Bilger, W. & Scherer, S. (1997). UV-B-induced synthesis of photoprotective pigments and extracellular polysaccharides in the terrestrial cyanobacterium *Nostoc commune*. *Journal of Bacteriology*, 179: 1940–1945.

Ettl, H. & Gärtner, G. (2014). *Syllabus der Boden-, Luft- und Flechtenalgen*. 2nd ed. Springer, Berlin.

16 🌀 A. BUSCH S. HESS

Fenton, J.H.C. (1983). Concentric fungal rings in Antarctic moss communities. *Transactions of the British Mycological Society*, **80**: 415–420.

Ferroni, L., Klisch, M., Pancaldi, S. & Häder, D.-P. (2010). Complementary UV-absorption of mycosporine-like amino acids and scytonemin is responsible for the UV-insensitivity of photosynthesis in *Nostoc flagelliforme*. *Marine Drugs*, **8**: 106–121.

Fritsch, F.E. (1922). The terrestrial alga. *Journal of Ecology*, **10**: 220–236.

Fučíková, K., Hall, J.D., Johansen, J.R. & Lowe, R. (2008). Desmid flora of the Great Smoky Mountains National Park, USA. *Bibliotheca Phycologica*, **113**: 1–59.

Furey, P.C., Lowe, R.L. & Johansen, J.R. (2007). Wet wall algal community response to in-field nutrient manipulation in the Great Smoky Mountains National Park, USA. *Algological Studies*, **125**: 17–43.

Galtier, N., Gouy, M. & Gautier, C. (1996). SEAVIEW and PHYLO_WIN: two graphic tools for sequence alignment and molecular phylogeny. *Bioinformatics*, **12**: 543–548.

Gao, Q. & Garcia-Pichel, F. (2011). Microbial ultraviolet sunscreens. *Nature Reviews Microbiology*, **9**: 791–802.

Garcia-Pichel, F. & Castenholz, R.W. (1991). Characterization and biological implications of scytonemin, a cyanobacterial sheath pigment. *Journal of Phycology*, **27**: 395–409.

Garcia-Pichel, F. & Castenholz, R.W. (1993). Occurrence of UV-absorbing, mycosporine-like compounds among cyanobacterial isolates and an estimate of their screening capacity. *Applied and Environmental Microbiology*, **59**: 163–169.

Garcia-Pichel, F., Sherry, N.D. & Castenholz, R.W. (1992). Evidence for an ultraviolet sunscreen role of the extracellular pigment scytonemin in the terrestrial cyanobacterium *Chlorogloeopsis* sp. *Photochemistry and Photobiology*, **56**: 17–23.

Garcia-Pichel, F., Wingard, C.E. & Castenholz, R.W. (1993). Evidence regarding the UV sunscreen role of a mycosporine-like compound in the cyanobacterium *Gloeocapsa* sp. *Applied and Environmental Microbiology*, **59**: 170–176.

Garduño-Solórzano, G., Martínez-García, M., Scotta Hentschke, G., Lopes, G., Castelo Branco, R., Vasconcelos, V.M.O., Campos, J.E., López-Cano, R. & Quintanar-Zúñiga, R.E. (2020). The phylogenetic placement of *Temnogametum* (Zygnemataceae) and description of *Temnogametum iztacalense* sp. nov., from a tropical high mountain lake in Mexico. *European Journal of Phycology*: doi: 10.1080/09670262.2020.1789226.

Gitzendanner, M.A., Soltis, P.S., Wong, G.K.-S., Ruhfel, B. R. & Soltis, D.E. (2018). Plastid phylogenomic analysis of green plants: a billion years of evolutionary history. *American Journal of Botany*, **105**: 291–301.

Gontcharov, A.A. (2008). Phylogeny and classification of Zygnematophyceae (Streptophyta): current state of affairs. *Fottea*, **8**: 87–104.

Gontcharov, A.A. & Melkonian, M. (2010). Molecular phylogeny and revision of the genus *Netrium* (Zygnematophyceae, Streptophyta): *Nucleotaenium* gen. nov. *Journal of Phycology*, **46**: 346–362.

Gontcharov, A.A., Marin, B. & Melkonian, M. (2003). Molecular phylogeny of conjugating green algae (Zygnemophyceae, Streptophyta) inferred from SSU rDNA sequence comparisons. *Journal of Molecular Evolution*, **56**: 89–104.

Gontcharov, A.A., Marin, B. & Melkonian, M. (2004). Are combined analyses better than single gene phylogenies? A case study using SSU rDNA and *rbc*L sequence

comparisons in the Zygnematophyceae (Streptophyta). *Molecular Biology and Evolution*, **21**: 612–624.

Gouy, M., Guindon, S. & Gascuel, O. (2010). SeaView version 4: a multiplatform graphical user interface for sequence alignment and phylogenetic tree building. *Molecular Biology and Evolution*, **27**: 221–224.

Gröniger, A. & Häder, D.-P. (2002). Induction of the synthesis of an UV-absorbing substance in the green alga *Prasiola stipitata*. *Journal of Photochemistry and Photobiology B: Biology*, **66**: 54–59.

Hall, J.D., Fučíková, K., Lewis, L.A. & Karol, K.G. (2010). An assessment of proposed DNA barcodes in freshwater green algae. *Cryptogamie Algologie*, **31**: 529–555.

Han, X., Chang, X., Zhang, Z., Chen, H., He, H., Zhong, B. & Deng, X.W. (2019). Origin and evolution of core components responsible for monitoring light environment changes during plant terrestrialization. *Molecular Plant*, **12**: 847–862.

Hargreaves, A., Taiwo, F.A., Duggan, O., Kirk, S.H. & Ahmad, S.I. (2007). Near-ultraviolet photolysis of β-phenylpyruvic acid generates free radicals and results in DNA damage. *Journal of Photochemistry and Photobiology B: Biology*, **89**: 110–116.

Hartmann, A., Glaser, K., Holzinger, A., Ganzera, M. & Karsten, U. (2020). Klebsormidin A and B, two new UV-sunscreen compounds in green microalgal *Interfilum* and *Klebsormidium* species (Streptophyta) from terrestrial habitats. *Frontiers in Microbiology*, **11**: 499.

Herburger, K., Remias, D. & Holzinger, A. (2016). The green alga *Zygogonium ericetorum* (Zygnematophyceae, Charophyta) shows high iron and aluminium tolerance: protection mechanisms and photosynthetic performance. *FEMS Microbiology Ecology*, **92**: doi: 10.1093/femsec/fiw103.

Hoffmann, L. (1989). Algae of terrestrial habitats. *The Botanical Review*, **55**: 77–105.

Holzinger, A., Albert, A., Aigner, S., Uhl, J., Schmitt-Kopplin, P., Trumhová, K. & Pichrtová, M. (2018). Arctic, Antarctic, and temperate green algae *Zygnema* spp. under UV-B stress: vegetative cells perform better than pre-akinetes. *Protoplasma*, **255**: 1239–1252.

Holzinger, A., Tschaikner, A. & Remias, D. (2010). Cytoarchitecture of the desiccation-tolerant green alga *Zygogonium ericetorum*. *Protoplasma*, **243**: 15–24.

Hooijmaijers, C.A.M. & Gould, K.S. (2007). Photoprotective pigments in red and green gametophytes of two New Zealand liverworts. *New Zealand Journal of Botany*, **45**: 451–461.

Hotter, V., Glaser, K., Hartmann, A., Ganzera, M. & Karsten, U. (2018). Polyols and UV-sunscreens in the *Prasiola*-clade (Trebouxiophyceae, Chlorophyta) as metabolites for stress response and chemotaxonomy. *Journal of Phycology*, **54**: 264–274.

Ingalls, A.E., Whitehead, K. & Bridoux, M.C. (2010). Tinted windows: the presence of the UV absorbing compounds called mycosporine-like amino acids embedded in the frustules of marine diatoms. *Geochimica et Cosmochimica Acta*, **74**: 104–115.

Jeffrey, S.W., MacTavish, H.S., Dunlap, W.C., Vesk, M. & Groenewoud, K. (1999). Occurrence of UVA- and UVB-absorbing compounds in 152 species (206 strains) of marine microalgae. *Marine Ecology Progress Series*, **189**: 35–51.

Karsten, U. (2008). Defense strategies of algae and cyanobacteria against solar ultraviolet radiation. In *Algal Chemical Ecology* (Amsler, C.D., editor), 273–296. Springer, Berlin.

Karsten, U. & Holzinger, A. (2014). Green algae in alpine biological soil crust communities: acclimation strategies

against ultraviolet radiation and dehydration. *Biodiversity and Conservation*, **23**: 1845–1858.

Karsten, U., Franklin, L.A., Lüning, K. & Wiencke, C. (1998). Natural ultraviolet radiation and photosynthetically active radiation induce formation of mycosporine-like amino acids in the marine macroalga *Chondrus crispus* (Rhodophyta). *Planta*, **205**: 257–262.

Karsten, U., Schumann, R. & Mostaert, A. (2007). Aeroterrestrial algae growing on man-made surfaces. In *Algae and Cyanobacteria in Extreme Environments* (Seckbach, J., editor), 583–597. Springer, Dordrecht.

Kitzing, C. & Karsten, U. (2015). Effects of UV radiation on optimum quantum yield and sunscreen contents in members of the genera *Interfilum*, *Klebsormidium*, *Hormidiella* and *Entransia* (Klebsormidiophyceae, Streptophyta). *European Journal of Phycology*, **50**: 279–287.

Klisch, M. & Häder, D.-P. (2002). Wavelength dependence of mycosporine-like amino acid synthesis in *Gyrodinium dorsum*. *Journal of Photochemistry and Photobiology B: Biology*, **66**: 60–66.

Kouwets, F. (2008). The species concept in desmids: the problem of variability, infraspecific taxa and the monothetic species definition. *Biologia*, **63**: 881–887.

Kräbs, G., Bischof, K., Hanelt, D., Karsten, U. & Wiencke, C. (2002). Wavelength-dependent induction of UV-absorbing mycosporine-like amino acids in the red alga *Chondrus crispus* under natural solar radiation. *Journal of Experimental Marine Biology and Ecology*, **268**: 69–82.

Kumar, S., Stecher, G., Li, M., Knyaz, C. & Tamura, K. (2018). MEGA X: molecular evolutionary genetics analysis across computing platforms. *Molecular Biology and Evolution*, **35**: 1547–1549.

Kützing, F.T. (1845). Phycologia germanica, d. i. Deutschlands Algen in bündigen Beschreibungen. Nebst einer Anleitung zum Untersuchen und Bestimmen dieser Gewächse für Anfänger. pp. [i]–x, [1] –340 ['240']. Nordhausen: zu finden bei Wilh. Köhne.

Lenzenweger, R. (2003). Desmidiaceenflora von Österreich, Teil 4. In *Bibliotheca Phycologica* (Cramer, J., editor), 1–87. Schweizerbart Science Publishers, Stuttgart.

Liang, H., Wei, T., Xu, Y., Li, L., Kumar Sahu, S., Wang, H., Li, H., Fu, X., Zhang, G., Melkonian, M., Liu, X., Wang, S. & Liu, H. (2019). Phylogenomics provides new insights into gains and losses of selenoproteins among Archaeplastida. *International Journal of Molecular Sciences*, **20**: 3020.

Lowe, R.L., Furey, P.C., Ress, J.A. & Johansen, J.R. (2007). Diatom biodiversity and distribution on wetwalls in Great Smoky Mountains National Park. *Southeastern Naturalist*, **6**: 135–152.

Mårtensson, O. & Nilsson, E. (1974). On the morphological colour of bryophytes. *Lindbergia*, **2**: 145–159.

Matasci, N., Hung, L.-H., Yan, Z., Carpenter, E.J., Wickett, N. J., Mirarab, S., Nguyen, N., Warnow, T., Ayyampalayam, S., Barker, M., Burleigh, J.G., Gitzendanner, M.A., Wafula E., Der, J.P., dePamphilis, C.W., Roure, B., Philippe, H., Ruhfel, B.R., Miles, N.W., Graham, S.W., Mathews, S., Surek, B., Melkonian, M., Soltis, D.E., Soltis, P.S., Rothfels, C., Pokorny, L., Shaw, J.A., DeGironimo, L., Stevenson, D.W., Villarreal, J.C., Chen, T., Kutchan, T.M., Rolf, M., Baucom, R.S., Deyholos, M.K., Samudrala, R., Tian, Z., Wu, X., Sun, X., Zhang, Y., Wang, J., Leebens-Mack, J. & Wong, G.K.-S. (2014). Data access for the 1,000 Plants (1KP) project. *Gigascience*, **3**: 2047-217X-3-17.

McCourt, R.M., Karol, K.G., Bell, J., Helm-Bychowski, K. M., Grajewska, A., Wojciechowski, M.F. & Hoshaw, R. W. (2000). Phylogeny of the conjugating green algae (Zygnemophyceae) based on *rbc*L sequences. *Journal of Phycology*, **36**: 747–758.

McFadden, G.I. & Melkonian, M. (1986). Use of Hepes buffer for microalgal culture media and fixation for electron microscopy. *Phycologia*, **25**: 551–557.

Nedbalová, L. & Sklenár, P. (2008). New records of snow algae from the Andes of Ecuador. *Arnaldoa*, **15**: 17–20.

Neustupa, J., Stastny, J. & Hodac, L. (2008). Temperature-related phenotypic plasticity in the green microalga *Micrasterias rotata*. *Aquatic Microbial Ecology*, **51**: 77–86.

Neustupa, J., Stastny, J., Nemjová, K., Mazalová, P., Goodyer, E., Poulíčková, A. & Škaloud, P. (2011). A novel, combined approach to assessing species delimitation and biogeography within the well-known desmid species *Micrasterias fimbriata* and *M. rotata* (Desmidiales, Steptophyta). *Hydrobiologia*, **667**: 223–239.

Newmaster, S.G., Fazekas, A.J. & Ragupathy, S. (2006). DNA barcoding in land plants: evaluation of *rbc*L in a multigene tiered approach. *Botany*, **84**: 335–341.

Oertel, A., Aichinger, N., Hochreiter, R., Thalhamer, J. & Lütz-Meindl, U. (2004). Analysis of mucilage secretion and excretion in *Micrasterias* (Chlorophyta) by means of immunoelectron microscopy and digital time lapse video microscopy. *Journal of Phycology*, **40**: 711–720.

Pattison, D.I. & Davies, M.J. (2006). Actions of ultraviolet light on cellular structures. In *Cancer: Cell Structures, Carcinogens and Genomic Instability* (Bignold, L.P., editor), 131–157. Birkhäuser, Basel.

Philippe, G., Sørensen, I., Jiao, C., Sun, X., Fei, Z., Domozych, D.S. & Rose, J.K. (2020). Cutin and suberin: assembly and origins of specialized lipidic cell wall scaffolds. *Current Opinion in Plant Biology*, **55**: 11–20.

Pichrtová, M., Remias, D., Lewis, L.A. & Holzinger, A. (2013). Changes in phenolic compounds and cellular ultrastructure of Arctic and Antarctic strains of *Zygnema* (Zygnematophyceae, Streptophyta) after exposure to experimentally enhanced UV to PAR ratio. *Microbial Ecology*, **65**: 68–83.

Pichrtová, M., Holzinger, A., Kulichová, J., Ryšánek, D., Šoljaková, T., Trumhová, K. & Nemcova, Y. (2018). Molecular and morphological diversity of *Zygnema* and *Zygnemopsis* (Zygnematophyceae, Streptophyta) from Svalbard (high Arctic). *European Journal of Phycology*, **53**: 492–508.

Portwich, A. & Garcia-Pichel, F. (2000). A novel prokaryotic UVB photoreceptor in the cyanobacterium *Chlorogloeopsis* PCC 6912. *Photochemistry and Photobiology*, **71**: 493–498.

Remias, D. & Lütz, C. (2007). Characterisation of esterified secondary carotenoids and of their isomers in green algae: a HPLC approach. *Algological Studies*, **124**: 85–94.

Remias, D., Holzinger, A., Aigner, S. & Lütz, C. (2012a). Ecophysiology and ultrastructure of *Ancylonema nordenskiöldii* (Zygnematales, Streptophyta), causing brown ice on glaciers in Svalbard (high Arctic). *Polar Biology*, **35**: 899–908.

Remias, D., Schwaiger, S., Aigner, S., Leya, T., Stuppner, H. & Lütz, C. (2012b). Characterization of an UV- and VIS-absorbing, purpurogallin-derived secondary pigment new to algae and highly abundant in *Mesotaenium berggrenii* (Zygnematophyceae, Chlorophyta), an extremophyte living on glaciers. *FEMS Microbiology Ecology*, **79**: 638–648.

Řezanka, T., Temina, M., Tolstikov, A.G. & Dembitsky, V.M. (2004). Natural microbial UV radiation filters – Mycosporine-like amino acids. *Folia Microbiologica*, **49**: 339–352.

18   A. BUSCH S. HESS

Rindi, F. & Guiry, M.D. (2004). Composition and spatial variability of terrestrial algal assemblages occurring at the bases of urban walls in Europe. *Phycologia*, 43: 225–235.

Rizzini, L., Favory, J.-J., Cloix, C., Faggionato, D., O'Hara, A., Kaiserli, E., Baumeister, R., Schäfer, E., Nagy, F., Jenkins, G.I. & Ulm, R. (2011). Perception of UV-B by the *Arabidopsis* UVR8 protein. *Science*, 332: 103–106.

Rosa, L.H., de Sousa, J.R.P., de Menezes, G.C.A., da Costa Coelho, L., Carvalho-Silva, M., Convey, P. & Câmara, P. E.A.S. (2020). Opportunistic fungi found in fairy rings are present on different moss species in the Antarctic Peninsula. *Polar Biology*, 43: 587–596.

Rozema, J., Björn, L.O., Bornman, J.F., Gaberščik, A., Häder, D.-P., Trošt, T., Germ, M., Klisch, M., Gröniger, A., Sinha, R.P., Lebert, M., He, Y.-Y., Buffoni-Hall, R., de Bakker, N.V.J., van de Staaij J. & Meijkamp, B.B. (2002). The role of UV-B radiation in aquatic and terrestrial ecosystems – an experimental and functional analysis of the evolution of UV-absorbing compounds. *Journal of Photochemistry and Photobiology B: Biology*, 66: 2–12.

Schagerl, M. & Zwirn, M. (2015). A brief introduction to the morphological species concept of *Spirogyra* and emanating problems. *Algological Studies*, 148: 67–86.

Schindelin, J., Arganda-Carreras, I., Frise, E., Kaynig, V., Longair, M., Pietzsch, T., Preibisch, S., Rueden, C., Saalfeld, S., Schmid, B., Tinevez, J.-Y., White, D.J., Hartenstein, V., Eliceiri, K., Tomancak, P. & Cardona, A. (2012). Fiji: an open-source platform for biological-image analysis. *Nature Methods*, 9: 676–682.

Singh, S.P., Häder, D.-P. & Sinha, R.P. (2010). Cyanobacteria and ultraviolet radiation (UVR) stress: mitigation strategies. *Ageing Research Reviews*, 9: 79–90.

Sinha, R.P., Klisch, M., Helbling, E.W. & Häder, D.-P. (2001). Induction of mycosporine-like amino acids (MAAs) in cyanobacteria by solar ultraviolet-B radiation. *Journal of Photochemistry and Photobiology B: Biology*, 60: 129–135.

Sinha, R.P., Ambasht, N.K., Sinha, J.P. & Häder, D.-P. (2003a). Wavelength-dependent induction of a mycosporine-like amino acid in a rice-field cyanobacterium, *Nostoc commune*: role of inhibitors and salt stress. *Photochemical & Photobiological Sciences*, 2: 171–176.

Sinha, R.P., Ambasht, N.K., Sinha, J.P., Klisch, M. & Häder, D.-P. (2003b). UV-B-induced synthesis of mycosporine-like amino acids in three strains of *Nodularia* (cyanobacteria). *Journal of Photochemistry and Photobiology B: Biology*, 71: 51–58.

Stancheva, R., Sheath, R.G. & Hall, J.D. (2012). Systematics of the genus *Zygnema* (Zygnematophyceae, Charophyta) from Californian watersheds. *Journal of Phycology*, 48: 409–422.

Stancheva, R., Hall, J.D., McCourt, R.M. & Sheath, R.G. (2013). Identity and phylogenetic placement of *Spirogyra* species (Zygnematophyceae, Charophyta) from California streams and elsewhere. *Journal of Phycology*, 49: 588–607.

Stastny, J., Skaloud, P., Langenbach, D., Nemjova, K. & Neustupa, J. (2013). Polyphasic evaluation of *Xanthidium antilopaeum* and *Xanthidium cristatum*

(Zygnematophyceae, Streptophyta) species complex. *Journal of Phycology*, 49: 401–416.

Storme, J.-Y., Golubic, S., Wilmotte, A., Kleinteich, J., Velázquez, D. & Javaux, E.J. (2015). Raman characterization of the UV-protective pigment gloeocapsin and its role in the survival of cyanobacteria. *Astrobiology*, 15: 843–857.

Takano, T., Higuchi, S., Ikegaya, H., Matsuzaki, R., Kawachi, M., Takahashi, F. & Nozaki, H. (2019). Identification of 13 *Spirogyra* species (Zygnemataceae) by traits of sexual reproduction induced under laboratory culture conditions. *Scientific Reports*, 9: 1–11.

Tamura, M., Tanabe, M., Valkonen, J.P.T. & Akita, M. (2019). Sunagoke moss (*Racomitrium japonicum*) used for greening roofs is severely damaged by *Sclerotium delphinii* and protected by a putative *Bacillus amyloliquefaciens* isolate. *Frontiers in Microbiology*, 10, doi: 10.3389/fmicb.2019.00372.

Timme, R.E., Bachvaroff, T.R. & Delwiche, C.F. (2012). Broad phylogenomic sampling and the sister lineage of land plants. *PLoS ONE*, 7: e29696. doi: 10.1371/journal.pone.0029696.

Vincent, W.F. & Neale, P.J. (2000). Mechanisms of UV damage to aquatic organisms. In *The Effects of UV Radiation in the Marine Environment* (de Mora, S.J., Demers, S. & Vernet, M., editors), 149–176. Cambridge University Press, Cambridge.

de Vries, J., Curtis, B.A., Gould, S.B. & Archibald, J.M. (2018). Embryophyte stress signaling evolved in the algal progenitors of land plants. *Proceedings of the National Academy of Sciences USA*, 115: E3471–E3480.

Wickett, N.J., Mirarab, S., Nguyen, N., Warnow, T., Carpenter, E., Matasci, N., Ayyampalayam, S., Barker, M.S., Burleigh, J.G., Gitzendanner, M.A., Ruhfel, B.R., Wafula, E., Der, J.P., Graham, S.W., Mathews, S., Melkonian, M., Soltis, D.E., Soltis, P.S., Miles, N.W., Rothfels, C.J., Pokorny, L., Shaw, A.J., DeGironimo, L., Stevenson, D.W., Surek, B., Villarreal, J.C., Roure, B., Philippe, H., dePamphilis, C. W., Chen, T., Deyholos, M.K., Baucom, R.S., Kutchan, T.M., Augustin, M.M., Wang, J., Zhang, Y., Tian, Z., Yan, Z., Wu, X., Sun, X., Wong, G.K.-S. & Leebens-Mack, J. (2014). Phylotranscriptomic analysis of the origin and early diversification of land plants. *Proceedings of the National Academy of Sciences USA*, 111: E4859–E4868.

Wodniok, S., Brinkmann, H., Glöckner, G., Heidel, A.J., Philippe, H., Melkonian, M. & Becker, B. (2011). Origin of land plants: do conjugating green algae hold the key? *BMC Evolutionary Biology*, 11: 1–10.

Wynn-Williams, D.D. & Edwards, H.G. (2002). Environmental UV radiation: biological strategies for protection and avoidance. In *Astrobiology* (Horneck, G. & Baumstark-Khan, C., editors), 245–260. Springer, Heidelberg.

Xu, Y., Wang, S., Li, L., Sahu, S.K., Petersen, M., Liu, X., Melkonian, M., Zhang, G. & Liu, H. (2019). Molecular evidence for origin, diversification and ancient gene duplication of plant subtilases (SBTs). *Scientific Reports*, 9: 1–10.

Supplementary information

for

'Sunscreen mucilage: a photoprotective adaptation found in terrestrial green algae (Zygnematophyceae)'

Busch & Hess, 2021

Supplementary Table S1: Studied *Serritaenia* strains and associated data (collection sites and accession numbers of the Central Collection of Algal Cultures (CCAC) and *rbc*L gene sequences).

Strain	Taxonomy	Collection site / coordinates	Sample information	CCAC	*rbc*L
DEL.1	*Serritaenia* sp.	Dellbrück, Cologne (DE) 50.974429, 7.091823	Blackish bryophytes on tree bark (forest)	CCAC 9318	MW159370
KH.1	*Serritaenia* sp.	Frei-Laubersheim, Bad Kreuznach (DE) 49.806280, 7.882115	Blackish bryophytes on dead wood (forest)	CCAC 9319	MW159371
OBE.1	*Serritaenia* sp.	Monsau, Wiehl (DE) 50.958607, 7.581137	Blackish forest soil and bryophytes	CCAC 9320	MW159369
CCAC 0155	*Serritaenia* sp.	Strohner Maarchen, Strohn (DE) 50.122289, 6.928597	Slurry with various desmids	CCAC 0155	FM992358
OBE.sm2	*Serritaenia* sp.	Wohlsberg, Wiehl (DE) 50.961667, 7.578056	Blackish bryophytes on dead wood (forest)	CCAC 9321	MW159373
OBE.sm1	*Serritaenia* sp.	Wohlsberg, Wiehl (DE) 50.961667, 7.578056	Blackish bryophytes on dead wood (forest)	CCAC 9322	MW159372
CCAC 3781	*Serritaenia* sp.	Naafbachtal (DE) n/a	Epiphytic bryophytes on tree bark	CCAC 3781	MW159374
GSM.5.thin	**S. testaceovaginata**	Clingmans Dome Rd, Great Smoky Mountains, NC (USA) 35.568104, -83.481939	Red-brown biofilm on wet rock surface	CCAC 9324	MW159377
GSM.5.thick	*Serritaenia* sp.	Clingmans Dome Rd, Great Smoky Mountains, NC (USA) 35.568104, -83.481939	Red-brown biofilm on wet rock surface	n/a	MW159376
GSM.4.4	*Serritaenia* sp.	Forney Ridge Trail, Great Smoky Mountains, NC (USA) 35.555917, -83.497417	Bryophytes with brown mucilage	CCAC 9323	MW159375

Supplementary Fig. S1: Unrooted Neighbour-Joining phylogeny of 43 zygnematophycean *rbc*L gene sequences displaying the polyphyly of *Mesotaenium* (red) and the position of the new genus *Serritaenia* (green). Support values are shown on the respective branches (NJ/ML). Branches with maximum support (100/100) are bold. The scale bar represents 0.02 nucleotide substitution per site.
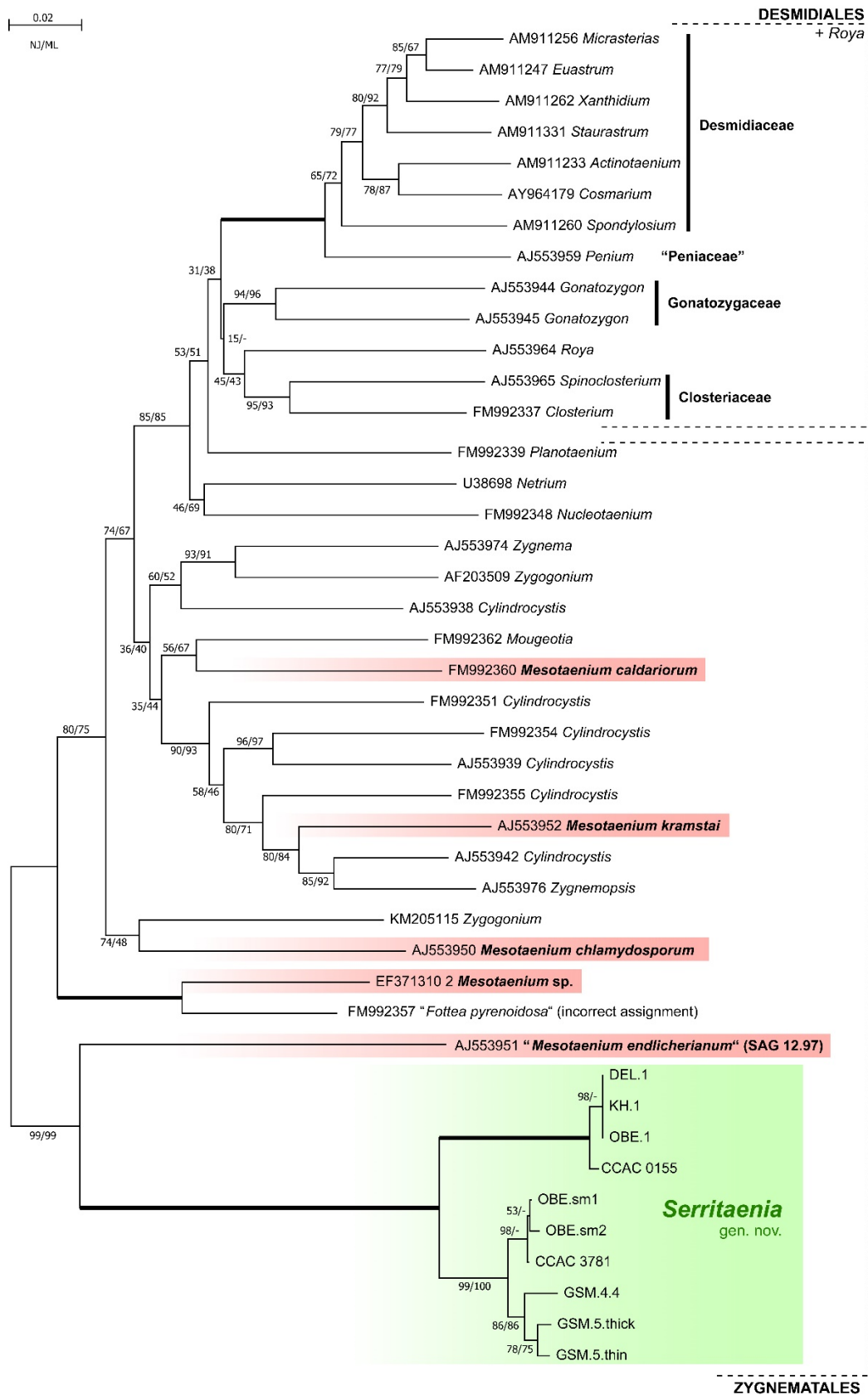
Supplementary Figs S2 and S3: Illustrations published with the original descriptions of *Mesotaenium braunii* (S2: *A*, *1-8*), *M. braunii* var. *minus* (S2: *A*, *9-11*), and *M. testaceovaginatum* (S3). The illustration of *M. testaceovaginatum* (S3) is designated as lectotype for this species.

S2
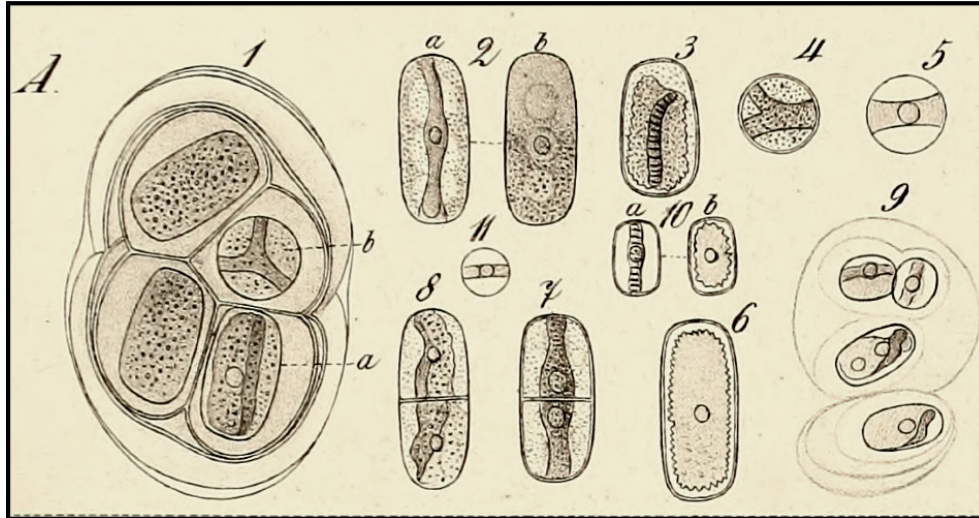
S3
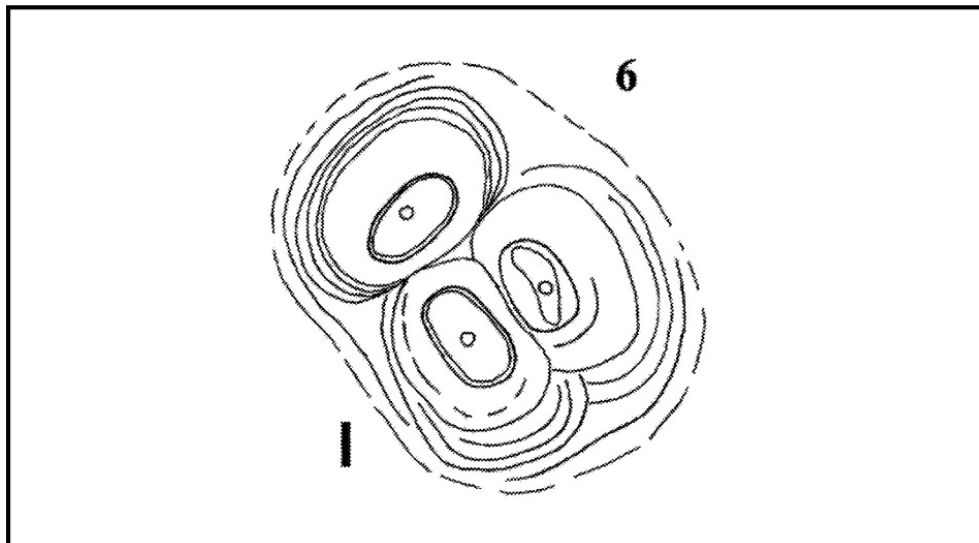
Supplementary Figs S4-S6: Microspectrophotometric measurements taken from the mucilage of *Serritaenia testaceovaginata* (strain GSM.5.thin) over a spectral range of 200–1600 nm. S4 and S5 display absorbance spectra of mucilage with varying degree of pigmentation from two independent wet mounts with 21 and 33 measurements, respectively. S6 displays 15 absorbance measurements of non-pigmented mucilage for comparison.

Supplementary Text:

Rationale for the new genus *Serritaenia* and taxonomy of its members

The studied algae resemble certain species of the ill-defined and polyphyletic genus *Mesotaenium* NÄGELI, which – according to AlgaeBase – contains 29 recognised species and 39 infraspecific taxa (Guiry & Guiry, 2020). As revealed by former molecular inferences (Gontcharov *et al.*, 2004; Gontcharov & Melkonian, 2010) and shown in our *rbc*L phylogeny as well, some of these *Mesotaenium* species fall in several (at least four) not directly related evolutionary lineages of the Zygnematophyceae. Al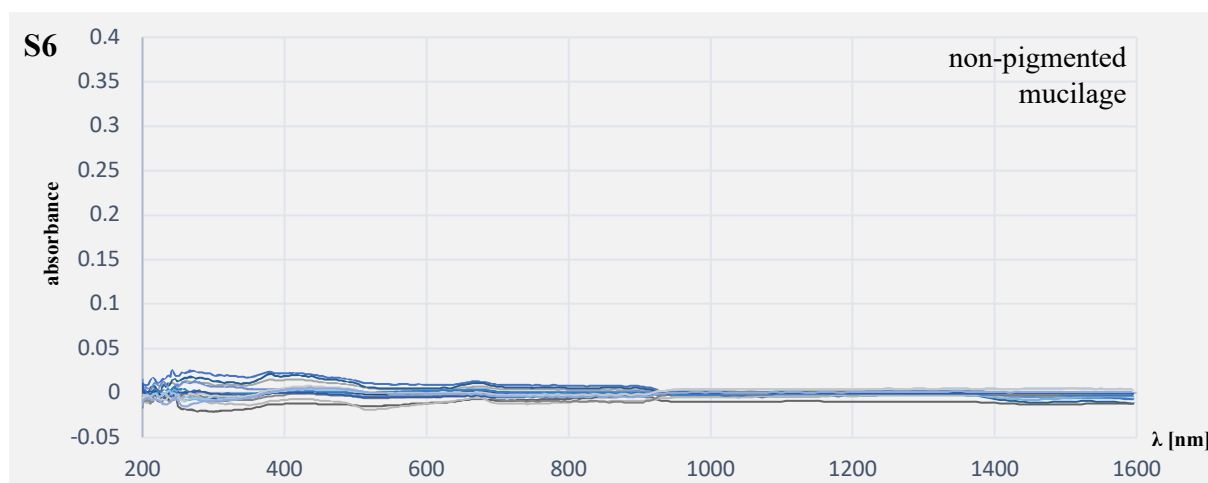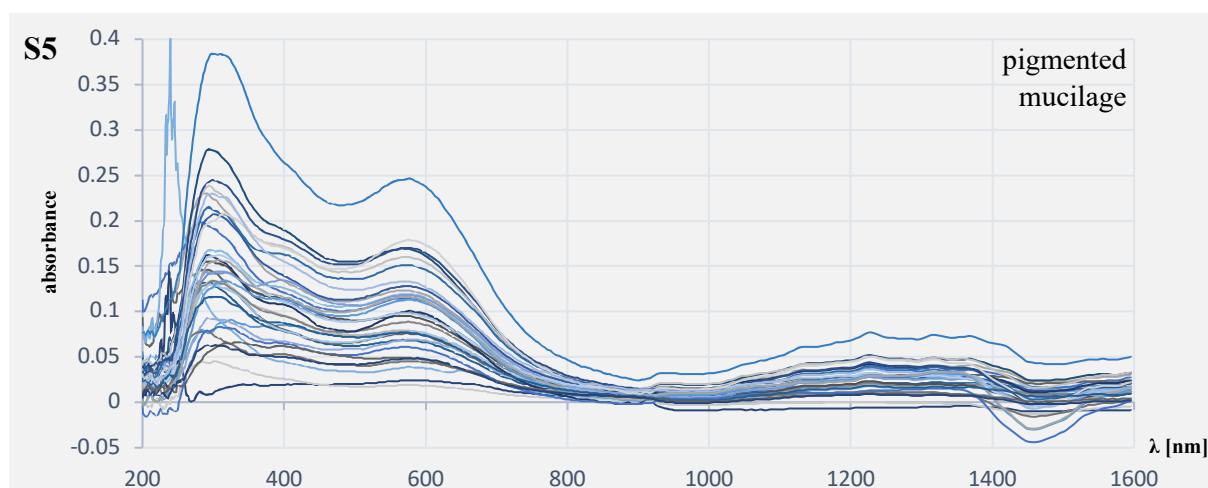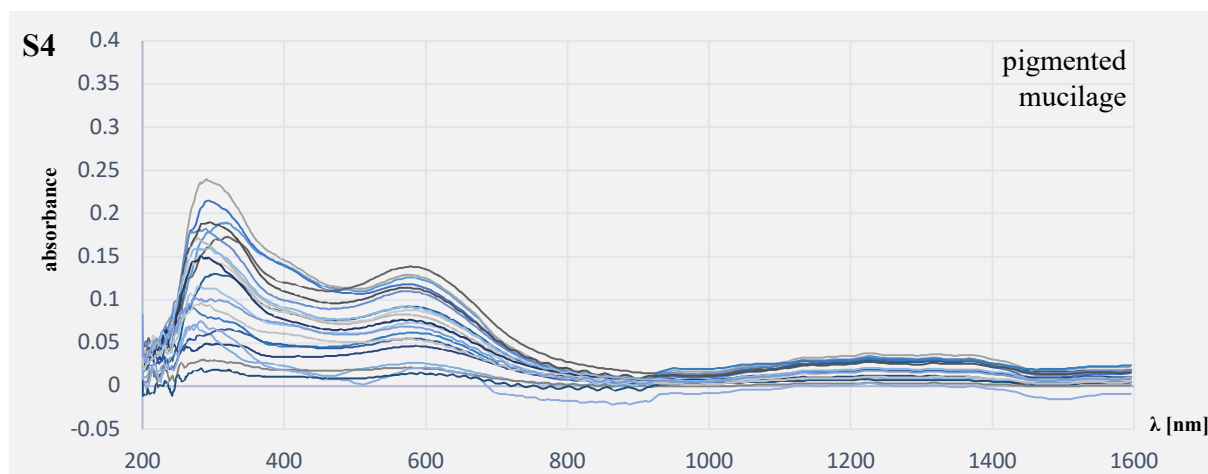though the members of these lineages exhibit clear differences in cellular details (Gontcharov, 2008), all of them are – until now – referred to as *Mesotaenium*, and a taxonomic revision of these algae is pending.

The following species resemble the algae studied in this work (with homotypic synonyms; ≡):

> ***M. braunii*** DE BARY

> ***M. braunii*** var. ***minus*** DE BARY
> > ≡ *M. macrococcum* var. *minus* (DE BARY) COMPÈRE
> > ≡ *Palmogloea macrococca* var. *minor* (DE BARY) RABENHORST

> ***M. macrococcum*** (KÜTZ.) J.ROY & BISSET
> > ≡ *Palmogloea macrococca* KÜTZ.

> ***M. testaceovaginatum*** FUČÍKOVÁ, J.D.HALL, J.R.JOHANS. & R.L.LOWE

Common defining characters of these species and our strains are cylindrical cells, a length-to-width ratio of maximum 2–3 (depending on the species), and a plate-like chloroplast in the centre of the cell (not parietal) with serrate or crenate edges. Furthermore, the cells are typically surrounded by mucilage (often in form of layered capsules) and thrive in terrestrial habitats (de Bary, 1858; West & West, 1904; Fučíková *et al.*, 2008). With that, these algae differ fundamentally from *M. endlicherianum* NÄGELI (the type species of the genus *Mesotaenium*), whose cells are more slender (length-to-width ratio 3–4), contain a chloroplast with smooth margins, and seem to lack conspicuous extracellular mucilage (Nägeli, 1849). In addition, *M. endlicherianum* is not reported to show the angled cell arrangement observed in our strains shortly after cell division, and, instead, divides in a chain-like manner.

Unfortunately, at present there is no algal strain available that closely matches the description of *M. endlicherianum*. This also applies to strain SAG 12.97 (the closest known relative of the algae studied here), which was probably misidentified and repeatedly referred to as '*M. endlicherianum*' (Gontcharov *et al.*, 2003, 2004; Gontcharov, 2008; Matasci *et al.*, 2014; Cheng *et al.*, 2019). Hence, we lack important phylogenetic information about the type species of *Mesotaenium* and cannot place this generic name with certainty. However, the marked phenotypic differences between *M. endlicherianum* NÄGELI and the algae studied here justify a separate genus name for the latter. In the context of potential genus names, it also has to be noted that *Mesotaenium macrococcum* was first described as *Palmogloea macrococca* KÜTZ. (Kützing, 1845). The genus *Palmogloea*, however, was established earlier (Kützing, 1843) with *P. protuberans* (SM.) KÜTZ. as the only species, which hence represents the type species of

the genus. This type species is considered a chlorophycean green alga (Fott & Nováková, 1971), so that the genus *Palmogloea* is not appropriate for zygnematophyceaen algae. Consequently, the studied algae require a new genus name and we here introduce *Serritaenia* gen. nov. (see main text for formal description).

The morphologically 'simple' *Mesotaenium* species have mostly been described on the basis of the cell shape and size of vegetative material. The lack of meaningful original descriptions in several cases and the resulting uncertainties led to a convoluted taxonomic history with a high number of infraspecific taxa and synonyms (Guiry & Guiry, 2020). At present there are a few names used for Zygnematophyceae that are here included in the genus *Serritaenia*. As detailed below, the available information about these taxa varies, and there are still some questions to be solved. Based on a careful comparison of our *Serritaenia* strains with published taxa (including original material), we follow a conservative approach and form only two new combinations (Art. 6.10. and 41 in Turland *et al.*, 2018) in this study. As the holotype of one species (*M. testaceovaginatum*) was evidently lost, we designate a cited illustration published along with the original description as lectotype (Art. 7.3. and 9.3. in Turland *et al.*, 2018) and provide a supporting epitype connected to genetic information (Art. 9.9. in Turland *et al.*, 2018). Some details about relevant species follow.

Mesotaenium macrococcum (KÜTZ.) J.ROY & BISSET is a widely accepted name for Zygnemato- phyceae that closely resemble *Serritaenia* species (Lenzenweger, 2003; Coesel & Meesters, 2007; Brook & Williamson, 2010; Ettl & Gärtner, 2014). As already mentioned above, it is a nomenclatural synonym of *Palmogloea macrococca* KÜTZ., a rather ill-defined species that caused much debate about its identity (Archer 1864, 1866; Hicks 1864). As far as we know, the question whether *P. macrococca* is a zygnematophycean green alga is still not solved, but the name *M. macrococcum* found its way in contemporary taxonomic literature. The current circumscription of this taxon in monographs and identification guides is quite broad and probably based on a variety of biological species as indicated by the stated cell sizes (e.g. cell width of 5–19 µm in Ettl & Gärtner, 2014). We here show that genetically separate *Serritaenia* strains have a relatively narrow and stable cell width range, emphasising the need to reflect the observed phenotypic diversity on the taxonomic level. Unfortunately, the description of *P. macrococca* is fairly meagre (Kützing, 1845), and the associated drawing difficult to interpret (Kützing, 1847). To assess whether *P. macrococca* is a *Serritaenia*-like alga and can be considered for a new combination, we studied the original material of that species (deposited at the Naturalis Biodiversity Center in Leiden, NL). Based on our microscopic examination alone, we cannot solve this question with certainty (genetic work in progress), so that we refrain from establishing a new combination of *P. macrococca* at this point. However, the cells of *P. macrococca* turned out to be markedly smaller than expected (about 10 µm wide) and, thus, are not identical with *M. braunii* (cells 15–19 µm wide). Consequently, the synonymy of these taxa seems to be unjustified and the name *M. braunii* becomes relevant for the large-celled representatives of the *Serritaenia*-clade.

Mesotaenium braunii DE BARY (illustrated in Supplementary Fig. S2) was established in a very detailed description and there is little doubt that this species belongs to the *Serritaenia*-clade. De Bary clearly depicted the chloroplast morphology, the mucilage capsules, and even mentioned the presence of an extracellular (violet) pigment (de Bary, 1858). The stated cell dimensions of *M. braunii* (15–19 µm) closely match those of our *Serritaenia* strains DEL.1, KH.1 and OBE.1. Here, we introduce a new combination, *Serritaenia braunii* comb. nov., but for now refrain from selecting a reference strain, as there might be the option to study original material of *M. braunii* in future (currently inaccessible to us).

***Mesotaenium braunii* var. *minus* DE BARY** (illustrated in Supplementary Fig. S2) was described as a smaller variety that reaches only half the size of *M. braunii* (= cell width 8–9.5 µm). Thus, it conforms with the small-celled *Serritaenia* strains OBE.sm1, OBE.sm2, CCAC3781 and GSM4.4, which show marked genetic distances to the large-celled *Serritaenia* strains. The small-celled strains are, however, not monophyletic, complicating the application of the name *M. braunii* var. *minus*. In addition, we found that the type material of *Palmogloea macrococca* resembles *M. braunii* var. *minus* in size, questioning the justification of the latter name due to priority (in case these organisms are indeed identical; pending genetic analyses). Because of this uncertainty, we refrain from creating any new combination at this point. *M. braunii* var. *minus* is also known under its homotypic synonyms *M. macrococcum* var. *minus* (DE BARY) COMPÈRE and *Palmogloea macrococca* var. *minor* (DE BARY) RABENHORST.

***Mesotaenium testaceovaginatum* FUČIKOVÁ, J.D.HALL, J.R.JOHANS. & R.L.LOWE** (illustrated in Supplementary Fig. S3) was most recently described from the Great Smoky Mountains National Park (North Carolina, USA) on a purely morphological basis (Fučíková *et al.*, 2008). In search of this species at its type locality, we found two morphotypes* (GSM.5.thin and GSM.5.thick), which differed in morphology, *rbc*L gene sequence, and their ability to grow under laboratory conditions. Both morphotypes matched the original description of *M. testaceovaginatum* to some extent: The cell dimensions provided in the written description (cell width 12–14 µm) and the drawing (Fig. 6 on p. 55 in Fučíková *et al.*, 2008) correspond to GSM.5.thin, while the cells depicted in the micrographs (Figs 26–28 on p. 55 in Fučíková *et al.*, 2008) rather resemble GSM.5.thick. As confirmed by one of the authors, a mix-up of the two co-occurring morphotypes in the description is, indeed, possible (pers. comm. K. Fučiková). Unfortunately, the holotype of *M. testaceovaginatum*, the aldehyde-fixed natural sample *GSM 10/23/04 J5A* (John Carroll University, Ohio), was lost. Furthermore, the holotype is very likely to contain both morphotypes, along with other algal taxa, so that the designation of a lectotype from the cited illustrations (as part of the original material) seems reasonable (Art. 9.3. in Turland *et al.*, 2018). In agreement with the cell dimensions given in the written description, we designate the drawing (Fig. 6 on p. 55 in Fučíková *et al.*, 2008; reproduced in Supplementary Fig. S3) as lectotype (see also Art. 9.14. in Turland *et al.*, 2018), and fixed cells of strain GSM.5.thin as supporting epitype. In addition, we establish a new combination, *Serritaenia testaceovaginata* comb. nov., and emend the written description of that species (see main text). As *S. testaceovaginata* currently has the most detailed (and unambiguous) description, we designate it as the type species of the genus *Serritaenia*.

Furthermore, there are some infraspecific taxa to be discussed. *M. macrococcum* var. *micrococcum* (KÜTZ.) WEST & G.S. WEST, synonymous with *M. micrococcum* (KÜTZ.) KIRCHN., is not considered for inclusion in the genus *Serritaenia*. Although these names were sometimes regarded as synonyms of *M. braunii* var. *minus* (Krieger, 1937), they are clearly based on *Palmogloea micrococca* KÜTZ. (see West & West 1904). The latter species, however, differs drastically from the algae studied here and rather represents *Coccomyxa* (Trebouxiophyceae, Chlorophyta) or relatives (Kützing, 1847, 1849). The varieties *M. macrococcum* var. *lagerheimii* WILLI KRIEG. and *M. macrococcum* var. *truncatum* (WEST & G.S. WEST) WILLI KRIEG. both display major morphological differences to *Serritaenia* and are not considered for inclusion in this genus as well. Finally, there is evidence of a species named *Palmogloea macrococca* var. *nigrescens* C. CRAMER in the *Index Nominum Algarum* database (Silva Center for Phycological Documentation, The University Herbarium at UC Berkeley, USA), but we were unable to locate its original description so far. Given the meaning of the name (Latin: *nigrescens* = blackening, darkening), it might be possible that Cramer's variety is a *Serritaenia*-clade member (name pointing to blackish extracellular pigmentation?). Future in-depth studies may shed some light on these orphan taxa.

---

* The term ‚morphotype' is here used in the broad sense and does not denote a taxonomic level.

References

Archer, W. (1864). Original Communications: An endeavour to identify *Palmogloea macrococca* (Kütz.) with description of the plant believed to be meant, and of a new species, both, however, referable rather to the genus *Mesotaenium* (Näg.). *Journal of Cell Science,* **s2-4:** 109–32.

Archer, W. (1866). Original Communication: Observations on the genera *Cylindrocystis* (Meneghini), *Mesotaenium* (Näg.), and *Spirotaenia* (Bréb.) (= *Palmogloea*, Kütz., pro maxima parte), mainly induced by a paper by Dr. J. Braxton Hicks, F.R.S., F.L.S., on the lower forms of algae. *Journal of Cell Science*, **s2-6:** 203–24.

de Bary, A. (1858). Untersuchungen über die Familie der Conjugaten (Zygnemeen und Desmidieen): Ein Beitrag zur physiologischen und beschreibenden Botanik. Förstnersche Buchhandlung, Leipzig.

Brook, A.J. & Williamson, D.B. (2010). A monograph on some British desmids. The Ray Society, London.

Cheng, S., Xian, W., Fu, Y., Marin, B., Keller, J., Wu, T., Sun, W., Li, X., Xu, Y., Zhang, Y., Wittek, S., Reder, T., Günther, G., Gontcharov, A., Wang, S., Li, L., Liu, X., Wang, J., Yang, H., Xu, X., Delaux, P.-M., Melkonian, B., Wong, G.K.-S. & Melkonian, M. (2019). Genomes of subaerial Zygnematophyceae provide insights into land plant evolution. *Cell*, **179:** 1057–1067.

Coesel, P.F.M. & Meesters, K.J. (2007). Desmids of the lowlands: Mesotaeniaceae and Desmidiaceae of the European lowlands. KNNV Publishing, Zeist.

Ettl, H. & Gärtner, G. (2014). Syllabus der Boden-, Luft- und Flechtenalgen, 2nd edition. Springer, Berlin, Heidelberg.

Fott, B. & Nováková, M. (1971). Taxonomy of the palmelloid genera *Gloeocystis* Nägeli and *Palmogloea* Kützing (Chlorophyceae). *Archiv für Protistenkunde*, **113:** 322–333.

Fučíková, K., Hall, J.D., Johansen, J.R. & Lowe, R. (2008)*.* Desmid flora of the Great Smoky Mountains National Park, USA. *Bibliotheca Phycologica*, **113:** 1–59.

Gontcharov, A.A. (2008). Phylogeny and classification of Zygnematophyceae (Streptophyta): current state of affairs. *Fottea*, **8:** 87–104.

Gontcharov, A.A., Marin, B. & Melkonian, M. (2003). Molecular phylogeny of conjugating green algae (Zygnemophyceae, Streptophyta) inferred from SSU rDNA sequence comparisons. *Journal of Molecular Evolution*, **56:** 89–104.

Gontcharov, A.A., Marin, B. & Melkonian, M. (2004). Are combined analyses better than single gene phylogenies? A case study using SSU rDNA and rbcL sequence comparisons in the Zygnematophyceae (Streptophyta). *Molecular biology and evolution*, **21:** 612–624.

Gontcharov, A.A. & Melkonian, M. (2010). Molecular phylogeny and revision of the genus *Netrium* (Zygnematophyceae, Streptophyta): *Nucleotaenium* gen. nov. *Journal of Phycology*, **46:** 346–362.

Guiry, M.D. & Guiry, G.M. AlgaeBase. World-wide electronic publication, National University of Ireland, Galway. https://www.algaebase.org/. (28 August 2020, date last accessed).

Hicks, J.B. (1864). Original Communications: Remarks on Mr. Archer's paper on algae. *Journal of Cell Science,* **s2-4:** 253–258.

Krieger, W. (1937). Die Desmidiaceen Europas mit Berücksichtigung der außereuropäischen Arten, 2nd edition. Akademische Verlagsgesellschaft, Leipzig.

Kützing, F.T. (1843). Phycologia generalis oder Anatomie, Physiologie und Systemkunde der Tange. Mit 80 farbig gedruckten Tafeln, gezeichnet und gravirt vom Verfasser. pp. [part 1]: [i]-xxxii, [1]-142, [part 2:] 143-458, 1, err.], pls 1-80. FA Brockhaus, Leipzig.

Kützing, F.T. (1845). Phycologia germanica, d. i. Deutschlands Algen in bündigen Beschreibungen. Nebst einer Anleitung zum Untersuchen und Bestimmen dieser Gewächse für Anfänger. pp. [i]-x, [1]-340 ['240']. Zu finden bei Wilh. Köhne, Nordhausen.

Kützing, F.T. (1847). Tabulae phycologicae; oder, Abbildungen der Tange. Vol. I, fasc. 3-5 pp. 17-36, pls 21-50. Gedruckt auf Kosten des Verfassers (in Commission bei W. Köhne), Nordhausen.

Kützing, F.T. (1849). Species algarum. FA Brockhaus, Leipzig.

Lenzenweger, R. (2003). Desmidiaceenflora von Österreich, Teil 4. In *Bibliotheca Phycologica* (Cramer, J., editor), 1-87. Schweizerbart Science Publishers, Stuttgart.

Matasci, N., Hung, L.-H., Yan, Z., Carpenter, E.J., Wickett, N.J., Mirarab, S., Nguyen, N., Warnow, T., Ayyampalayam, S., Barker, M., Burleigh, J.G., Gitzendanner, M.A., Wafula E., Der J.P., dePamphilis, C.W., Roure, B., Philippe, H., Ruhfel, B.R., Miles, N.W., Graham, S.W., Mathews, S., Surek, B., Melkonian, M., Soltis, D.E., Soltis, P.S., Rothfels, C., Pokorny, L., Shaw, J.A., DeGironimo, L., Stevenson, D.W., Villarreal, J.C., Chen, T., Kutchan, T.M., Rolf, M., Baucom, R.S., Deyholos, M.K., Samudrala, R., Tian, Z., Wu, X., Sun, X., Zhang, Y., Wang, J., Leebens-Mack, J. & Wong, G.K.-S. (2014). Data access for the 1,000 Plants (1KP) project. *Gigascience*, **3:** 2047-217X-3-17.

Nägeli, C. (1849). Gattungen einzelliger Algen: physiologisch und systematisch bearbeitet. Friedrich Schulthess, Zürich.

Turland, N.J., Wiersema, J.H., Barrie, F.R., Greuter, W., Hawksworth, D.L., Herendeen, P.S., Knapp, S., Kusber, W.H., Li, D.Z., Marhold, K. & May, T.W. (2018). International Code of Nomenclature for algae, fungi, and plants (Shenzhen Code) adopted by the Nineteenth International Botanical Congress Shenzhen, China, July 2017. Koeltz Botanical Books, Oberreifenberg.

West, W. & West, G.S. (1904). A monograph of the British Desmidiaceae. The Ray Society, London.

Comparative transcriptomics elucidates the cellular responses of an aeroterrestrial zygnematophyte to UV radiation

Chapter II

RESEARCH PAPER

Comparative transcriptomics elucidates the cellular responses of an aeroterrestrial zygnematophyte to UV radiation

Anna Busch[1,*] [ID], Jennifer V. Gerbracht[1], Kevin Davies[2], [ID], Ute Hoecker[3], [ID], and Sebastian Hess[1,†]

[1] Department of Biology, University of Cologne, Zülpicher Str. 47b, D-50674 Cologne, Germany
[2] The New Zealand Institute for Plant and Food Research Limited, Private Bag 11600, Palmerston North 4442, New Zealand
[3] Institute for Plant Sciences and Cluster of Excellence on Plant Sciences (CEPLAS), Biocenter, University of Cologne, Zülpicher Strasse 47b, D-50674, Cologne, Germany
[†] Present address: Department of Biology, Technical University of Darmstadt, Schnittspahnstr. 3, D-64287 Darmstadt, Germany.

* Correspondence: anna.busch@uni-koeln.de

Abstract

The zygnematophytes are the closest relatives of land plants and comprise several lineages that adapted to a life on land. Species of the genus *Serritaenia* form colorful, mucilaginous capsules, which surround the cells and block harmful solar radiation, one of the major terrestrial stressors. In eukaryotic algae, this 'sunscreen mucilage' represents a unique photoprotective strategy, whose induction and chemical background are unknown. We generated a *de novo* transcriptome of *Serritaenia testaceovaginata* and studied its gene regulation under moderate UV radiation (UVR) that triggers sunscreen mucilage under experimental conditions. UVR induced the repair of DNA and the photosynthetic apparatus as well as the synthesis of aromatic specialized metabolites. Specifically, we observed pronounced expressional changes in the production of aromatic amino acids, phenylpropanoid biosynthesis genes, potential cross-membrane transporters of phenolics, and extracellular, oxidative enzymes. Interestingly, the most upregulated enzyme was a secreted class III peroxidase, whose embryophyte homologs are involved in apoplastic lignin formation. Overall, our findings reveal a conserved, plant-like UVR perception system (UVR8 and downstream factors) in zygnematophyte algae and point to a polyphenolic origin of the sunscreen pigment of *Serritaenia*, whose synthesis might be extracellular and oxidative, resembling that of plant lignins.

Keywords: Lignin, peroxidase, phenolics, phenylpropanoid, streptophyte algae, UV radiation, UVR8, *Zygnematophyceae*.

Introduction

The conjugating green algae (*Zygnematophyceae*) represent an algal class of ~4000 described species, which inhabit diverse freshwater-fed systems (Hall and McCourt, 2015). They colonize standing waters, from eutrophic lakes to dystrophic moorlands, but also thrive on terrestrial surfaces (e.g. rocks, bark, and deadwood) and even glaciers. Hence, these algae display a wide ecological variation, and, at the same time, relatively simple growth forms (unicells or filaments). It appears that their ecological variation is likely to be underpinned by physiological specialties that evolved in distinct zygnematophyte taxa.

Furthermore, the zygnematophytes are the key to understanding the evolution of plant metabolism and the process of terrestrialization, as these algae represent the sister clade of the land plants (Wodniok *et al.*, 2011; Timme *et al.*, 2012; Ruhfel *et al.*, 2014; Wickett *et al.*, 2014; Leebens-Mack *et al.*, 2019). Indeed, the zygnematophytes are gaining increasing attention by various biological disciplines. Well-studied aspects include cell wall synthesis and composition (Domozych, 2014; Domozych *et al.*, 2014), physiological reactions to abiotic stressors and metabolic networks (Pichrtová *et al.*, 2014; de Vries *et al.*, 2020; de Vries and Ischebeck, 2020; Permann *et al.*, 2022), genome evolution (Cheng *et al.*, 2019), and phylogenetics (Gontcharov *et al.*, 2004; Gontcharov, 2008; Hess *et al.*, 2022). Overall, it is thought that algal (pre-)adaptations concerning various cellular and metabolic traits might have paved the way for the evolution of the land plants (de Vries and Archibald, 2018; Jiao *et al.*, 2020). However, so far, relatively few zygnematophyte species (e.g. from the genera *Mesotaenium*, *Mougeotia*, *Spirogloea*, *Penium*, and *Zygnema*) have been subjected to in-depth genomic or transcriptomic analyses (Cheng *et al.*, 2019; Jiao *et al.*, 2020; Fürst-Jansen *et al.*, 2021; Dadras *et al.*, 2023a; Feng *et al.*, 2023, Preprint). These revealed taxon-specific differences (e.g. the triploid genome of *Spirogloea*) and showed that our picture of the zygnematophyte specialized metabolism, perception of environmental factors, and signaling is still fragmentary. This is not surprising given the enormous diversity of zygnematophytes and their lifestyles. Hence, we need data of various species to tell apart common and species-specific traits, and to gain insights into how certain zygnematophyte lineages adapted to their specific environments.

Aeroterrestrial zygnematophytes are of particular interest as they cope with abiotic stressors that might have been crucial during the evolution of land plants, namely limited water supply, frequent desiccation, high temperature amplitudes, and intense sunlight. Interestingly, several distinct zygnematophyte lineages exhibit a terrestrial lifestyle or thrive in otherwise extreme habitats such as glaciers and alpine lakes (Remias *et al.*, 2012a; Aigner *et al.*, 2013; Garduño-Solórzano *et al.*, 2021; Busch and Hess, 2022). Under these conditions, high light exposure is a serious stressor as UV radiation (UVR) damages

nucleic acids and proteins, and thus can disturb vital metabolic functions (Karentz *et al.*, 1991; Lao and Glazer, 1996; Buma *et al.*, 2003). It appears that some zygnematophyte lineages evolved photoprotective strategies that reduce cellular damage under high light conditions. For example, representatives of the distantly related genera *Ancylonema*, *Temnogametum*, and *Zygogonium* produce colorful intracellular compounds that are thought to be sunscreens (Newsome and van Breemen, 2012; Remias *et al.*, 2012b; Aigner *et al.*, 2013; Garduño-Solórzano *et al.*, 2021). It has been established that these compounds, identified as purpurogallin derivates or gallic acid polymers, have a phenolic origin and effectively absorb light and UVR. However, the biosynthesis of these pigments is still unknown, as zygnematophytes from extreme habitats are difficult to cultivate (Remias and Procházková, 2023) and no associated genomic and metabolomic data are available (but see Bowles *et al.*, 2023, Preprint).

A very different photoprotective strategy can be found in the genus *Serritaenia*, whose members inhabit forests, moorlands, and heathlands in temperate regions of Europe and North America (Busch and Hess, 2021). These unicellular zygnematophytes form gelatinous colonies that stick to plant and rock surfaces, and produce a colorful extracellular pigment (Fig. 1). The pigment is often secreted in a directional manner and, as shown by microspectrophotometry, effectively blocks UVR. So far, *Serritaenia* is the only known zygnematophyte lineage able to produce this extracellular 'sunscreen mucilage', and hence represents a unique organismal system. The closest analogy can be found in the photoprotective sheath pigments (gloeocapsin and scytonemin) of cyanobacteria (Proteau *et al.*, 1993; Storme *et al.*, 2015), which, however, have different properties and are unlikely to occur in eukaryotic algae. They can be readily extracted with methanol/ethyl acetate mixtures or acetone, while the sunscreen pigment of *Serritaenia* appeared to be resistant to various solvents and harsh acidic hydrolysis (Busch and Hess, 2021), and was intractable to standard chemical analyses. However, *Serritaenia* species can be cultivated in the laboratory and triggered by artificial UVR to produce their extracellular pigmentation. Thus, these algae are excellent laboratory models to study the reaction of zygnematophytes to
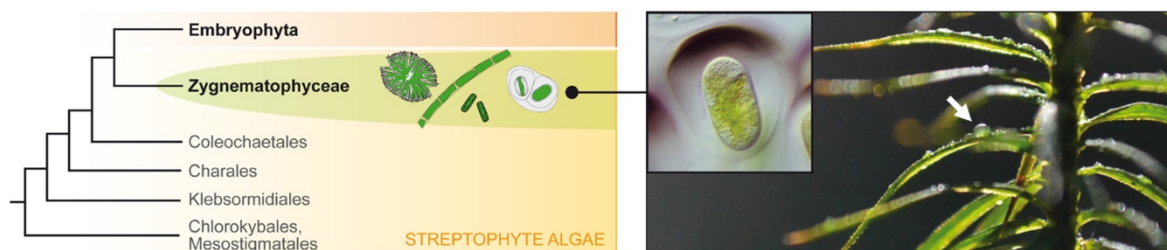
Fig. 1. Phylogenetic affinity and aeroterrestrial lifestyle of *Serritaenia* species. *Serritaenia* belongs to the *Zygnematophyceae*, which have a key position in the streptophyte phylogeny. Several *Serritaenia* species colonize bryophytes (arrow) and form pigmented 'sunscreen mucilage' (inset). Topology of the phylogenetic tree according to Wickett *et al.* (2014).

UVR and to gain insights into the formation of the sunscreen mucilage by transcriptomic methods.

Here, we generated a *de novo* transcriptome of *Serritaenia testaceovaginata* and explored the transcriptional reactions of this species to moderate UVR exposure. Besides general cellular processes such as DNA repair, photosynthesis, and reactive oxygen species (ROS) scavenging, we examined the photoreceptor systems and the specialized metabolism of aromatic compounds. A special focus is set on highly regulated oxidative enzymes known from lignin formation in higher plants, whose functions in zygnematophytes are still unknown.

Materials and methods

Experimental set-up

Algae were pre-grown in tissue culture flasks in liquid culture medium KW (Supplementary Table S1) at 30 µmol m^{-2} s^{-1} photosynthetically active radiation (PAR) (LinearZ SunLike LEDs, 5700 K, Lumitronix, Hechingen) with a 14/10 h light/dark cycle for 4 weeks. Before the start of the light experiment, the cells were transferred to Petri dishes with fresh medium and acclimatized to higher PAR conditions (120 µmol m^{-2} s^{-1}, 14/10 h) for 10 d. During the experiment, the algae were exposed to the above-mentioned LEDs and the UVB Broadband TL fluorescent tube lamp (20 W, Philips, Hamburg), resulting in 120 µmol m^{-2} s^{-1} PAR, 400 µW cm^{-2} UV-B (280–315 nm), and 150 µW cm^{-2} UV-A (315–400 nm). While PAR was applied in the regular 14/10 h photoperiod, UVR was applied for 4 h at noon. Control cells were covered with a Makrolon® polycarbonate plate that blocks UVR <390 nm (Busch and Hess, 2021). The experiment was run in triplicate for 3 d at 16 °C. After the third UVR exposure, when the algae displayed slight extracellular pigmentation, all samples were subjected to RNA isolation. Brightfield microscopy and photo-documentation of experimental cultures were carried out with the Motic AE2000 inverted microscope (Motic, Hong Kong) equipped with a MikroLive 6.4MP CMOS camera (MikroLive, Oppenau).

RNA isolation and RNA sequencing

Algal cells were collected by centrifugation (500 *g*, 5 min), lysed as described in Gerbracht *et al.* (2022), and subjected to RNA isolation with the TRIzol Reagent (Thermo Fisher Scientific Inc., Waltham, MA, USA) according to the manufacturer's protocol. The RNA samples (see Supplementary Fig. S1 for gel picture) were submitted to the Cologne Center for Genomics (Cologne, Germany) for paired-end mRNA library preparation (Illumina TruSeq mRNA stranded, Illumina, San Diego, CA, USA) and RNA sequencing (RNA-seq; ~20 million reads/sample) on a NovaSeq 6000 platform (Illumina).

Transcriptome assembly

K-mer-based error correction was done with R-Corrector version 1.0.4 (Song and Florea, 2015), and quality and adapter trimming with Trim Galore version 0.6.6 (https://github.com/FelixKrueger/TrimGalore). Processed reads from all conditions were pooled (267 756 958 reads in total) and assembled *de novo* with Trinity version 2.0.6 (Grabherr *et al.*, 2011) in the strand-specific mode. To detect potential contaminants, the resulting transcriptome was blasted against the nt database (megablast, version 2.20.1), and sequences with a length >100 nucleotides and >95% identity with ribosomal, bacterial, or viral sequences were removed. ORFs were predicted with Transdecoder version 2.1.0 (https://github.com/TransDecoder/TransDecoder). Transcriptome assembly statistics

were obtained with Trinity toolkit utilities (TrinityStats.pl) and BUSCO version 4.0.6 (Seppey *et al.*, 2019).

Functional annotation

The predicted ORF sequences were compared with the nr database (release 2020_06) using DIAMOND blastp version 2.0.7 (Buchfink *et al.*, 2021) with an e-value cut-off of 1 × 10^{-6}. Furthermore, we applied EggNOG mapper version 2.1.7 (Cantalapiedra *et al.*, 2021) for a gene ontology (GO) annotation in the DIAMOND mode. InterProScan version 5.22-61.0 (Blum *et al.*, 2021) was used running the following analyses: CDD-3.14, Coils-2.2.1, Gene3D-3.5.0, Hamap-201605.11, MobiDBLite-1.0, PANTHER-11.1, Pfam-30.0, PIRSF-3.01, PRINTS-42.0, ProDom-2006.1, ProSitePatterns-20.119, ProSiteProfiles-20.119, SFLD-2, SignalP_EUK-4.1, SMART-7.1, SUPERFAMILY-1.75, TIGRFAM-15.0, and TMHMM-2.0c. The knumbers were annotated using KAAS annotation (Moriya *et al.*, 2007) in SBH (single-directional best hit) mode using defined organisms as reference (organism abbreviations: ath, boe, gmx, rcu, pop, qsu, vvi, sly, psom, osa, zma, mus, ppp, cre, mng, apro, olu, mpp, cme, ccp, mdm, spen, nta, and to). Furthermore, Ghost Koala version 2.2 (Kanehisa *et al.*, 2016) was used with the KEGG (Kyoto Encyclopedia of Genes and Genomes) database 'genus_prokaryotes+family_eukaryotes' and Kofam Koala version 101.0 (Aramaki *et al.*, 2020) with an e-value cut-off of 0.01. To get the most complete picture (see UpSet plot in Supplementary Fig. S2), retrieved knumbers from KAAS, Ghost Koala, and Kofam Koala were merged and the resulting dataset was used for KEGG pathway mapping using *Arabidopsis thaliana* as a reference (Kanehisa and Sato, 2020; Kanehisa *et al.*, 2022). Transmembrane domains and signal peptides were predicted for selected protein sequences with DeepLoc 2.0 (Almagro Armenteros *et al.*, 2017; Thumuluri *et al.*, 2022) in high-quality mode, DeepTMHMM (Hallgren *et al.*, 2022, Preprint), and SignalP 6.0 (Teufel *et al.*, 2022). Binding sites and the active site of class III peroxidase were predicted by conserved domain search on NCBI (Lu *et al.*, 2020). Furthermore, for the first 50 upregulated genes, the predicted ORF sequences were compared with the refseq_protein database (15 January 2024) using blastp version 2.15.0 (Altschul *et al.*, 1990) with an e-value cut-off of 1 × 10^{-10}. The hit with the lowest e-value with functional information from eukaryotes was chosen, while annotations from plants and green algae were preferred.

Homology searches of specific protein groups

Homologs of enzymes scavenging ROS and class III peroxidases were searched in the output files of EggNOG mapper and InterProScan by EC number and protein name searches. Homologs of photosynthesis proteins and enzymes of specialized metabolite pathways were searched by knumber annotation (see above) and KEGG pathway mapping (map00195, map00940, map00941, map00942, map00944, map00943, and map00965). Furthermore, photosynthesis-associated proteins (from *A. thaliana* and *Chlamydomonas reinhardtii*), jasmonate pathway-related proteins (from *A. thaliana* and *Glycine max*), photoreceptors and photoreceptor-associated proteins (from *A. thaliana*, *C. reinhardtii*, and *Mougeotia scalaris*), and proteins related to the biosynthesis of scytonemin and mycosporine-like amino acids (from cyanobacteria) were used to search for homologs in *S. testaceovaginata* by blastp searches (Altschul *et al.*, 1990). For blastp searches, only putative homologs with an e-value <1 × 10^{-10}, a percentage identity >30%, and a minimal alignment length >50% of the query sequence were chosen.

Differential expression analysis

The processed reads were mapped to the *de novo* transcriptome with bowtie2 version 2.4.1 (Langmead and Salzberg, 2012), and transcript abundance was quantified with Salmon version 1.14.1 in the alignment-based mode

(Patro *et al.*, 2017). Transcript-level abundances, estimated counts, and transcript lengths were imported with tximport version 1.18.0 (Soneson *et al.*, 2016) and summarized into a matrix. Only contigs with a counts per million (CPM) >1 in two or more samples were kept. The differential expression analysis was carried out with DESeq2 version 1.30.0 (Love *et al.*, 2014).

Global enrichment analyses

GO term enrichment analysis was performed with GOseq version 1.42.0 (Young *et al.*, 2010). The sequence lengths required for the analysis were computed with the script 'fasta_seq_length.pl' from the Trinity toolkit utilities. GO terms were retrieved by EggNOG mapper version 2.1.7 (Cantalapiedra *et al.*, 2021). The adjusted *P*-value was set to <0.01 and log2fold change (FC) >1 (upregulated) or <1 (downregulated). Upregulated genes within the term 'Response to UV' were assigned to putative homologs based on EggNOG and InterProScan descriptions, and blastp searches against the UniProtKB/Swiss-Prot database (performed in May 2022). For blastp searches, only putative homologs with an e-value $<1 \times 10^{-10}$, a percentage identity >30%, and a minimal alignment length >50% of the query sequence were chosen.

Protein structure predictions and phylogenetic analyses

Protein structure predictions were performed with I-TASSER (Yang and Zhang, 2015) and visualized with iCn3D (J. Wang *et al.*, 2020). For phylogenetic analysis of class III peroxidases, we created a multiple sequence alignment with streptophyte sequences (all algae and selected embryophytes) from RedOxiBase (Savelli *et al.*, 2019), published sequences from Morgenstern *et al.* (2008), two selected sequences from the RCSB protein data bank (3HDL, 1BGP), and homologs from the algal transcriptomes and genomes listed in Supplementary Table S2. The latter homologs were extracted by Blast searches (e-value $<1 \times 10^{-10}$, length >250 amino acids, percentage identity >30%) with the sequence of StesPRX01 (TRINITY_DN14219) as query. The sequences were aligned with MAFFT version 7.471 (Katoh and Standley, 2013) in 'auto' mode and trimmed with trimAl version 1.4.rev15 (Capella-Gutiérrez *et al.*, 2009) using the 'automated1' setting. The substitution model with the best fit was determined by the ModelFinder function of IQ-TREE version 4.5.1 (Minh *et al.*, 2020), and maximum likelihood phylogenies were inferred with IQ-TREE. After manually reducing sequence redundancy, a final phylogenetic analysis (124 sequences, 248 sites; alignment in Supplementary Dataset S1) was run with the substitution model Q.pfam+R7 and 1000 bootstrap replicates.

Supporting phylogenetic analyses for shikimate and betalain pathway-related genes were conducted within the Geneious Prime sequence analysis software package (Biomatters, New Zealand). The candidate transcriptome sequences were hand-annotated and then translated to provide the deduced amino acid sequences, which were aligned using ClustalOmega or MUSCLE, and the alignments manually adjusted as necessary. Phylogenetic trees were inferred from conserved regions using MrBayes (Ronquist *et al.*, 2012) with an outlier sequence and the default parameters. For assisting with assigning putative function, the trees contained sequences of confirmed function from land plants, along with related sequences from other species of interest. Sequence accession numbers are given within the phylogenies.

Results and discussion

Capturing the reaction of *Serritaenia* to UV radiation by RNA-seq

Based on previous observations on the visible reactions of *S. testaceovaginata* to UVR (Busch and Hess, 2021), we treated the algae with two well-defined conditions over 3 d (Fig. 2A). Control cells experienced a daily 14 h photoperiod of PAR, with a continuous spectrum provided by sun-mimicking LEDs (Fig. 2B). The UVR treatment was characterized by the same PAR spectrum but supplemented with UVR for 4 h per photoperiod (Fig. 2A). The applied UVR had its main emission in the UV-B and far UV-A region, plus a narrow secondary peak at 365 nm (Fig. 2C). While the mucilage of control cells remained colorless (Fig. 2D), cells under the UVR treatment displayed a faint bluish pigmentation after the third photoperiod of the experiment (Fig. 2E). This indicated the ongoing formation of *Serritaenia*'s typical photoprotection triggered by UVR (Busch and Hess, 2021). At this stage, *Serritaenia* cells from both conditions were processed for Illumina RNA sequencing. As there was no reference genome of *Serritaenia* available, we assembled a *de novo* transcriptome from read data of both conditions (six samples). The transcriptome was 77.9% complete according to the BUSCO analysis (Benchmarking Universal Single-Copy Orthologs; Seppey *et al.*, 2019) with the *Viridiplantae* dataset as reference (Fig. 2F). We also checked the completeness of the >60 000 predicted ORFs and found that >60% of them were annotated as complete protein sequences (Fig. 2F). The number of predicted ORFs might seem high, but roughly aligns with the inferred gene numbers of other zygnematophytes (this varies strongly across species from ~11 000 to >50 000 genes; Feng *et al.*, 2023, Preprint). However, it has to be noted that the ORFs of a *de novo* assembled transcriptome cannot be equated to the gene content of the organism. Yet, our *de novo* transcriptome of *S. testaceovaginata* should provide a fairly complete picture of the relevant transcriptomic landscape in this species, and served well for the differential expression analysis. As shown by a principal component analysis, the replicates of the two experimental conditions grouped in two tight and distinct clusters (Fig. 2G), indicating that the experimental set-up led to consistent reactions of the algae under the chosen conditions.

UV radiation triggers cellular reprogramming, repair, and unexpected signaling components

We identified GO terms that were significantly enriched in upregulated genes under the UVR treatment. The majority of these enriched GO terms were related to RNA processing, protein degradation (ubiquitination), and protein modification (Fig. 3A, left). This indicates major expressional changes and a pronounced reprogramming of the cells under UVR. The enriched GO term 'Response to UV' contained 27 upregulated genes and was of particular interest as it allows for some comparisons with other well-studied systems (Fig. 3A, right; Supplementary Table S3). Several genes with a known function in DNA repair and chromatin remodeling were upregulated, indicating that the applied UVR caused damage to the DNA of *Serritaenia* during this early phase of sunscreen production. In particular, this included factors of the eukaryote nucleotide excision
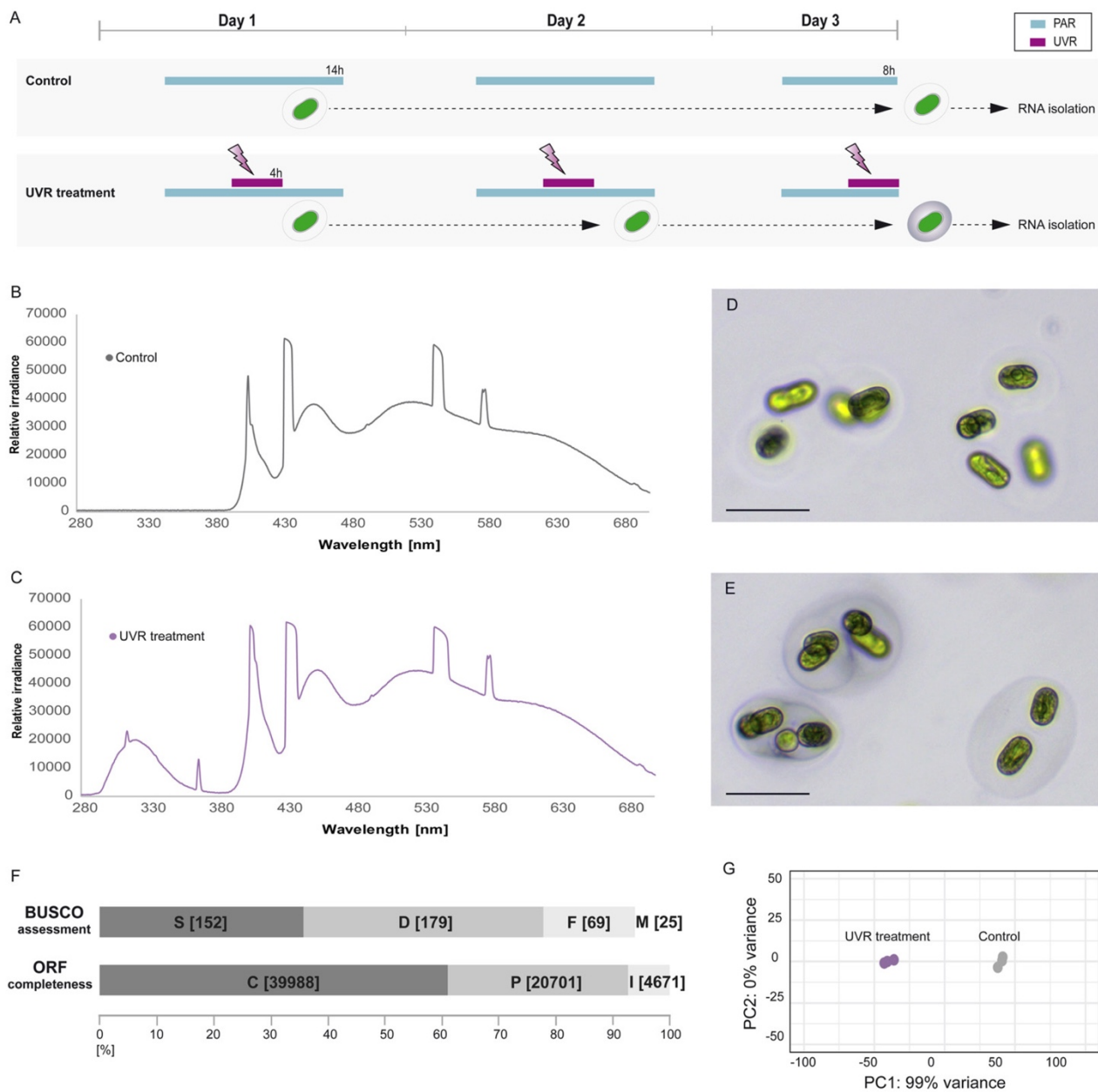
Fig. 2. Experimental set-up and *de novo* transcriptome assembly of *Serritaenia testaceovaginata*. (A) PAR/UVR exposure of cells under the two experimental conditions over the course of 3 d. (B) Relative spectral power distribution under the PAR-only treatment ('Control'). (C) Relative spectral power distribution under the PAR+UVR treatment ('UVR treatment'). (D and E) Cells of *S. testaceovaginata* from the control (D) and the UVR treatment (E) at harvest. Scale bars 50 µm. (F) BUSCO assessment of the assembled transcriptome (top) and completeness of the predicted ORFs (bottom). The BUSCO analysis was performed with the 'Viridiplantae' dataset. The absolute numbers of single-copy orthologs for the categories S (complete and single-copy), D (complete and duplicated), F (fragmented), and M (missing) are shown in brackets. The absolute numbers of ORFs (bottom) for the categories C (complete), P (partial), and I (internal) are also shown in brackets. (G) Principal component analysis (PCA) based on the expression level of all transcripts for each replicate included in the experiment.

Fig. 3. Gene ontology (GO) enrichment analysis, and gene regulation of the photosynthetic machinery and anti-ROS factors. (A) Enriched GO terms associated with upregulated genes under the UVR treatment. GO terms are ranked according to the –log10 false discovery rate (FDR)-corrected *P*-value. Only terms with an FDR-corrected *P*-value <0.05 are shown. The numbers in the circles indicate the number of contigs of upregulated genes

associated with the listed GO terms. The color of the circles indicates the ontology of the respective term: turquoise (biological process, BP), yellow (cellular component, CC), orange (molecular function, MF). Functionally annotated genes of the GO term 'Response to UV' are shown in detail with their upregulation under the UVR treatment (log2FC depicted by violet stars). (B) Regulation of the photosynthetic machinery under the UVR treatment versus the control illustrated by color-coded proteins/boxes: red (upregulated, log2FC ≥1, adjusted P-value <0.001), blue (downregulated, log2FC ≤1, adjusted P-value <0.001), white with black letters (no significant regulation, log2FC −1 to 1, adjusted P-value <0.001). Proteins with gray letters could not be recovered in the transcriptome. (C) Detected anti-ROS factors with their expression levels under the two conditions in transcripts per million (TPM) and predicted cellular localization. Red and blue arrowheads indicate upregulation (log2FC ≥1, adjusted P-value <0.001) and downregulation (log2FC ≤1, adjusted P-value <0.001), respectively, with the log2FC of the respective gene. Cellular localizations predicted on the basis of partial ORFs are indicated by asterisks. The gray box highlights the class III peroxidase StesPrx01, which might have other functions (biosynthesis of phenylpropanoids; see main text).

repair pathway (Supplementary Fig. S3), namely DDB2, XPC, XPB, TFIIH2, XPF, and ERCC1 (global genome repair, GGR); and CSB, UVSSA, POLR2, XPG, and RPA (transcription-coupled repair, TCR). This pathway is responsible for the removal of various types of DNA damage caused by UVR exposure and other damaging agents (Kimura and Sakaguchi, 2006). Most genes of the eukaryote base excision repair and mismatch repair pathways, which are known to remove damaged bases and erroneous base mutations that arise during DNA replication and recombination (Kimura and Sakaguchi, 2006), did not show significant regulation (Supplementary Figs S4, S5). There were also pronounced reactions related to protein degradation and folding, especially factors with chaperone-like functions. This includes homologs of the mitochondrial GrpE2 protein and ABC transporter 1 (Cardazzo et al., 1998), both of which were shown to be triggered by UV-B in plants and algae such as A. thaliana (Hu et al., 2012) and Volvox carteri (Razeghi and Kianianmomeni, 2019), respectively. A specific search for differentially expressed heat shock protein (HSP) sequences in the Serritaenia transcriptome revealed 11 upregulated HSP genes (Supplementary Table S4), all predicted to act as molecular chaperones assisting in a wide range of folding processes of proteins (Mayer and Bukau, 2005; Qiu et al., 2006; Guo et al., 2020). Beneficial effects of HSPs under UV-B stress were reported for plants and algae, such as A. thaliana (Swindell et al., 2007), the marine diatom Odontella sinensis (Döhler et al., 1995), and the cyanobacterium Synechocystis sp. (Balogi et al., 2008). Furthermore, chloroplastic factors associated with UVR responses in higher plants were upregulated in Serritaenia (Fig. 3A, right). Two Chl a/b-binding proteins (ELIP, early light-induced protein; and SEP2, stress enhanced protein 2), for example, accumulate upon UV-B exposure in vascular plants and prevent excess accumulation of free chlorophyll, thereby protecting against photo-oxidative damage (Heddad and Adamska, 2000; Hutin et al., 2003; Sävenstrand et al., 2004). These factors have also been found in chlorophyte green algae such as V. carteri (Razeghi and Kianianmomeni, 2019) and C. reinhardtii (Allorent and Petroutsos, 2017), and might represent a universal mechanism in the green chloroplasts of the Viridiplantae at least. Similar to these other organisms, Serritaenia has several ELIP genes, most of which, however, were not upregulated. All in all, these results reveal that the zygnematophyte Serritaenia has a UVR-responsive toolkit dedicated to repair

and protection that in many ways reflects that of higher plants. The GO terms enriched in the downregulated genes included those for signaling, chloroplast restructuring, phosphor-related processes, sugar metabolism, and cell cycle-related processes (Supplementary Fig. S6), suggesting that Serritaenia under UVR stress slows down some energy-costly processes such as cell growth and multiplication.

A surprising finding was upregulated components of the GO term 'Jasmonic acid mediated signaling pathway'. In vascular plants, the hormone jasmonic acid (JA) functions in defense, growth, and stress response, and in A. thaliana JA levels were shown to increase upon UV-B exposure (Mackerness et al., 1999). So far, JA has not been reported to be involved in UVR- or stress-related signaling cascades in streptophyte green algae. In fact, recent studies suggest that JA signaling evolved in land plants and is absent in algal relatives (Rieseberg et al., 2022). Overall, the pattern of detected proteins involved in JA synthesis, transport, and perception is patchy in streptophyte algae (Holzinger and Becker, 2015; S. Wang et al., 2020). In Serritaenia, we found homologs of digalactosyldiacylglycerol synthase 1 (DGD1; chloroplast), OPDA reductases (OPR2 and OPR3, chloroplast), 'Novel Interactor of JAZ' (NINJA; nucleus), and NAC transcription factors (NAC019, NAC055, and NAC072; nuclear) to be upregulated. However, given the lack of other important JA-related factors (Supplementary Tables S5, S6), the functions of these proteins in Serritaenia and other zygnematophytes remain elusive.

Responses of the photosynthetic machinery and anti-ROS factors

We also analyzed the regulation of genes associated with the photosynthetic machinery in Serritaenia in response to UVR (Fig. 3B; Supplementary Table S7). Almost all components of PSI and PSII, light-harvesting complexes, the cytochrome b_6f complex, and photosynthetic electron transport were downregulated or not differentially expressed. A marked exception were the four genes encoding PsbA (D1), PsbD (D2), PsbC (cp43), and PsbB (cp47) in the reaction center of PSII, which were upregulated under the UVR treatment. It is known from plants that UV-B radiation or strong PAR exposure leads to the inactivation of PSII, by damaging first the oxygen-evolving complex followed by the reaction center (Ohnishi et al., 2005).

The damaged proteins are then replaced by *de novo* synthesis (Hakala *et al.*, 2005). This appears to be a quite common effect in photosynthetic organisms, as even cyanobacteria lose D1 and D2 after the exposure to moderate levels of UV-B (Wu *et al.*, 2011). Hence, the upregulation of D1, D2, cp43, and cp47 points to a specific degradation of the PSII reaction center of *Serritaenia*, which is compensated by the *de novo* synthesis of the damaged components. By contrast, PSI seems not to be affected by UVR in that way, which is in accordance with observations on plants (Iwanzik *et al.*, 1983; Kulandaivelu and Noorudeen, 1983). However, two important components of the cyclic electron flow at PSI, PGR5 and PGR5-like, were upregulated. As in higher plants, the cyclic electron transport in *Serritaenia* might eliminate excess electrons (potentially accumulating due to the damage on PSII), and thereby reduce chlorophyll excitation and oxidative damage. Taken together, under the UVR treatment, the photosynthetic machinery of *Serritaenia* seems to be specifically damaged by UV-B at the reaction center of PSII, which might be compensated by the replacement of broken proteins and cyclic electron flow. Other factors known to be involved in photoprotective quenching in algae and land plants, for example CONSTANS, LHCSR, and PSBS (Suárez-López *et al.*, 2001; Serrano-Bueno *et al.*, 2009; Alboresi *et al.*, 2010; Furukawa *et al.*, 2019; Tokutsu *et al.*, 2019), were not upregulated, indicating that the chloroplast experiences specific damage rather than typical light stress.

Elevated PAR and harmful wavebands such as UV-B are known to initiate the formation of ROS within the cell. ROS can play a regulatory role in gene expression as a response to UV-B radiation (Green and Fluhr, 1995; Surplus *et al.*, 1998; Mackerness *et al.*, 1999), but also cause cell damage by the degradation of various biomolecules (Czarnocka and Karpiński, 2018). To prevent high concentrations of ROS, organisms contain a plethora of enzymes from different families which eliminate the different forms of reactive oxygen. In the *Serritaenia* transcriptome, we found homologs of all of these typical ROS scavengers and predicted their cellular localization (Fig. 3C; Supplementary Table S8). Most of the 27 candidates were downregulated or not differentially expressed, including factors such as ascorbate peroxidases (APXs), glutathione reductases, and a glutathione peroxidase, which in *A. thaliana* were found upregulated under UVR stress (Ulm *et al.*, 2004). It appears that glutathione-associated ROS scavenging does not play a marked role in *Serritaenia* under the UVR treatment. However, the downregulation of superoxide dismutases (SODs), dehydroascorbate reductases (DHARs), and APXs in the algae reflects the situation of UVR-treated *A. thaliana* (Ulm *et al.*, 2004). Only two putative ROS scavengers were highly expressed and upregulated under the UVR treatment, namely a cytoplasmic catalase and an extracellular class III peroxidase (StesPrx01) (Fig. 3C, StesPrx01 highlighted by a gray box). While catalases have a clear function as ROS-scavenging enzymes catalyzing the dismutation of hydrogen peroxide (H_2O_2) into water (H_2O) and oxygen (O_2), class III peroxidases

can have various biological roles, including the biosynthesis of polyphenols such as lignin in the apoplast. Although lignin is unlikely to occur in zygnematophytes, class III peroxidases might have biosynthetic functions in *Serritaenia* as discussed below. Both the specific reaction of the photosynthetic machinery and the limited upregulation of typical ROS scavengers indicate that *Serritaenia* under UVR treatment was not in a stage of broad physiological stress.

How does *Serritaenia* sense light and UV radiation?

We identified components of all major plant photoreceptor systems in *Serritaenia*, including the red-light phytochrome (PHY) system, the blue-light phototropin (PHOT), cryptochrome (CRY), and ZEITLUPE (ZTL) systems, and the UV RESISTANCE LOCUS 8 (UVR8) system (Fig. 4A; Supplementary Table S9). With the exception of the phototropins, components of all photoreceptor systems showed expressional changes upon UV-B treatment (Fig. 4A, right). The interpretation of their functions in microalgae remains difficult, as several molecular components have mainly been studied in higher plants and are associated with processes such as germination and flowering (Kevei *et al.*, 2006; Paik and Huq, 2019). However, we know that the photoprotective reaction in *Serritaenia*, namely the synthesis of its extracellular sunscreen pigment, can be specifically triggered by UV-B radiation (Busch and Hess, 2021). Our *de novo* transcriptome of *Serritaenia* contained homologs of all components of the UVR8 photoreceptor system (Fig. 4A), which is known to perceive UV-B in land plants (Rizzini *et al.*, 2011) and might have a similar function in the distantly related chlorophyte algae (Tilbrook *et al.*, 2016). The UVR8 homolog of *Serritaenia* showed a 65% sequence identity with the UVR8 receptor of *A. thaliana*, and its amino acid sequence contained all sequence motifs necessary for UV-B absorption (tryptophan residues at W233, W285, and W337) and interaction with regulatory factors [a valine–proline (VP) domain at the C-terminus] (Lau *et al.*, 2019) (Fig. 4B). Furthermore, the *in silico* predicted tertiary structure of the UVR8 homolog of *Serritaenia* is similar to the crystal structure of the UVR8 of *A. thaliana* (Wu *et al.*, 2012) (Fig. 4C), and its closest hit in the RCSB protein data bank (TM score 0.976) was the cryo-EM structure of the UV-B-activated UVR8 in complex with CONSTITUTIVE PHOTOMORPHOGENIC 1 (COP1) from *A. thaliana* (entry 7VGG). While the putative UVR8 receptor of *Serritaenia* did not show significant expressional changes under the UVR treatment, two components of the UVR8 signaling network, COP1 and REPRESSOR OF UV-B PHOTOMORPHOGENESIS (RUP), were clearly upregulated (Fig. 4D). In plants, UVR8 dimers split into monomers upon UV-B exposure, which then interact with the E3 ubiquitin ligase COP1. This reduces the ubiquitin-mediated breakdown of the transcription factor ELONGATED HYPOCOTYL 5 (HY5) by COP1, and thus mediates the transcription of UV-B-responsive genes responsible for UV-B
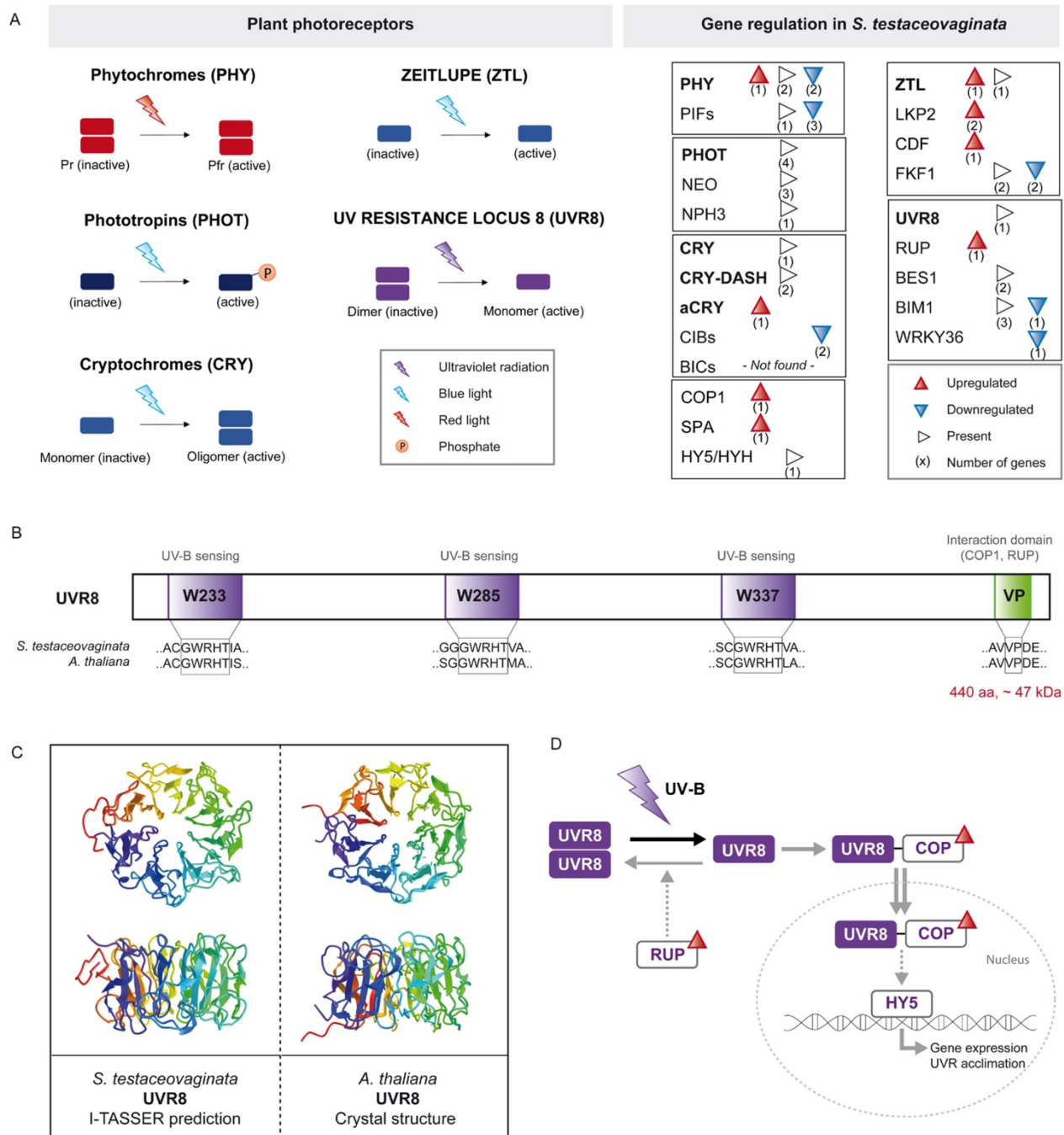
Fig. 4. Presence and regulation of putative photoreceptor systems in *S. testaceovaginata*, with details on UVR8. (A) Schematic illustration of detected photoreceptors (left) and gene regulation of these photoreceptor systems including associated proteins (right). Regulation under the UVR treatment versus the control is indicated by colored arrowheads: red (upregulated, log2FC ≥1, adjusted *P*-value <0.001), blue (downregulated, log2FC ≤1, adjusted *P*-value <0.001), white (no significant regulation, log2FC −1 to 1, adjusted *P*-value <0.001). Numbers in parentheses below the arrowheads indicate the number of annotated ORFs (blastp, e-value cut-off of 1×10^{-10}). PHY, phytochromes; PIFs, PHYTOCHROME INTERACTING FACTORS; PHOT, phototropins; NEO, neochromes; NPH3, NONPHOTOTROPIC HYPOCOTYL 3; CRY, cryptochromes; CRY-DASH, *Drosophila*, Arabidopsis, *Synechocystis*, human (DASH)-type cryptochromes; aCRY, animal-like cryptochromes; CIBs, CRYPTOCHROME2-INTERACTING-BASIC-HELIX–LOOP–HELIX proteins; BICs, blue-light inhibitors of cryptochromes; COP1, CONSTITUTIVE PHOTOMORPHOGENIC 1; SPA, SUPPRESSOR OF PHYA-105;

HY5, ELONGATED HYPOCOTYL 5; HYH, HY5-HOMOLOG; ZTL, ZEITLUPE; LKP2, LOV KELCH PROTEIN 2; CDF, CYCLIC DOF FACTORS; FKF1, FLAVIN-BINDING, KELCH REPEAT, F-BOX 1; UVR8, UV-RESISTANCE LOCUS 8; RUP, REPRESSOR OF UV-B PHOTOMORPHOGENESIS; BES1, BRI1(BRASSINOSTEROID INSENSITIVE 1)-EMS (EXTRA MICROSPOROCYTES)-SUPRESSOR 1; BIM1, BES1-INTERACTING MYC-LIKE 1; WRKY36, WRKY DNA-BINDING PROTEIN 36. (B) Scheme of the UVR8 photoreceptor from *S. testaceovaginata* with the three conserved tryptophan motifs (W233, W285, and W337) responsible for UV-B sensing and the VP domain responsible for the interaction with COP and RUP. (C) *In silico* structure prediction of the UVR8 photoreceptor from *S. testaceovaginata* next to the resolved crystal structure of the UVR8 from *A. thaliana* (pdb entry 4DNU) (Wu *et al.*, 2012). (D) Scheme of the UVR8 signaling cascade triggered by UV-B radiation. Components upregulated under the UVR treatment are marked by red arrowheads.

acclimation (Oravecz *et al.*, 2006; Tilbrook *et al.*, 2013; Liang *et al.*, 2019). RUP, in contrast, maintains the photoequilibrium when the UVR8 dimer/monomer cycling rate increases by facilitating the re-dimerization of UVR8, and thereby reduces again the transcription of UV-B-responsive genes (Liao *et al.*, 2020). This negative feedback loop can be understood as a counterbalancing reaction to UV-B-induced signaling. The existence of a UVR8 homolog with conserved functional sites and the pronounced regulation of COP1 and RUP as part of the UVR8 signaling network suggest that the zygnematophyte *Serritaenia* has a functional UVR8 system that may be a central component of its cellular reaction to harmful wavebands.

Specialized metabolite pathways and their reaction to UV radiation

One of the most interesting questions is the metabolic origin of the extracellular sunscreen pigment of *Serritaenia*. A similar but probably analogous phenomenon can be found in the world of prokaryotes. Cyanobacteria produce sheath pigments such as scytonemin and gloeocapsin, which are formed and deposited in the extracellular matrix (Proteau *et al.*, 1993; Storme *et al.*, 2015). The biosynthesis of the well-studied scytonemin is based on the cyanobacterial 'Scytonemin gene cluster' (Soule *et al.*, 2007, 2009; Bennett and Soule, 2022). In *Serritaenia*, we did not detect most of these scytonemin-related genes, except potential homologs of trpA–E, aroB, and aroG, and a tyrosinase (Supplementary Table S10). Only one of the latter (trpE) was upregulated under the UVR treatment. As expected due to the vast evolutionary distance of streptophyte green algae and cyanobacteria, and their fundamental differences in cellular organization, it seems unlikely that the sunscreen compound of *Serritaenia* is related to scytonemin biosynthesis. Another well-known group of sun screening compounds of algae are the colorless mycosporines and mycosporine-like amino acids (MAAs). They have been found in phylogenetically diverse phototrophs, including cyanobacteria, green algae, rhodophytes, dinoflagellates, and diatoms (Garcia–Pichel and Castenholz, 1993; Karsten *et al.*, 1998; Řezanka *et al.*, 2004; Hotter *et al.*, 2018; Hartmann *et al.*, 2020). However, so far, there is no evidence of these compounds in zygnematophytes. We screened the *Serritaenia* transcriptome for MAA biosynthesis genes known from cyanobacteria (Balskus and Walsh, 2010; Singh *et al.*, 2020), and found potential homologs of Ava3855, Ava3857, Ava3859, and NpR5599. Except Ava3859, these genes were not upregulated

under UVR treatment (Supplementary Table S11), and other relevant factors of MAA biosynthesis (Ava3856, Ava3858, NpR5597, and NpR5598) were not detected at all. It might well be that the *Zygnematophyceae* do not possess a functional MAA biosynthesis pathway.

In the world of higher plants, most UVR-screening compounds have an aromatic origin and are derived from the shikimate pathway (Ferreyra *et al.*, 2021; Davies *et al.*, 2022). Zygnematophytes have also been shown to contain phenolic compounds, some of which are enriched under enhanced UVR and/or PAR levels (Aigner *et al.*, 2013; Pichrtová *et al.*, 2013; Holzinger *et al.*, 2018). However, the biosynthesis of such zygnematophycean compounds, including the colorful vacuolar gallic acid derivates (Remias *et al.*, 2012b; Newsome and van Breemen, 2012), remains unknown. Interestingly, the GO term 'Cellular aromatic compound metabolic process' was enriched in *Serritaenia* under UV-B treatment (Fig. 3A). Hence, we studied the presence and regulation of candidate sequences for enzymes from diverse plant specialized metabolite pathways in *Serritaenia* upon UV-B radiation, with a focus on aromatic compounds. The shikimate pathway was fully recovered and the subsequent synthesis of aromatic amino acids (phenylalanine and tyrosine) from chorismic acid was strongly upregulated (Fig. 5A; Supplementary Table S12), indicating an enhanced production of specialized metabolites derived from these aromatic amino acids. Aromatic amino acids are the primary building blocks for the phenylpropanoid pathway, which also leads to flavonoids such as anthocyanins, isoflavonoids, sphagnorubins, and auronidins, and to lignins (Vanholme *et al.*, 2019; Davies *et al.*, 2022). The colorful sphagnorubins and auronidins, in particular, are known from non-vascular plants, namely mosses (sphagnorubins) and liverworts (auronidins), and typically accumulate in the cell wall (Rudolph and Vowinkel, 1969; Rudolph *et al.*, 1981; Berland *et al.*, 2019). However, there were few components of the canonical plant polyphenolic metabolite pathways leading to flavonoids and anthocyanins in the transcriptome, and these pathways are probably not functional in *Serritaenia* (Fig. 5A). The few genes putatively assigned to these pathways were all downregulated and may, in fact, also not be flavonoid related. In our protein phylogenies, the putative CHS homologs branch clearly outside the polyketide synthases from land plants that are known to be involved in phenylpropanoid biosynthesis (e.g. chalcone synthase, bibenzyl synthase, and stilbene synthase). Instead, one of the two candidate genes is nested in oxoalkylresorcinol synthases of

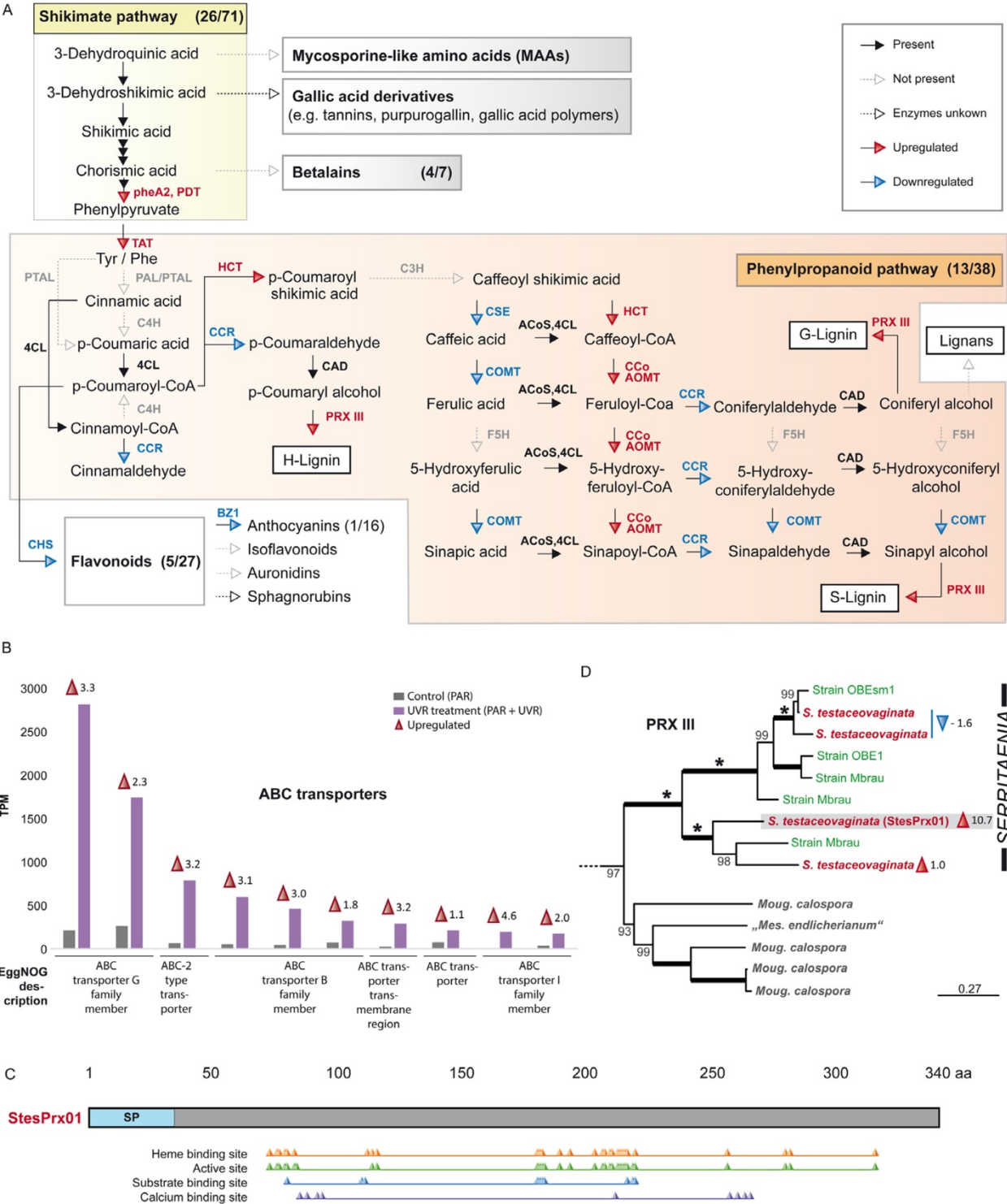**Fig. 5.** Regulation of specialized metabolite pathways and details on ABC transporters and class III peroxidases. (A) Scheme of the shikimate pathway and downstream specialized metabolite pathways. Presence, absence, and regulation under the UVR treatment are indicated by the design and color of arrows (see key). The numbers in parentheses indicate the number of detected versus total knumbers of the respective pathway as a measure of

completeness. PAL, phenylalanine ammonia-lyase; PTAL, phenylalanine/tyrosine ammonia-lyase; C4H, cinnamate 4-hydroxylase; 4CL, 4-coumarate-CoA ligase; CCR, cinnamoyl-CoA reductase; C3H, 4-coumarate 3-hydroxylase; CAD, cinnamyl-alcohol dehydrogenase; CSE, caffeoylshikimate esterase-like; COMT, catechol-*O*-methyltransferase; F5H, ferulate-5-hydroxylase; HCT, hydroxycinnamoyl CoA:shikimate/quinate hydroxycinnamoyltransferase; CCoAOMT, caffeoyl-CoA *O*-methyltransferase; ACoS, acyl-CoA synthetase; PRX III, class III peroxidase. Scale bars: 10 µm. (B) Top 10 most highly expressed ABC transporters under the UVR treatment with their expression levels in transcripts per million (TPM). Red and blue arrowheads indicate upregulation (log2FC ≥1, adjusted *P*-value <0.001) and downregulation (log2FC ≤1, adjusted *P*-value <0.001), respectively, with the log2FC of the respective gene. (C) Scheme of the highly upregulated class III peroxidase StesPrx01 (log2FC 10.7) depicting the signal peptide (SP), heme-binding site, active site, substrate-binding site, and calcium-binding site. (D) Section of the phylogenetic tree of class III peroxidases with genes of the genera *Serritaenia*, *Mougeotiopsis*, and *Mesotaenium* (the full tree is given in Supplementary Fig. S16). Ultrafast bootstrap values are shown at the branches, except when 100% (bold branches). Asterisks highlight potential gene duplication events in the genus *Serritaenia*, and colored arrowheads indicate upregulation (log2FC ≥1) and downregulation (log2FC ≤1) under the UVR treatment with the log2FC.

bryophytes (Supplementary Fig. S7). The other one, which was strongly upregulated during UVR treatment, did not branch with anything known. The *Serritaenia* gene annotated as CHI branches in the clade of fatty acid-binding protein b (FAPb), and not with the flavonoid enzyme clades of CHI and CHI-Like (Supplementary Fig. S8). Overall, the candidates annotated using KEGG as CHS, CHI, and UDP-glycosyltransferases (UGT) are not closely related to known genes with defined functions in flavonoid synthesis (Fig. 5A; Supplementary Figs S7–S9). Nevertheless, multiple flavonoid compounds were detected in the model zygnematophyte *Penium margaritaceum* and, as already suggested (Jiao *et al.*, 2020), this could be based on cryptic activities of known enzymes, novel enzymes, or even alternative biosynthetic routes such as that discovered for fungi that produce flavonoids (Zhang *et al.*, 2023). The synthesis of betalains from tyrosine branching of the shikimate pathway appears to be absent in *Serritaenia*, since the genes mapped to this pathway did not branch close to betalain-related genes of land plants (Supplementary Fig. S10). This is not surprising as betalains are only known from a single order of land plants (*Caryophyllales*) and some fungi (Stintzing and Schliemann, 2007; Babos *et al.*, 2011; Timoneda *et al.*, 2019).

However, *Serritaenia* expressed a number of genes that may encode enzymes that in land plants function in the core phenylpropanoid pathway and lignin biosynthesis. In agreement with previous studies (de Vries *et al.*, 2021; Rieseberg *et al.*, 2022; Dadras *et al.*, 2023b), these land plant-based pathways are only fragmentarily recovered in streptophyte green algae, and some important enzymes such as phenylalanine ammonia-lyase (PAL), cinnamate 4-hydroxylase (C4H), 4-coumarate 3-hydroxylase (C3H), and ferulate–5-hydroxylase (F5H) could not be detected in the *Serritaenia* transcriptome. The lack of these enzymes in zygnematophytes (e.g. *Penium* and *Zygnema*) is known, but it is uncertain whether these algae perform the metabolic steps in question with different enzymes or evolved alternative pathways for phenylpropanoid synthesis. Overall, there is compelling evidence that zygnematophytes should be able to produce such compounds, as indicated by reports of the occurrence of flavonoids and phenylpropanoids in a wide range of green algae including chlorophytes (Aigner *et al.*, 2013; Pichrtová *et al.*, 2013; Goiris *et al.*, 2014; Jiao *et al.*, 2020). Specifically, we detected genes annotated as caffeoylshikimate esterase-like

(CSE), hydroxylcinnamoyl–CoA:shikimate hydroxycinnamoyl transferase (HCT), cinnamyl–alcohol dehydrogenase (CAD), cinnamoyl–CoA reductase (CCR), 4-coumarate-CoA ligase (4CL), catechol-*O*-methyltransferase (COMT), caffeoyl–CoA *O*-methyltransferase (CCoAOMT), and class III peroxidases, most of which show significant regulation in response to UVR (Fig. 5A). For some candidates (e.g. CSE and HCT), the true activity remains unknown, as in our gene phylogenies they occupy distant positions to characterized plant enzymes (Supplementary Figs S11, S12), or are in a clade that also contains land plant genes with different activities (CAD and CCR; Supplementary Fig. S13; see also (de Vries *et al.* (2021). Furthermore, some core monolignol biosynthetic enzymes have related homologs that are involved in the primary metabolism, which makes functional annotation in phylogenetically distant organisms difficult (Weng and Chapple, 2010). Yet, the upregulated acetyltransferase (HCT-annotated) and methyltransferase (CCoAOMT-annotated; Supplementary Fig. S14) sequences might encode proteins that act on hydroxycinnamic acids and thus are part of the phenylpropanoid pathway. The 4CL homolog branches with credible reference genes of other streptophytes as well (Supplementary Fig. S15). The CCoAOMT homologs, in particular, are interesting candidates as they show similarities in functional residues for ligand binding with plant enzymes and originated at the base of the *Phragmoplastophyta* (including *Charophyceae*, *Coleochaetophyceae*, *Zygnematophyceae*, and embryophytes) (de Vries *et al.*, 2021). We still require both further transcriptomic profiling of zygnematophyte representatives and experimental studies on such protein candidates to shed light on their functions in unicellular green algae. Certainly, we cannot exclude that the enzymes encoded by some of the weakly annotated metabolic genes of *Serritaenia* are involved in other, as yet unknown pathways, which are not present in higher plants and, hence, not represented in current databases. These major discrepancies on the level of specialized metabolism clearly illustrate the deep evolutionary split between land plants and their closest algal relatives.

Oxidative enzymes in the extracellular space

In plants, the products of the lignin–related phenylpropanoid pathway—the lignin precursors (monolignols,

monolignol-ferulate ester, and flavone tricin)—are synthesized in the cytoplasm and transported to the apoplast (Barros *et al.*, 2015). Several mechanisms of transport, namely passive diffusion, active transport via G-family ATP-binding cassette (ABC) transporters, and secretion via vesicle–membrane fusion (especially for glucosylated monolignols), have been debated, but the relative contribution of these routes in the secretion of phenylpropanoids is still poorly understood (Barros *et al.*, 2015; Perkins *et al.*, 2019; Xin and Herburger, 2021). The ABCG transporters form a large, gene-rich family and transport various substrates, especially hydrophobic organic compounds (e.g. cutin monomers, lipids, wax components, and fatty acids), with varying specificity (Gräfe and Schmitt, 2021; Xin and Herburger, 2021). In streptophyte algae, such transporters are underexplored and uncharacterized, and their substrates might differ from those in land plants. Yet, these proteins may have important roles in the secretion of known and unknown algal specialized metabolites. We screened the transcriptome of *Serritaenia* for ABC transporters and found 28 genes that were upregulated under the UVR treatment. Two candidates, both annotated as ABCG22, showed extreme upregulation and expression (Fig. 5B; Supplementary Table S13). Interestingly, transporters of this family have been suspected to be involved in lignification in *A. thaliana*, as they were co-expressed with AtABCG29, which evidently transports monolignols (Alejandro *et al.*, 2012), and other lignification-associated factors (Takeuchi *et al.*, 2018a). In fact, several homologs of the ABCG transporters from *A. thaliana* have been associated with lignification and the transport of phenylpropanoids on the basis of expression patterns, for example ABCG30, ABCG33, ABCG34, and ABCG37 (Takeuchi *et al.*, 2018b). However, experimental evidence for most plant ABCG transporters is still lacking and the evolutionary significance of their diversity is unknown. As already proposed by plant biologists (Xin and Herburger, 2021), the study of algal ABC transporters might be an informative, complementing approach. The two ABCG22 homologs found to be strongly expressed during UVR-induced pigment production in *Serritaenia* might be interesting candidates.

The final part of the lignin-related phenylpropanoid pathway in plants is the oxidative polymerization of lignin precursors in the apoplast. This reaction is performed by extracellular enzymes such as heme-containing peroxidases of class III (Marjamaa *et al.*, 2009; Fagerstedt *et al.*, 2010). These enzymes are secreted into the extracellular space and catalyze the reduction of H_2O_2 by transferring electrons from various donor molecules, such as phenolic compounds, lignin precursors, auxin, or secondary metabolites, and can also function as generators of ROS (Weng and Chapple, 2010; Shigeto and Tsutsumi, 2016). The KEGG annotations of the *Serritaenia* transcriptome revealed the presence of a class III peroxidase (Fig. 5A), which turned out to be the gene with the highest upregulation (log2FC=10.7) in the transcriptome. The hypothetical protein of 340 amino acids contains a signal peptide

(likelihood 0.99) and is predicted to be localized in the extracellular space (probability 0.8) according to SignalP 6.0 (Teufel *et al.*, 2022) and DeepLoc 2.0 (Thumuluri *et al.*, 2022), respectively. Blast annotations with the RedOxiBase dataset (Savelli *et al.*, 2019) confirmed its affinity for plant class III peroxidases; the three closest hits from *A. thaliana* were AtPrx30, AtPrx53, and AtPrx54. Despite the relatively low sequence identity with plant homologs (<50%), the *Serritaenia* peroxidase contains residues predicted to bind heme, calcium ions, and the substrate ferulic acid (Fig. 5C). We also performed an *in silico* structure prediction with I-TASSER (Yang and Zhang, 2015), which confirmed the heme- and calcium-binding sites (C-scores 0.77 and 0.03, respectively). The most similar hits from the RCSB protein data bank were a highly glycosylated peroxidase from the royal palm tree *Roystonea regia* [RPTP (3HDL; TM score 0.865] and peroxidase A2 from *A. thaliana* [AtPrx53 (1PA2); TM score 0.862]. The RPTP is an extracellular enzyme with superior stability (Zamorano *et al.*, 2008), which showed high activity on ferulic acid, a central phenolic compound in the phenylpropanoid pathway (Sakharov *et al.*, 2001, 2002). The peroxidase A2 (AtPrx53) from *A. thaliana* was suggested to have a role in lignification, as this protein was highly expressed in lignifying cells and tissues, and the substrate-binding site was predicted to bind and oxidize lignin precursors, especially *p*-coumaroyl and coniferyl alcohols (Ostergaard *et al.*, 2000). However, class III peroxidases are involved in various biological processes and have a broad substrate spectrum. Hence, it is not possible to assign specific functions on the basis of annotations or sequence homology.

Class III peroxidases have already been detected in streptophyte green algae (Buschmann and Holzinger, 2020; Mbadinga Mbadinga *et al.*, 2020), but the algal homologs are still vastly underexplored and uncharacterized. We collected peroxidase sequences from 23 streptophyte algae (including 15 zygnematophytes) and performed phylogenetic inferences to assess the diversity of these proteins and to understand the evolution of the peroxidases of *Serritaenia* (Fig. 5D). Even though the deeper branches are not well resolved due to limited phylogenetic signal, we observed a number of algal peroxidase clades with pronounced diversification of these proteins in several taxa, especially in the genera *Chaetosphaeridium* and *Coleochaete* (Supplementary Fig. S16). The facts that (i) the algal clades are nested within the embryophyte peroxidases and (ii) the peroxidases of a single algal species occur at different positions in the tree, suggest that a certain degree of diversification happened well before the evolution of land plants. The class III peroxidases of the zygnematophyte order *Serritaeniales* form a single well-supported clade, reflecting the phylogeny of the organisms (Hess *et al.*, 2022). We added information of three other *Serritaenia* strains (two sequenced in this study), which represent the phylogenetic diversity of the genus. The peroxidases of the *Serritaenia* strains were closely related and stem from a single ancestor. According to our phylogeny, there were up to four potential gene duplication events, some of which

may have occurred before the diversification of the *Serritaenia* species. However, only one of the four homologs (StesPrx01) found in *S. testaceovaginata* displayed massive upregulation and pronounced expression upon UVR exposure, indicating that the class III peroxidases differ in function and/or biological relevance (Fig. 5D). This is the first report of UVR-related upregulation of a secreted class III peroxidase in a streptophyte alga, similar to the reaction of vascular plants such as *Nicotiana tabacum* (Rácz *et al.*, 2018), *Helianthus annuus* (Yannarelli *et al.*, 2006), and *A. thaliana* (Rao *et al.*, 1996). This finding, along with some highly upregulated multicopper oxidase domain-containing proteins (Supplementary Table S14), points to increased oxidative reactions in the cell wall and/or mucilage of *Serritaenia* when exposed to UVR. In land plants, such enzymes perform various important roles, including ROS scavenging, signaling, and the polymerization of extracellular phenolics (McCaig *et al.*, 2005; Shigeto and Tsutsumi, 2016). Just recently, the multicopper oxidase-like enzymes of the SKS family have been shown to be required for coumaroylation of sporopollenin in pollen (Xu *et al.*, 2023). While phenolic polymers, referred to as 'lignin-like substances', have been detected in other streptophyte green algae (*Coleochaete* and *Nitella*; Delwiche *et al.*, 1989; Ligrone *et al.*, 2008), there is currently no evidence for them in the zygnematophytes. Given the pronounced regulation of phenylpropanoid-related enzymes, ABCG transporters, and oxidative enzymes predicted in the extracellular environment, it might well be that polymeric phenylpropanoids enriched in the algal mucilage fulfill the remarkable sunscreen function in *Serritaenia*. The connection between extracellular (cuticular) phenolics and the 'pre-lignin' pathway was already established for bryophytes (Renault *et al.*, 2017). With this study, we provide expression data and sequence information of UVR-responsive candidate genes, that will enable us to experimentally test the role of such a 'pre-lignin' pathway and its products in the closest algal relatives of land plants.

Conclusion

With comparative transcriptomics, this study sheds some light on the cellular changes of a non-model zygnematophyte with a unique sunscreen mechanism. Overall, the data suggest that fundamental processes such as photosynthesis and light/UVR perception are relatively conserved and react similarly to what is known from land plants. However, the plant-based specialized metabolism was only fragmentarily recovered, which reflects the large evolutionary split between plants and zygnematophytes, and points to a major lack of knowledge concerning algal metabolic processes. Two important specialized metabolite pathways (flavonoid biosynthesis, including flavones and flavonols, or anthocyanins), which in plants have significant roles in UVR protection, do not appear to play a role in *Serritaenia*'s reaction to UV-B. Instead, we discovered marked regulation of enzymes mapped on the shikimate and phenylpropanoid pathway, potential cross-membrane transporters of

phenolics, and oxidative enzymes targeted to the extracellular space. Plant homologs of the latter are known to act on extracellular phenolics to form polymeric lignin in the apoplast, which is mainly associated with the mechanical properties of plant tissues. However, given the substrate promiscuity of class III peroxidases and the extent of uncharacterized homologs, these enzymes might produce many more extracellular compounds of varying function in plants and algae. The extracellular pigment of *Serritaenia* is surprisingly resistant to solvents and hydrolysis, and, despite its different function, might share a common origin with plant lignins.

Supplementary data

The following supplementary data are available at *JXB* online.
　　Fig. S1. RNA samples used for sequencing.
　　Fig. S2. UpSet plot of knumber annotations.
　　Fig. S3. KEGG pathway nucleotide excision repair.
　　Fig. S4. KEGG pathway base excision repair.
　　Fig. S5. KEGG pathway mismatch repair.
　　Fig. S6. GO terms enriched in downregulated genes.
　　Fig. S7. Phylogenetic tree of CHS.
　　Fig. S8. Phylogenetic tree of CHALCONE ISOMERASE (CHI) and CHI-Like (CHIL).
　　Fig. S9. Phylogenetic tree of UGT.
　　Fig. S10. Phylogenetic tree of ligB genes.
　　Fig. S11. Phylogenetic tree of caffeoylshikimate esterases.
　　Fig. S12. Phylogenetic tree of BAHD acyltransferases.
　　Fig. S13. Phylogenetic tree of NAD(P)H-dependent reductases (CAD and CCR-like).
　　Fig. S14. Phylogenetic tree of *O*-methyltransferases.
　　Fig. S15. Phylogenetic tree of 4-coumaroyl CoA:ligase (4CL).
　　Fig. S16. Phylogenetic tree of class III peroxidases (PRXIII) from streptophyte representatives (algae, bryophytes, ferns, and flowering plants).
　　Table S1. Recipe of algal culture medium KW.
　　Table S2. Streptophyte green algal transcriptomes and genomes screened for class III peroxidases.
　　Table S3. Enriched gene ontology term 'response to UV' (GO:0009411) of upregulated genes.
　　Table S4. Heat shock proteins.
　　Table S5. BlastP result of selected jasmonate pathway-related proteins.
　　Table S6. Potential homologs of jasmonate pathway-related proteins in *S. testaceovaginata*.
　　Table S7. Photosynthesis-related proteins.
　　Table S8. Anti-ROS factors.
　　Table S9. Photoreceptors and associated proteins.
　　Table S10. BlastP result of scytonemin biosynthesis-related proteins.
　　Table S11. BlastP result of mycosporine-like amino acids biosynthesis-related proteins.

Acknowledgements

Author contributions

AB and SH: conceptualization, performing the experiments, and writing the draft manuscript; AB and JVG: performing bioinformatic analysis; KD: performing phylogenetic analyses of metabolic enzymes. All authors discussed the results and commented on the manuscript.

Conflict of interest

No conflict of interest declared.

Funding

Data availability

The data that support the findings of this study are openly available. The RNA-seq reads can be found on ArrayExpress at https://www.ebi.ac.uk/biostudies/arrayexpress, accession E-MTAB-13832. The transcriptome assemblies can be found on ENA (European Nucleotide Archive) at https://www.ebi.ac.uk/ena/browser/home, accession PRJEB72628. Gene expression data and functional annotations of transcripts are publicly available in Zenodo at https://doi.org/10.5281/zenodo.10680943.

References

Aigner S, Remias D, Karsten U, Holzinger A. 2013. Unusual phenolic compounds contribute to ecophysiological performance in the purple-colored green alga *Zygogonium ericetorum* (Zygnematophyceae, Streptophyta) from a high-alpine habitat. Journal of Phycology **49**, 648–660.

Alboresi A, Gerotto C, Giacometti GM, Bassi R, Morosinotto T. 2010. *Physcomitrella patens* mutants affected on heat dissipation clarify the evolution of photoprotection mechanisms upon land colonization. Proceedings of the National Academy of Sciences, USA **107**, 11128–11133.

Alejandro S, Lee Y, Tohge T, *et al*. 2012. AtABCG29 is a monolignol transporter involved in lignin biosynthesis. Current Biology **22**, 1207–1212.

Allorent G, Petroutsos D. 2017. Photoreceptor-dependent regulation of photoprotection. Current Opinion in Plant Biology **37**, 102–108.

Almagro Armenteros JJ, Sønderby CK, Sønderby SK, Nielsen H, Winther O. 2017. DeepLoc: prediction of protein subcellular localization using deep learning. Bioinformatics **33**, 3387–3395.

Altschul SF, Gish W, Miller W, Myers EW, Lipman DJ. 1990. Basic local alignment search tool. Journal of Molecular Biology **215**, 403–410.

Aramaki T, Blanc-Mathieu R, Endo H, Ohkubo K, Kanehisa M, Goto S, Ogata H. 2020. KofamKOALA: KEGG Ortholog assignment based on profile HMM and adaptive score threshold. Bioinformatics **36**, 2251–2252.

Babos M, Halász K, Zagyva T, Zöld-Balogh A, Szegő D, Bratek Z. 2011. Preliminary notes on dual relevance of ITS sequences and pigments in *Hygrocybe* taxonomy. Persoonia **26**, 99–107.

Balogi Z, Cheregi O, Giese KC, Vierling E, Vass I, Vígh L, Horváth I. 2008. A mutant small heat shock protein with increased thylakoid association provides an elevated resistance against UV-B damage in *Synechocystis* 6803. Journal of Biological Chemistry **283**, 22983–22991.

Balskus EP, Walsh CT. 2010. The genetic and molecular basis for sunscreen biosynthesis in cyanobacteria. Science **329**, 1653–1656.

Barros J, Serk H, Granlund I, Pesquet E. 2015. The cell biology of lignification in higher plants. Annals of Botany **115**, 1053–1074.

Bennett J, Soule T. 2022. Expression of scytonemin biosynthesis genes under alternative stress conditions in the cyanobacterium *Nostoc punctiforme*. Microorganisms **10**, 427.

Berland H, Albert NW, Stavland A, *et al*. 2019. Auronidins are a previously unreported class of flavonoid pigments that challenges when anthocyanin biosynthesis evolved in plants. Proceedings of the National Academy of Sciences, USA **116**, 20232–20239.

Blum M, Chang H-Y, Chuguransky S, *et al*. 2021. The InterPro protein families and domains database: 20 years on. Nucleic Acids Research **49**, D344–D354.

Bowles AM, Williams TA, Donoghue PC, Campbell DA, Williamson CJ. 2023. Genome of the glacier alga *Ancylonema* and its insights into the evolution of streptophyte life on ice and land. bioRxiv 2023-10. [Preprint].

Buchfink B, Reuter K, Drost H-G. 2021. Sensitive protein alignments at tree-of-life scale using DIAMOND. Nature Methods **18**, 366–368.

Buma AGJ, Boelen P, Jeffrey WH. 2003. UVR-induced DNA damage in aquatic organisms. In: Helbling EW, Zagarese HE, eds. UV effects in aquatic organisms and ecosystems. Comprehensive Series in Photochemical and Photobiological Sciences. Cambridge: The Royal Society of Chemistry, 291–327.

Busch A, Hess S. 2021. Sunscreen mucilage: a photoprotective adaptation found in terrestrial green algae (Zygnematophyceae). European Journal of Phycology **57**, 107–124.

Busch A, Hess S. 2022. A diverse group of underappreciated zygnematophytes deserves in-depth exploration. Applied Phycology **3**, 306–323.

Buschmann H, Holzinger A. 2020. Understanding the algae to land plant transition. Journal of Experimental Botany **71**, 3241–3246.

Cantalapiedra CP, Hernández-Plaza A, Letunic I, Bork P, Huerta-Cepas J. 2021. eggNOG-mapper v2: functional annotation, orthology assignments, and domain prediction at the metagenomic scale. Molecular Biology and Evolution **38**, 5825–5829.

Capella-Gutiérrez S, Silla-Martínez JM, Gabaldón T. 2009. trimAl: a tool for automated alignment trimming in large-scale phylogenetic analyses. Bioinformatics **25**, 1972–1973.

Cardazzo B, Hamel P, Sakamoto W, Wintz H, Dujardin G. 1998. Isolation of an *Arabidopsis thaliana* cDNA by complementation of a yeast abc1 deletion mutant deficient in complex III respiratory activity. Gene **221**, 117–125.

Cheng S, Xian W, Fu Y, *et al*. 2019. Genomes of subaerial zygnematophyceae provide insights into land plant evolution. Cell **179**, 1057–1067.e14.

Czarnocka W, Karpiński S. 2018. Friend or foe? Reactive oxygen species production, scavenging and signaling in plant response to environmental stresses. Free Radical Biology and Medicine **122**, 4–20.

Page 16 of 19 | Busch *et al*.

Dadras A, Fürst-Jansen JMR, Darienko T, et al. 2023a. Environmental gradients reveal stress hubs pre-dating plant terrestrialization. Nature Plants **9**, 1419–1438.

Dadras A, Rieseberg TP, Zegers JMS, Fürst-Jansen JMR, Irisarri I, de Vries J, de Vries S. 2023b. Accessible versatility underpins the deep evolution of plant specialized metabolism. Phytochemistry Reviews https://doi.org/10.1007/s11101-023-09863-2

Davies KM, Landi M, van Klink JW, et al. 2022. Evolution and function of red pigmentation in land plants. Annals of Botany **130**, 613–636.

Delwiche CF, Graham LE, Thomson N. 1989. Lignin-like compounds and sporopollen in *Coleochaete*, an algal model for land plant ancestry. Science **245**, 399–401.

de Vries J, Archibald JM. 2018. Plant evolution: landmarks on the path to terrestrial life. New Phytologist **217**, 1428–1434.

de Vries J, de Vries S, Curtis BA, et al. 2020. Heat stress response in the closest algal relatives of land plants reveals conserved stress signaling circuits. The Plant Journal **103**, 1025–1048.

de Vries J, Ischebeck T. 2020. Ties between stress and lipid droplets pre-date seeds. Trends in Plant Science **25**, 1203–1214.

de Vries S, Fürst-Jansen JMR, Irisarri I, Dhabalia Ashok A, Ischebeck T, Feussner K, Abreu IN, Petersen M, Feussner I, de Vries J. 2021. The evolution of the phenylpropanoid pathway entailed pronounced radiations and divergences of enzyme families. The Plant Journal **107**, 975–1002.

Döhler G, Hoffmann M, Stappel U. 1995. Pattern of proteins after heat shock and UV-B radiation of some temperate marine diatoms and the Antarctic *Odontella weissflogii*. Botanica Acta **108**, 93–98.

Domozych DS. 2014. *Penium margaritaceum*: a unicellular model organism for studying plant cell wall architecture and dynamics. Plants **3**, 543–558.

Domozych DS, Sørensen I, Popper ZA, et al. 2014. Pectin metabolism and assembly in the cell wall of the charophyte green alga *Penium margaritaceum*. Plant Physiology **165**, 105–118.

Fagerstedt KV, Kukkola EM, Koistinen VVT, Takahashi J, Marjamaa K. 2010. Cell wall lignin is polymerised by class III secretable plant peroxidases in Norway Spruce. Journal of Integrative Plant Biology **52**, 186–194.

Feng X, Zheng J, Irisarri I, et al. 2023. Chromosome-level genomes of multicellular algal sisters to land plants illuminate signaling network evolution. bioRxiv 2023.01.31.526407. [Preprint].

Ferreyra MLF, Serra P, Casati P. 2021. Recent advances on the roles of flavonoids as plant protective molecules after UV and high light exposure. Physiologia Plantarum **173**, 736–749.

Fürst-Jansen JMR, de Vries S, Lorenz M, von Schwartzenberg K, Archibald JM, de Vries J. 2021. Submergence of the filamentous Zygnematophyceae *Mougeotia* induces differential gene expression patterns associated with core metabolism and photosynthesis. Protoplasma **259**, 1157–1174.

Furukawa R, Aso M, Fujita T, Akimoto S, Tanaka R, Tanaka A, Yokono M, Takabayashi A. 2019. Formation of a PSI–PSII megacomplex containing LHCSR and PsbS in the moss *Physcomitrella patens*. Journal of Plant Research **132**, 867–880.

Garcia-Pichel F, Wingard CE, Castenholz RW. 1993. Evidence regarding the UV sunscreen role of a mycosporine-like compound in the cyanobacterium *Gloeocapsa* sp. Applied and Environmental Microbiology **59**, 170–176.

Garduño-Solórzano G, Martínez-García M, Scotta Hentschke G, Lopes G, Castelo Branco R, Vasconcelos VMO, Campos JE, López-Cano R, Quintanar-Zúñiga RE. 2021. The phylogenetic placement of *Temnogametum* (Zygnemataceae) and description of *Temnogametum iztacalense* sp. nov., from a tropical high mountain lake in Mexico. European Journal of Phycology **56**, 159–173.

Gerbracht JV, Harding T, Simpson AGB, Roger AJ, Hess S. 2022. Comparative transcriptomics reveals the molecular toolkit used by an algivorous protist for cell wall perforation. Current Biology **32**, 3374–3384.e5.

Goiris K, Muylaert K, Voorspoels S, Noten B, De Paepe D, Baart GJ E, De Cooman L. 2014. Detection of flavonoids in microalgae from different evolutionary lineages. Journal of Phycology **50**, 483–492.

Gontcharov AA. 2008. Phylogeny and classification of Zygnematophyceae (Streptophyta): current state of affairs. Fottea **8**, 87–104.

Gontcharov AA, Marin B, Melkonian M. 2004. Are combined analyses better than single gene phylogenies? A case study using SSU rDNA and rbcL sequence comparisons in the Zygnematophyceae (Streptophyta). Molecular Biology and Evolution **21**, 612–624.

Grabherr MG, Haas BJ, Yassour M, et al. 2011. Trinity: reconstructing a full-length transcriptome without a genome from RNA-Seq data. Nature Biotechnology **29**, 644–652.

Gräfe K, Schmitt L. 2021. The ABC transporter G subfamily in *Arabidopsis thaliana*. Journal of Experimental Botany **72**, 92–106.

Green R, Fluhr R. 1995. UV-B-induced PR-1 accumulation is mediated by active oxygen species. The Plant Cell **7**, 203–212.

Guo L-M, Li J, He J, Liu H, Zhang H-M. 2020. A class I cytosolic HSP20 of rice enhances heat and salt tolerance in different organisms. Scientific Reports **10**, 1383.

Hakala M, Tuominen I, Keränen M, Tyystjärvi T, Tyystjärvi E. 2005. Evidence for the role of the oxygen-evolving manganese complex in photoinhibition of Photosystem II. Biochimica et Biophysica Acta **1706**, 68–80.

Hall JD, McCourt RM. 2015. Conjugating green algae including desmids. In: Wehr JD, Sheath RG, Kociolek JP, eds. Aquatic ecology. Freshwater algae of North America. 2nd edn. Boston: Academic Press, 429–457.

Hallgren J, Tsirigos KD, Pedersen MD, Armenteros JJA, Marcatili P, Nielsen H, Krogh A, Winther O. 2022. DeepTMHMM predicts alpha and beta transmembrane proteins using deep neural networks. bioRxiv 2022.04.08.487609. [Preprint].

Hartmann A, Glaser K, Holzinger A, Ganzera M, Karsten U. 2020. Klebsormidin A and B, two new UV-sunscreen compounds in green microalgal *Interfilum* and *Klebsormidium* species (Streptophyta) from terrestrial habitats. Frontiers in Microbiology **11**, 499.

Heddad M, Adamska I. 2000. Light stress-regulated two-helix proteins in *Arabidopsis thaliana* related to the chlorophyll a/b-binding gene family. Proceedings of the National Academy of Sciences, USA **97**, 3741–3746.

Hess S, Williams SK, Busch A, et al. 2022. A phylogenomically informed five-order system for the closest relatives of land plants. Current Biology **32**, 4473–4482.

Holzinger A, Albert A, Aigner S, Uhl J, Schmitt-Kopplin P, Trumhová K, Pichrtová M. 2018. Arctic, Antarctic, and temperate green algae *Zygnema* spp. under UV-B stress: vegetative cells perform better than pre-akinetes. Protoplasma **255**, 1239–1252.

Holzinger A, Becker B. 2015. Desiccation tolerance in the streptophyte green alga *Klebsormidium*: the role of phytohormones. Communicative & Integrative Biology **8**, e1059978.

Hotter V, Glaser K, Hartmann A, Ganzera M, Karsten U. 2018. Polyols and UV-sunscreens in the *Prasiola*-clade (Trebouxiophyceae, Chlorophyta) as metabolites for stress response and chemotaxonomy. Journal of Phycology **54**, 264–274.

Hu C, Lin S, Chi W, Charng Y. 2012. Recent gene duplication and sub-functionalization produced a mitochondrial GrpE, the nucleotide exchange factor of the Hsp70 complex, specialized in thermotolerance to chronic heat stress in *Arabidopsis*. Plant Physiology **158**, 747–758.

Hutin C, Nussaume L, Moise N, Moya I, Kloppstech K, Havaux M. 2003. Early light-induced proteins protect *Arabidopsis* from photooxidative stress. Proceedings of the National Academy of Sciences, USA **100**, 4921–4926.

Iwanzik W, Tevini M, Dohnt G, Voss M, Weiss W, Gräber P, Renger G. 1983. Action of UV-B radiation on photosynthetic primary reactions in spinach chloroplasts. Physiologia Plantarum **58**, 401–407.

Jiao C, Sørensen I, Sun X, et al. 2020. The *Penium margaritaceum* genome: hallmarks of the origins of land plants. Cell **181**, 1097–1111.e12.

Kanehisa M, Sato Y. 2020. KEGG Mapper for inferring cellular functions from protein sequences. Protein Science **29**, 28–35.

Kanehisa M, Sato Y, Kawashima M. 2022. KEGG mapping tools for uncovering hidden features in biological data. Protein Science **31**, 47–53.

Kanehisa M, Sato Y, Morishima K. 2016. BlastKOALA and GhostKOALA: KEGG tools for functional characterization of genome and metagenome sequences. Journal of Molecular Biology **428**, 726–731.

Karentz D, Cleaver JE, Mitchell DL. 1991. Cell survival characteristics and molecular responses of antarctic phytoplankton to ultraviolet-B radiation. Journal of Phycology **27**, 326–341.

Karsten U, Franklin LA, Lüning K, Wiencke C. 1998. Natural ultraviolet radiation and photosynthetically active radiation induce formation of mycosporine-like amino acids in the marine macroalga *Chondrus crispus* (Rhodophyta). Planta **205**, 257–262.

Katoh K, Standley DM. 2013. MAFFT multiple sequence alignment software version 7: improvements in performance and usability. Molecular Biology and Evolution **30**, 772–780.

Kevei E, Gyula P, Hall A, et al. 2006. Forward genetic analysis of the circadian clock separates the multiple functions of ZEITLUPE. Plant Physiology **140**, 933–945.

Kimura S, Sakaguchi K. 2006. DNA repair in plants. Chemical Reviews **106**, 753–766.

Kulandaivelu G, Noorudeen AM. 1983. Comparative study of the action of ultraviolet-C and ultraviolet-B radiation on photosynthetic electron transport. Physiologia Plantarum **58**, 389–394.

Langmead B, Salzberg SL. 2012. Fast gapped-read alignment with Bowtie 2. Nature Methods **9**, 357–359.

Lao K, Glazer AN. 1996. Ultraviolet-B photodestruction of a light-harvesting complex. Proceedings of the National Academy of Sciences, USA **93**, 5258–5263.

Lau K, Podolec R, Chappuis R, Ulm R, Hothorn M. 2019. Plant photoreceptors and their signaling components compete for COP1 binding via VP peptide motifs. The EMBO Journal **38**, e102140.

Leebens-Mack JH, Barker MS, Carpenter EJ, et al. 2019. One thousand plant transcriptomes and the phylogenomics of green plants. Nature **574**, 679–685.

Liang T, Yang Y, Liu H. 2019. Signal transduction mediated by the plant UV-B photoreceptor UVR8. New Phytologist **221**, 1247–1252.

Liao X, Liu W, Yang H-Q, Jenkins GI. 2020. A dynamic model of UVR8 photoreceptor signalling in UV-B-acclimated *Arabidopsis*. New Phytologist **227**, 857–866.

Ligrone R, Carafa A, Duckett JG, Renzaglia KS, Ruel K. 2008. Immunocytochemical detection of lignin-related epitopes in cell walls in bryophytes and the charalean alga *Nitella*. Plant Systematics and Evolution **270**, 257–272.

Love MI, Huber W, Anders S. 2014. Moderated estimation of fold change and dispersion for RNA-seq data with DESeq2. Genome Biology **15**, 550.

Lu S, Wang J, Chitsaz F, et al. 2020. CDD/SPARCLE: the conserved domain database in 2020. Nucleic Acids Research **48**, D265–D268.

Mackerness SA-H, Surplus SL, Blake P, John CF, Buchanan-Wollaston V, Jordan BR, Thomas B. 1999. Ultraviolet-B-induced stress and changes in gene expression in *Arabidopsis thaliana*: role of signalling pathways controlled by jasmonic acid, ethylene and reactive oxygen species. Plant, Cell & Environment **22**, 1413–1423.

Marjamaa K, Kukkola EM, Fagerstedt KV. 2009. The role of xylem class III peroxidases in lignification. Journal of Experimental Botany **60**, 367–376.

Mayer MP, Bukau B. 2005. Hsp70 chaperones: cellular functions and molecular mechanism. Cellular and Molecular Life Sciences **62**, 670–684.

Mbadinga Mbadinga DL, Li Q, Ranocha P, Martinez Y, Dunand C. 2020. Global analysis of non-animal peroxidases provides insights into the evolution of this gene family in the green lineage. Journal of Experimental Botany **71**, 3350–3360.

McCaig BC, Meagher RB, Dean JFD. 2005. Gene structure and molecular analysis of the laccase-like multicopper oxidase (LMCO) gene family in *Arabidopsis thaliana*. Planta **221**, 619–636.

Minh BQ, Schmidt HA, Chernomor O, Schrempf D, Woodhams MD, von Haeseler A, Lanfear R. 2020. IQ-TREE 2: new models and efficient methods for phylogenetic inference in the genomic era. Molecular Biology and Evolution **37**, 1530–1534.

Morgenstern I, Klopman S, Hibbett DS. 2008. Molecular evolution and diversity of lignin degrading heme peroxidases in the Agaricomycetes. Journal of Molecular Evolution **66**, 243–257.

Moriya Y, Itoh M, Okuda S, Yoshizawa AC, Kanehisa M. 2007. KAAS: an automatic genome annotation and pathway reconstruction server. Nucleic Acids Research **35**, W182–W185.

Newsome AG, van Breemen R. 2012. Characterization of the purple vacuolar pigment of *Zygogonium ericetorum* alga. Planta Medica **78**, PJ20.

Ohnishi N, Allakhverdiev SI, Takahashi S, Higashi S, Watanabe M, Nishiyama Y, Murata N. 2005. Two-step mechanism of photodamage to photosystem II: step 1 occurs at the oxygen-evolving complex and step 2 occurs at the photochemical reaction center. Biochemistry **44**, 8494–8499.

Oravecz A, Baumann A, Máté Z, Brzezinska A, Molinier J, Oakeley EJ, Ádám E, Schäfer E, Nagy F, Ulm R. 2006. CONSTITUTIVELY PHOTOMORPHOGENIC1 is required for the UV-B response in *Arabidopsis*. The Plant Cell **18**, 1975–1990.

Ostergaard L, Teilum K, Mirza O, Mattsson O, Petersen M, Welinder KG, Mundy J, Gajhede M, Henriksen A. 2000. *Arabidopsis* ATP A2 peroxidase. Expression and high-resolution structure of a plant peroxidase with implications for lignification. Plant Molecular Biology **44**, 231–243.

Paik I, Huq E. 2019. Plant photoreceptors: multi-functional sensory proteins and their signaling networks. Seminars in Cell & Developmental Biology **92**, 114–121.

Patro R, Duggal G, Love MI, Irizarry RA, Kingsford C. 2017. Salmon provides fast and bias-aware quantification of transcript expression. Nature Methods **14**, 417–419.

Perkins M, Smith RA, Samuels L. 2019. The transport of monomers during lignification in plants: anything goes but how? Current Opinion in Biotechnology **56**, 69–74.

Permann C, Pierangelini M, Remias D, Lewis LA, Holzinger A. 2022. Photophysiological investigations of the temperature stress responses of *Zygnema* spp (Zygnematophyceae) from subpolar and polar habitats (Iceland, Svalbard). Phycologia **61**, 299–311.

Pichrtová M, Kulichová J, Holzinger A. 2014. Nitrogen limitation and slow drying induce desiccation tolerance in conjugating green algae (Zygnematophyceae, Streptophyta) from polar habitats. PLoS One **9**, e113137.

Pichrtová M, Remias D, Lewis LA, Holzinger A. 2013. Changes in phenolic compounds and cellular ultrastructure of arctic and antarctic strains of *Zygnema* (Zygnematophyceae, Streptophyta) after exposure to experimentally enhanced UV to PAR ratio. Microbial Ecology **65**, 68–83.

Proteau PJ, Gerwick WH, Garcia-Pichel F, Castenholz R. 1993. The structure of scytonemin, an ultraviolet sunscreen pigment from the sheaths of cyanobacteria. Experientia **49**, 825–829.

Qiu X-B, Shao Y-M, Miao S, Wang L. 2006. The diversity of the DnaJ/Hsp40 family, the crucial partners for Hsp70 chaperones. Cellular and Molecular Life Sciences **63**, 2560–2570.

Rácz A, Hideg E, Czégény G. 2018. Selective responses of class III plant peroxidase isoforms to environmentally relevant UV-B doses. Journal of Plant Physiology **221**, 101–106.

Rao MV, Paliyath G, Ormrod DP. 1996. Ultraviolet-B- and ozone-induced biochemical changes in antioxidant enzymes of *Arabidopsis thaliana*. Plant Physiology **110**, 125–136.

Razeghi J, Kianianmomeni A. 2019. UV-B response is modulated by cell-type specific signaling pathway in multicellular green algae *Volvox carteri*. Plant Growth Regulation **87**, 303–315.

Remias D, Holzinger A, Aigner S, Lütz C. 2012a. Ecophysiology and ultrastructure of *Ancylonema nordenskiöldii* (Zygnematales, Streptophyta), causing brown ice on glaciers in Svalbard (high arctic). Polar Biology **35**, 899–908.

Remias D, Procházková L. 2023. The first cultivation of the glacier ice alga *Ancylonema alaskanum* (Zygnematophyceae, Streptophyta): differences in

Page 18 of 19 | Busch *et al*.

morphology and photophysiology of field vs laboratory strain cells. Journal of Glaciology **69**, 1080–1084.

Remias D, Schwaiger S, Aigner S, Leya T, Stuppner H, Lütz C. 2012b. Characterization of an UV- and VIS-absorbing, purpurogallin-derived secondary pigment new to algae and highly abundant in *Mesotaenium berggrenii* (Zygnematophyceae, Chlorophyta), an extremophyte living on glaciers. FEMS Microbiology Ecology **79**, 638–648.

Renault H, Alber A, Horst NA, et al. 2017. A phenol-enriched cuticle is ancestral to lignin evolution in land plants. Nature Communications **8**, 14713.

Řezanka T, Temina M, Tolstikov AG, Dembitsky VM. 2004. Natural microbial UV radiation filters—mycosporine-like amino acids. Folia Microbiologica **49**, 339–352.

Rieseberg TP, Dadras A, Fürst-Jansen JMR, Dhabalia Ashok A, Darienko T, de Vries S, Irisarri I, de Vries J. 2022. Crossroads in the evolution of plant specialized metabolism. Seminars in Cell & Developmental Biology **134**, 37–58.

Rizzini L, Favory J-J, Cloix C, et al. 2011. Perception of UV-B by the *Arabidopsis* UVR8 protein. Science **332**, 103–106.

Ronquist F, Teslenko M, van der Mark P, Ayres DL, Darling A, Höhna S, Larget B, Liu L, Suchard MA, Huelsenbeck JP. 2012. MrBayes 3.2: efficient Bayesian phylogenetic inference and model choice across a large model space. Systematic Biology **61**, 539–542.

Rudolph H, Krause H-J, Blaicher M, Herms E. 1981. Investigations of the shikimic acid metabolism in *Sphagnum magellanicum* during synthesis of sphagnorubin induced by chilling. Biochemie und Physiologie der Pflanzen **176**, 728–736.

Rudolph H, Vowinkel E. 1969. Sphagnorubin, ein kristallines Membranochrom aus *Sphagnum magellanicum*. Zeitschrift für Naturforschung B **24**, 1211–1212.

Ruhfel BR, Gitzendanner MA, Soltis PS, Soltis DE, Burleigh JG. 2014. From algae to angiosperms—inferring the phylogeny of green plants (Viridiplantae) from 360 plastid genomes. BMC Evolutionary Biology **14**, 23.

Sakharov IY, Vesga BMK, Galaev IY, Sakharova IV, Pletjushkina OY. 2001. Peroxidase from leaves of royal palm tree *Roystonea regia*: purification and some properties. Plant Science **161**, 853–860.

Sakharov IY, Vesga Blanco MK, Sakharova IV. 2002. Substrate specificity of African oil palm tree peroxidase. Biochemistry **67**, 1043–1047.

Savelli B, Li Q, Webber M, Jemmat AM, Robitaille A, Zamocky M, Mathé C, Dunand C. 2019. RedoxiBase: a database for ROS homeostasis regulated proteins. Redox Biology **26**, 101247.

Sävenstrand H, Olofsson M, Samuelsson M, Strid A. 2004. Induction of early light-inducible protein gene expression in *Pisum sativum* after exposure to low levels of UV-B irradiation and other environmental stresses. Plant Cell Reports **22**, 532–536.

Seppey M, Manni M, Zdobnov EM. 2019. BUSCO: assessing genome assembly and annotation completeness. Methods in Molecular Biology **1962**, 227–245.

Serrano-Bueno G, Herrera-Palau R, Romero JM, Serrano A, Coupland G, Valverde F. 2009. *Chlamydomonas constans* and the evolution of plant photoperiodic signaling.

Shigeto J, Tsutsumi Y. 2016. Diverse functions and reactions of class III peroxidases. New Phytologist **209**, 1395–1402.

Singh DK, Pathak J, Pandey A, Singh V, Ahmed H, Kumar D, Sinha RP. 2020. Ultraviolet-screening compound mycosporine-like amino acids in cyanobacteria: biosynthesis, functions, and applications. In: Singh PK, Kumar A, Singh VK, Shrivastava AK, eds. Advances in cyanobacterial biology. Academic Press, 219–233.

Soneson C, Love MI, Robinson MD. 2016. Differential analyses for RNA-seq: transcript-level estimates improve gene-level inferences. F1000Research **4**, 1521.

Song L, Florea L. 2015. Rcorrector: efficient and accurate error correction for Illumina RNA-seq reads. GigaScience **4**, 48.

Soule T, Palmer K, Gao Q, Potrafka RM, Stout V, Garcia-Pichel F. 2009. A comparative genomics approach to understanding the biosynthesis of the sunscreen scytonemin in cyanobacteria. BMC Genomics **10**, 336.

Soule T, Stout V, Swingley WD, Meeks JC, Garcia-Pichel F. 2007. Molecular genetics and genomic analysis of scytonemin biosynthesis in *Nostoc punctiforme* ATCC 29133. Journal of Bacteriology **189**, 4465–4472.

Stintzing F, Schliemann W. 2007. Pigments of fly agaric (*Amanita muscaria*). Zeitschrift fur Naturforschung C **62**, 779–785.

Storme J-Y, Golubic S, Wilmotte A, Kleinteich J, Velázquez D, Javaux EJ. 2015. Raman characterization of the UV-protective pigment gloeocapsin and its role in the survival of cyanobacteria. Astrobiology **15**, 843–857.

Suárez-López P, Wheatley K, Robson F, Onouchi H, Valverde F, Coupland G. 2001. CONSTANS mediates between the circadian clock and the control of flowering in *Arabidopsis*. Nature **410**, 1116–1120.

Surplus SL, Jordan BR, Murphy AM, Carr JP, Thomas B, Mackerness SA-H. 1998. Ultraviolet-B-induced responses in *Arabidopsis thaliana*: role of salicylic acid and reactive oxygen species in the regulation of transcripts encoding photosynthetic and acidic pathogenesis-related proteins. Plant, Cell & Environment **21**, 685–694.

Swindell WR, Huebner M, Weber AP. 2007. Transcriptional profiling of *Arabidopsis* heat shock proteins and transcription factors reveals extensive overlap between heat and non-heat stress response pathways. BMC Genomics **8**, 125.

Takeuchi M, Kegasa T, Watanabe A, Tamura M, Tsutsumi Y. 2018a. Expression analysis of transporter genes for screening candidate monolignol transporters using *Arabidopsis thaliana* cell suspensions during tracheary element differentiation. Journal of Plant Research **131**, 297–305.

Takeuchi M, Watanabe A, Tamura M, Tsutsumi Y. 2018b. The gene expression analysis of *Arabidopsis thaliana* ABC transporters by real-time PCR for screening monolignol-transporter candidates. Journal of Wood Science **64**, 477–484.

Teufel F, Almagro Armenteros JJ, Johansen AR, Gíslason MH, Pihl SI, Tsirigos KD, Winther O, Brunak S, von Heijne G, Nielsen H. 2022. SignalP 6.0 predicts all five types of signal peptides using protein language models. Nature Biotechnology **40**, 1023–1025.

Thumuluri V, Almagro Armenteros JJ, Johansen AR, Nielsen H, Winther O. 2022. DeepLoc 2.0: multi-label subcellular localization prediction using protein language models. Nucleic Acids Research **50**, W228–W234.

Tilbrook K, Arongaus AB, Binkert M, Heijde M, Yin R, Ulm R. 2013. The UVR8 UV-B photoreceptor: perception, signaling and response. The Arabidopsis Book **11**, e0164.

Tilbrook K, Dubois M, Crocco CD, Yin R, Chappuis R, Allorent G, Schmid-Siegert E, Goldschmidt-Clermont M, Ulm R. 2016. UV-B perception and acclimation in *Chlamydomonas reinhardtii*. The Plant Cell **28**, 966–983.

Timme RE, Bachvaroff TR, Delwiche CF. 2012. Broad phylogenomic sampling and the sister lineage of land plants. PLoS One **7**, e29696.

Timoneda A, Feng T, Sheehan H, Walker-Hale N, Pucker B, Lopez-Nieves S, Guo R, Brockington S. 2019. The evolution of betalain biosynthesis in Caryophyllales. New Phytologist **224**, 71–85.

Tokutsu R, Fujimura-Kamada K, Matsuo T, Yamasaki T, Minagawa J. 2019. The CONSTANS flowering complex controls the protective response of photosynthesis in the green alga *Chlamydomonas*. Nature Communications **10**, 4099.

Ulm R, Baumann A, Oravecz A, Máté Z, Ádám E, Oakeley EJ, Schäfer E, Nagy F. 2004. Genome-wide analysis of gene expression reveals function of the bZIP transcription factor HY5 in the UV-B response of *Arabidopsis*. Proceedings of the National Academy of Sciences, USA **101**, 1397–1402.

Vanholme R, De Meester B, Ralph J, Boerjan W. 2019. Lignin biosynthesis and its integration into metabolism. Current Opinion in Biotechnology **56**, 230–239.

Wang J, Youkharibache P, Zhang D, et al. 2020. iCn3D, a web-based 3D viewer for sharing 1D/2D/3D representations of biomolecular structures. Bioinformatics **36**, 131–135.

Wang S, Li L, Li H, et al. 2020. Genomes of early-diverging streptophyte algae shed light on plant terrestrialization. Nature Plants **6**, 95–106.

Weng J, Chapple C. 2010. The origin and evolution of lignin biosynthesis. New Phytologist **187**, 273–285.

Wickett NJ, Mirarab S, Nguyen N, *et al*. 2014. Phylotranscriptomic analysis of the origin and early diversification of land plants. Proceedings of the National Academy of Sciences, USA **111**, E4859–E4868.

Wodniok S, Brinkmann H, Glöckner G, Heidel AJ, Philippe H, Melkonian M, Becker B. 2011. Origin of land plants: do conjugating green algae hold the key? BMC Evolutionary Biology **11**, 104.

Wu D, Hu Q, Yan Z, *et al* 2012. Structural basis of ultraviolet-B perception by UVR8. Nature **484**, 214–219.

Wu H, Abasova L, Cheregi O, Deák Z, Gao K, Vass I. 2011. D1 protein turnover is involved in protection of Photosystem II against UV-B induced damage in the cyanobacterium *Arthrospira* (*Spirulina*) *platensis*. Journal of Photochemistry and Photobiology B: Biology **104**, 320–325.

Xin A, Herburger K. 2021. Mini review: transport of hydrophobic polymers into the plant apoplast. Frontiers in Plant Science **11**, 590990.

Xu L, Tang Y, Yang Y, Wang D, Wang H, Du J, Bai Y, Su S, Zhao C, Li L. 2023. Microspore-expressed SCULP1 is required for p-coumaroylation of sporopollenin, exine integrity, and pollen development in wheat. New Phytologist **239**, 102–115.

Yang J, Zhang Y. 2015. I-TASSER server: new development for protein structure and function predictions. Nucleic Acids Research **43**, W174–W181.

Yannarelli GG, Gallego SM, Tomaro ML. 2006. Effect of UV-B radiation on the activity and isoforms of enzymes with peroxidase activity in sunflower cotyledons. Environmental and Experimental Botany **56**, 174–181.

Young MD, Wakefield MJ, Smyth GK, Oshlack A. 2010. Gene ontology analysis for RNA-seq: accounting for selection bias. Genome Biology **11**, R14.

Zamorano LS, Pina DG, Arellano JB, *et al*. 2008. Thermodynamic characterization of the palm tree *Roystonea regia* peroxidase stability. Biochimie **90**, 1737–1749.

Zhang W, Zhang X, Feng D, *et al*. 2023. Discovery of a unique flavonoid biosynthesis mechanism in fungi by genome mining. Angewandte Chemie **135**, e202215529.

Supplementary Data

Comparative transcriptomics elucidates the cellular responses of an aeroterrestrial zygnematophyte to UV radiation

Anna Busch, Jennifer V. Gerbracht, Kevin Davies, Ute Hoecker, Sebastian Hess

Fig. S1 RNA samples used for sequencing. RNA denaturing gel of isolated RNA from *Serritaenia testaceovaginata* under condition 1 (NK) and condition 2 (UV) in triplicates.
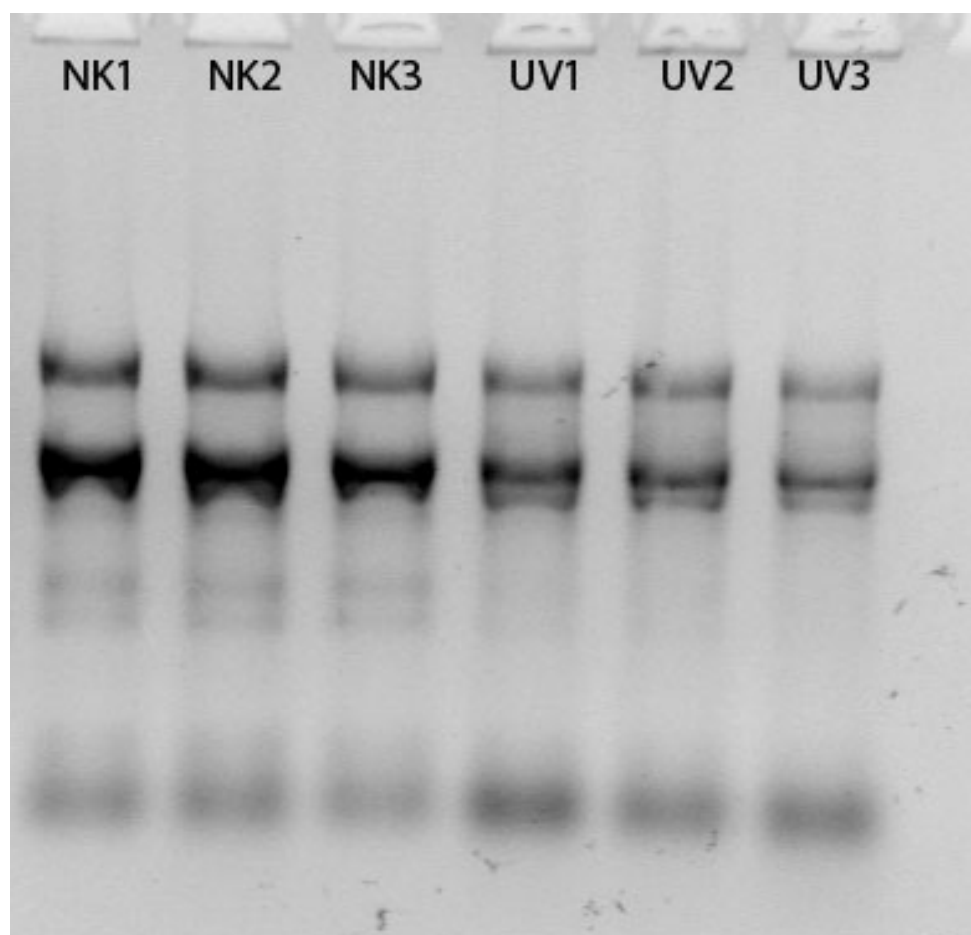
Fig. S2 UpSet plot of knumber annotations. UpSet plot showing the number of ORFs (intersection size) annotated by the indicated annotation tools and databases and their combinations.

Fig. S3 KEGG pathway nucleotide excision repair. Presence and regulation in *S. testaceovaginata* are indicated by the color of the boxes.
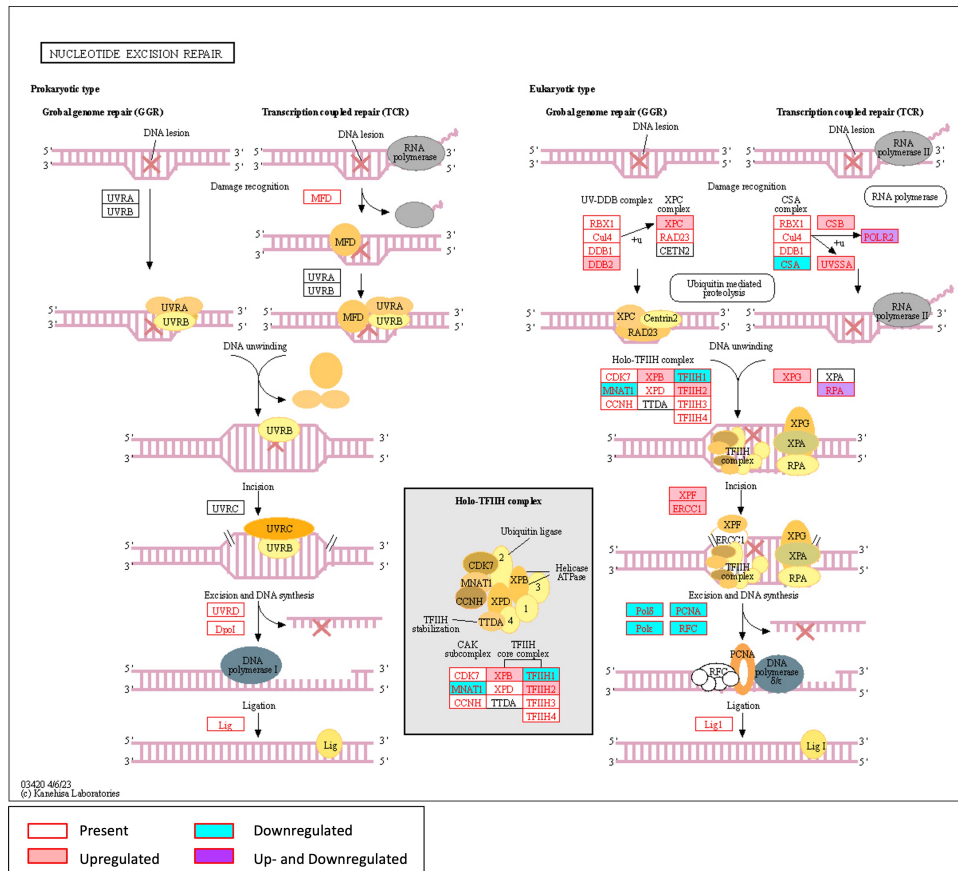
Fig. S4 KEGG pathway base excision repair. Presence and regulation in *S. testaceovaginata* are indicated by the color of the boxes.

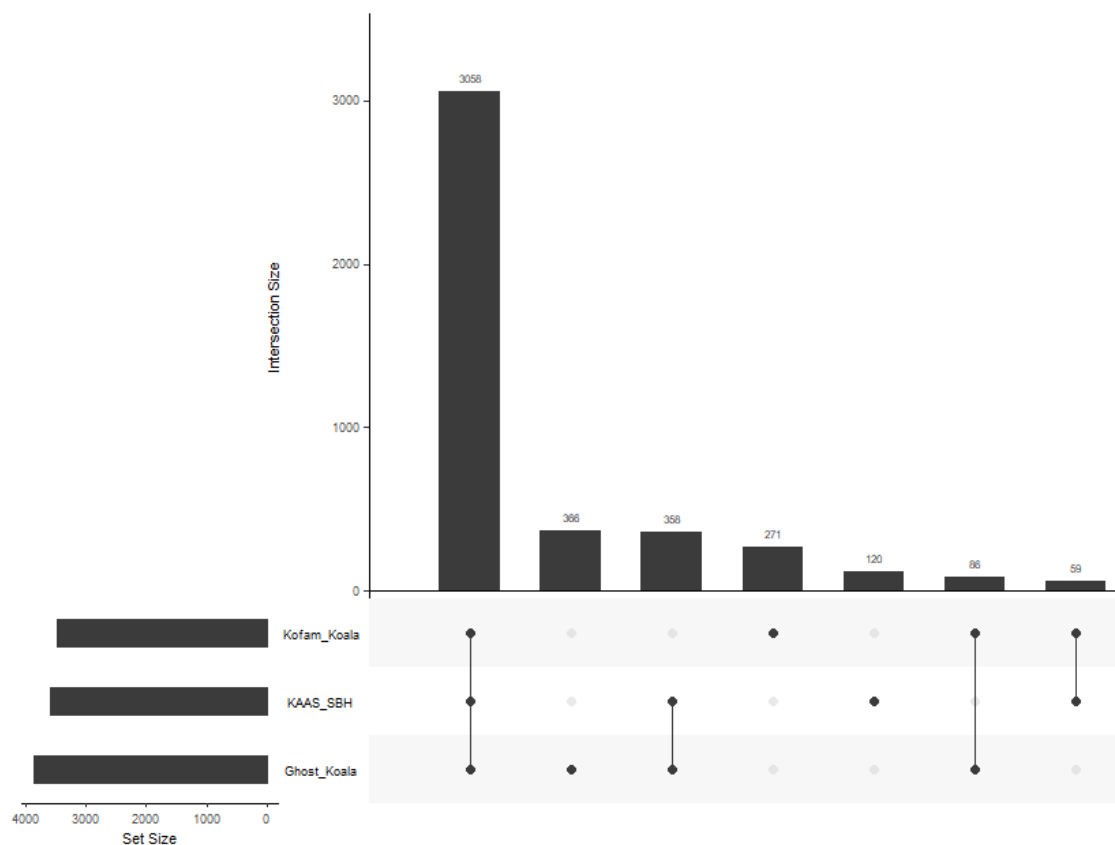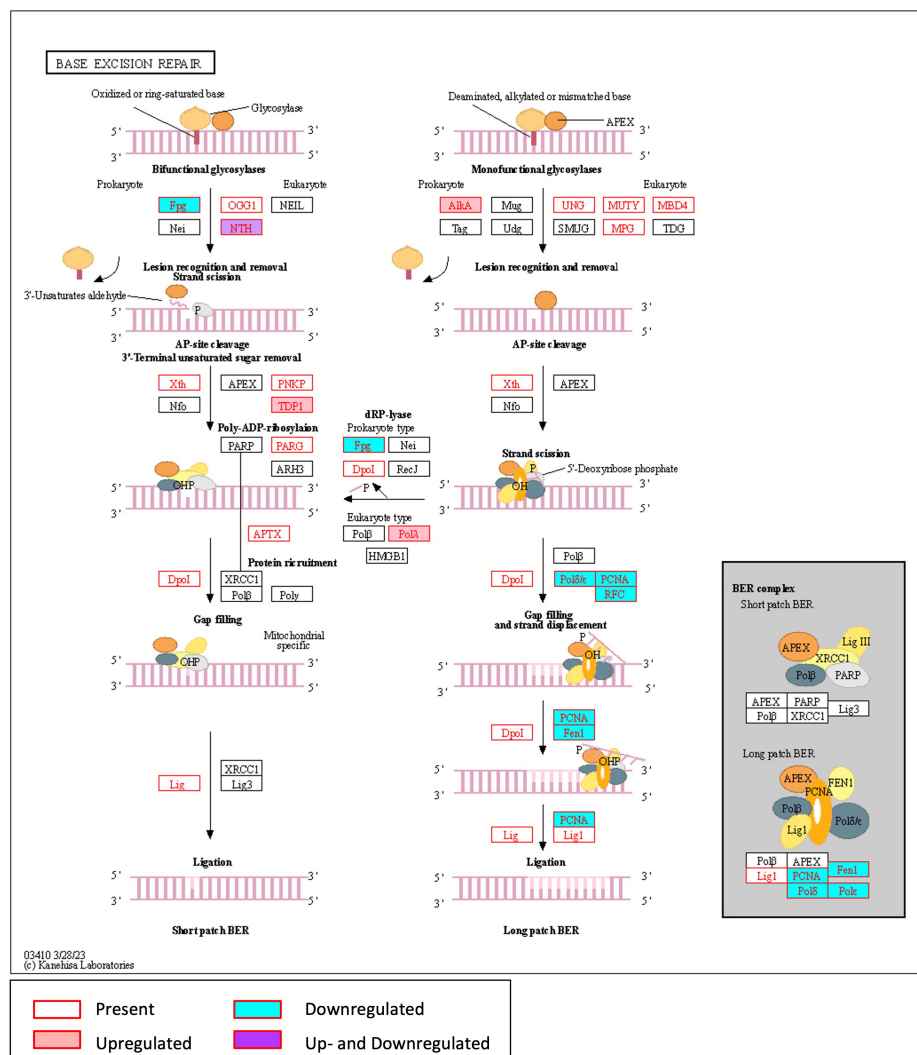**Fig. S5 KEGG pathway mismatch repair.** Presence and regulation in *S. testaceovaginata* are indicated by the color of the boxes.

Fig. S6 GO terms enriched in downregulated genes.

Fig. S7 Phylogenetic tree of CHS.

Fig. S8 Phylogenetic tree of CHALCONE ISOMERASE (CHI) and CHI-Like (CHIL).

Fig. S9 Phylogenetic tree of UGT.

Fig. S10 Phylogenetic tree of ligB genes.

Fig. S11 Phylogenetic tree of caffeoylshikimate esterases.

MONOACYLGLYCEROL LIPASES (MAGLS)/ESTERASE FAMILY

Fig. S12 Phylogenetic tree of BAHD acyltransferases.

Fig. S13 Phylogenetic tree of NAD(P)H-dependent reductases (CAD and CCR-like).

Fig. S14 Phylogenetic tree of *O*-methyltransferases.

O-METHYLTRANSFERASES

Danio rerio (Zebrafish) A4IG53 Catechol OMT
Rattus norvegicus P22734 Catechol O-methyltransferase
Dunaliella salina KAF5838081 putative SAM-MT
Klebsormidium nitens GAQ84666 putative OMT
Selaginella moellendorffii XP_002979270 catechol-OMT
Marchantia paleacea KAG6558114 Caffeic acid-OMT
Haplomitrium mnioides QCG81601 CCoAOMT
TRINITY_DN5278_c0_g1_i2.p1
TRINITY_DN7410_c0_g2_i1.p1
TRINITY_DN7410_c0_g1_i2.p1
TRINITY_DN7410_c0_g1_i6.p1
TRINITY_DN2526_c2_g1_i16.p2
TRINITY_DN2526_c2_g1_i15.p1
TRINITY_DN6561_c0_g1_i14.p1
TRINITY_DN6561_c0_g1_i10.p2
TRINITY_DN6561_c0_g1_i8.p1
TRINITY_DN6561_c0_g1_i6.p1
Zea mays CAB45149 caffeoyl-CoA OMT
Pinus taeda Q9ZTT5 CCoAMT
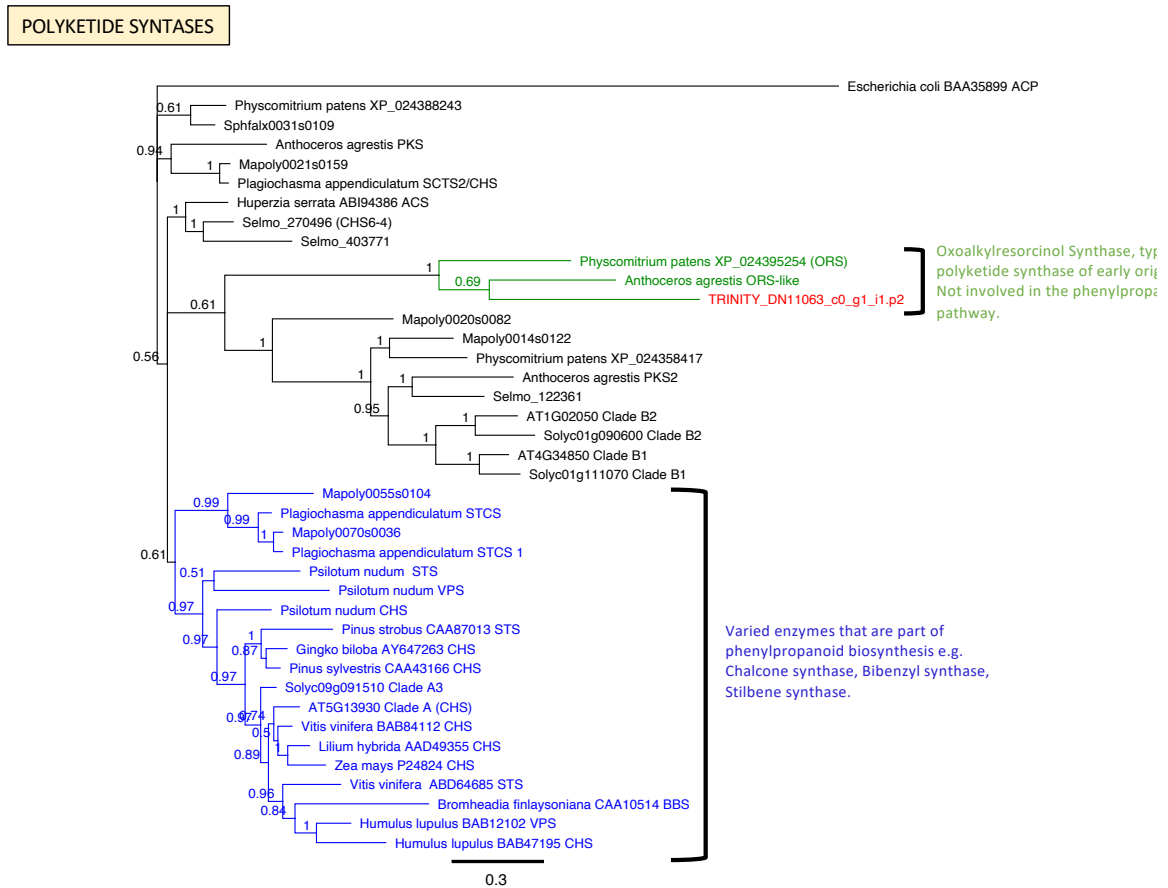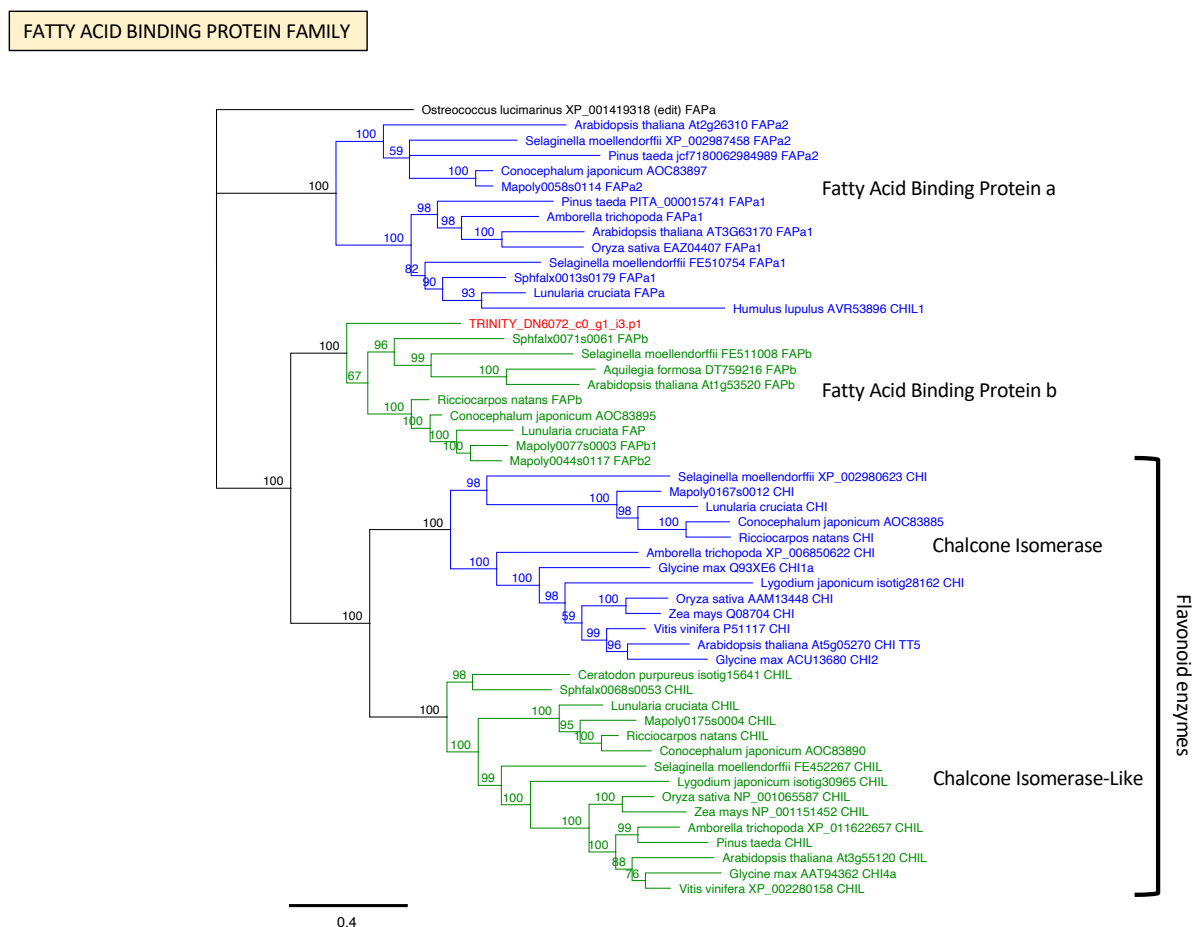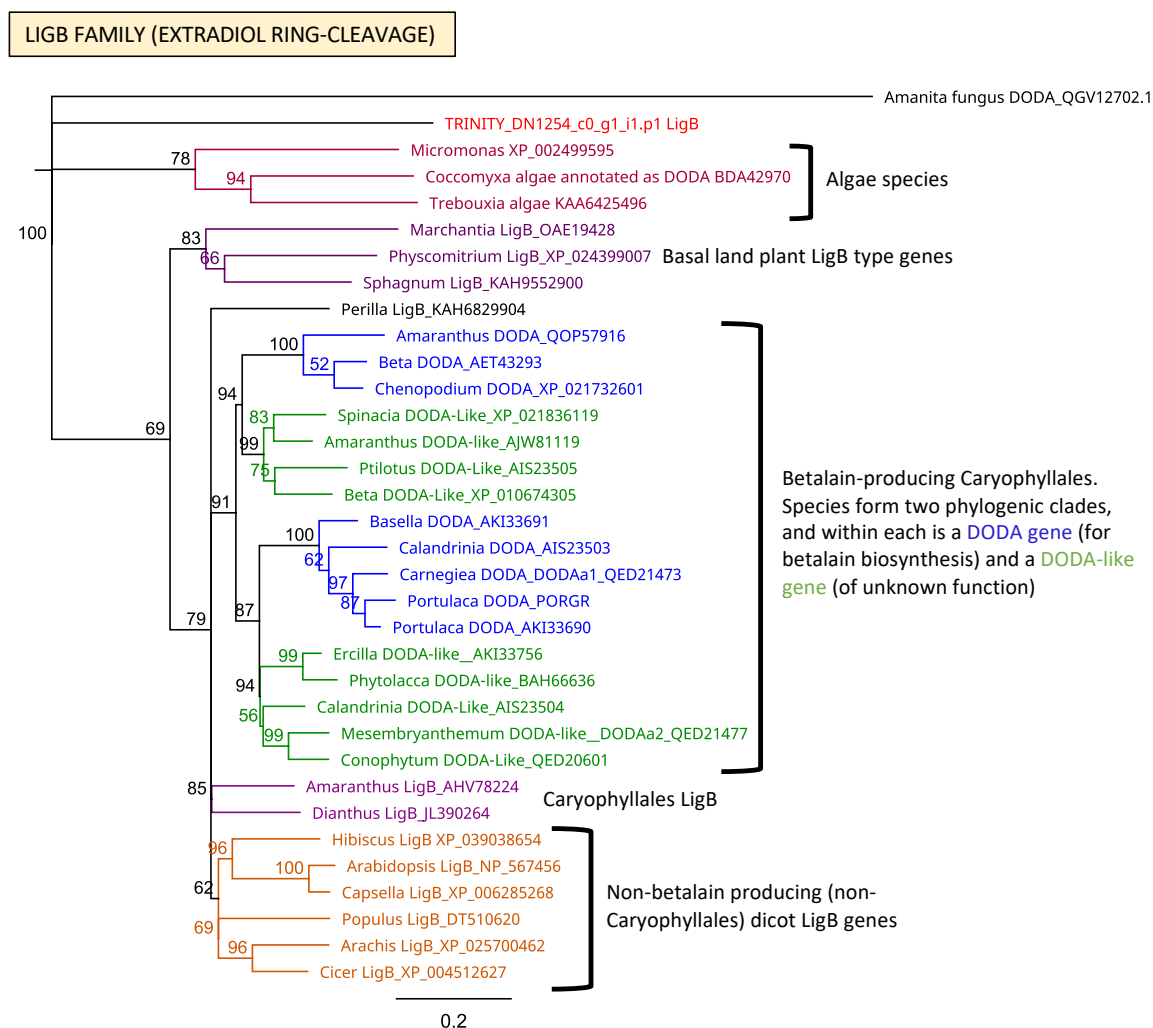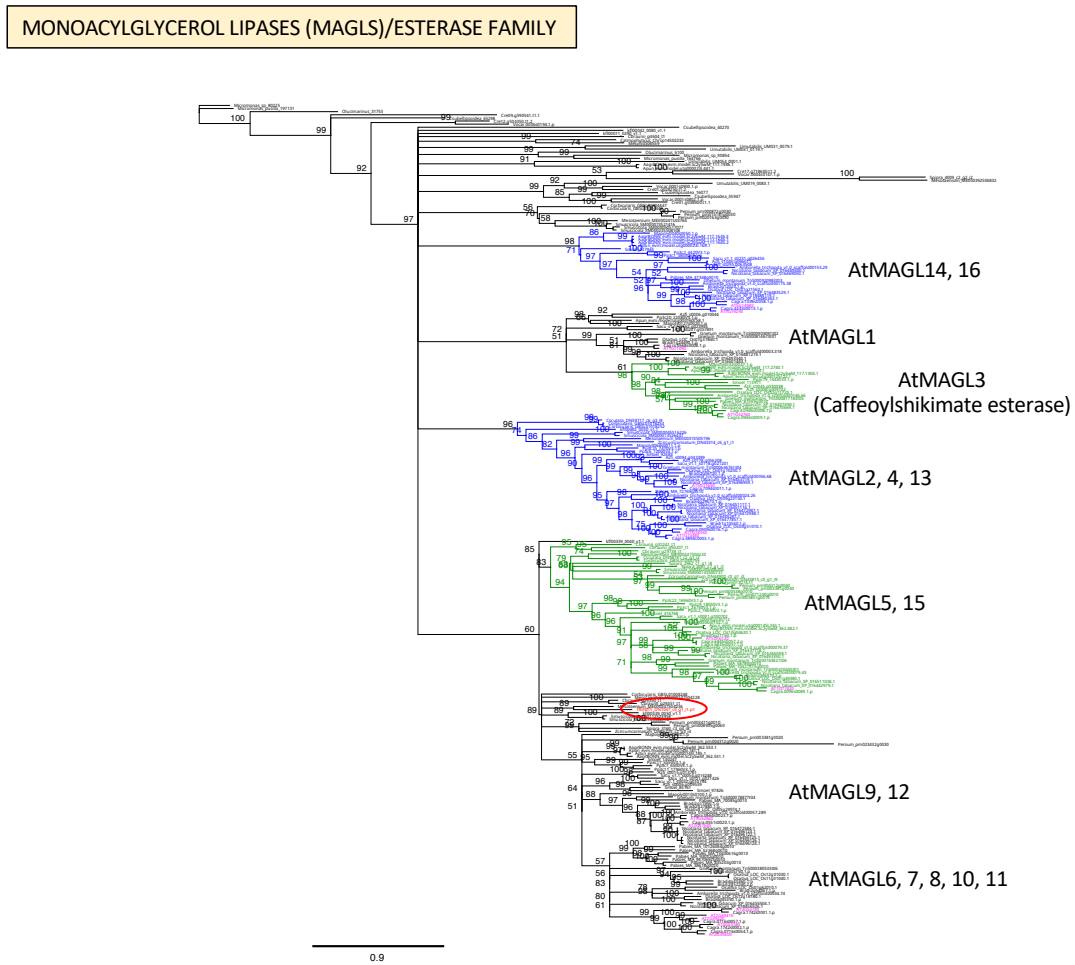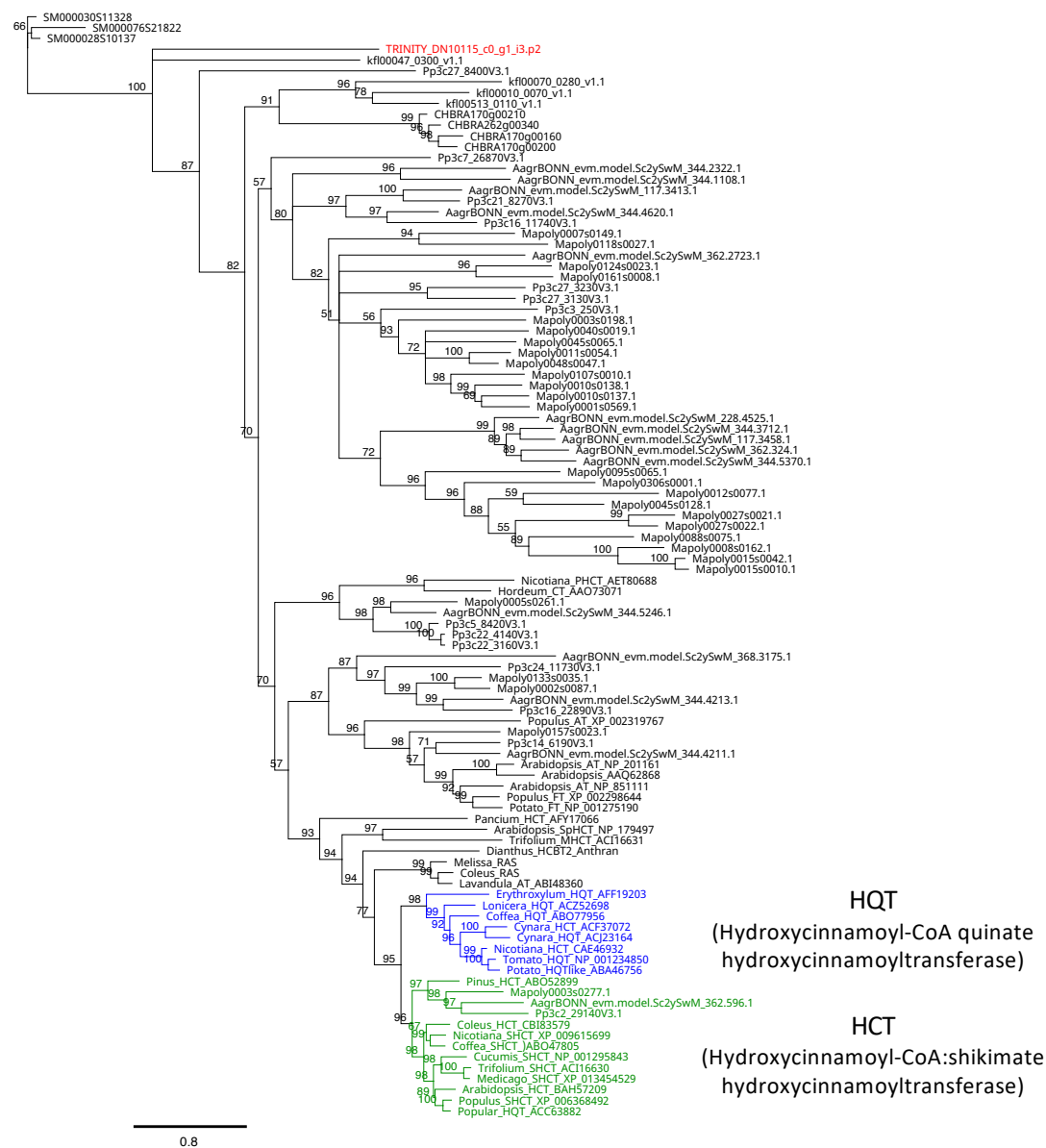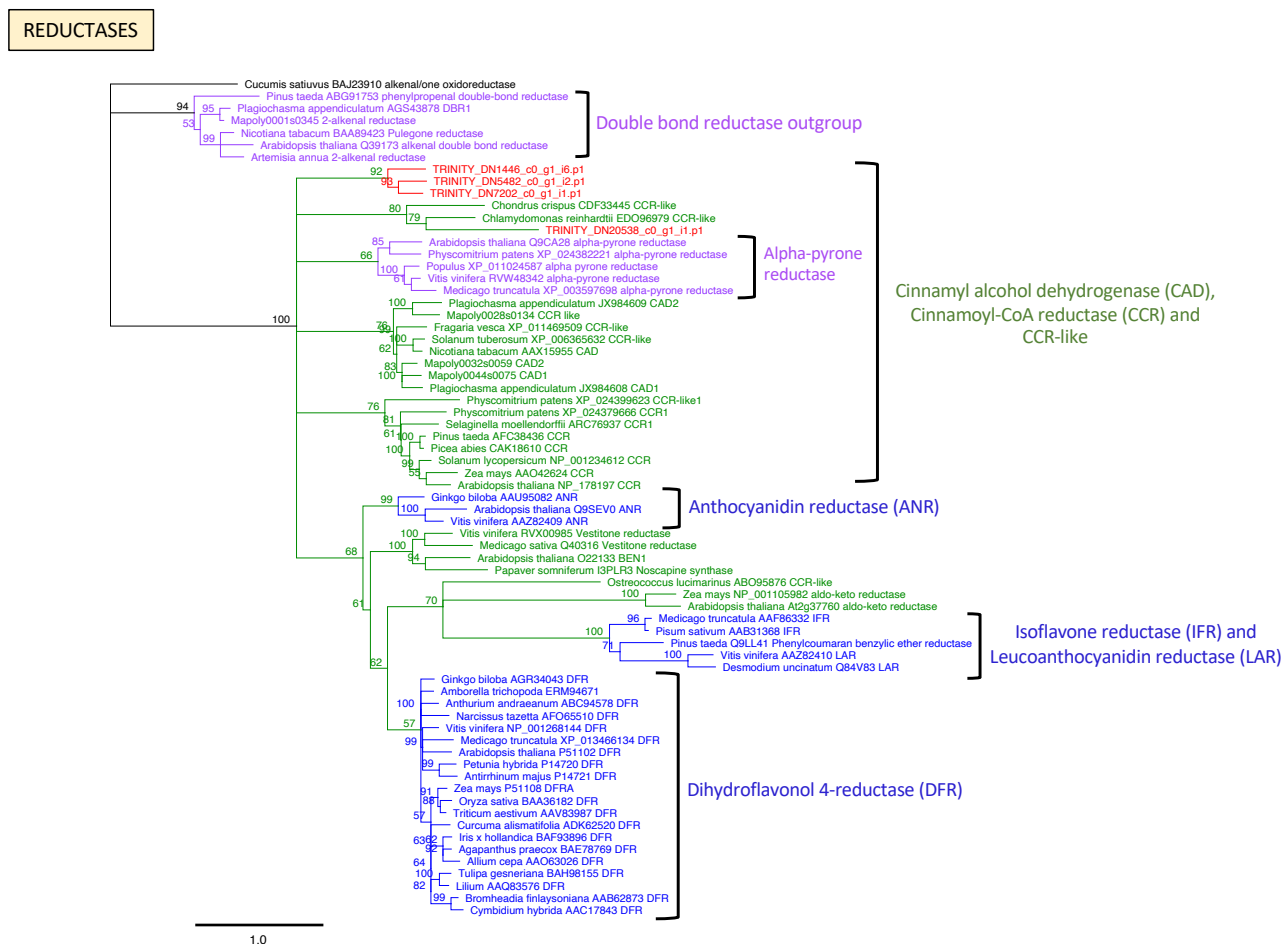Arabidopsis thaliana AAM64800 caffeoyl-CoA OMT
Cyclamen persicum BAK74804 anthocyanin OMT
Petunia hybrida AIE77047 anthocyanin OMT
Torenia hybrida BAP74301 anthocyanin 3'5'-OMT
Sesamum indicum XP_011086775 flavonoid 3',5'-OMT
Vitis vinifera C7AE94 Anthocyanin-OMT
Fragaria vesca XP_004299737 flavonoid 3',5'-OMT
TRINITY_DN8655_c0_g2_i1.p1
Prunus mume XP_008241354 Caffeic acid 3-OMT
Mapoly0044s0121
Mapoly0044s0123
Mapoly0044s0122
Plagiochasma appendiculatum COMT4
Plagiochasma appendiculatum ARS23163 F4'OMT
Mapoly0681s0001
Mapoly0136s0036
Mapoly0040s0105
Mapoly0002s0065
Mapoly0002s0063
Mapoly0002s0334
Mapoly0129s0005
Mapoly0015s0023
Mapoly0055s0090
Mapoly0055s0089
Mapoly0015s0025
Mapoly0129s0006
Mapoly0015s0024
Mapoly0013s0033
Mapoly0337s0001
Mapoly0015s0026
Hevea Reticuline XP_021682741 7 OMT
Pinus sylvestris AQX17822 COMYT like
Morus notabilis XP_010094294 Norcoclaurine 6 OMT
Arabidopsis thaliana Q9T003 Acetylserotonin OMT
Ocimum basilicum AFU50300 Flavonoid OMT6
Mentha x piperita AAR09602 Flavonoid 4'OMT
Ocimum basilicum AFU50295 Flavonoid OMT1
Mentha x piperita AAR09599 Flavonoid 7OMT
Thalictrum flavum Q5C9L7.1 norcoclaurine 6OMT
Papaver somniferum Q6WUC1 norcoclaurine 6OMT
Ocimum basilicum Q93WU2 (Iso)eugenol OMT
Catharanthus roseus Q8GSN1 MyricetinOMT
Mentha x piperita Q6VMW0 Flavonoid 8OMT
Vitis vinifera resveratrol B6VJS4 di-OMT
Hordeum vulgare CAA54616 Flavonoid 7OMT
Glycine max C6TAY1 Flavonoid 4'OMT SOMT2
Glycyrrhiza echinata Q84KK6 Isoflavone 4'-OMT
Pisum sativum O24305 (+)-6a-hydroxymaackiain 3-OMT
Lotus japonicus Q84KK4 Isoflavone 4'-OMT
Selaginella moellendorffii ADE88153 COMT like
Asparagus officinalis XP_020260885 caffeic acid 3 OMT
Thalictrum flavum Scoulerine 9OMT
Pinus sylvestris Pinosylvin-OMT
Gingko bilboa AER35881 OMT
Mentha x piperita AAR09601 Flavonoid 3'OMT
Chrysosplenium americanum Q42653 Flavonoid 3OMT
Arabidopsis thaliana XP_020871511 Flavonoid 3'OMT
Triticum aestivum Q38J50 Flavonoid 3'4'5'-OMT
Oryza glaberrima XP_052165229 flavone 3'-OMT
Oryza sativa Q6ZD89 Flavonoid 3'OMT1
Zea mays NP_001106047 caffeic acid-OMT
Oryza sativa BAM13734 Caffeic acid 7OMT
Citrus sinensis XP_006493515 Anthranilate NMT
Solanum pennellii XP_015079768 Caffeic acid 3OMT
Solanum lycopersicum flavonol 3'OMT
Cicer arietinum Isoliquiritigenin XP_004491872 2'OMT
Epimedium sagittatum AIS92510 Caffeic acid OMT
Populus trichocarpa XP_002302677 Eugenol OMT
Nicotiana tormentosiformis XP_018625480 caffeic acid 3-OMT
Capsicum annuum XP_016545476 cs caffeic acid 3-OMT
Solanum lycopersicum NP_001306101 catechol-OMT
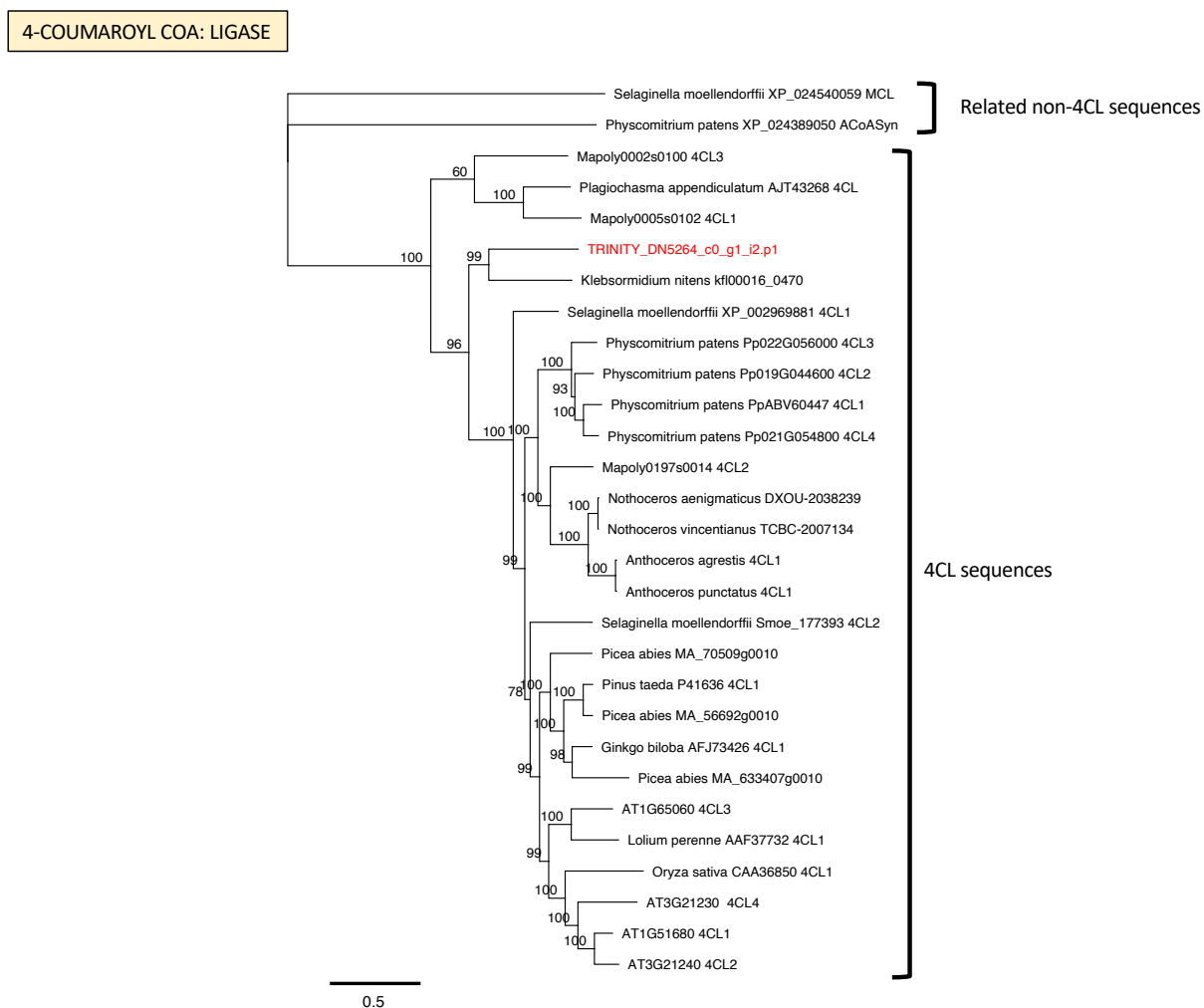Lycium ferocissimum XP_059301525 catechol OMT

0.9

Fig. S15 Phylogenetic tree of 4-Coumaroyl CoA: ligase (4CL).

Fig. S16 Phylogenetic tree of class III peroxidases (PRXIII) from streptophyte representatives (algae, bryophytes, ferns and flowering plants). Sequences of streptophyte algae are highlighted in red and ultrafast bootstrap values are shown at the branches. Scale bar = number of expected substitutions per site. * annotation stems from RedOxiBase (samples were wrongly annotated in the 1kp dataset and might originate from *Zygnema* sp.)

Table S1 Recipe of algal culture medium KW. One milliliter of each stock solution is added to one liter of demineralized water. The pH should be around 6.

Components	Stock solution
HEPES	238.1 g/l dH$_2$O
KNO$_3$	100 g/ l dH$_2$O
MgSO$_4$ x 7 H$_2$O	20 g/l dH$_2$O
NaH$_2$PO$_4$ x H$_2$O	0.69 g/50 ml
Na$_2$HPO$_4$ x 2 H$_2$O	0.89 g /50 ml
CaCl$_2$ x 2 H$_2$O	14.7 g/l dH$_2$O
P-II Metals stock solution	
EDTA (Titriplex III)	3.00 g/l dH2O
H$_3$BO$_3$	1.14 g/l dH2O
MnCl$_2$ x 4 H$_2$O	144.00 mg/l dH2O
ZnSO$_4$ x 7 H$_2$O	21.00 mg/l dH2O
CoCl$_2$ x 6 H$_2$O	4.00 mg/l dH2O
Fe-EDTA stock solution	
EDTA (Titriplex II)	5.22 g / l dH2O
FeSO$_4$ x 7 H$_2$O	4.98 g / l dH2O
1N KOH	54.00 ml / l dH2O

Table S2 Streptophyte green algal transcriptomes and genomes screened for class III peroxidases.

| Strain	Data type	Source of data	Data availability
Penium margaritaceum AEKF	Transcriptome	1kp project	https://www.onekp.com/public_data.html
Chaetosphaeridium globosum DRGY	Transcriptome	1kp project	https://www.onekp.com/public_data.html
Netrium digitus FFGR	Transcriptome	1kp project	https://www.onekp.com/public_data.html
Klebsormidium subtile FQLP	Transcriptome	1kp project	https://www.onekp.com/public_data.html
Spirogyra sp. HAOX	Transcriptome	1kp project	https://www.onekp.com/public_data.html
Cylindrocystis cushleckae JOJQ	Transcriptome	1kp project	https://www.onekp.com/public_data.html
Spirotaenia minuta NNHQ	Transcriptome	1kp project	https://www.onekp.com/public_data.html
Coleochaete irregularis QPDY	Transcriptome	1kp project	https://www.onekp.com/public_data.html
Cosmarium ochthodes STKJ	Transcriptome	1kp project	https://www.onekp.com/public_data.html
Coleochaete scutata VQBJ	Transcriptome	1kp project	https://www.onekp.com/public_data.html
Mesotaenium endlicherianum WDCW	Transcriptome	1kp project	https://www.onekp.com/public_data.html
Roya obtusa XRTZ	Transcriptome	1kp project	https://www.onekp.com/public_data.html
Cylindrocystis brebissonii YOXI	Transcriptome	1kp project	https://www.onekp.com/public_data.html
Mougeotia sp. ZRMT	Transcriptome	1kp project	https://www.onekp.com/public_data.html
Mesotaenium endlicherianum	Genome	Cheng et al., 2019	https://figshare.com/articles/dataset/Genomes_of_subaerial_Zygnematophyceae_provide_insights_into_land_plant_evolution/9911876/1
Spirogloea muscicola	Genome	Cheng et al., 2019	https://figshare.com/articles/dataset/Genomes_of_subaerial_Zygnematophyceae_provide_insights_into_land_plant_evolution/9911876/1
Chaetosphaeridium globosum SAG26.98	Transcriptome	Cooper and Delwiche, 2016	https://figshare.com/articles/dataset/Green_algal_transcriptomes_for_phylogenetics_and_comparative_genomics/1604778
Coleochaete orbicularis	Transcriptome	Cooper and Delwiche, 2016	https://figshare.com/articles/dataset/Green_algal_transcriptomes_for_phylogenetics_and_comparative_genomics/1604778
Klebsormidium flaccidum UTEX 321	Transcriptome	Cooper and Delwiche, 2016	https://figshare.com/articles/dataset/Green_algal_transcriptomes_for_phylogenetics_and_comparative_genomics/1604778
Mougeotia scalaris SAG164.80	Transcriptome	Cooper and Delwiche, 2016	https://figshare.com/articles/dataset/Green_algal_transcriptomes_for_phylogenetics_and_comparative_genomics/1604778
Nitella mirabilis transcriptomes of lower and upper tissues	Transcriptome	Cooper and Delwiche, 2016	https://figshare.com/articles/dataset/Green_algal_transcriptomes_for_phylogenetics_and_comparative_genomics/1604778
Penium margaritaceum SAG22.82	Transcriptome	Cooper and Delwiche, 2016	https://figshare.com/articles/dataset/Green_algal_transcriptomes_for_phylogenetics_and_comparative_genomics/1604778
Spirogyra pratensis UTEX 921	Transcriptome	Cooper and Delwiche, 2016	https://figshare.com/articles/dataset/Green_algal_transcriptomes_for_phylogenetics_and_comparative_genomics/1604778
Spirogyra sp. Transcriptome Au1	Transcriptome	Cooper and Delwiche, 2016	https://figshare.com/articles/dataset/Green_algal_transcriptomes_for_phylogenetics_and_comparative_genomics/1604778

Serritaenia sp. OBE.sm1	Transcriptome	This study	https://www.ebi.ac.uk/ena/browser/view/PRJEB72628
Serritaenia sp. OBE.1	Transcriptome	This study	https://www.ebi.ac.uk/ena/browser/view/PRJEB72628
Cylindrocystis crassa SAG23.97	Transcriptome	This study	https://www.ebi.ac.uk/ena/browser/view/PRJEB72628
Mesotaenium endlicherianum SAG12.97	Transcriptome	Dadras et al., 2022	https://mesotaenium.uni-goettingen.de/download.html
Mougeotiopsis calospora MZCH580	Transcriptome	Hess et al., 2022	https://www.ncbi.nlm.nih.gov/Traces/wgs/?val=GJZN01

A diverse group of underappreciated zygnematophytes deserves in-depth exploration

Published in Applied Phycology

Chapter III
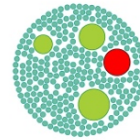
British Phycological Society
Understanding and using algae

Taylor & Francis
Taylor & Francis Group

OPEN ACCESS   Check for updates

A diverse group of underappreciated zygnematophytes deserves in-depth exploration

Anna Busch and Sebastian Hess

Institute for Zoology, University of Cologne, Cologne, Germany

ABSTRACT

The conjugating green algae (Zygnematophyceae) are the closest relatives of land plants and hence are of great evolutionary interest. Besides the popular placoderm desmids and the filamentous species, there is an underappreciated diversity of unicellular zygnematophytes with a much "simpler" morphology and smooth cell walls – traditionally referred to as "saccoderm desmids". These saccoderm desmids have a broad geographic distribution and are ecologically diverse. Many species inhabit terrestrial habitats such as dead wood, rock surfaces and glacial ice. Furthermore, several of the saccoderm genera have turned out to be highly polyphyletic and are typically poorly captured by environmental sequencing approaches. One of these genera is *Mesotaenium* Nägeli, with ~70 described species and infraspecific taxa united only by a relatively simple (plate- or ribbon-like) chloroplast structure. Here, we shed some light on these inconspicuous yet important members of the algal flora and present an updated *rbc*L gene phylogeny of the conjugating green algae, including several new lineages of *Mesotaenium*-like zygnematophytes. We depict the subtle morphological differences among these lineages and discuss our updated phylogeny in the light of ecology and cell biology. In addition, we review published knowledge on photoprotective strategies of zygnematophytes, the latest insights into their evolutionary innovations, and address some technical challenges in exploring this elusive group of microalgae. Some new observations of saccoderm desmids in undersampled habitats and of their microbial associates (e.g., parasites) point to interesting avenues for future research.

Introduction

It is now well established that the conjugating green algae (Zygnematophyceae , Streptophyta) represent the sister clade of all land plants (Figure 1(a); Cheng et al. (2019); Timme, Bachvaroff, & Delwiche (2012); Wickett et al. (2014); Wodniok et al., 2011). Hence, these algae are of special interest as they can provide information on how members of the "green lineage" (Viridiplantae) became multicellular and conquered the land in a process termed "terrestrialization" (Delaux, Nanda, Mathé, Sejalon-Delmas, & Dunand, 2012; Gerrienne, Servais, & Vecoli, 2016). The sequence of evolutionary events and the physiological adaptations that might have paved the way to a "life on land" represent an exciting and timely field of research that has already led to some view-changing insights (Cannell et al., 2020; Cheng et al., 2019; de Vries, Curtis, Gould, & Archibald, 2018; Wang et al., 2021). Several cellular and metabolic features that were initially known only from land plants have also been found in streptophyte green algae. This includes a number of specific stress responses (de Vries et al., 2020; Holzinger et al., 2014),

homologues of phytohormone receptors (de Vries et al., 2018; Sun et al., 2019), and key enzymes of the phenyl-propanoid pathway (de Vries, de Vries, Slamovits, Rose, & Archibald, 2017). Furthermore, the evolutionary importance of the zygnematophytes was demonstrated in a genomic study that revealed horizontal gene transfer from soil bacteria to unicellular, terrestrial representatives of this algal class, most notably genes encoding homologues of GRAS transcription factors and PYR/PYL/RCAR-like abscisic acid receptors, which might have had roles in the terrestrialization of these algae (Cheng et al., 2019).

The Zygnematophyceae are stunningly diverse in terms of cellular organization, physiology and ecology (Brook & Williamson, 2010; Coesel & Meesters, 2007; Ettl & Gärtner, 2014; Guiry, 2013; Hall & McCourt, 2015). They probably encompass far more than the ca. 4,000 described species (Gerrath, 1993; Gontcharov, 2008; Šťastný & Kouwets, 2012), which are traditionally divided into three groups: the placoderm desmids, the saccoderm desmids and the filamentous forms (Figure 1(b)). Most in-depth studies on cell biology, ecology and genetics have been on
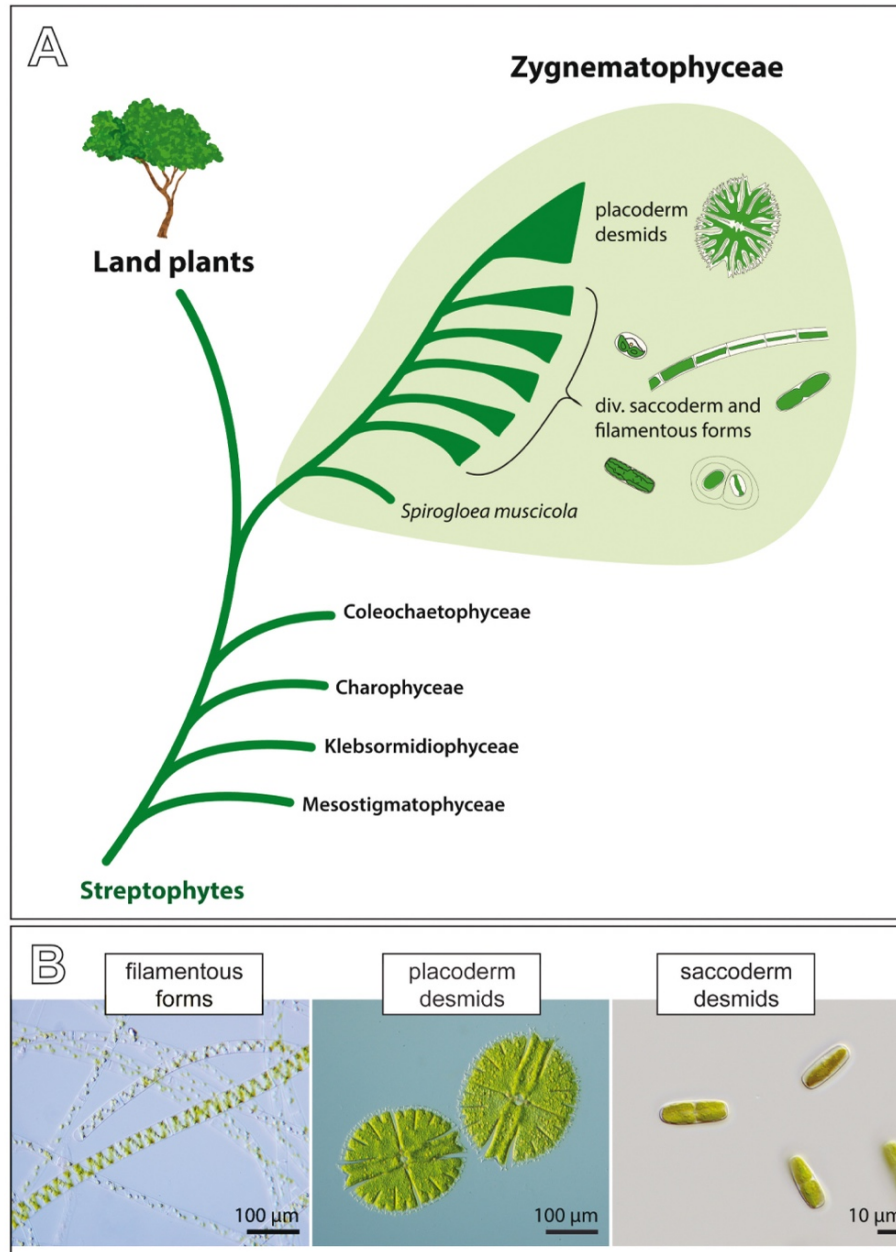
Figure 1. Evolutionary history of the Zygnematophyceae and depiction of the three morphologically defined groups of these algae. (a) Schematic phylogenetic tree of the Streptophyta showing the sister relationship of the Zygnematophyceae and land plants, and the internal diversity of zygnematophytes. Note that the saccoderm desmids plus the filamentous forms (traditionally referred to as "Zygnematales") are paraphyletic. Most of the internal phylogeny is unresolved except the deepest-branching position of *Spirogloea*. (b) Three traditional groups of zygnematophytes defined by gross cell morphology: filamentous zygnematophytes (*Spirogyra* spp.), placoderm desmids (*Micrasterias* sp.) with isthmus and obvious symmetry, and saccoderm desmids without isthmus and cell wall ornamentations (strain SAG 12.97, for details see main text).

the beautiful placoderm desmids, which are characterized by two symmetrical semi-cells, and on the filamentous species (e.g., de Vries et al., 2018; Hainz, Wöber, & Schagerl, 2009; Holzinger & Pichrtová, 2016; Kawai et al., 2022; Lütz-Meindl, 2016; Stastny, Skaloud, Langenbach, Nemjova, & Neustupa, 2013; Zhou, Wilkens, Hanelt, & von Schwartzenberg, 2021). The unicellular, structurally much simpler saccoderm desmids have not had as much attention in the more recent past – probably due to their relatively plain appearance and the difficulties in differentiating species and genera. In fact, the saccoderm desmids have turned out to be highly polyphyletic (Gontcharov,

2008; Gontcharov, Marin, & Melkonian, 2003, 2004). However, they are still lumped into a few ill-defined genera, most importantly *Mesotaenium* and *Cylindrocystis* (Guiry & Guiry, 2021), and their true diversity remains largely unrecognized (see also Mollenhauer, 1986). This is an impediment to science, as the saccoderm desmids vary greatly in ecology and cellular adaptations. They show a wide geographic distribution (including polar regions) and occur in habitats that vary strongly in temperature, chemical conditions and water availability (e.g., Busch & Hess, 2021; West & West, 1904; Williamson et al., 2020). Most notably, many saccoderm desmids colonize terrestrial habitats (Brook & Williamson, 2010; Ettl & Gärtner, 2014; Fučíková, Hall, Johansen, & Lowe, 2008) and might be valuable for exploring adaptive strategies to terrestrial stressors (Cheng et al., 2019).

In this work, we explored saccoderm desmids of the *Mesotaenium* type, i.e., unicellular zygnematophytes with a ribbon- or plate-like chloroplast, and provide an updated molecular phylogeny with 12 distinct lineages of these algae. A new, provisional clade nomenclature emphasizes the true genetic diversity of these organisms and enables unambiguous communication about them. Based on this system, we summarize the structural and ecological variations found in *Mesotaenium*-like zygnematophytes and discuss their photoprotective adaptations, which we trust will inspire future research on these underappreciated microalgae.

Material and methods

Sampling, isolation and maintenance of algal strains

Natural samples (mostly algal biofilms on surfaces) were collected at several sites in Germany and in the Great Smoky Mountains, USA, as listed in Supplementary table S1. The samples were suspended in water, and single algal cells were isolated with a micropipette, washed in sterile water and transferred into the liquid growth medium Waris-H (McFadden & Melkonian, 1986). After several weeks of growth under artificial light (white LEDs, photon fluence rate 30 µmol m^{-2} s^{-1}, 14:10 h light–dark cycle) at 16°C, the resulting cells were ultrasonicated on ice (max. 10 s) with the XL-2000 ultrasonicator (Misonix Inc., USA) or the UW 2070 ultrasonicator (Bandeline electronic, DE) to liberate cells from the mucilage and sprayed onto solidified culture medium Waris-H (1.5% agar) with pressurized air. After a few days of incubation at 16°C, bacteria-free cells picked and transferred to liquid culture medium were used as sources of the axenic cultures used in this study. Very homogeneous natural samples

of *Mesotaenium*-like zygnematophytes were directly ultrasonicated and spray-plated as detailed above. The liquid cultures were maintained at a photon fluence rate of 30 µmol m^{-2} s^{-1}, a 14:10 h light–dark cycle, at 16°C, and were subcultured about every 2 months. Cultures on agar slants (solidified Waris-H) were maintained at 10°C and subcultured every 6 months. As indicated in Supplementary table S1, several of the studied strains were obtained from public culture collections, namely the Culture Collection of Algae at the University of Cologne (CCAC, now Central Collection of Algal Cultures in Essen, Germany), Culture Collection of Algae at Göttingen University (SAG, Germany) and the Coimbra Culture Collection of Algae (ACOI, Portugal). The strains isolated during this study can be obtained from the corresponding author (SH) upon request.

Light microscopy and photography

Images of algal growth types were taken with a Nikon D3100 digital single-lens reflex camera (Nikon, Tokyo, Japan) equipped with RAYNOX Macro Conversion Lenses (Yoshida Industry Co., Ltd., Tokyo, Japan). Regular brightfield microscopy and photodocumentation of cultures used the Motic AE2000 inverted microscope (Motic Hong Kong Limited, Hong Kong) equipped with a MikroLive 6.4MP CMOS camera (MikroLive, Oppenau). For high-resolution imaging, the Zeiss IM35 inverted microscope (Carl Zeiss, Oberkochen, Germany) equipped with the objective lenses Plan 40×/0.65 and Planapochromat 63×/1.4, electronic flash and the Canon EOS 6D digital single-lens reflex camera (Canon, Tokyo, Japan) was used, or the Zeiss Axio Observer inverted microscope equipped with the objective lenses Plan-Neofluar 40×/1.3 and Plan-Neofluar 100×/1.3 and the Axiocam 512 colour (Carl Zeiss, Oberkochen, Germany) was used. The colour balance and contrast of micrographs were adjusted with Photoshop CS4 (Adobe Inc., California, USA).

DNA sequencing, alignment and molecular phylogenetics

Algal material from 2 ml of a running culture was collected by centrifugation (5,000 *g*, 5 min), resuspended in sterile water and lysed by ultrasonication on ice (5 × 5 s) with the XL-2000 ultrasonicator or by grinding in liquid nitrogen. In the case of ultrasonicated material, insoluble debris was pelleted by centrifugation (5,000 *g*, 1 min) and the supernatant was used directly as a template for PCR (details below). The ground material was subjected to Chelex extraction as follows: 1–10 µl of

the algal suspension/frozen material was mixed with 50 µl Tris-HCl buffer (10 mM; pH 8.5), Chelex 100 beads (5%; Sigma-Aldrich) and 2 µl proteinase K (20 mg ml^{-1}; Thermo Fisher Scientific, Massachuesetts, USA), then incubated at 56°C for 45 min and finally at 98°C for 20 min. The samples were centrifuged at 17 000 g for 3 min, and the supernatant was used for PCR. The chloroplast-encoded gene for the large chain of the ribulose bisphosphate carboxylase (rbcL) was amplified by a semi-nested PCR with the primers MaGo1F, MaGo2F and MaGo3R (Gontcharov et al., 2004) and Invitrogen Taq DNA Polymerase (Thermo Fisher Scientific, Massachuesetts, USA) or the repliQa HiFi ToughMix (Quanta Bio, Massachuesetts, USA), sequenced and assembled as previously described (Busch & Hess, 2021). The generated rbcL gene sequences have been deposited in GenBank under the accession numbers OM241454–OM241471. The sequences were manually aligned with rbcL gene sequences of other Zygnematophyceae (alignment from Busch & Hess, 2021) using the SeaView 4.5.4 alignment editor (Galtier, Gouy, & Gautier, 1996; Gouy, Guindon, & Gascuel, 2010). The resulting dataset of 92 sequences and 1295 sites (including all codon positions) was subjected to phylogenetic inferences with neighbour joining (NJ) and maximum likelihood (ML) methods using MEGA software version X (Kumar et al., 2018). For ML analyses, we applied the GTR+I +G model (discrete Gamma distribution; five categories). Branch support was assessed with 1000 bootstrap repetitions.

Results and discussion

Genetic and phenotypic diversity of Mesotaenium-like zygnematophytes

The structurally simplest zygnematophytes have mainly been assigned to the genus *Mesotaenium*. These inconspicuous, unicellular algae are characterized by a smooth cell wall and a more or less ribbon-like plastid (Nägeli, 1849). According to AlgaeBase, the genus *Mesotaenium* contains 29 recognized species and 39 infraspecific taxa (including synonyms; Guiry & Guiry, 2021), most of which were described on the basis of gross morphological characters such as the cell shape and size of vegetative material. Unfortunately, the lack of meaningful original descriptions has complicated species identification of these life forms, which is reflected in the conflicting information in different monographs about desmids (e.g., Brook & Williamson, 2010; Coesel & Meesters, 2007; Ettl & Gärtner, 2014; Lenzenweger, 2003). Molecular sequence information for a few of these species revealed that the genus

Mesotaenium is polyphyletic and that *Mesotaenium*-like zygnematophytes form at least six separate lineages within the conjugating green algae (Busch & Hess, 2021; Gontcharov, 2008; Gontcharov & Melkonian, 2010). Despite the available phylogenetic information, most of these lineages have not been studied in detail and we lack proper genus names for them. This leads to a general underappreciation of their actual genetic and ecological diversity. However, exceptions are the *Mesotaenium*-like zygnematophytes of the genera *Ancylonema* Berggren and *Serritaenia* A.Busch & S.Hess, which have recently been subjected to a more detailed characterization and a taxonomic treatment (Busch & Hess, 2021; Procházková, Řezanka, Nedbalová, & Remias, 2021). Increasing amounts of data for certain strains on the genomic, cell biological and ecological levels necessitates a clear nomenclatural separation of distinct phylogenetic lineages to avoid a mix-up in evolutionary interpretations. The genome-sequenced strain SAG 12.97, for example, has repeatedly been referred to as "*Mesotaenium endlicherianum*" (Cheng et al., 2019; Gontcharov, 2008; Gontcharov et al., 2003, 2004; Matasci et al., 2014), although, in our opinion, it does not match the original description of that species very well (Nägeli, 1849). Even though taxonomic problems will take much more time and effort to be resolved (e.g., by assessing original material from several species in question), an unambiguous naming system for the different lineages of *Mesotaenium*-like zygnematophytes and more biological data on them is desirable.

To further explore the diversity of *Mesotaenium*-like zygnematophytes, we sampled various aquatic and terrestrial habitats (see below for details) and obtained additional strains from public and private culture collections. In total, we studied 31 strains (listed in Supplementary table S1) and inferred a phylogenetic tree of the Zygnematophyceae based on the most widely available genetic marker for that algal class, the gene for the large chain of the ribulose bisphosphate carboxylase (rbcL gene). As shown in several published phylogenies, this gene is unable to resolve the deepest branches within the phylogeny but was well suited to differentiate new zygnematophycean lineages at the genus level (Figure 2). Our culture-based approach resulted in the identification of 12 lineages of *Mesotaenium*-like zygnematophytes, which are phylogenetically distinct; several of them could be distinguished by morphology as well (see below for details). Two lineages are credibly assigned to existing genera, namely the *Ancylonema* lineage and the *Serritaenia* lineage (Figure 2; Busch & Hess, 2021; Procházková et al., 2021). Taxonomic assignment of strains from other lineages will need
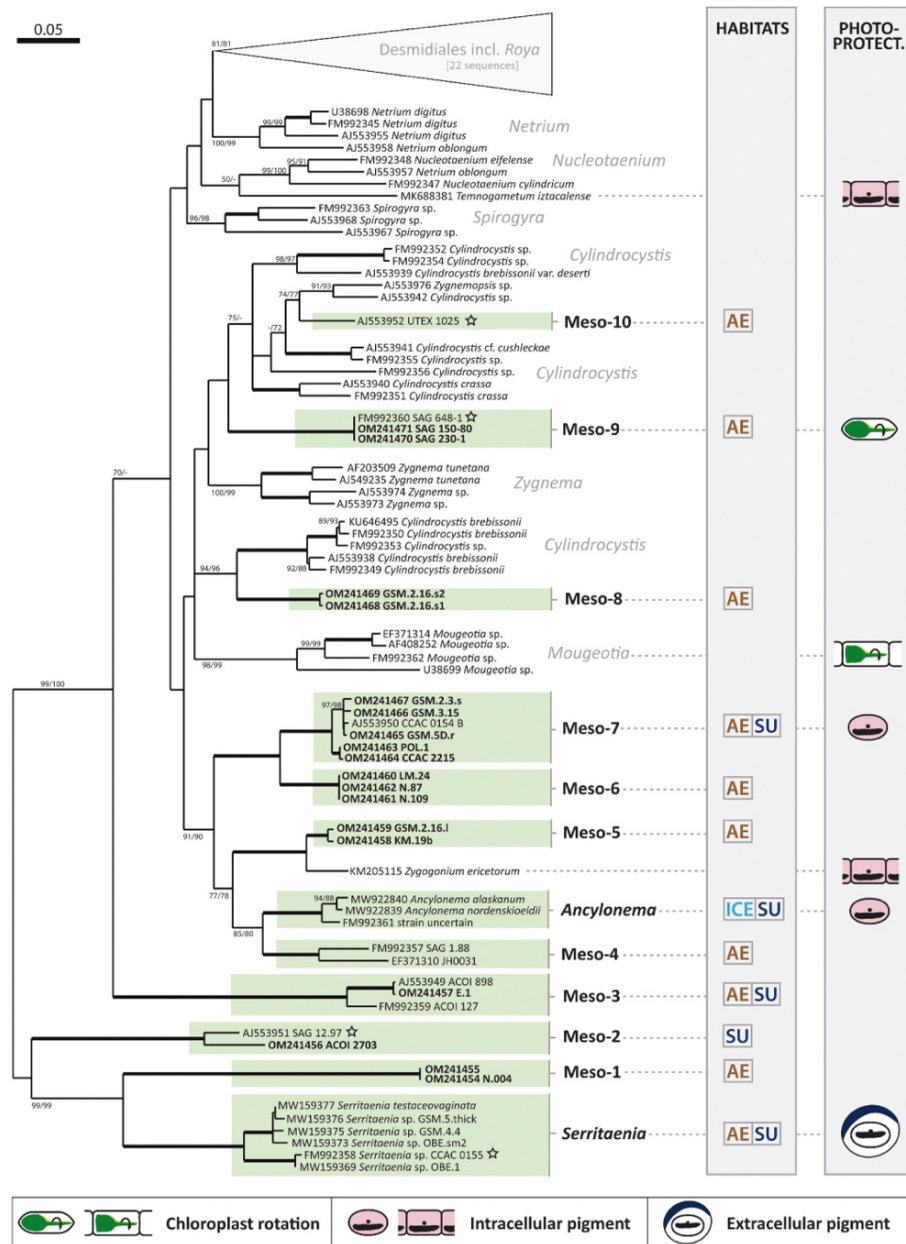
Figure 2. Maximum likelihood phylogeny of the Zygnematophyceae inferred from *rbc*L gene sequences revealing 12 lineages of *Mesotaenium*-like zygnematophytes (highlighted in green). Bootstrap support values (1000 replicates) are shown at the branches (ML/NJ), except for those with full support (100%; bold branches) or support below 50% with the ML inference (omitted). New sequences generated in this study are in bold and *Mesotaenium*-like zygnematophytes with genome or transcriptome data are denoted by stars. The two grey columns on the right indicate the habitat types (AE = aerophytic, SU = submerged, ICE = ice/snow) and photoprotective adaptations (see legend at the bottom of the figure) of *Mesotaenium*-like algae and some other zygnematophytes. The scale bar represents 0.05 expected substitutions per site.

careful re-evaluation, as detailed in the lineage-specific sections below. For these lineages, we introduce a provisional nomenclature from "Meso-1" to "Meso-10" (Figure 2). Similar approaches have been used to name phylogenetic clades in other groups of microbial

eukaryotes, e.g., in the rhizarians (e.g., Bass & Cavalier-Smith, 2004; Bass et al., 2009), alveolates (e.g., Guillou et al., 2008) and stramenopiles (e.g., Massana et al., 2004; Massana, Del Campo, Sieracki, Audic, & Logares, 2014). Some lineages in our phylogeny are

directly related to each other but still have distinct designations (e.g., Meso-1, Meso-2 and the *Serritaenia* lineage). This is based on clear-cut phenotypic differences and marked genetic distances.

An overview of the morphological diversity of *Mesotaenium*-like zygnematophytes from different lineages is given in Figure 3. All cells have a smooth cell wall and no isthmus but vary largely in size. While some strains are smaller than 10 μm, others exceed 100 μm in length (compare Meso-1 and Meso-10 in Figure 3). Important diagnostic characters include the cell shape, chloroplast number in interphase,

chloroplast morphology and position, pyrenoid morphology and position of the nucleus. Cell shapes can be roughly categorized as cylindrical (e.g., *Serritaenia*, Meso-1), elliptical (e.g., Meso-7) or elongate with rounded (e.g., Meso-6), conical (e.g., Meso-3, Meso-9) or truncate (e.g., Meso-2) cell ends. The chloroplasts range in number from one (*Serritaenia*, Meso-1 and Meso-2) to two (Meso-4, Meso-5 and Meso-7) and can occupy a parietal (e.g., Meso-2, Meso-6 and Meso-7) or axial position (e.g., *Serritaenia*, Meso-3 and Meso-8). True ribbon-like, axial chloroplasts as described for the type species of the genus *Mesotaenium*

Figure 3. Morphological diversity of *Mesotaenium*-like zygnematophytes (differential interference contrast). (a) Strain GSM.5.thin (*Serritaenia testaceovaginata*). (b) Strain KH.2.sm (lineage Meso-1). (c) Strain SAG 12.97 sometimes referred to as "*M. endlicherianum*" (lineage Meso-2). (d) Strain E.1 (lineage Meso-3). (e) Strain GSM.2.16.s2 (lineage Meso-8). (f) Strain SAG 230–1 (lineage Meso-9). (g) Strain GSM.2.16.l (lineage Meso-5). (h) Strain SAG 1.88 (lineage Meso-4). (i) Strain LM.24 (lineage Meso-6). (j) Strain CCAC 2215 (lineage Meso-7). (k) Strain UTEX 1025 (lineage Meso-10). Scale bar in (a) is 10 μm and applies to all panels.

(*M. endlicherianum* Nägeli) have so far only been found in the lineages Meso-3 and Meso-9, suggesting that the genus *Mesotaenium* might belong to one of these lineages. However, currently, there is no strain that clearly matches the original description of *M. endlicherianum*, so that this important genus name cannot be applied with certainty. More common are lenticular (e.g., Meso-1 and Meso-7) and channel-like chloroplasts (Meso-2). Almost all lineages have chloroplasts with smooth margins, with the exception of *Serritaenia* (serrate/dentate margins) and Meso-2 (undulating margins). Pyrenoids are present in all lineages and vary in shape (circular or lentiform), size and conspicuousness. The nuclei of all studied strains are fairly inconspicuous but can be identified by the central spherical nucleolus. The position of the nucleus within the cell is of great diagnostic value. It is either central, i.e., on the longitudinal cell axis (often nested between the chloroplasts: Meso-5, Meso-6, Meso-7 and Meso-8), or displaced by the chloroplast (*Serritaenia*, Meso-1 and Meso2). It is important to note that some characters, especially chloroplast morphology, can vary with environmental conditions (e.g., *Serritaenia* species develop additional chloroplast ridges in laboratory culture; Busch & Hess, 2021) and that chloroplasts can be largely obscured by colourless globules (depending on the physiological state of the cells). Hence, cultures grown under defined conditions can have advantages in assessing the morphology of *Mesotaenium*-like zygnematophytes. This also applies to the chloroplast number, which doubles before cell division.

Mesotaenium-like zygnematophytes show also various "growth forms" in laboratory cultures, which probably result from differences in cell division and mucilage secretion. In liquid culture, cells can be solitary (Figure 4 (a); e.g., Meso-6, Meso-7), or form chains (Figure 4(b); e.g., Meso-2, Meso-5), gelatinous films on submerged surfaces and/or discrete gelatinous "colonies" (Figure 4 (c); e.g., *Serritaenia*, Meso-1). Colony morphology and colour on solid media show marked differences as well. While some lineages form irregular gelatinous masses (e.g., *Serritaenia*), others produce flat, film-like plaques with even (Figure 4(d); Meso-4) or erose (Figure 4(e); Meso-3) margins or raised colonies with irregular surface (Figure 4(f); Meso-1). All these observations on cell morphology and growth forms indicate profound biological variation in the 12 lineages of *Mesotaenium*-like zygnematophytes identified in this study. Short summaries of each of these lineages are provided in the following.

The *Serritaenia* lineage is the sister lineage of Meso-1 in our phylogeny with robust bootstrap support (99/99). The separation of the two lineages is based on clear-cut morphological differences and significant genetic
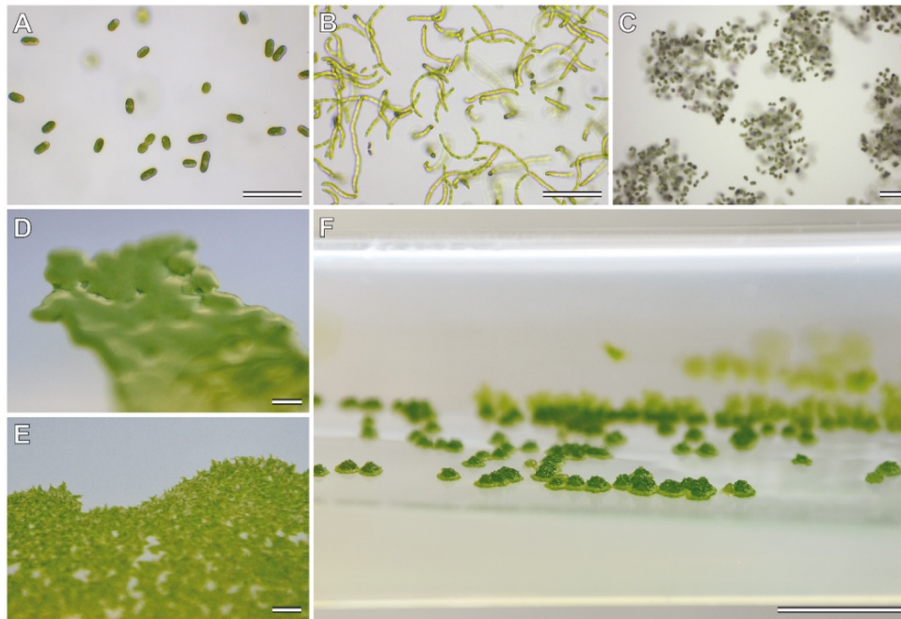

Figure 4. Growth forms of *Mesotaenium*-like zygnematophytes in culture. (a) Single cells in liquid culture, strain GSM.2.3.s (lineage Meso-7). (b) Cell chains in liquid culture, strain KM.19b (lineage Meso-5). (c) Colony-like mucilaginous aggregates in liquid culture, strain GSM.5.thin (*Serritaenia testaceovaginata*). (d) Shiny, smooth plaque with even margins on agar, strain SAG 1.88 (Meso-4) (e) Rough plaque with erose margins on agar, strain ACOI 127 (Meso-3). (f) Raised colonies with irregular surface on agar, strain KH.2.sm (Meso-1). Scale bars 100 μm in (a)–(c); 1 mm in (d) and (e); 5 mm in (f).

distance (Figures 2 and 3). The genus *Serritaenia* encompasses strains that were formerly associated with the species names *Mesotaenium macrococcum, M. braunii* and *M. testaceovaginatum*, but correct application of the two first names needs additional taxonomic research on difficult-to-obtain original material (for details see Busch & Hess, 2021). Interphase cells of *Serritaenia* species are mostly cylindrical with rounded cell ends (Figure 3(a)), while cells shortly after division are ovoid and show a typical angled arrangement. Chain formation was never observed in *Serritaenia*. The single chloroplast is an axial plate with serrated or indented margins (Figure 3(a)). The chloroplast can develop one or two additional ridges and thereby become more complex. In liquid laboratory cultures, *Serritaenia* cells can form irregular, gelatinous colonies (Figure 4(c)) or confluent mucilage films. However, the mucilage can be dissolved under certain environmental conditions, and the cells become solitary. *Serritaenia* species are most prominent in terrestrial habitats and are known from central Europe, the United Kingdom, North America and South America. Some species can form mass developments in the form of gelatinous biofilms on various substrates (dead wood, leaf litter, soil, and bryophytes). Furthermore, *Serritaenia* represents the only known lineage of the Zygnematophyceae whose members produce an extracellular sunscreen pigment (Busch & Hess, 2021). Despite some (questionable) statements in the older literature, intracellular (pinkish) pigments have never been observed by the authors of this study (potentially these statements are based on confusion with lineage Meso-7).

Lineage Meso-1 contains two strains which have identical *rbc*L gene sequences (Figure 2). The cells measure <15 μm in length and are cylindrical with rounded, rather flat cell ends. The plate-like or lenticular chloroplast with smooth margins is mostly parietal, rarely axial (Figure 3(b)). Both strains were isolated from bryophytes on dead wood in temperate forests of Germany. In these habitats, cells of lineage Meso-1 are entirely embedded in mucilage (which can form tube-like structures) and can co-occur with *Serritaenia* species. The cells of lineage Meso-1 resemble *Mesotaenium macrococcum* var. *lagerheimii* Willi Krieg. to some extent (Krieger, 1933).

Lineage Meso-2 includes two strains characterized by elongated cells with flat, almost truncated cell ends (Figure 3(c)). The single chloroplast can be plate-like but is frequently parietal with folded lateral sides, resulting in a channel-like morphology. The chloroplast bears undulate margins and rather prominent, lentiform pyrenoids. In culture, cells of lineage Meso-2 readily form chains through cell division and terminal mucilage

secretion (Figure 3(c)). Both strains were isolated from aquatic habitats, from freshwater plankton in Portugal (SAG 12.97) and from a brook in Spain (ACOI 2703). The genome-sequenced strain SAG 12.97 has been of interest (e.g., Bonnot et al., 2019; Cannell et al., 2020; Cheng et al., 2019; Donoghue & Paps, 2020; Wang et al., 2021) and was repeatedly referred to as *Mesotaenium endlicherianum*, but this designation is probably based on a misidentification as suggested by major morphological differences to the original description of that species (Nägeli, 1849).

Lineage Meso-3 comprises three strains, which match the description of *Mesotaenium caldariorum* (Lagerheim) Hansgirg (Hansgirg, 1886) and are listed under this name in public culture collections (see Supplementary table S1 for strain names). The cells are elongated with conical cell ends and contain an axial, ribbon-like chloroplast with clearly visible circular pyrenoids (Figure 3(d)). In the top view, the chloroplast matches the shape of the cell (i.e., with tapered ends), while in the side view, it appears as a thin ribbon. The strains ACOI 127 and ACOI 898 were isolated from moist soil (Portugal) and flowing water (Madeira, Portugal), respectively. Strain E.1 derives from wet moss from a waterfall (Germany). Interestingly, the lineage Meso-3 is morphologically indistinct from lineage Meso-9 but shows a high genetic divergence (Figure 2). Whether Meso-3 and Meso-9 are sister lineages remains to be solved by multigene phylogenies.

Lineage Meso-4 contains two strains, whose cells are cylindrical, sometimes slightly bent, with rounded cell ends (Figure 3(h)). Each cell contains two parietal, plate-like chloroplasts situated at opposing lateral sides of the cell. Some cells can have four chloroplasts (before cell division). The strain SAG 1.88 derives from the Signy Islands (Antarctica) and was isolated from bare mineral soil (Broady, 1976). For the strain JH0031, no sampling information is available. Strain SAG 1.88 was previously assigned to the genus *Fottea* (*Fottea pyrenoidosa*; Broady, 1976), which, however, belongs to the chlorophytes (with its type species *F. cylindrica* Hindák). Hence, the species was transferred to the genus *Mesotaenium* (Petlovany, 2014) and is currently named *Mesotaenium pyrenoidosum* (P.A. Broady) Petlovany (Guiry & Guiry, 2021; Petlovany, 2014). However, the morphology of strain SAG 1.88 is certainly in conflict with that of the type species of *Mesotaenium* (*M. endlicherianum*).

The *Ancylonema* lineage contains three sequences, two of which are from the ice-dwelling species *Ancylonema nordenskioeldii* and *Ancylonema alaskanum* (here the epithet of the latter species is corrected in gender according to Articles 62.2 (c), 23.5 and 32.2;

see Turland et al., 2018). The latter species was formerly known as *Mesotaenium berggrenii* (Procházková et al., 2021). For the third *rbc*L gene sequence, no strain information is available (Fig 2). The cells are cylindrical or elongated with broadly rounded cell ends. They have one or two parietal, lenticular or cup-shaped chloroplasts with a circular pyrenoid and a central nucleus (Remias, Holzinger, & Lütz, 2009, 2012). As far as we know, there are no cultivated strains available, despite several attempts to cultivate these glacier algae (Remias et al., 2009, 2012) (see below for geographic information), where they can form blooms (Procházková et al., 2021; Remias et al., 2012; Williamson et al., 2020). Despite their close relationship, the two *Ancylonema* species differ drastically in cell size and shape. Cell chain formation is known in *A. nordenskioeldii*. Both *A. nordenskioeldii* and *A. alaskanum* contain red-brown vacuolar pigments, suspected sunscreen compounds (see below for details).

Lineage Meso-5 is closely related to the filamentous, terrestrial green alga *Zygogonium ericetorum*, with full bootstrap support (Figure 2). The lineage comprises two strains, which cannot be assigned to an existing species with certainty, but show some similarities to the species *Mesotaenium truncatum* West & G.S.West (West & West, 1904). The cells are elongated with rather flat, almost truncated cell ends and contain a parietal plate-like chloroplast with a marked central indentation. This creates the impression of two chloroplasts, but there is a bridge between the two lobes. The nucleus is situated in the central region between the two chloroplast lobes (Figure 3(g)). Both strains readily form cell chains and floating films at the air–water interface in liquid culture. They were isolated from moist and acidic terrestrial surfaces in Germany (strain KM.19b) and Tennessee, USA (strain GSM.2.16.l).

Lineage Meso-6 contains three strains, which are morphologically similar to *Mesotaenium chlamydosporum* De Bary (De Bary, 1858). The cells are elongated with broadly rounded cell ends and contain one or two shovel-like chloroplasts, which are always parietal (Figure 3(i)). The cytoplasm often contains small, granular inclusions that can cover the nucleus and the chloroplast (Figure 3(i)). The three strains derive from terrestrial samples (Germany).

Lineage Meso-7 contains six strains, which are morphologically similar to *Mesotaenium mirificum* W. Archer (Archer, 1864). Except for the elliptical shape, the cells are similar to those of lineage Meso-6 (compare Figure 3(i, j)). The parietal, shovel-shaped chloroplasts and the nucleus are often surrounded by small granules (Figure 3(j)). The strains were isolated from different freshwater and terrestrial habitats in

Germany, Poland, the Great Smoky Mountains (USA), and Ontario, Canada (see Supplementary table S1 for details). Members of this lineage were found with copious mucilage in their natural habitats, which, however, is often lost in liquid culture. Strain GSM.5D.r was observed with pink cell content in its natural habitat (wet rocks, Great Smoky Mountains, Tennessee, USA).

Lineage Meso-8 contains two strains and has not been detected before (Figure 2). The cells are cylindrical or slightly elongated with round cell ends (Figure 3(e)). There are two parietal, shovel-shaped chloroplasts per cell, and the cytoplasm contains numerous small granules, often surrounding the nucleus in the form of a chain. Both strains were isolated from black-greenish mucilage on soil in the Great Smoky Mountains (Tennessee, USA).

Lineage Meso-9 is represented by three strains, which have identical *rbc*L gene sequences (Figure 2). The strains are morphologically similar to *Mesotaenium caldariorum* (Lagerheim) (Hansgirg, 1886) and are also named as such in culture collections and in published phylogenies (e.g., Surek, Beemelmanns, Melkonian, & Bhattacharya, 1994). As mentioned above, lineage Meso-9 is morphologically indistinct from lineage Meso-3 (compare Figure 3(d, f)) but shows high genetic divergence (Figure 2). The cells are elongated with conical cell ends and contain a central ribbon-like chloroplast with clearly visible, circular pyrenoids (Figure 3 (f)). The strains were isolated from moist terrestrial surfaces, a boggy meadow in Austria (SAG 150.80) and a wet brick in the Czech Republic (SAG 648.1). For SAG 230–1, no sampling information is available. Furthermore, the plastid movement and phytochromes of the strain SAG 648–1 (=UTEX 41) were studied intensively (see below for details).

Lineage Meso-10 is represented by one strain (UTEX 1025), which is morphologically similar to *Mesotaenium kramstai* (Lemmermann, 1896) and also named as such in culture collections as well as in published phylogenies (e.g., Gontcharov et al., 2003). The cells are long, rod-shaped with rounded cell ends, and the chloroplast is a ribbon with folded margins (Figure 3(k)). The chloroplast is, however, quite variable in shape. The strain derives from Texas (USA) from "air". It is the largest known zygnematophyte associated with the genus *Mesotaenium*.

The updated *rbc*L phylogeny reveals massive polyphyly of the genus *Mesotaenium* and, furthermore, reveals a so far hidden diversity of small, unicellular zygnematophytes. Probably, there are still many more new lineages to discover. As we show here, *Mesotaenium*-like algae are morphologically diverse, and specific cellular details can be used to distinguish some but not all lineages of these algae.

Distribution and ecology of Mesotaenium-like zygnematophytes

Mesotaenium-like zygnematophytes appear to be distributed over the whole globe as indicated by accounts from all over Europe, Africa, North and South America, Australia, certain areas in Asia, as well as the Arctic and Antarctic (e.g., De Bary, 1858; Hansgirg, 1886; Krieger, 1937; Ling & Seppelt, 1990; Remias et al., 2012; West & West, 1904). They inhabit various aquatic and terrestrial habitat types, including extreme habitats such as glacial ice (details below). Hence, different Mesotaenium-like zygnematophytes appear to vary strongly in their ecology. The phylogenetic tree in Figure 2 gives a rough overview of the habitat preferences of the 12 lineages defined in this study. The strains labelled as "aerophytic" were isolated from terrestrial surfaces that are subjected to periodic desiccation, while those associated with the term "submerged" come from flowing or standing waters that ensure permanent supply of water. All except two of the 12 lineages contain aerophytic strains, with seven lineages exclusively known from terrestrial habitats. Hence, a "life on land" appears to be very common among Mesotaenium-like zygnematophytes.

The habitats of representatives with a submerged lifestyle such as strains of the lineages Meso-2 and Meso-3 include puddles, boggy pools, brooks and streamlets (Gontcharov et al., 2004; West & West, 1904). Strain E.1 of lineage Meso-3 was isolated from wet moss in a waterfall, which is also considered a submerged habitat (Figure 5(a)). Blooms of suspended cells seem to be rare, but in certain cases, Mesotaenium-like zygnematophytes can form a skin on the water surface as reported for an aquatic species determined as M. endlicherianum (Hansgirg, 1886).

The aerophytic strains of lineages Meso-1, Meso-5, Meso-7, Meso-8 and Serritaenia from temperate zones colonize tree bark (Figure 5(b)), dead wood (Figure 5 (c)), rock surfaces (Figure 5(d)), soil and bryophytes. There are also accounts of Mesotaenium-like zygnematophytes on damp soil in heathers and warm houses (Hansgirg, 1886; West & West, 1901), and it seems that most species occur on acidic substrates. They are often part of multi-species communities, e.g., intermingled with chlorophyte green algae, cyanobacteria or moss protonema. However, Serritaenia species and the members of lineage Meso-7 can also form uni-algal, gelatinous patches that are visible with the naked eye (Busch & Hess, 2021; De Bary, 1858; West & West, 1904). In some instances, we observed mass developments of Serritaenia species that covered relatively large areas in moist German spruce forests and Molinia-dominated heathland (Figure 5(e) and Busch & Hess,

2021). In these areas, Serritaenia can overgrow entire bryophytes (e.g., various acrocarpous and pleurocarpous mosses) with severe effects on the plants (Figure 5(f, g)). Similar mass developments were reported for M. chlamydosporum and M. mirificum (Hansgirg, 1886; West & West, 1901), which might belong to the lineages Meso-6 and Meso-7, respectively. Furthermore, one Serritaenia strain (not yet sequenced) was isolated from a rock in an Araucaria forest in the Nahuelbuta National Park, Chile (Figure 5(h)). According to the collectors, the algal material was extracted from cracks in the rock, suggesting a chasmoendolithic lifestyle (pers. comm. Tatyana Darienko).

Mesotaenium-like zygnematophytes also colonize extreme habitats and are especially well known from glacial ice and snow in alpine or polar regions (e.g., Procházková et al., 2021; Yallop et al., 2012). The two cryophilic algal species Ancylonema nordenskioeldii and Ancylonema alaskanum (formerly known as Mesotaenium breggrenii) were found in the Arctic (e.g., Harding, Jungblut, Lovejoy, & Vincent, 2011; Uetake, Naganuma, Hebsgaard, Kanda, & Kohshima, 2010; Williamson et al., 2020), Alaska (Takeuchi, 2001), the Antarctic (Izaguirre & Pizarro, 1997; Ling & Seppelt, 1990), on a Himalayan glacier (Yoshimura, Kohshima, & Ohtani, 1997), a Chilean glacier (Takeuchi & Kohshima, 2004) and in the European Alps (Procházková et al., 2021). In these habitats, Ancylonema species can bloom in the ice, which results in large, grey or brown areas (Figure 5(i)). This darkening caused by a reddish-brown, intracellular pigments (details below) leads to increased absorption of solar radiation and melting rates of glacial ice (Takeuchi, Kohshima, & Seko, 2001; Williamson et al., 2018, 2020).

Despite their broad distribution and ecological versatility, Mesotaenium-like zygnematophytes are poorly captured by environmental sequence data, and most of the known diversity stems from culture-based approaches. Large environmental sequencing studies have been conducted in the open oceans and the pelagic zone of lakes (e.g., Boenigk et al., 2018; de Vargas et al., 2015), which are typically not very rich in zygnematophytes. Studies on terrestrial samples and microbial communities on trees often focus on bacteria, fungi and heterotrophic protists (e.g., Heger et al., 2018; Nacke et al., 2011; O'Brien, Parrent, Jackson, Moncalvo, & Vilgalys, 2005; Walden et al., 2021). There are, however, several environmental sequencing studies on biological soil crusts in dry polar regions and on glacial ice, which detected zygnematophycean amplicons, including those of the cryophilic Ancylonema nordenskioeldii (Büdel, Dulić, Darienko, Rybalka, & Friedl,

Figure 5. Habitats and biotic interactions of *Mesotaenium*-like zygnematophytes. (a) Waterfall with wet moss cushions (near Nohn, Eifel, Germany) inhabited by a species of lineage Meso-3. (b) Tree trunk with black algal crust (nature reserve "Heiliges Meer", Recke, Germany). (c) Decaying dead wood with green, mucilaginous layer (nature reserve "Schwarzes Wasser", Wesel, Germany). (d) Rock surface of "wet walls" colonized by various microalgae, including species of *Serritaenia* and Meso-7 (Great Smoky Mountains, North Carolina, USA). (e) *Molinia caerulea* (purple moor grass) in a *Molinia*-dominated degeneration phase of a heathland is heavily colonized by *Serritaenia* species (nature reserve "Heiliges Meer", Recke, Germany). (f) Undetermined pleurocarpous moss almost entirely covered by a black crust (Wiehl, Germany). (g) Same moss plant as shown in (f) after rehydration in water. The moss is heavily colonized by a *Serritaenia* species that forms globular colonies. (h) Araucarian forest (Nahuelbuta National Park, Chile) with rocks colonized by a potentially chasmoendolithic *Serritania* species (courtesy of T. Darienko). (i) Glacial ice inhabited by *Ancylonema* species (Morteratsch Glacier, Switzerland; courtesy of D. Remias). (j) Vampyrellid amoeba extracting the content of a *Serritaenia* species shown during feeding (brightfield; courtesy of H. Schulp). (k) Digestive cyst of the same vampyrellid species shown in (j) next to two perforated and emptied algal cells (brightfield; courtesy of H. Schulp). (l) Gelatinous colony of *Serritaenia testaceovaginata* with (fungal?) hyphae (differential interference contrast). (m) Cell of *Serritaenia testaceovaginata* from the population shown in (l) penetrated by the filamentous, fungus-like parasite (differential interference contrast). Scale bars 10 μm in (l) and (m), not available for (j) and (k).

2016; Garcés-Pastor et al., 2019; Lutz, Anesio, Edwards, & Benning, 2017; Rippin, 2018; Rippin, Lange, Sausen, & Becker, 2018; Samolov et al., 2020). The typical habitats of mesophilic saccoderm desmids, i.e., various surfaces in temperate forests, heathers and moorlands, remain undersampled. Based on our microscopic observations and the historical literature, we expect that environmental sequencing directed towards algal

biofilms in temperate zones will be a useful method to further expand our phylogenetic knowledge about unicellular zygnematophytes and reveal more of their ecological preferences.

Furthermore, there are observations that point to interesting biotic interactions between *Mesotaenium*-like zygnematophytes and other microbes. An unidentified, potentially undescribed vampyrellid amoeba (Vampyrellida, Rhizaria) was documented to extract the cellular contents of *Serritaenia* cells in a terrestrial sample (Figure 5(j, k)). These "protoplast feeders" often have a narrow prey range (Hess & Suthaus, 2022), and the undersampled microhabitats mentioned above might contain their own heterotrophic microfauna. In addition, we repeatedly observed (fungal?) hyphae running through the gelatinous colonies of *Serritaenia* species from different geographic localities in Europe and North America (Figure 5(l), arrowheads). These potentially biotrophic parasites penetrate algal cells and eventually lead to cell death (Figure 5(m)). So far, we know almost nothing about these heterotrophic associates of terrestrial microalgae, but our first attempts to isolate them promise to change this situation.

Cellular adaptations of *Mesotaenium*-like zygnematophytes to environmental factors

As shown above, various *Mesotaenium*-like zygnematophytes have a terrestrial lifestyle (Figure 2). Hence, they face strong fluctuations in water availability and temperature and increased exposure to sunlight. *Mesotaenium*-like zygnematophytes certainly have cellular adaptations to these abiotic stressors, for instance, the excessive mucilage secretion observed in *Serritaenia* and lineage Meso-7 that probably results in an increased water-holding capacity and extended photosynthetic periods. However, the cellular reactions of *Mesotaenium*-like zygnematophytes to desiccation are unstudied, in contrast to those of the filamentous forms. We know that *Zygnema* and *Zygogonium* accumulate osmolytes (sucrose), upregulate aquaporins and stress-related molecules (early light-inducible proteins, chaperones, late embryogenesis abundant proteins and DNA repair proteins), and they alter the thickness and composition of their cell walls (de Vries et al., 2018; Fuller, 2013; Herburger & Holzinger, 2015; Herburger, Remias, Holzinger, & Elster, 2016; Herburger, Xin, & Holzinger, 2019; Holzinger, Tschaikner, & Remias, 2010; Rippin, Becker, & Holzinger, 2017; Sørensen et al., 2011). In natural material of *Mesotaenium*-like zygnematophytes, one can observe pronounced cellular changes as well, which deserve future analysis.

Three remarkable photoprotective strategies have been studied in *Mesotaenium*-like zygnematophytes: (i) rotary chloroplast movement, (ii) vacuolar pigmentation and (iii) sunscreen mucilage. As shown in our phylogeny, these strategies are not necessarily limited to a single lineage but can also be found in other, even filamentous members (Figure 2). Rotary chloroplast movement was intensely studied in strain SAG 648–1 (referred to as *Mesotaenium caldariorum*) of lineage Meso-9 and in the filamentous zygnematophyte *Mougeotia scalaris*, both of which have a similar, ribbon-like chloroplast morphology (Haupt & Scheuerlein, 1990; Wada, Grolig, & Haupt, 1993). Depending on the light conditions, these algae re-arrange the chloroplast within the cell by axial rotation and alter the chloroplast surface that faces the light source between maximum (chloroplast in top view) and minimum surface (chloroplast in profile view). In both algae, an interplay of two photosensory receptors, phytochromes and cryptochromes, was found to trigger this photo-orientation of the chloroplast, and it has been hypothesized that the movement is mediated by the actin cytoskeleton (Haupt, 1991; Klein, Wagner, & Blatt, 1980; Kraml, Büttner, Haupt, & Herrmann, 1988; Wagner, Haupt, & Laux, 1972). However, research on chloroplast rotation in unicellular zygnematophytes ceased more than 20 years ago, and we suspect that there is much more to explore. Relatively recently, time-lapse microscopy of *Spirogloea muscicola* revealed an oscillating rotation of its helical chloroplast (Cheng et al., 2019), but it is yet unknown whether this relates to photoprotection (e.g., through rotational self-shading of the chloroplast).

The two cryophilic species of the *Ancylonema* lineage are well known for their intense, intracellular pigmentation (Remias, Holzinger, Aigner, & Lütz, 2012; Remias et al., 2009). The water-soluble, red-brown pigments are localized in one or more vacuoles of the cell and can largely obscure other cellular details (Figure 6(a, b)). The pigment of *A. alaskanum* was isolated from natural material and identified as a glycosylated purpurogallin derivative by nuclear magnetic resonance spectroscopy (Remias et al., 2012). The isolated substance was shown to absorb both ultraviolet radiation and visible light, suggesting a function as an intracellular sunscreen (Remias et al., 2012). Another study corroborated the strong UV absorbance of the abundant *Ancylonema* pigments and revealed their pronounced effect on overall cellular energy absorption (increased 50-fold by phenolic pigments; Williamson et al., 2020). This enables *Ancylonema* species to withstand the extreme solar irradiance present in glacier environments, while the chloroplasts are still low-light adapted (Williamson et al., 2020). The absorbed short-wavelength radiation is converted to heat and leads to melting of the glacier ice. This
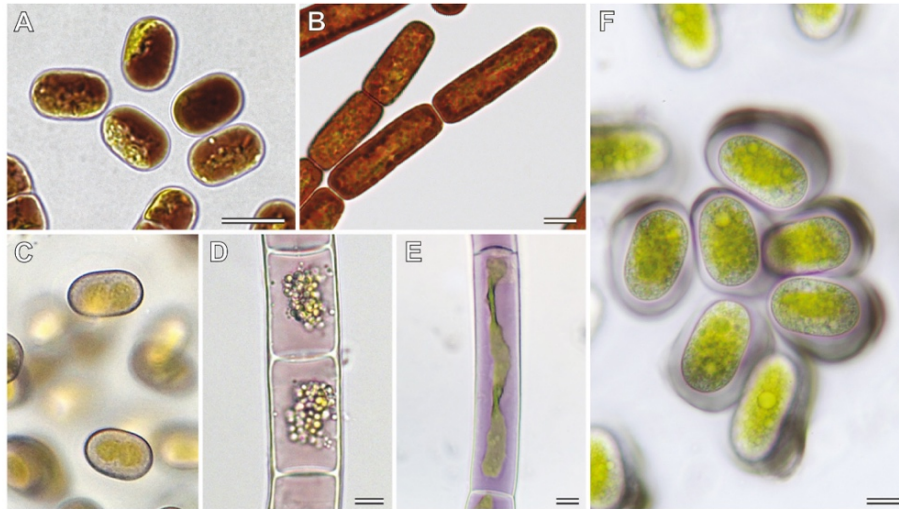
Figure 6. Non-photosynthetic pigments of *Mesotaenium*-like algae and other zygnematophytes. (a) *Ancylonema alaskanum* with dark-red vacuolar contents (Morteratsch Glacier, Switzerland; courtesy of D. Remias). (b) *Ancylonema nordenskioeldii* with red cellular contents (Morteratsch Glacier, Switzerland; micrograph from Procházková et al., 2021). (c) Cells of lineage Meso-7 with rose cellular contents (Wet walls, Great Smoky Mountains, North Carolina, USA). (d) *Zygogonium ericetorum* with pink vacuolar contents (Streamlet, Schoenwieskopf, Tyrol, Austria; micrograph from Aigner et al., 2013). (e) *Temnogametum iztacalense* with purple vacuolar contents (Lake La Luna, Nevado de Toluca, Mexico; courtesy of G. Garduño Solorzano). (f) *Serritaenia* sp. with purple-blue pigment in extracellular mucilage (from moss shown in Fig 5(f,g)). Scale bars 10 μm, scale information for (c) not available.

has severe impact on the integrity of the Greenland Ice Sheet, which experiences blooms of *Anyclonema* species (Williamson et al., 2018, 2020; Yallop et al., 2012). However, vacuolar pigments are not limited to the cryophilic species of the *Ancylonema* lineage but have been observed in several other zygnematophytes that colonize habitats of increased solar radiation (e.g., sun-exposed dead wood, ground in heathlands and shallow high mountain lakes). This includes members of lineage Meso-7 (Figure 6(c)), *Cylindrocystis brebissonii* f. *cryophila* (no genetic information available) and the filamentous zygnematophytes *Zygogonium ericetorum* (Figure 6(d)) and *Temnogametum iztacalense* (Figure 6(e)) (Aigner, Remias, Karsten, Holzinger, & Bassi, 2013; Garduño-Solórzano et al., 2021; Nedbalová & Sklenár, 2008). Hence, the production of intracellular pigments occurs in several distinct lineages of the Zygnematophyceae (Figure 2), and differences in colour (red-brown vs. purple) indicate variations in chemical structure and physical properties. In fact, the purple pigment of *Zygogonium ericetorum* might be a highly branched polymer of glucose with traces of ester-linked polyphenolic moieties (e.g., gallic acid) that form a colourful complex with ferric iron (Newsome & van Breemen, 2012). In addition, Holzinger et al. (2010) detected two water-soluble compounds that mainly absorb UV light, suggesting that the chemical photoprotection of zygnematophytes can be composed of several compounds.

Another sunscreen strategy, which appears to be unique among zygnematophytes, is found in the genus *Serritaenia*. These algae produce mucilaginous capsules with an extracellular, insoluble pigment that may function as external sunscreen (Figure 6(f)). The pigmented mucilage occupies a perfect position to shade the entire cell and was shown to effectively absorb over the UV–vis range, with a peak at about 300 nm (Busch & Hess, 2021). The synthesis of *Serritaenia*'s sunscreen mucilage is not constitutive and can be specifically induced by UVB radiation under laboratory conditions. The colouration of the mucilage varies in nature (bright red, brown, black and blue), which is (partially) influenced by the pH value of the surrounding medium. All *Serritaenia* species tested so far produce blueish mucilage under our culture conditions. The chemical structure of the pigment involved is as yet unknown.

All three photoprotective strategies found in the zygnematophytes (chloroplast movements, intracellular and extracellular pigments) provide interesting analogies to phenomena known from land plants, e.g., chloroplast avoidance movement (Kasahara et al., 2002), vacuolar anthocyanins (Steyn, Wand, Holcroft, & Jacobs, 2002) and cell walls with potentially photoprotective pigments (Hooijmaijers & Gould, 2007; Mårtensson & Nilsson, 1974). Yet, most of the cellular and biochemical background of such adaptations in

14 🖄 A. BUSCH AND S. HESS

zygnematophytes is still unresolved, and the unicellular *Mesotaenium*-like zygnematophytes might be useful laboratory models for future research.

Perspectives for future research

The available cultures of diverse *Mesotaenium*-like zygnematophytes enable various experimental studies. Ecophysiological comparisons concerning light preferences, freezing and drought tolerance may provide explanations for the unexpected diversity of these otherwise inconspicuous algae. A very obvious difference between the lineages is the varying propensity to form extracellular mucilage and the varying properties of the latter (e.g., confluent, capsular, hierarchical layers and terminal mucilage pillows). The mucilaginous, extracellular polymers of zygnematophytes have mainly been studied in *Penium*, *Micrasterias*, *Netrium* and several filamentous forms (e.g., Domozych, 2014; Eder & Lütz-Meindl, 2010; Eder & Lütz-Meindl, 2008; Palacio-López, Tinaz, Holzinger, & Domozych, 2019; Pfeifer et al., 2021), leaving the exopolymers of unicellular, terrestrial zygnematophytes biochemically unexplored. The sophisticated experiments performed on the studied zygnematophytes already revealed how complex the extracellular polymers of these algae are, containing pectic substances, hemicelluloses, arabinogalactan-proteins and rhamnogalactan proteins (Domozych et al., 2014; Palacio-López, Tinaz, Holzinger, & Domozych, 2019; Pfeifer et al., 2021; Sørensen et al., 2011 and references therein). It would certainly be very interesting to extend such studies to some terrestrial members of the *Mesotaenium*-like algae.

Despite the numerous phylogenetic studies performed on zygnematophytes, the deeper branches of this algal class are still unresolved (e.g., Gontcharov, 2008; Hall, Karol, McCourt, & Delwiche, 2008). In addition, we demonstrated that with manageable effort, one can find zygnematophycean lineages that have not been detected before. To better understand the evolution of the zygnematophytes, we need increased sampling and cultivation (including cells that look similar to known strains/species) as well as genomic or transcriptomic data from all relevant lineages. The latter can be used for multigene phylogenies, which, hopefully, will better resolve the branching pattern of major zygnematophycean clades in the future. At the moment, such data from *Mesotaenium*-like zygnematophytes are still scarce, limited to four out of 12 lineages (*Serritaenia*, Meso-2, Meso-9 and Meso-10; see stars in Figure 2). However, next-generation sequencing data from additional lineages are in progress.

The in-depth analysis of genomic and transcriptomic data also provides information on molecular innovations that might relate to major evolutionary transitions. The genomic analysis of strain SAG 12.97 (lineage Meso-2), for example, revealed expanded orthogroups that likely evolved in the common ancestor of the zygnematophytes and land plants. This includes genes for transcription factors, phytohormone signalling and genes involved in the biosynthesis and remodelling of the cell wall (Cheng et al., 2019). An interesting gene expansion was discovered for the GRAS transcription factor family, with a potential origin from soil bacteria by horizontal gene transfer (Cheng et al., 2019). Another interesting example is small RNA pathway-related genes that possibly contribute to pathogen defence and antibacterial immunity, a topic poorly explored in unicellular algae (Wang et al., 2021). To really understand the evolution of such mechanisms, dense genomic sampling at a phylogenetic level will be essential. Hence, biodiversity exploration is crucial, including inconspicuous life forms such as desmids of the *Mesotaenium*-type.

Disclosure statement

No potential conflict of interest was reported by the author(s).

ORCID

Anna Busch http://orcid.org/0000-0002-5377-7150
Sebastian Hess http://orcid.org/0000-0003-1262-8201

References

Aigner, S., Remias, D., Karsten, U., Holzinger, A., & Bassi, R. (2013). Unusual phenolic compounds contribute to ecophysiological performance in the purple-colored green alga *Zygogonium ericetorum* (Zygnematophyceae, Streptophyta) from a high-alpine habitat. *Journal of Phycology*, 49, 648–660.

Archer, W. (1864). Original communications: An endeavour to identify *Palmogloea macrococca* (Kütz.) with description of the plant believed to be meant, and of a new species, both, however, referable rather to the genus *Mesotaenium* (Näg.). *Journal of Cell Science*, 2, 109–132.

Bass, D., & Cavalier-Smith, T. (2004). Phylum-specific environmental DNA analysis reveals remarkably high global biodiversity of Cercozoa (Protozoa). *International Journal of Systematic and Evolutionary Microbiology*, 54, 2393–2404.

Bass, D., Chao, E. E.-Y., Nikolaev, S., Yabuki, A., Ishida, K., Berney, C., ... Cavalier-Smith, T. (2009). Phylogeny of novel naked filose and reticulose Cercozoa: Granofilosea cl. n. and Proteomyxidea revised. *Protist*, 160, 75–109.

Boenigk, J., Wodniok, S., Bock, C., Beisser, D., Hempel, C., Grossmann, L., ... Jensen, M. (2018). Geographic distance and mountain ranges structure freshwater protist communities on a European scale. *Metabarcoding and Metagenomics*, 2, e21519.

Bonnot, C., Hetherington, A. J., Champion, C., Breuninger, H., Kelly, S., & Dolan, L. (2019). Neofunctionalisation of basic helix–loop–helix proteins occurred when embryophytes colonised the land. *New Phytologist*, 223, 993–1008.

Broady, P. A. (1976). Six new species of terrestrial algae from Signy Island, South Orkney Islands, Antarctica. *British Phycological Journal*, 11, 387–405.

Brook, A. J., & Williamson, D. B. (2010). *A monograph on some British desmids*. London: Ray Society.

Büdel, B., Dulić, T., Darienko, T., Rybalka, N., & Friedl, T. (2016). Cyanobacteria and algae of biological soil crusts. In B. Weber, B. Büdel, & J. Belnap (Eds.), *Biological soil crusts: An organizing principle in drylands* (Vol. 226, pp. 55–80). Basel: Springer International Publishing.

Busch, A., & Hess, S. (2021). Sunscreen mucilage: A photoprotective adaptation found in terrestrial green algae (Zygnematophyceae). *European Journal of Phycology*, 1–18.

Cannell, N., Emms, D. M., Hetherington, A. J., MacKay, J., Kelly, S., Dolan, L., & Sweetlove, L. J. (2020). Multiple metabolic innovations and losses are associated with major transitions in land plant evolution. *Current Biology*, 30, 1783–1800.e11.

Cheng, S., Xian, W., Fu, Y., Marin, B., Keller, J., Wu, T., ... Melkonian, M. (2019). Genomes of subaerial Zygnematophyceae provide insights into land plant evolution. *Cell*, 179, 1057–1067.e14.

Coesel, P. F. M., & Meesters, K. J. (2007). *Desmids of the Lowlands: Mesotaeniaceae and Desmidiaceae of the European Lowlands*. Leiden: BRILL.

De Bary, A. (1858). *Untersuchungen über die Familie der Conjugaten: 91 pp*. Leipzig.

de Vargas, C., Audic, S., Henry, N., Decelle, J., Mahé, F., Logares, R., ... Velayoudon, D., et al. (2015). Eukaryotic plankton diversity in the sunlit ocean. *Science*, 348, 1261605.

de Vries, J., de Vries, S., Slamovits, C. H., Rose, L. E., & Archibald, J. M. (2017). How embryophytic is the biosynthesis of phenylpropanoids and their derivatives in streptophyte algae? *Plant & Cell Physiology*, 58, 934–945.

de Vries, J., Curtis, B. A., Gould, S. B., & Archibald, J. M. (2018). Embryophyte stress signaling evolved in the algal progenitors of land plants. *Proceedings of the National Academy of Sciences*, 115, E3471–E3480.

de Vries, J., de Vries, S., Curtis, B. A., Zhou, H., Penny, S., Feussner, K., ... Archibald, J. M. (2020). Heat stress response in the closest algal relatives of land plants reveals conserved stress signaling circuits. *The Plant Journal*, 103, 1025–1048.

Delaux, P.-M., Nanda, A. K., Mathé, C., Sejalon-Delmas, N., & Dunand, C. (2012). Molecular and biochemical aspects of plant terrestrialization. *Perspectives in Plant Ecology, Evolution and Systematics*, 14, 49–59.

Domozych, D. S., Sørensen, I., Popper, Z. A., Ochs, J., Andreas, A., Fangel, J. U., ... Willats, W. G. (2014). Pectin metabolism and assembly in the cell wall of the charophyte green alga *Penium margaritaceum*. *Plant Physiology*, 165, 105–118.

Domozych, D. S. (2014). *Penium margaritaceum*: A unicellular model organism for studying plant cell wall architecture and dynamics. *Plants*, 3, 543–558.

Donoghue, P., & Paps, J. (2020). Plant evolution: Assembling land plants. *Current Biology*, 30, R81–R83.

Eder, M., & Lütz-Meindl, U. (2008). Pectin-like carbohydrates in the green alga *Micrasterias* characterized by cytochemical analysis and energy filtering TEM. *Journal of Microscopy*, 231, 201–214.

Eder, M., & Lütz-Meindl, U. (2010). Analyses and localization of pectin-like carbohydrates in cell wall and mucilage of the green alga *Netrium digitus*. *Protoplasma*, 243, 25–38.

Ettl, H., & , and Gärtner, G. (2014). *Syllabus der Boden-, Luft- und Flechtenalgen*. Berlin Heidelberg: Springer Spektrum.

Fučíková, K., Hall, J. D., Johansen, J. R., & Lowe, R. (2008). Desmid flora of the Great Smoky Mountains National Park, USA. *Bibliotheca Phycologica*, 113, 1–59.

Fuller, C. L. (2013). *Examining morphological and physiological changes in Zygnema irregulare during a desiccation and recovery period* (PhD Thesis).

Galtier, N., Gouy, M., & Gautier, C. (1996). Seaview and phylo_win: Two graphic tools for sequence alignment and molecular phylogeny. *Bioinformatics*, 12, 543–548.

Garcés-Pastor, S., Wangensteen, O. S., Pérez-Haase, A., Pèlachs, A., Pérez-Obiol, R., Cañellas-Boltà, N., ... Vegas-Vilarrúbia, T. (2019). DNA metabarcoding reveals modern and past eukaryotic communities in a high-mountain peat bog system. *Journal of Paleolimnology*, 62, 425–441.

Garduño-Solórzano, G., Martínez-García, M., Scotta Hentschke, G., Lopes, G., Castelo Branco, R., Vasconcelos, V. M. O., ... Quintanar-Zúñiga, R. E. (2021). The phylogenetic placement of *Temnogametum* (Zygnemataceae) and description of *Temnogametum iztacalense* sp. nov., from a tropical high mountain lake in Mexico. *European Journal of Phycology*, 56, 159–173.

16 🜊 A. BUSCH AND S. HESS

Gerrath, J. F. (1993). The biology of desmids: A decade of progress. *Progress in Phycological Research*, 9, 79–192.

Gerrienne, P., Servais, T., & Vecoli, M. (2016). Plant evolution and terrestrialization during Palaeozoic times—The phylogenetic context. *Review of Palaeobotany and Palynology*, 227, 4–18.

Gontcharov, A. A., Marin, B., & Melkonian, M. (2003). Molecular phylogeny of conjugating green algae (Zygnemophyceae, Streptophyta) inferred from SSU rDNA sequence comparisons. *Journal of Molecular Evolution*, 56, 89–104.

Gontcharov, A. A., Marin, B., & Melkonian, M. (2004). Are combined analyses better than single gene phylogenies? A case study using SSU rDNA and rbcL sequence comparisons in the Zygnematophyceae (Streptophyta). *Molecular Biology and Evolution*, 21, 612–624.

Gontcharov, A. A. (2008). Phylogeny and classification of Zygnematophyceae (Streptophyta): Current state of affairs. *Fottea*, 8, 87–104.

Gontcharov, A. A., & Melkonian, M. (2010). Molecular phylogeny and revision of the genus *Netrium* (Zygnematophyceae, Streptophyta): *Nucleotaenium* gen. nov. *Journal of Phycology*, 46, 346–362.

Gouy, M., Guindon, S., & Gascuel, O. (2010). SeaView Version 4: A multiplatform graphical user interface for sequence alignment and phylogenetic tree building. *Molecular Biology and Evolution*, 27, 221–224.

Guillou, L., Viprey, M., Chambouvet, A., Welsh, R. M., Kirkham, A. R., Massana, R., ... Worden, A. Z. (2008). Widespread occurrence and genetic diversity of marine parasitoids belonging to Syndiniales (Alveolata). *Environmental Microbiology*, 10, 3349–3365.

Guiry, M. D. (2013). Taxonomy and nomenclature of the Conjugatophyceae (= Zygnematophyceae). *ALGAE*, 28, 1–29.

Guiry, M. D., & Guiry, G. M. (2021, December 21). AlgaeBase. *World-wide electronic publication*, Galway: National University of Ireland. https://www.algaebase.org

Hainz, R., Wöber, C., & Schagerl, M. (2009). The relationship between *Spirogyra* (Zygnematophyceae, Streptophyta) filament type groups and environmental conditions in Central Europe. *Aquatic Botany*, 91, 173–180.

Hall, J. D., Karol, K. G., McCourt, R. M., & Delwiche, C. F. (2008). Phylogeny of the conjugating green algae based on chloroplast and mitochondrial nucleotide sequence data (1). *Journal of Phycology*, 44, 467–477.

Hall, J. D., & McCourt, R. M. (2015). Chapter 9 - Conjugating green algae including desmids. In J. D. Wehr, R. G. Sheath, & J. P. Kociolek (Eds.), *Freshwater Algae of North America (Second Edition)* (pp. 429–457). San Diego: Academic Press. doi:10.1016/B978-0-12-385876-4.00009-8

Hansgirg, A. (1886). *Prodromus der Algenflora von Böhmen. 1. Theil [Teil]. Enthaltend die Rhodophyceen, Phaeophyceen und einen Teil der Chlorophyceen.* Řivnáč.

Harding, T., Jungblut, A. D., Lovejoy, C., & Vincent, W. F. (2011). Microbes in high Arctic snow and implications for the cold biosphere. *Applied and Environmental Microbiology*, 77, 3234–3243.

Haupt, W., & Scheuerlein, R. (1990). Chloroplast movement. *Plant, Cell & Environment*, 13, 595–614.

Haupt, W. (1991). Phytochrome and cryptochrome: Coaction or interaction in the control of chloroplast orientation. In Riklis E.(ed.), *Photobiology* (pp. 479–489). New York: Springer.

Heger, T. J., Giesbrecht, I. J. W., Gustavsen, J., Del Campo, J., Kellogg, C. T. E., Hoffman, K. M., ... Keeling, P. J. (2018). High-throughput environmental sequencing reveals high diversity of litter and moss associated protist communities along a gradient of drainage and tree productivity. *Environmental Microbiology*, 20, 1185–1203.

Herburger, K., & Holzinger, A. (2015). Localization and quantification of callose in the streptophyte green algae *Zygnema* and *Klebsormidium*: Correlation with desiccation tolerance. *Plant & Cell Physiology*, 56, 2259–2270.

Herburger, K., Remias, D., Holzinger, A., & Elster, J. (2016). The green alga *Zygogonium ericetorum* (Zygnematophyceae, Charophyta) shows high iron and aluminium tolerance: Protection mechanisms and photosynthetic performance. *FEMS Microbiology Ecology*, 92, fiw103.

Herburger, K., Xin, A., & Holzinger, A. (2019). Homogalacturonan accumulation in cell walls of the green alga *Zygnema* sp. (Charophyta) increases desiccation resistance. *Frontiers in Plant Science*, 10, 540.

Hess, S., & Suthaus, A. (2022). The vampyrellid amoebae (Vampyrellida, Rhizaria). *Protist*, 173, 1–27. doi:10.1016/j.protis.2021.125854

Holzinger, A., Tschaikner, A., & Remias, D. (2010). Cytoarchitecture of the desiccation-tolerant green alga *Zygogonium ericetorum*. *Protoplasma*, 243, 15–24.

Holzinger, A., Kaplan, F., Blaas, K., Zechmann, B., Komsic-Buchmann, K., Becker, B., & Araujo, W. L. (2014). Transcriptomics of desiccation tolerance in the streptophyte green alga *Klebsormidium* reveal a land plant-like defense reaction. *PLOS ONE*, 9, e110630.

Holzinger, A., & Pichrtová, M. (2016). Abiotic stress tolerance of charophyte green algae: New challenges for omics techniques. *Frontiers in Plant Science*, 7, 678.

Hooijmaijers, C. A. M., & Gould, K. S. (2007). Photoprotective pigments in red and green gametophytes of two New Zealand liverworts. *New Zealand Journal of Botany*, 45, 451–461.

Izaguirre, I., & Pizarro, H. (1997). Epilithic algae in a glacial stream at Hope Bay (Antarctica). *Polar Biology*, 19, 24–31.

Kasahara, M., Kagawa, T., Oikawa, K., Suetsugu, N., Miyao, M., & Wada, M. (2002). Chloroplast avoidance movement reduces photodamage in plants. *Nature*, 420, 829–832.

Kawai, J., Kanazawa, M., Suzuki, R., Kikuchi, N., Hayakawa, Y., & Sekimoto, H. (2022). Highly efficient transformation of the model zygnematophycean alga *Closterium peracerosum-strigosum-littorale* complex by square-pulse electroporation. *New Phytologist*, 233, 569–578.

Klein, K., Wagner, G., & Blatt, M. R. (1980). Heavy-meromyosin-decoration of microfilaments from *Mougeotia* protoplasts. *Planta*, 150, 354–356.

Kraml, M., Büttner, G., Haupt, W., & Herrmann, H. (1988). Chloroplast orientation in *Mesotaenium*: The phytochrome effect is strongly potentiated by interaction with blue light. In Tazawa M.(ed.), *Cell Dynamics* (pp. 172–179). Wien: Springer.

Krieger, W. (1933). 39. Die Desmidiaceen. *Rabenhorst's Kryptogamen-Flora von Deutschland, Österreich Und Der Schweiz, 13*.

Krieger, W. (1937). Die Desmidiaceen Europas mit Berücksichtigung der außereuropäischen Arten. Rabenhorst's Kryptogamen Flora. *Dt, Österr. Schweiz., 3,* 377–712.

Kumar, S., Stecher, G., Li, M., Knyaz, C., Tamura, K., & Battistuzzi, F. U. (2018). MEGA X: Molecular evolutionary genetics analysis across computing platforms. *Molecular Biology and Evolution, 35,* 1547–1549.

Lemmermann, E. (1896). *Zur Algenflora des Riesengebirges.* Berlin: Friedländer & Sohn.

Lenzenweger, R. (2003). *Desmidiaceenflora von Österreich, Teil 4.* Stuttgart: Schweizerbart'sche Verlagsbuchhandlung. https://www.schweizerbart.de/publications/detail/isbn/9783443600389/Desmidiaceenflora-von-sterreich-Teil-4

Ling, H. U., & Seppelt, R. D. (1990). Snow algae of the Windmill Islands, continental Antarctica. *Mesotaenium berggrenii* (Zygnematales, Chlorophyta) the alga of grey snow. *Antarctic Science, 2,* 143–148.

Lutz, S., Anesio, A. M., Edwards, A., & Benning, L. G. (2017). Linking microbial diversity and functionality of *Arctic* glacial surface habitats: *Arctic* glacial surface habitats. *Environmental Microbiology, 19,* 551–565.

Lütz-Meindl, U. (2016). *Micrasterias* as a model system in plant cell biology. *Frontiers in Plant Science, 7,* 999.

Mårtensson, O., & Nilsson, E. (1974). On the morphological colour of bryophytes. *Lindbergia, 2,* 145–159.

Massana, R., Castresana, J., Balagué, V., Guillou, L., Romari, K., Groisillier, A., . . . Pedrós-Alió, C. (2004). Phylogenetic and ecological analysis of novel marine stramenopiles. *Applied and Environmental Microbiology, 70,* 3528–3534.

Massana, R., Del Campo, J., Sieracki, M. E., Audic, S., & Logares, R. (2014). Exploring the uncultured microeukaryote majority in the oceans: Reevaluation of ribogroups within stramenopiles. *The ISME Journal, 8,* 854–866.

Matasci, N., Hung, L.-H., Yan, Z., Carpenter, E. J., Wickett, N. J., Mirarab, S., . . . Wong, G. K. S., et al. (2014). Data access for the 1,000 Plants (1KP) project. *GigaScience, 3,* 2047–217X-3–17.

McFadden, G. I., & Melkonian, M. (1986). Use of Hepes buffer for microalgal culture media and fixation for electron microscopy. *Phycologia, 25,* 551–557.

Mollenhauer, D. (1986). Concepts and strategies for research in Mesotaeniaceae. *Beiheft Zur Nova Hedwigia, 56,* 43–60.

Nacke, H., Thürmer, A., Wollherr, A., Will, C., Hodac, L., Herold, N., . . . Daniel, R. (2011). Pyrosequencing-based assessment of bacterial community structure along different management types in German forest and grassland soils. *PLOS ONE, 6,* e17000.

Nägeli, C. (1849). *Gattungen einzelliger Algen: Physiologisch und systematisch bearbeitet.* Zürich: Friedrich Schulthess.

Nedbalová, L., & Sklenár, P. (2008). New records of snow algae from the Andes of Ecuador. *Arnaldoa, 15,* 17–20.

Newsome, A. G., & van Breemen, R. B. (2012). Characterization of the purple vacuolar pigment of *Zygogonium ericetorum* alga. *Planta Medica, 78,* J20.

O'Brien, H. E., Parrent, J. L., Jackson, J. A., Moncalvo, J.-M., & Vilgalys, R. (2005). Fungal community analysis by large-scale sequencing of environmental samples. *Applied and Environmental Microbiology, 71,* 5544–5550.

Palacio-López, K., Tinaz, B., Holzinger, A., & Domozych, D. S. (2019). Arabinogalactan proteins and the extracellular matrix of charophytes: A sticky business. *Frontiers in Plant Science, 10,* 447.

Petlovany, O. V. (2014). Zygnematales. In Tsarenko, P. M., Wasser, S. P., Nevo, E.(Eds.), *Algae of Ukraine: Diversity, nomenclature, taxonomy, ecology and geography* (Vol. 4, pp. 11–61). Königstein: Koeltz Botanical Books.

Pfeifer, L., Utermöhlen, J., Happ, K., Permann, C., Holzinger, A., von Schwartzenberg, K., & Classen, B. (2021). Search for evolutionary roots of land plant arabinogalactan-proteins in charophytes: Presence of a rhamnogalactan-protein in *Spirogyra pratensis* (Zygnematophyceae). *The Plant Journal, 109,* 568–584.

Procházková, L., Řezanka, T., Nedbalová, L., & Remias, D. (2021). Unicellular versus filamentous: The glacial alga *Ancylonema alaskana* comb. et stat. nov. and its ecophysiological relatedness to *Ancylonema nordenskioeldii* (Zygnematophyceae, Streptophyta). *Microorganisms, 9,* 1103.

Remias, D., Holzinger, A., & Lütz, C. (2009). Physiology, ultrastructure and habitat of the ice alga *Mesotaenium berggrenii* (Zygnemaphyceae, Chlorophyta) from glaciers in the European Alps. *Phycologia, 48,* 302–312.

Remias, D., Schwaiger, S., Aigner, S., Leya, T., Stuppner, H., & Lütz, C. (2012). Characterization of an UV- and VIS-absorbing, purpurogallin-derived secondary pigment new to algae and highly abundant in *Mesotaenium berggrenii* (Zygnematophyceae, Chlorophyta), an extremophyte living on glaciers. *FEMS Microbiology Ecology, 79,* 638–648.

Remias, D., Holzinger, A., Aigner, S., & Lütz, C. (2012). Ecophysiology and ultrastructure of *Ancylonema nordenskiöldii* (Zygnematales, Streptophyta), causing brown ice on glaciers in Svalbard (high Arctic). *Polar Biology, 35,* 899–908.

Rippin, M., Becker, B., & Holzinger, A. (2017). Enhanced desiccation tolerance in mature cultures of the streptophytic green alga *Zygnema circumcarinatum* revealed by transcriptomics. *Plant & Cell Physiology, 58,* 2067–2084.

Rippin, M., Lange, S., Sausen, N., & Becker, B. (2018). Biodiversity of biological soil crusts from the Polar regions revealed by metabarcoding. *FEMS Microbiology Ecology, 94.* doi:10.1093/femsec/fiy036

Rippin, M., Borchhardt, N., Williams, L., Colesie, C., Jung, P., Büdel, B., Becker, B. (2018). Genus richness of microalgae and Cyanobacteria in biological soil crusts from Svalbard and Livingston Island: Morphological versus molecular approaches. *Polar Biology, 15,* 909–923.

Samolov, E., Baumann, K., Büdel, B., Jung, P., Leinweber, P., Mikhailyuk, T., . . . Glaser, K. (2020). Biodiversity of algae and cyanobacteria in biological soil crusts collected along a climatic gradient in Chile using an integrative approach. *Microorganisms, 8,* 1047.

Sørensen, I., Pettolino, F. A., Bacic, A., Ralph, J., Lu, F., O'Neill, M. A., . . . Willats, W. G. T. (2011). The charophycean green algae provide insights into the early origins of plant cell walls. *The Plant Journal, 68,* 201–211.

Stastny, J., Skaloud, P., Langenbach, D., Nemjova, K., & Neustupa, J. (2013). Polyphasic evaluation of *Xanthidium antilopaeum* and *Xanthidium cristatum* (Zygnematophyceae, Streptophyta) species complex. *Journal of Phycology, 49,* 401–416.

Šťastný, J., & Kouwets, F. A. C. (2012). New and remarkable desmids (Zygnematophyceae, Streptophyta) from Europe: Taxonomical notes based on LM and SEM observations. *Fottea*, 12, 293–313.

Steyn, W. J., Wand, S. J. E., Holcroft, D. M., & Jacobs, G. (2002). Anthocyanins in vegetative tissues: A proposed unified function in photoprotection. *New Phytologist*, 155, 349–361.

Sun, Y., Harpazi, B., Wijerathna-Yapa, A., Merilo, E., de Vries, J., Michaeli, D., … Mosquna, A. (2019). A ligand-independent origin of abscisic acid perception. *Proceedings of the National Academy of Sciences*, 116, 24892–24899.

Surek, B., Beemelmanns, U., Melkonian, M., & Bhattacharya, D. (1994). Ribosomal RNA sequence comparisons demonstrate an evolutionary relationship between Zygnematales and charophytes. *Plant Systematics and Evolution*, 191, 171–181.

Takeuchi, N. (2001). The altitudinal distribution of snow algae on an Alaska glacier (Gulkana Glacier in the Alaska Range). *Hydrological Processes*, 15, 3447–3459.

Takeuchi, N., Kohshima, S., & Seko, K. (2001). Structure, formation, and darkening process of albedo-reducing material (cryoconite) on a Himalayan glacier: A granular algal mat growing on the glacier. *Arctic, Antarctic, and Alpine Research*, 33, 115–122.

Takeuchi, N., & Kohshima, S. (2004). A snow algal community on Tyndall Glacier in the southern Patagonia icefield, Chile. *Arctic, Antarctic, and Alpine Research*, 36, 92–99.

Timme, R. E., Bachvaroff, T. R., & Delwiche, C. F. (2012). Broad phylogenomic sampling and the sister lineage of land plants. *PLOS ONE*, 7, e29696.

Turland, N. J., Wiersema, J. H., Barrie, F. R., Greuter, W., Hawksworth, D. L., Herendeen, P. S., … Smith, G. et al. (Eds.). (2018). *International code of nomenclature for algae, fungi, and plants (Shenzhen Code) adopted by the Nineteenth International Botanical Congress Shenzhen, China, July 2017*. Regnum Vegetabile 159. Glashütten: Koeltz Botanical Books. doi:10.12705/Code.2018

Uetake, J., Naganuma, T., Hebsgaard, M. B., Kanda, H., & Kohshima, S. (2010). Communities of algae and cyanobacteria on glaciers in west Greenland. *Polar Science*, 4, 71–80.

Wada, M., Grolig, F., & Haupt, W. (1993). New trends in photobiology: Light-oriented chloroplast positioning. Contribution to progress in photobiology. *Journal of Photochemistry and Photobiology. B, Biology*, 17, 3–25.

Wagner, G., Haupt, W., & Laux, A. (1972). Reversible inhibition of chloroplast movement by cytochalasin B in the green alga *Mougeotia*. *Science*, 176, 808–809.

Walden, S., Jauss, R.-T., Feng, K., Fiore-Donno, A. M., Dumack, K., Schaffer, S., … Bonkowski, M. (2021). On the phenology of protists: Recurrent patterns reveal seasonal variation of protistan (Rhizaria: Cercozoa and Endomyxa) communities in tree canopies. *FEMS Microbiology Ecology*, 97, fiab081.

Wang, S., Liang, H., Xu, Y., Li, L., Wang, H., Sahu, D. N., … Liu, H. (2021). Genome-wide analyses across Viridiplantae reveal the origin and diversification of small RNA pathway-related genes. *Communications Biology*, 4, 1–11.

West, W., & West, G. S. (1901). *The alga-flora of Yorkshire: A complete account of the known freshwater algae of the county, with many notes on their affinities and distribution* (Vol. 5). York: Yorkshire Naturalists' Union.

West, W., & West, G. S. (1904). *A monograph of the British Desmidiaceae* (Vol. 1). London: Ray Society.

Wickett, N. J., Mirarab, S., Nguyen, N., Warnow, T., Carpenter, E., Matasci, N., … Leebens-Mack, J. (2014). Phylotranscriptomic analysis of the origin and early diversification of land plants. *Proceedings of the National Academy of Sciences*, 111, E4859–E4868.

Williamson, C. J., Anesio, A. M., Cook, J., Tedstone, A., Poniecka, E., Holland, A., … Yallop, M. L. (2018). Ice algal bloom development on the surface of the Greenland Ice Sheet. *FEMS Microbiology Ecology*, 94, fiy025.

Williamson, C. J., Cook, J., Tedstone, A., Yallop, M., McCutcheon, J., Poniecka, E., … Anesio, A. (2020). Algal photophysiology drives darkening and melt of the Greenland ice sheet. *Proceedings of the National Academy of Sciences*, 117, 5694–5705.

Wodniok, S., Brinkmann, H., Glöckner, G., Heidel, A. J., Philippe, H., Melkonian, M., & Becker, B. (2011). Origin of land plants: Do conjugating green algae hold the key? *BMC Evolutionary Biology*, 11, 104.

Yallop, M. L., Anesio, A. M., Perkins, R. G., Cook, J., Telling, J., Fagan, D., … Roberts, N. W. (2012). Photophysiology and albedo-changing potential of the ice algal community on the surface of the Greenland ice sheet. *The ISME Journal*, 6, 2302–2313.

Yoshimura, Y., Kohshima, S., & Ohtani, S. (1997). A community of snow algae on a Himalayan glacier: Change of algal biomass and community structure with altitude. *Arctic and Alpine Research*, 29, 126.

Zhou, H., Wilkens, A., Hanelt, D., & von Schwartzenberg, K. (2021). Expanding the molecular toolbox for Zygnematophyceae – Transient genetic transformation of the desmid *Micrasterias radians* var. *evoluta*. *European Journal of Phycology*, 56, 51–60.

Supplementary Data

A diverse group of underappreciated zygnematophytes deserves in-depth exploration

Anna Busch & Sebastian Hess

Supplementary Table S1: Studied strains with lineage affiliations, sampling sites, coordinates of sampling sites, and details on sampled material. Strains sequenced in this study are bold. Lacking information is indicated by NA.

Strain	Lineage	Sampling site	Coordinates of sampling site	Type of sample
OBE.1	*Serritaenia*	Monsau, Wiehl (DE)	50.958607, 7.581137	soil and bryophytes
CCAC 0155	*Serritaenia*	Strohner Maarchen, Eifel (DE)	NA	paste of desmids
OBE.sm.2	*Serritaenia*	Wohlsberg, Wiehl (DE)	50.961667, 7.578056	blackish crust on bryophyte growing on tree bark
GSM.4.4	*Serritaenia*	wet surfaces on way to Andrews Bold, Great Smoky Mountains (US)	35.555917, -83.497417	brown mucilage on bryophyte
GSM.5.thick	*Serritaenia*	wet walls on way to clingmans dome, Great Smoky Mountains (US)	35.568104, -83.481939	black-greenish mucilage on wet wall
GSM.5.thin	*Serritaenia*	wet walls on way to clingmans dome, Great Smoky Mountains (US)	35.568104, -83.481939	black-greenish mucilage on wet wall
N.004	Meso-1	Kermeter, Eifel (DE)	50.621944, 6.430000	bryophyte on beech
KH.2.sm	Meso-1	Frei-Laubersheimer Wald, Bad Kreuznach (DE)	49.806280, 7.882115	blackish crust on bryophyte growing on dead wood
ACOI 2703	Meso-2	between Ceada and Miranda do Douro (ESP)	NA	brook
SAG 12.97	Meso-2	Lagoa das Bracas, Quiaios (PT)	NA	freshwater
ACOI 127	Meso-3	Ladeira das Alpenduradas, Coimbra (PT)	NA	moist soil
E.1	Meso-3	Waterfall Dreihmühlen, near Nohn, Eifel (DE)	50.324807, 6.768928	squeezed, wet moss
ACOI 898	Meso-3	Bica do Carmo, Madeira (PT)	NA	flowing water
SAG 1.88	Meso-4	Signy Island, South Orkney (AQ)	NA	mineral soil (pH 5.2)
KM.19b	Meso-5	Moorland near Dellbrück, Cologne (DE)	50.987350, 7.079390	algal biofilm on wet peat
GSM.2.16.l	Meso-5	Cades Cove trail, Great Smoky Mountains (US)	35.604444, -83.868611	black-greenish mucilage on ground with interwoven bryophyte
N.109	Meso-6	Mariawald, Eifel (DE)	NA	rock surface
N.87	Meso-6	Sauerbach, Eifel (DE)	NA	terrestrial sample near trail
LM.24	Meso-6	Moorland near Dellbrück, Cologne (DE)	50.987350, 7.079390	squeezed Sphagnum
CCAC 2215	Meso-7	Experimental Lake Area (Lake 114), Ontario (CA)	NA	freshwater
POL.1	Meso-7	near Szczecin (POL)	NA	Epiphytic bryophytes with mucilage
GSM.5D.r	Meso-7	wet walls on way to Clingmans Dome, Great Smoky Mountains (US)	35.568104, -83.481939	brown-reddish mucilage on wet wall
CCAC 0154	Meso-7	Monschau, Eifel (DE)	NA	freshwater
GSM.3.15	Meso-7	Grotto falls trail, Great Smoky Mountains (US)	35.676667, -83.452972	green mucilage on dead wood
GSM.2.3.s	Meso-7	Cades Cove trail, Great Smoky Mountains (US)	35.611261, -83.881739	blackish crust on bryophyte
GSM.2.16.s1	Meso-8	Cades Cove trail, Great Smoky Mountains (US)	35.604444, -83.868611	black-greenish mucilage on ground with interwoven bryophyte
GSM.2.16.s2	Meso-8	Cades Cove trail, Great Smoky Mountains (US)	35.604444, -83.868611	black-greenish mucilage on ground with interwoven bryophyte
SAG 230-1	Meso-9	NA	NA	freshwater
SAG 150-80	Meso-9	Pitztal, Tyrol, (AT)	NA	boggy meadow

SAG 648-1	Meso-9	Klobouk near Brno (CZ)	NA	wet brick, together with *Porphyridium cruentum*
UTEX 1025	Meso-10	Austin, Texas (US)	NA	air

A mesophilic relative of common glacier algae, *Ancylonema palustre* sp. nov., provides insights into the induction of vacuolar pigments in zygnematophytes

Chapter IV

Title

A mesophilic relative of common glacier algae, *Ancylonema palustre* sp. nov., provides insights into the induction of vacuolar pigments in zygnematophytes

Running Title

Vacuolar pigments in *Ancylonema palustre*

Authors

Anna Busch[1]*, Emilia Slominski[1], Daniel Remias[2], Lenka Procházková[3], Sebastian Hess[1,4]

Affiliations:

[1] Department of Biology, University of Cologne, Zülpicher Str. 47b, 50674 Cologne, Germany

[2] Department of Environment & Biodiversity, University of Salzburg, Hellbrunnerstr. 34, 5020 Salzburg, Austria

[3] Department of Ecology, Faculty of Science, Charles University, Viničná 7, 128 00 Prague, Czech Republic

[4] Department of Biology, Technical University of Darmstadt, Schnittspahnstr. 3, 64287 Darmstadt, Germany

*Correspondence:

Anna Busch

e-mail: anna.busch@uni-koeln.de

Co-author e-mail addresses:

Emilia Slominski: emilia.slominski@gmail.com

Daniel Remias: daniel.remias@plus.ac.at

Lenka Procházková: lenkacerven@gmail.com

Sebastian Hess: sebastian.hess@uni-koeln.de

The authors declare no conflict of interest.

Abstract

The zygnematophyte green algae of the genus *Ancylonema* are common colonizers of glaciers in several distinct regions around the globe. In their natural habitat they exhibit a remarkable reddish-brown pigmentation due to vacuolar compounds related to gallic acid. Blooms of these algae result in glacier darkening and enhanced melting rates. The currently known *Ancylonema* species are true psychrophiles, which impairs experimental work and limits our functional understanding of these algae. For example, the biosynthesis, inducing factors and biological function of *Ancylonema'*s secondary pigments are not known. Here, we report a mesophilic *Ancylonema* species, *A. palustre* sp. nov. from temperate moorlands, which forms the sister lineage to all known psychrophilic strains. Despite its morphological resemblance to the latter, it shows unique autecological and photophysiological characteristics, and let us describe vegetative and sexual cellular processes in great detail. Furthermore, we experimentally tested for abiotic factors that induce the secondary pigments of zygnematophytes and found that low nutrient conditions combined with ultraviolet B radiation result in vacuolar pigmentation, indicating a sunscreening function. Our well-growing, bacteria-free cultures of *A. palustre* will facilitate comparative genomic studies of meso- and extremophilic zygnematophytes and might hold the key in understanding how *Ancylonema* species colonized the worlds glaciers.

Key words: Conjugatophyceae, peat bog, phenolic compounds, photoprotection, streptophyte algae, UV radiation, Zygnematophyceae

Introduction

The conjugating green algae (Zygnematophyceae) comprise about 4,000 described species with rather simple growth forms, ranging from non-flagellated unicells to filaments (Brook & Williamson, 2010; Coesel & Meesters, 2007; Hall & McCourt, 2015). As revealed by several phylogenomic studies, these algae are the closest relatives of the land plants and hence important research subjects to understand the transition from aquatic to terrestrial life (Timme et al., 2012; Wickett et al., 2014; Wodniok et al., 2011). Of particular interest are physiological adaptations to terrestrial conditions that potentially predated the origin of the land plants and thereby facilitated their evolution (de Vries et al., 2017, 2020; Fürst-Jansen et al., 2020). Most zygnematophytes thrive in freshwater-fed systems of various trophic levels, including ponds, lakes and moorlands. However, some lineages colonize more extreme habitats such as rock surfaces, deadwood, tree bark, and even glacial ice (Busch & Hess, 2022a; Remias et al., 2009). Only very few known zygnematophytes adapted to the freezing temperatures and high solar radiation existent on glaciers. The two most widespread zygnematophyte species inhabiting such extreme habitats are *Ancylonema nordenskioeldii* and *A. alaskanum* (Procházková et al., 2021). They have been found on glaciers of the European Alps, Greenland, Alaska, Svalbard, the Altai Mountains, the Himalaya and Antarctica (Kol, 1942; Ling & Seppelt, 1990; Remias et al., 2009; Takeuchi, 2001; Takeuchi et al., 2006, 2019; Williamson et al., 2018; Yoshimura et al., 1997), and occasionally grow at high densities. In the recent years, glacier algae gained much attention, since their blooms have detrimental effects on glaciers. A dark cover of algal cells, anthropogenic black carbon and mineral debris reduces the albedo of glacial ice surfaces, absorbs solar radiation and thereby accelerates glacial melting during summer (Cook et al., 2020; Stibal et al., 2017; Williamson et al., 2018, 2019; Yallop et al., 2012). The coloration caused by *Ancylonema* blooms results, in part, from reddish-brown, non-photosynthetic pigments, which accumulate in vacuoles of the algal cells (Remias et al., 2009). These secondary pigments are of phenolic origin, and a main compound from *A. alaskanum* was previously identified as purpurogallin carboxylic acid-6-O-β-d-glucopyranoside, which shows a broad absorbance the UV-VIS portion of sunlight (Remias, Schwaiger, et al., 2012). In the natural habitat, these phenolics equip the algal cells with a remarkable, dark brown coloration. Hence, several biological functions of *Ancylonema*'s secondary pigments have been proposed, including a function as sunscreen, chemical defense agent, and ice-melting agent (Remias, Schwaiger, et al., 2012). A photoprotective function seems most likely, as these compounds very effectively absorb UVR and VIS and are supposed to shade the low-light-adapted chloroplasts (Williamson et al., 2020). However, this hypothesis was never experimentally tested as the psychrophilic nature of the known *Ancylonema* species is a hurdle for experimental research. The recently established cultures depend on low temperatures (≤ 5 °C), grow very slowly and are not axenic (Jensen et al., 2023; Remias & Procházková, 2023). So far, we lack any knowledge about the biosynthetic pathway of intracellular pigments of zygnematophytes and the environmental factors that trigger their biosynthesis.

In the temperate moorlands of Germany, we discovered mesophilic *Ancylonema* strains, which showed a remarkable resemblance to their psychrophilic relatives, including the reddish-brown intracellular pigmentation. We established well-growing, axenic cultures, which were used to pinpoint the evolutionary origin of these algae by molecular phylogenetics, and to characterize the vegetative cell cycle and sexual processes, including zygospore formation. Furthermore, we studied the photosynthetic performance of the mesophilic strains and tested abiotic factors (nutrient conditions, light regimes) for their effect on the biosynthesis of secondary pigments. Overall, this is the first report and detailed characterization of a mesophilic *Ancylonema* species, here described as *A. palustre* sp. nov., setting the ground for future comparative genomic and ecophysiological studies.

Experimental procedures

Collection and cultivation of algae

Natural samples were collected at two moorlands in Germany (see Table S1 for detailed sampling information) and screened for algal cells. Single cells were isolated with a micropipette under visual control with a Motic AE2000 inverted microscope (Motic, Hong Kong), washed in sterile water, and transferred into the liquid growth medium Waris-H (McFadden & Melkonian, 1986). The isolated cells were incubated at low, artificial light from white LEDs (< 30 µmol photons m^{-2} s^{-1}), which resulted in well grown cultures. These cultures were used to establish bacteria-free strains by spray-plating as previously described (Busch & Hess, 2022a). The bacteria-free cultures were grown at 15 °C under a 14/10 h light/dark cycle with a photon fluence rate of about 30 µmol photons m^{-2} s^{-1} photosynthetically active radiation (PAR) supplied by LinearZ SunLike LEDs (5700 K, Lumitronix, Hechingen; see Figure 1A for spectral power distribution). The established algal strains, N3 and V5, are available through the senior author (S.H.) of this study.

Light and scanning electron microscopy

Time-lapse microscopy and photodocumentation of experimental cultures were done with the Motic AE2000 inverted microscope (Motic, Hong Kong) equipped with a MikroLive 6.4MP CMOS camera (MikroLive, Oppenau). For high-resolution imaging, the Zeiss Axio Observer inverted microscope equipped with the objective lenses Plan-Neofluar 40×/1.3 and Plan-Neofluar 100×/1.3 and the Axiocam 512 color (Carl Zeiss, Oberkochen) was used. For scanning electron microscopy, cells were collected by sedimentation, fixed with 2.5% glutaraldehyde and 1% osmium tetroxide in MT buffer (30 mM HEPES, 15 mM KCl, 5 mM EGTA, 5 mMMgSO4, pH 7), dehydrated in a graded series of ethanol:water mixtures, transferred into hexamethyldisilazane, and finally dried in the fume hood as previously described (Moye et al., 2022). The dry samples were sputter-coated with gold and examined with a ZEISS Neon 40 scanning electron microscope at 2.5 kV acceleration voltage (Carl Zeiss, Oberkochen). Brightness and contrast of micrographs were adjusted with Photoshop CS4 (Adobe Inc., Dublin).

DNA sequencing, alignment and molecular phylogenetics

Algal material from 15 ml of an axenic culture was collected by centrifugation (500 g, 10 min), washed twice with sterile, ultrapure water, and again collected by centrifugation. The resulting pellet was snap frozen in liquid nitrogen and lyophilized with the freeze-drying system BETA 1-8 LD plus (Christ, Osterode am Harz). Twenty SiLibeads Type ZY 6.0 of about 3 mm (Sigmund Lindner GmbH, Warmensteinach) were added to each sample, followed by mechanical lysis of the freeze-dried cells in a TissueLyser II (QIAGEN, Hilden). The samples were subjected to two minutes of shaking with a frequency of 30 min^{-1}. To extract DNA, the samples were further processed with the DNeasy PowerLyzer PowerSoil Kit (QIAGEN, Hilden) according to the manufacturer's instructions. The chloroplast encoded gene for the RuBisCO large subunit (rbcL) was amplified by a semi-nested PCR with the primers MaGo1F, MaGo2F and MaGo3R as previously described (Busch & Hess, 2022a; Gontcharov et al., 2004). The nucleus-encoded gene for the 18S rRNA was amplified with the universal eukaryotic primers EukA and EukB (without terminal polylinker; (Medlin et al., 1988)) after the following protocol: initial denaturation (95 °C, 180 s), followed by 35 cycles of denaturation (95 °C, 45 s), annealing (55 °C, 60 s), and elongation (72 °C, 180 s). All PCRs were done with the Taq DNA Polymerase (Invitrogen, Waltham, MA, USA) according to the manufacturers protocol. The PCR products were subjected to commercial Sanger sequencing (Eurofins Genomics, Ebersberg) with the primers MaGo2F and MaGo3R (rbcL gene) and EukA and EukB (18S rRNA gene). The nearly complete rbcL and 18S rRNA gene sequences were assembled from two overlapping reads using the AlignIR™ 2.0 software (LI-COR Biosciences, Lincoln, US) and deposited at GenBank (https://www.ncbi.nlm.nih.gov/genbank/) under the accessions PP555606, PP555607, PP555608 (rbcL gene) and PP544794, PP544795 (18S rRNA gene). The sequences were manually aligned with available gene sequences of other Zygnematophyceae using the SeaView 4.5.4 alignment editor (Galtier et al., 1996; Gouy et al., 2010). For the rbcL gene, we used an existent alignment (Busch & Hess, 2022a), while 18S rRNA gene sequences were retrieved from the National Center for Biotechnology Information (https://www.ncbi.nlm.nih.gov/). This resulted in two final datasets: (1) 35 zygnematophycean rbcL gene sequences with 1,290 sites, (2) 15 zygnematophycean 18S rRNA gene sequences with 1,675 sites. They were subjected to phylogenetic inferences with maximum likelihood (ML), neighbour joining (NJ) and maximum parsimony (MP) methods using the MEGA11 software (Tamura et al., 2021). The ML analyses were done with the GTR+I+G model (discrete Gamma distribution; 5 categories), NJ analyses with the P-distance model with the "partial deletion" option, and MP analyses with the Subtree-pruning-regrafting (SPR) algorithm. To assess statistical support of the branches, we performed 1,000 bootstrap repetitions for every analysis and added the resulting values to the ML topology shown in the results and the supplements. A pairwise distance analysis of six selected rbcL gene sequences was performed with 1,304 sites. All codon positions were included, but ambiguous positions were removed for each sequence pair (pairwise deletion option).

Pulse–amplitude modulated fluorometry

Cells of strains N3 and V5 were grown in Waris-H medium under the standard culturing conditions (see above) and then acclimated to two light conditions (12/12 h light/dark cycle), here termed "low light" (PAR: 19-22 μmol photons m^{-2} s^{-1}, UVA: 0.05-0.06 W m^{-2}, UVB: 0.005-0.006 W m^{-2}) and "high light" (PAR: 140-170 μmol photons m^{-2} s^{-1}, UVA: 0.3 W m^{-2}, UVB 0.02-0.03 W m^{-2}) for one week. During acclimatization the cells were kept at 15 °C and agitated by shaking at 150 rpm. After harvest by sedimentation, the cells were subjected to pulse–amplitude modulated fluorometry with a Walz PAM 2500 in a KS-2500 suspension cuvette (0.4 ml) at 15 °C. To determine the relative electron transport rates (rETR) of photosystem II, the apparent quantum yield for electron transport (α) and the light saturation point (I_k), we performed rapid light curve (RLC) measurements with photon flux densities (PFD) of 5, 34, 67, 104, 201, 366, 622, 984, 1389, 1666 and 2018 μmol photons m^{-2} s^{-1} for 30 s each. For each density, four independent replicates were measured. Data analysis was done as previously described (Procházková et al., 2018).

High PAR treatments

Algal material (strain N3) was suspended in fresh KW medium (see Table S2 for recipe) and distributed to 35 mm suspension tissue culture dishes (Sarstedt, Nümbrecht). The cells were then exposed to the SunLike high-power LED (5,000 K, 50 W, Seoul Semiconductor, Ansan) in a 14/10 h light/dark cycle (see Figure 1B for spectral power distribution). Different irradiance settings (100-1,300 μmol photons m^{-2} s^{-1}) were realized by adjusting the distance to the lamp. The algal cells were observed and photo-documented over at least 14 days. PAR irradiance was measured with the MQ-500 Full-Spectrum Quantum Sensor (Apogee Instruments Inc., Utah) through the lids of the used Petri dishes. The experiments were done in triplicates.

UVR treatments

Algal material (strain N3) was suspended in fresh KW medium (see Table S2 for recipe) and distributed to 100 mm tissue culture dishes (VWR international, Darmstadt). The "UVA treatment" was achieved with the TL-D Blacklight Blue fluorescent tube lamp (18 W, Philips, Hamburg), the "UVB treatment" with the UVB Broad Band TL (20 W, Phillips, Hamburg). For both treatments, cells were exposed for 4 h during the light phase of a 14/10 h light/dark cycle with PAR emitted by LinearZ SunLike LEDs (5,700K, Lumitronix, Hechingen) (see Figure 1C,D for spectral power distribution). Different irradiance settings (1-8 W m^{-2} for UVA, 0.2-2.0 W m^{-2} for UVB) were realized by adjusting the distance to the lamps. The algal cells were observed and photo-documented over at least 14 days. UVA and UVB irradiances were measured with the digital UV radiometers Solarmeter® Model 4.2 and Solarmeter® Model 6.2, respectively (Solar Light Company Inc., Pennsylvania) through the lids of the Petri dishes. The experiments were done in triplicates.

Nutrient limitation treatments

We designed three variations of the KW medium, which were limited in nitrate (-N), phosphate (-P) or both (-P-N) (see Table S2 for recipes). Well-growing material of strain N3 was suspended in these media, distributed in six-well tissue culture plates (VWR international, Darmstadt), and subjected to different light regimes. The latter included a treatment with moderate/high PAR (200 µmol photons m^{-2} s^{-1}), UVA at 8 W m^{-2}, and UVB at 0.6 W m^{-2} (selected on the basis of our previous experiments with varying irradiances). The experiments were done in triplicates and cells were photo-documented over at least 14 days.

Results

Habitat characteristics and natural material

Two monoclonal and axenic strains of *Ancylonema palustre* (N3 and V5) were established in this study. Both strains derive from moorlands in western Germany (Figure 2A). The strain N3 was isolated from squeezed *Sphagnum* moss of a waterlogged area in the spring bog of Neuenhähnen, Waldbröl, Germany (Figure 2B,C). The strain V5 was found in the organic, oxygenated sediment of a shallow bog pond with acidic, brown water, close to a disturbed raised bog system of the moorland Großes Veen, Hamminkeln, Germany (Figure 2D). Cells from this site displayed reddish-brown cytoplasm (Figure 2E), which was lost during cultivation. The climate of both sampling sites is temperate/oceanic (annual temperature average: Neuenhähnen 9.4 °C, Hamminkeln 10.8 °C) with considerable rainfall (>850 mm/year), classified as Cfb after Köppen (Geiger, 1954).

Morphology and cell division

Vegetative cells from laboratory cultures were bright green and rod-shaped with rounded cell poles (Figure 3A). Cells of both strains were very similar in size, with a cell width of around 7 µm and a cell length ranging from 16 to 34 µm (n=100, see Figure S1 for boxplots). While the cell width appeared to be relatively uniform, the cell length varied considerably due to cell growth between cell divisions. At interphase, each cell contained a single nucleus of about 3.6 µm in diameter (n=40) with a spherical nucleolus of about 1.7 µm (n=40). The nucleus was located in the cell's center between two chloroplasts (Figure 3A,B). These chloroplasts were mostly parietal and shovel-shaped with smooth margins, and there was no sign of a connecting bridge between them (Figure 3B). Each of the chloroplasts typically contained a single, circular or slightly elliptic pyrenoid of about 2.5 µm in diameter (n=80; Figure 3B). Only rarely, we observed additional smaller pyrenoids. Time-lapse microscopy revealed the sequence of cellular events during the cell cycle (Figure 3C, Movie S1). The cell division started with the duplication of the pyrenoids, which was followed by nuclear division (Figure 3D, stages 1-3). The two new nuclei then migrated into the cell's halves and subsequently a cross wall was formed in the center of the cell, starting with an increased vesicle movement (Figure 3D, stages 4, 5). Once the cross wall became more defined, the chloroplasts started to divide. The nearly synchronous divisions of the cell and the chloroplasts resulted in two firmly attached daughter cells with two chloroplasts each (Figure

3D, stage 5). The daughter cells separated slowly and attained the typical rod-shaped morphology by subsequent longitudinal cell growth (Figure 3D, stages 6, 1). We did not observe any pronounced formation of cell chains.

Molecular phylogeny

Figure 4A displays the best *rbc*L gene phylogeny (ML topology) of the genus *Ancylonema* plus selected outgroup lineages (Meso-4 – Meso-7 and *Zygogonium ericetorum*). Our new strains N3 and V5 are closely related to an available *rbc*L sequence (FM992361) of an alga isolated from wet rock in a forest of the Eifel, Germany (A. Gontscharov, pers. comm., no strain information available, Procházková et al., 2021). This alga might be identical to an uncharacterized algal strain of the Central Collection of Algal Cultures (CCAC2248), which was also sequenced in this study. Together, the four sequences of mesophilic algae form a highly supported clade (100/100/99), whose members are here assigned to the new species *A. palustre*. The *A. palustre* clade shows a sister relationship to the known sequences from psychrophilic *Ancylonema* strains. This grouping is very robust as well (100/100/99), so that we include the new, mesophilic strains in the genus *Ancylonema*. The subclade of psychrophilic representatives contains sequences from recently established cultures (OQ222865, OQ584255- OQ584267) as well as from field material (OQ202166, MW922839, MW922839). They stem from the Greenland ice sheet (violet circles) and the Alps (blue squares), and do not group according to their geographic origin. The *rbc*L gene phylogeny further reveals that the sequence MW922840, previously assigned to the species *A. alaskanum* (Procházková et al., 2021) is not identical or directly related to the cultivated *A. alaskanum* strain WP251 (Remias & Procházková, 2023). This points to some prevailing taxonomic problems concerning the species concepts of *A. alaskanum* and *A. nordenskioeldii*.

The mesophilic strains N3 and V5 showed only minor genetic differences in the *rbc*L gene. Pairwise distance analysis revealed a difference < 0.5 % between the four *A. palustre* sequences, while the genetic difference between these sequences and those of *A. alaskanum* (OQ222865) and *A. nordenskioeldii* (MW922839) were 2.8 and 3 %, respectively (see Table S3 for details). Overall, we recognize two genetically distinct subclades of the genus *Ancylonema*, which correlate with the ecological preferences of the strains (psychrophilic vs. mesophilic). We also generated sequence data of the 18S rRNA gene and inferred an 18S rRNA gene phylogeny. Even though the taxon sampling was not as broad and the phylogenetic signal of the 18S rRNA gene relatively weak, we observed a split of psychrophilic and mesophilic *Ancylonema* species in two subclades as well (Figure S2).

Photophysiology of laboratory cultures

For both strains (N3, V5), we collected rapid light curves of cells acclimated to "low light" and "high light" conditions, respectively (Figure 4B,C). The maximum electron transport rate (ETR_{max}) was markedly higher in the high light adapted cells, which also showed a slightly higher light saturation point (I_k). The low-light utilization efficiency α ranged from 36 to 42 in both strains, with higher values in low light adapted cells. Both strains showed signs of photoinhibition irrespective of the acclimatization conditions. In strain N3 the onset of photoinhibition was at about 200 µmol photons

$m^{-2} s^{-1}$, in strain V5 it was somewhat earlier at about 100 µmol photons $m^{-2} s^{-1}$. Overall, short-term acclimatization of *A. palustre* cells to higher light conditions resulted in lower α, higher I_k and enhanced ETR_{max}.

Cellular reactions to different light and nutrient conditions

Under our standard laboratory conditions (30 µmol photons $m^{-2} s^{-1}$; 15 °C, Waris-H medium) the cells of *A. palustre* lost their reddish-brown, intracellular pigmentation. However, in very old cultures we observed the sporadic occurrence of slightly reddish cells, pointing to an effect of the nutrient availability on the production of secondary pigments. Furthermore, it is already established that other saccoderm desmids (*Serritaenia* spp.) can be triggered to form other dark sunscreen pigments (extracellular) by experimental UVB exposure (Busch & Hess, 2022b). To test whether the production of vacuolar pigments in *A. palustre* can be experimentally induced, we subjected cells of strain N3 to different light and nutrient conditions.

The cells were exposed to three different spectral power distributions, termed "High PAR", "UVA" and "UVB" (Figure 1B-D), at varying irradiances, and showed distinct cellular reactions (Figure 5A-I). All three spectral ranges triggered the formation of vacuolar pigments (referred to as "pigmentation" in the following) after two to seven days, but with very different effectiveness. While high PAR (> 200 µmol photons $m^{-2} s^{-1}$) and UVA (> 1 W m^{-2}) resulted in very faintly pigmentated cells (Figure 5C,F), UVB at > 0.2 W m^{-2} led to a marked vacuolar pigmentation (Figure 5H,I). The varying extent of the dark pigmentation was confirmed with high resolution brightfield microscopy (Figure 6A-C). Furthermore, we observed a significant shrinkage of the chloroplasts under very high PAR and UVB conditions (Figure 5C,I). High PAR (> 500 $µmol^{-2} s^{-1}$) had clearly adverse effects on the cells, including the deformation and bleaching of the chloroplasts, the formation of unusual pigment inclusions (vacuoles of reddish-brown color), and cell death (Figure 5C). The formation of pigment inclusions was also observed under very high UVA exposure (> 8 W m^{-2}, Figure S2).

Limitation of nitrate (-N) and phosphate (-P) in the culture medium showed clear effects on the cells of *A. palustre* under standard light conditions. While the absence of phosphate in the medium alone did not have any visible effect on the cells (Figure 5J), nitrate limitation led to the formation of large colorless globules within the cytoplasm (Figure 5K). The strongest effect was observed under combined phosphate/nitrate limitation (-P-N), including the formation of colorless globules and reddish cytoplasm. These effects were already apparent after four days of treatment, but increased further with time (Figure 5L,M). High resolution microscopy also revealed a pronounced shrinkage of the chloroplast under P-N-limitation (Figure 6D).

Finally, we tested the cumulative effects of -P-N limitation and three light conditions that triggered the intracellular pigments, but did not harm the cells (PAR: max. 200 µmol photons $m^{-2} s^{-1}$, UVA: max. 8 W m^{-2}, UVB: max. 0.6 W m^{-2}). All combinations led to pigmented cytoplasm (Figure 5N-P), which was most intense under the UVA and UVB treatments. After 45 days of treatment, cells under -P-N limitation and UVB exposure displayed strongly colored cytoplasm and relatively small but green

chloroplasts, resembling the *Ancylonema* cells found in nature (Figures 5Q, 6E). Under all tested conditions the intracellular secondary pigments had a reddish color.

Formation and morphology of zygospores

Under -N limitation and -P-N limitation both *A. palustre* strains formed roundish zygospores by conjugation of monoclonal cells, leaving behind two empty parental cell walls (Figure 6F). These cell walls exhibited a roundish hole with a dilatated margin of porous/fibrillar texture (Figure 6G). Mature zygospores measured 13–21 μm (n=20) and had a multifaceted morphology with three discernible cell walls (Figure 6H). The latter may correspond to the exo-, meso- and endospore of other Zygnematophyceae (Permann et al., 2023). The inner zygospore wall (endospore) had a round outline and tightly surrounded the protoplast, while the middle wall (mesospore) created the polyhedral appearance by folds and/or ribs (Figure 6H). In scanning electron micrographs, it became apparent that the polygonal faces of the zygospores were not flat but rather represented depressions (Figure 6I). Most of the zygospores were likely to have 12 faces, as most observed faces had five adjacent faces (comparable to a dodecahedron). The surface of the polyhedral wall (mesospore) was granular due to fine warts, but in many cases partially covered by a smooth, skin-like envelope, the potential exospore (Figure 6J). This envelope appeared to be ruptured and displayed fairly long fibrils (potentially cellulose) at the edges (Figure 6J, inset). Time-lapse microscopy of the zygospore maturation revealed that the zygospores of *A. palustre* started as spherical cells with a smooth cell wall, which then increased in thickness and was subsequently slightly deformed by another secondary cell wall (Figure 6K, Movie S2). This secondary cell wall grew bigger and produced the polyhedral geometry of the zygospore. On top of this secondary wall were some remains of a smooth cell wall, which may correspond to the ruptured, skin-like layer observed in the scanning electron microscope. The formation of a third cell wall, which tightly surrounds the spherical protoplast could not be captured very well, but this is likely to be the last event during zygospore maturation (compare with Figure 6H).

Discussion

Until now, *Ancylonema* species have only been known from glacial ice (rarely snow) and represent the best studied psychrophilic streptophyte algae. Hence, the discovery of mesophilic *Ancylonema* strains from temperate moorlands raise the question of how they differ from the known species. From the morphological point of view, they appear similar at first glance. Both the psychrophilic species (*A. alaskanum*, *A. nordenskioeldii*) and the new mesophilic species form rod-shaped cells with rounded cell poles, and contain shovel-shaped chloroplasts with smooth margins and circular pyrenoids. However, our morphological analysis revealed distinct differences concerning the cell width, the number of observed chloroplasts, conjugation and zygospore morphology. In the saccoderm desmids, the cell width appears to be a relatively stable character of taxonomic significance. This character can differ between genetically distinct strains, but was shown to remain unaltered in natural vs. cultivated material (Barcytė

et al., 2020; Busch & Hess, 2022b). The new species *A. palustre* is more slender than the cultivated strain of *A. alaskanum* (7 vs. 8,5 μm) and the natural material of *A. nordenskioeldii* (>10 μm) (Procházková et al., 2021; Remias & Procházková, 2023). Our time-lapse studies on *A. palustre* revealed that this species (in culture) has always two chloroplasts per cell throughout the cell cycle. This is because the division of the chloroplasts coincides with the formation of a new cross wall. In natural and cultivated material of *A. alaskanum*, cells with only one chloroplast have frequently been documented (Procházková et al., 2021; Remias et al., 2009; Remias & Procházková, 2023). Of course, cell cycle processes might be influenced by environmental conditions and future in-depth studies on cultivated glacier species have to complete our picture. Under nutrient-poor conditions (esp. nitrate limitation), *A. palustre* forms zygospores by conjugation of monoclonal cells, which exit the parent cell walls during the process and form a spherical zygote. This effect of nitrate limitation is consistent with published observations on other genera, e.g. *Mesotaenium*, *Spirogyra*, and *Closterium* (Hogetsu & Yokoyama, 1979; Tiflickjian & Raybum, 1986; Yamashita & Sasaki, 1979; Zwirn et al., 2013). The zygote of *A. palustre* develops into a zygospore with three cell wall layers, which correspond to the endo-, meso- and exospore layers (Permann et al., 2023). The relatively thick mesospore of *A. palustre* exhibits a remarkable multifaceted morphology, most closely resembling a dodecahedron. In some other species (e.g. *Spirogyra*, *Mougeotia*) the mesospore was shown to contain lipids and aromatic compounds and is thought to be responsible for the high resistance of zygospores against environmental factors (Permann et al., 2022; Permann, Herburger, Felhofer, et al., 2021; Permann, Herburger, Niedermeier, et al., 2021). Furthermore, the mesospore represents a defining character of taxonomic value, as it can vary in color (e.g. brown, yellow, purple), shape and ornamentation depending on the species (Pichrtová et al., 2018; Poulíčková et al., 2007; Takano et al., 2019). As far as we know, mature zygospores have not been documented for the psychrophilic *Ancylonema* species. However, Remias et al. (Remias, Holzinger, et al., 2012) found conjugating *A. nordenskioeldii* cells, which apparently do not exit the parent cells and, thereby, produce more irregular zygotes with a prominent conjugation bridge. There is another account for zygospores of psychrophilic *Ancylonema* strains from continental Antarctica (Ling & Seppelt, 1990). These algae, referred to as "*Mesotaenium berggrenii*", lack any genetic information and show a conspicuous variation in cell sizes, potentially pointing to more than one species. In contrast to *A. nordenskioeldii*, the documented zygotes are spherical. As they have a smooth cell wall and no discernible mesospore, they might be immature and further studies have yet to show whether these psychrophilic strains form multifaceted mesospores similar to those of *A. palustre*.

The molecular phylogenies of two marker genes (*rbc*L, 18S rRNA) confirm the separation of mesophilic and psychrophilic *Ancylonema* species, which form two distinct clades and show clear genetic divergence in the *rbc*L gene (> 2.8%). Hence, we are confident in proposing a new species for the three mesophilic *Ancylonema* strains (N3, V5, CCAC2248), accepting minor genetic differences (< 0.5%) among them, as we did not recognize any marked phenotypic differences. The taxonomic situation in the psychrophilic clade appears to be more difficult. Both psychrophilic morphospecies *A.*

nordenskioeldii and *A. alaskanum* are part of a genetically shallow branch of sequences from environmental samples and crude cultures, that still lack a sound taxonomic treatment (Jensen et al., 2023). Furthermore, two separate isolates assigned to *A. alaskanum* occupy distinct positions, being non-monophyletic (MW922840 and sequences of WP251). The sequences derived from the same Austrian glacier, but were sampled in different years (2017 and 2020). Overall, the genetic variation visible in the psychrophilic clade indicates that the actual diversity of these algae might be greater than reasonably represented by only two described species. The morphological variability of *Ancylonema* cells in the field, e.g. the range of cell width (4-12 µm) observed by different authors for cells assigned to *A. alaskanum* (Remias et al., 2009), supports this hypothesis, and just recently Remias et al. (Remias et al., 2023) recognized another undescribed species in glacier ice samples from Svalbard, the Alps of Switzerland and Austria, and Sweden by environmental ITS2 sequencing (reference ITS2 sequence: PP138441). We conclude that the genus *Ancylonema* probably hides more species than currently recognized, which deserve to be characterized by integrative taxonomy and ecophysiological studies in the future.

The strains of the two main *Ancylonema* clades occur in very different habitats. While glacial habitats are characterized by low temperatures close to the freezing mark, moorlands (including ponds) in the sampled zones can warm up considerably during summer (the maximum ambient temperatures in these zones are well above 15 °C). This climatic difference is reflected by the preferred temperatures of the available *Ancylonema* cultures. While *A. alaskanum* dies at temperatures above 10 °C (unpubl. observation, D. Remias), *A. palustre* grows well at 15 °C and higher. Furthermore, the two habitat types differ strongly in the level of solar radiation experienced by the algae. The lower altitudes of the sampled moorlands, potential shading by plants, debris and sediment, and absorbance by the water column (especially when humic substances are present), should reduce light and UV irradiances considerably (as compared to glacier surface habitats).

Our photophysiological measurements show that the two mesophilic *Ancylonema* strains (N3 and V5) reacted partly similar at higher irradiances, if grown under "low light" conditions: The onset of photoinhibition (a decline in rETR) was noticed. This happened at relatively low light levels, when compared to the *Ancylonema* strain from glacier ice (< 200 vs. 366 µmol photons m^{-2} s^{-1}; (Remias & Procházková, 2023)). Consistently, a typical low-light (i.e. reduced I_k, increased alpha) or high-light (i.e. increased I_k, reduced alpha) acclimation of the photosystems was noticed. There are, however, significant differences between the photosynthetic performance of the glacier ice alga *A. alaskanum* and the two mesophilic strains, if grown under high light: First, the light saturation point of the psychrophile was one magnitude higher (I_k=472; (Remias & Procházková, 2023)) when compared to the mesophiles. Second, the psychrophile reached the highest rETR at very high light levels (rETR of 42 at 1500-2100 µmol photons m^{-2} s^{-1}; (Remias & Procházková, 2023)). Third, the glacier ice alga showed very low utilization efficiency at low light (alpha = 0.09; (Remias & Procházková, 2023)). In contrast, the mesophiles showed no chlorophyll fluorescence from 1000 µmol photons m^{-2} s^{-1} on, but were able to

keep a high utilization efficiency at low light levels, irrespective of the acclimation conditions. Overall, these differences indicate that *Ancylonema* strains from the two very different habitat types (moorlands vs. glaciers) display pronounced ecological adaptations.

Interestingly, the mesophilic *Anyclonema* strains produce a secondary pigmentation, which is surprisingly similar to that found in the glacier species. Based on the visual resemblance of the pigmented cells and the phylogenetic proximity of the algae, we assume that the pigmentation is based on the same or similar phenolic compounds as those detected in *A. alaskanum*, namely purpurogallin derivates (Remias, Schwaiger, et al., 2012). Even though a role of these substances as sunscreen is likely, other functions have been proposed as well. For example, antimicrobial effects and a thawing function through heat dissipation (Remias, Schwaiger, et al., 2012). Most of the currently known zygnematophytes that produce striking intracellular pigments (e.g. *Zygogonium ericetorum*, *Temnogametum iztacalense*, psychrophilic *Ancylonema* species) are either uncultivated or difficult to grow, as they occur in extreme habitats in terms of temperature and/or nutrient composition (Aigner et al., 2013; Garduño-Solórzano et al., 2021; Remias et al., 2009). Here, we used our well-growing cultures of *A. palustre* to test for abiotic inducing factors of intracellular zygnematophycean pigments and found that both nutrient availability and radiation influence the secondary pigment biosynthesis. It might seem remarkable that -N-P limited conditions alone lead to a slight reddish pigmentation in *A. palustre* (esp. over longer periods of time), while this was not regularly observed in richer media (e.g. Waris-H). However, the habitats of *A. palustre* were oligotrophic (strain N3) or dystrophic (strain V5), so that a culture medium poor in nitrate and phosphate might better reflect natural nutrient conditions and favor a close-to-natural metabolism – including the production of phenolic pigments. A very strong induction was observed under ultraviolet radiation, in particular UVB, which suggests that the reddish-brown pigments in *Ancylonema* are indeed specific reactions to harmful wavebands. Even though we cannot exclude that the strong vacuolar pigmentation has other functions, especially in psychrophilic strains (e.g. thawing agent to create liquid water), the occurrence of these pigments in mesophilic strains and their induction by UVB support a primary function in photoprotection.

With these experiments we optimized the experimental production of the intracellular phenolics of zygnematophytes and were able to create strongly pigmented cells with a close-to-natural phenotype in the laboratory. This paves the way for molecular and analytical follow-up studies on how these pigments are composed and synthetized. In particular, the application of genomic techniques, which often depend on high cell numbers, will be applicable to *A. palustre* and may help to answer the question of how psychrophiles evolved in one particular lineage of zygnematophytes.

<u>Taxonomy</u>

Class **Zygnematophyceae** Round ex Guiry 2013

Genus *Ancylonema* Berggren, 1872

Ancylonema palustre sp. nov.

Description: Cells rod-shaped, 6-8 µm wide and 16-34 µm long, with rounded apices. Two parietal or axial chloroplasts per cell, with smooth edges and a single more or less circular pyrenoid per chloroplast of about 2.5 µm. Nucleus vesicular, about 3.6 µm in diameter, often located in the cell's center between the chloroplasts, with spherical nucleolus of about 1.7 µm. Cytoplasm colorless or reddish due to secondary pigments. Zygospores form outside of parent cells, with three cell walls including a multifaceted (dodecahedron-like), colorless mesospore, 13-21 µm in diameter.

Etymology: The species name is derived from *paluster* (neuter *palustre*) [Latin] = living in the swamp; referring to the natural habitat.

Type (here designated): Permanent slide with fixed material of strain N3 deposited in *Herbarium Berolinense* (Botanic Garden and Botanical Museum Berlin), accession B 40 >>To be added after review<<, locality: Neuenhähnen, North Rhine-Westphalia, Germany; collected 2020, leg. S. Hess.

Reference sequence: PP555607 (*rbc*L gene sequence of strain N3).

PhycoBank ID: >>To be added after review<<

<u>Acknowledgements</u>

<u>Author Contributions</u>

Conceptualization: A.B., S.H.; investigation: all authors; writing – original draft: A.B.; writing – review & editing: all authors; visualization: A.B., L.P.; funding acquisition: S.H.

References

Aigner, S., Remias, D., Karsten, U., & Holzinger, A. (2013). Unusual phenolic compounds contribute to ecophysiological performance in the purple-colored green alga *Zygogonium ericetorum* (Zygnematophyceae, Streptophyta) from a high-alpine habitat. *Journal of phycology*, *49*(4), Article 4.

Barcytė, D., Pilátová, J., Mojzeš, P., & Nedbalová, L. (2020). The arctic *Cylindrocystis* (Zygnematophyceae, Streptophyta) green algae are genetically and morphologically diverse and exhibit effective accumulation of polyphosphate. *Journal of Phycology*, *56*(1), Article 1.

Brook, A. J., & Williamson, D. B. (2010). A monograph on some British desmids. *The Ray Society. London: UK*, 364.

Busch, A., & Hess, S. (2022a). A diverse group of underappreciated zygnematophytes deserves in-depth exploration. *Applied Phycology*, 1–18.

Busch, A., & Hess, S. (2022b). Sunscreen mucilage: A photoprotective adaptation found in terrestrial green algae (Zygnematophyceae). *European Journal of Phycology*, *57*(1), 107–124. https://doi.org/10.1080/09670262.2021.1898677

Coesel, P. F. M., & Meesters, K. J. (2007). *Desmids of the Lowlands: Mesotaeniaceae and Desmidiaceae of the European Lowlands*. BRILL.

Cook, J. M., Tedstone, A. J., Williamson, C., McCutcheon, J., Hodson, A. J., Dayal, A., Skiles, M., Hofer, S., Bryant, R., McAree, O., McGonigle, A., Ryan, J., Anesio, A. M., Irvine-Fynn, T. D. L., Hubbard, A., Hanna, E., Flanner, M., Mayanna, S., Benning, L. G., … Tranter, M. (2020). Glacier algae accelerate melt rates on the south-western Greenland Ice Sheet. *The Cryosphere*, *14*(1), 309–330. https://doi.org/10.5194/tc-14-309-2020

de Vries, J., de Vries, S., Curtis, B. A., Zhou, H., Penny, S., Feussner, K., Pinto, D. M., Steinert, M., Cohen, A. M., von Schwartzenberg, K., & Archibald, J. M. (2020). Heat stress response in the closest algal relatives of land plants reveals conserved stress signaling circuits. *The Plant Journal*, *103*(3), 1025–1048. https://doi.org/10.1111/tpj.14782

de Vries, J., de Vries, S., Slamovits, C. H., Rose, L. E., & Archibald, J. M. (2017). How Embryophytic is the Biosynthesis of Phenylpropanoids and their Derivatives in Streptophyte Algae? *Plant and Cell Physiology*, *58*(5), 934–945. https://doi.org/10.1093/pcp/pcx037

Fürst-Jansen, J. M. R., de Vries, S., & de Vries, J. (2020). Evo-physio: On stress responses and the earliest land plants. *Journal of Experimental Botany*, *71*(11), 3254–3269. https://doi.org/10.1093/jxb/eraa007

Galtier, N., Gouy, M., & Gautier, C. (1996). SEAVIEW and PHYLO_WIN: Two graphic tools for sequence alignment and molecular phylogeny. *Bioinformatics*, *12*(6), Article 6.

Garduño-Solórzano, G., Martínez-García, M., Scotta Hentschke, G., Lopes, G., Castelo Branco, R., Vasconcelos, V. M. O., Campos, J. E., López-Cano, R., & Quintanar-Zúñiga, R. E. (2021). The phylogenetic placement of Temnogametum (Zygnemataceae) and description of Temnogametum iztacalense sp. Nov., from a tropical high mountain lake in Mexico. *European Journal of Phycology*, *56*(2), 159–173. https://doi.org/10.1080/09670262.2020.1789226

Geiger, R. (1954). Klassifikation der klimate nach W. Köppen. In *Landolt-Börnstein: Zahlenwerte und Funktionen aus Physik, Chemie, Astronomie, Geophysik und Technik* (Bd. 3, S. 603–607). Springer.

Gontcharov, A. A., Marin, B., & Melkonian, M. (2004). Are combined analyses better than single gene phylogenies? A case study using SSU rDNA and rbc L sequence comparisons in the Zygnematophyceae (Streptophyta). *Molecular biology and evolution*, *21*(3), Article 3.

Gouy, M., Guindon, S., & Gascuel, O. (2010). SeaView version 4: A multiplatform graphical user interface for sequence alignment and phylogenetic tree building. *Molecular biology and evolution*, *27*(2), Article 2.

Hall, J. D., & McCourt, R. M. (2015). Chapter 9—Conjugating Green Algae Including Desmids. In J. D. Wehr, R. G. Sheath, & J. P. Kociolek (Hrsg.), *Freshwater Algae of North America (Second Edition)* (S. 429–457). Academic Press. https://doi.org/10.1016/B978-0-12-385876-4.00009-8

Hogetsu, T., & Yokoyama, M. (1979). Light, a nitrogen-depleted medium and cell-cell interaction in the conjugation process of Closterium ehrenbergii Meneghini. *Plant and Cell Physiology*, *20*(4), 811–817. https://doi.org/10.1093/oxfordjournals.pcp.a075873

Jensen, M. B., Perini, L., Halbach, L., Jakobsen, H., Haraguchi, L., Ribeiro, S., Tranter, M., Benning, L. G., & Anesio, A. M. (2023). The dark art of cultivating glacier ice algae. *Botany Letters*, *0*(0), 1–10. https://doi.org/10.1080/23818107.2023.2248235

Kol, E. (1942). The Snow and ice algae of Alaska. *THE SMITHSONIAN INSTITUTION*, *101*(16).

Ling, H. U., & Seppelt, R. D. (1990). Snow algae of the Windmill Islands, continental Antarctica. Mesotaenium berggrenii (Zygnematales, Chlorophyta) the alga of grey snow. *Antarctic Science*, *2*(2), Article 2. https://doi.org/10.1017/S0954102090000189

McFadden, G. I., & Melkonian, M. (1986). Use of Hepes buffer for microalgal culture media and fixation for electron microscopy. *Phycologia*, *25*(4), Article 4.

Medlin, L., Elwood, H. J., Stickel, S., & Sogin, M. L. (1988). The characterization of enzymatically amplified eukaryotic 16S-like rRNA-coding regions. *Gene*, *71*(2), 491–499. https://doi.org/10.1016/0378-1119(88)90066-2

Moye, J., Schenk, T., & Hess, S. (2022). Experimental evidence for enzymatic cell wall dissolution in a microbial protoplast feeder (Orciraptor agilis, Viridiraptoridae). *BMC Biology*, *20*(1), 267. https://doi.org/10.1186/s12915-022-01478-x

Permann, C., Gierlinger, N., & Holzinger, A. (2022). Zygospores of the green alga Spirogyra: New insights from structural and chemical imaging. *Frontiers in Plant Science*, *13*. https://doi.org/10.3389/fpls.2022.1080111

Permann, C., Herburger, K., Felhofer, M., Gierlinger, N., Lewis, L. A., & Holzinger, A. (2021). Induction of Conjugation and Zygospore Cell Wall Characteristics in the Alpine Spirogyra mirabilis (Zygnematophyceae, Charophyta): Advantage under Climate Change Scenarios? *Plants*, *10*(8), Article 8. https://doi.org/10.3390/plants10081740

Permann, C., Herburger, K., Niedermeier, M., Felhofer, M., Gierlinger, N., & Holzinger, A. (2021). Cell wall characteristics during sexual reproduction of Mougeotia sp. (Zygnematophyceae) revealed by electron microscopy, glycan microarrays and RAMAN spectroscopy. *Protoplasma*, *258*(6), 1261–1275. https://doi.org/10.1007/s00709-021-01659-5

Permann, C., Pichrtová, M., Šoljaková, T., Herburger, K., Jouneau, P.-H., Uwizeye, C., Falconet, D., Marechal, E., & Holzinger, A. (2023). 3D-reconstructions of zygospores in Zygnema vaginatum (Charophyta) reveal details of cell wall formation, suggesting adaptations to extreme habitats. *Physiologia Plantarum*, *175*(4), e13988. https://doi.org/10.1111/ppl.13988

Pichrtová, M., Holzinger, A., Kulichová, J., Ryšánek, D., Šoljaková, T., Trumhová, K., & Nemcova, Y. (2018). Molecular and morphological diversity of Zygnema and Zygnemopsis (Zygnematophyceae, Streptophyta) from Svalbard (high Arctic). *European journal of phycology*, *53*(4), Article 4.

Poulíčková, A., Žižka, Z., Hašler, P., & Benada, O. (2007). Zygnematalean zygospores: Morphological features and use in species identification. *Folia Microbiologica*, *52*(2), 135–145. https://doi.org/10.1007/BF02932152

Procházková, L., Remias, D., Řezanka, T., & Nedbalová, L. (2018). Chloromonas nivalis subsp. tatrae, subsp. nov. (Chlamydomonadales, Chlorophyta): Re–examination of a snow alga from the High Tatra Mountains (Slovakia). *Fottea (Praha)*, *18*(1), 1–18. https://doi.org/10.5507/fot.2017.010

Procházková, L., Řezanka, T., Nedbalová, L., & Remias, D. (2021). Unicellular versus Filamentous: The Glacial Alga Ancylonema alaskana comb. et stat. nov. and Its Ecophysiological Relatedness to Ancylonema nordenskioeldii (Zygnematophyceae, Streptophyta). *Microorganisms*, *9*(5), Article 5. https://doi.org/10.3390/microorganisms9051103

Remias, D., Holzinger, A., Aigner, S., & Lütz, C. (2012). Ecophysiology and ultrastructure of Ancylonema nordenskiöldii (Zygnematales, Streptophyta), causing brown ice on glaciers in Svalbard (high arctic). *Polar Biology*, *35*(6), Article 6.

Remias, D., Holzinger, A., & Lütz, C. (2009). Physiology, ultrastructure and habitat of the ice alga Mesotaenium berggrenii (Zygnemaphyceae, Chlorophyta) from glaciers in the European Alps. *Phycologia*, *48*(4), Article 4. https://doi.org/10.2216/08-13.1

Remias, D., & Procházková, L. (2023). The first cultivation of the glacier ice alga Ancylonema alaskanum (Zygnematophyceae, Streptophyta): Differences in morphology and photophysiology of field vs laboratory strain cells. *Journal of Glaciology*, *69*(276), 1080–1084. https://doi.org/10.1017/jog.2023.22

Remias, D., Procházková, L., Nedbalová, L., Benning, L. G., & Lutz, S. (2023). Novel insights in cryptic diversity of snow and glacier ice algae communities combining 18S rRNA gene and ITS2

amplicon sequencing. *FEMS Microbiology Ecology*, *99*(12), fiad134. https://doi.org/10.1093/femsec/fiad134

Remias, D., Schwaiger, S., Aigner, S., Leya, T., Stuppner, H., & Lütz, C. (2012). Characterization of an UV-and VIS-absorbing, purpurogallin-derived secondary pigment new to algae and highly abundant in M esotaenium berggrenii (Z ygnematophyceae, Chlorophyta), an extremophyte living on glaciers. *FEMS microbiology ecology*, *79*(3), Article 3.

Stibal, M., Box, J. E., Cameron, K. A., Langen, P. L., Yallop, M. L., Mottram, R. H., Khan, A. L., Molotch, N. P., Chrismas, N. A. M., Calì Quaglia, F., Remias, D., Smeets, C. J. P. P., van den Broeke, M. R., Ryan, J. C., Hubbard, A., Tranter, M., van As, D., & Ahlstrøm, A. P. (2017). Algae Drive Enhanced Darkening of Bare Ice on the Greenland Ice Sheet. *Geophysical Research Letters*, *44*(22), 11,463-11,471. https://doi.org/10.1002/2017GL075958

Takano, T., Higuchi, S., Ikegaya, H., Matsuzaki, R., Kawachi, M., Takahashi, F., & Nozaki, H. (2019). Identification of 13 Spirogyra species (Zygnemataceae) by traits of sexual reproduction induced under laboratory culture conditions. *Scientific reports*, *9*(1), Article 1.

Takeuchi, N. (2001). The altitudinal distribution of snow algae on an Alaska glacier (Gulkana Glacier in the Alaska Range). *Hydrological Processes*, *15*(18), 3447–3459. https://doi.org/10.1002/hyp.1040

Takeuchi, N., Tanaka, S., Konno, Y., Irvine-Fynn, T. D. L., Rassner, S. M. E., & Edwards, A. (2019). Variations in Phototroph Communities on the Ablating Bare-Ice Surface of Glaciers on Brøggerhalvøya, Svalbard. *Frontiers in Earth Science*, *7*. https://doi.org/10.3389/feart.2019.00004

Takeuchi, N., Uetake, J., Fujita, K., Aizen, V. B., & Nikitin, S. D. (2006). A snow algal community on Akkem glacier in the Russian Altai mountains. *Annals of Glaciology*, *43*, 378–384. https://doi.org/10.3189/172756406781812113

Tamura, K., Stecher, G., & Kumar, S. (2021). MEGA11: Molecular Evolutionary Genetics Analysis Version 11. *Molecular Biology and Evolution*, *38*(7), 3022–3027. https://doi.org/10.1093/molbev/msab120

Tiflickjian, J. D., & Raybum, W. R. (1986). Nutritional Requirements for Sexual Reproduction in Mesotaenium Kramstai (chlorophyta) 1. *Journal of Phycology*, *22*(1), 1–8. https://doi.org/10.1111/j.1529-8817.1986.tb02508.x

Timme, R. E., Bachvaroff, T. R., & Delwiche, C. F. (2012). Broad phylogenomic sampling and the sister lineage of land plants. *PLoS one*, *7*(1), Article 1.

Walsby, A. E. (1997). Modelling the daily integral of photosynthesis by phytoplankton: Its dependence on the mean depth of the population. *Hydrobiologia*, *349*(1), 65–74. https://doi.org/10.1023/A:1003045528581

Wickett, N. J., Mirarab, S., Nguyen, N., Warnow, T., Carpenter, E., Matasci, N., Ayyampalayam, S., Barker, M. S., Burleigh, J. G., & Gitzendanner, M. A. (2014). Phylotranscriptomic analysis of the origin and early diversification of land plants. *Proceedings of the National Academy of Sciences*, *111*(45), Article 45.

Williamson, C. J., Anesio, A. M., Cook, J., Tedstone, A., Poniecka, E., Holland, A., Fagan, D., Tranter, M., & Yallop, M. L. (2018). Ice algal bloom development on the surface of the Greenland Ice Sheet. *FEMS Microbiology Ecology*, *94*(3), fiy025. https://doi.org/10.1093/femsec/fiy025

Williamson, C. J., Cameron, K. A., Cook, J. M., Zarsky, J. D., Stibal, M., & Edwards, A. (2019). Glacier Algae: A Dark Past and a Darker Future. *Frontiers in Microbiology*, *10*. https://doi.org/10.3389/fmicb.2019.00524

Williamson, C. J., Cook, J., Tedstone, A., Yallop, M., McCutcheon, J., Poniecka, E., Campbell, D., Irvine-Fynn, T., McQuaid, J., Tranter, M., Perkins, R., & Anesio, A. (2020). Algal photophysiology drives darkening and melt of the Greenland Ice Sheet. *Proceedings of the National Academy of Sciences*, *117*(11), 5694–5705. https://doi.org/10.1073/pnas.1918412117

Wodniok, S., Brinkmann, H., Glöckner, G., Heidel, A. J., Philippe, H., Melkonian, M., & Becker, B. (2011). Origin of land plants: Do conjugating green algae hold the key? *BMC Evolutionary Biology*, *11*(1), Article 1.

Yallop, M. L., Anesio, A. M., Perkins, R. G., Cook, J., Telling, J., Fagan, D., MacFarlane, J., Stibal, M., Barker, G., Bellas, C., Hodson, A., Tranter, M., Wadham, J., & Roberts, N. W. (2012). Photophysiology and albedo-changing potential of the ice algal community on the surface of

the Greenland ice sheet. *The ISME Journal*, *6*(12), 2302–2313. https://doi.org/10.1038/ismej.2012.107

Yamashita, T., & Sasaki, K. (1979). Conditions for the induction of the mating process and changes in contents of carbohydrates and nitrogen compounds during the mating process of Spirogyra. *Journal of the Faculty of Science, Hokkaido University*, *11*, 279–287.

Yoshimura, Y., Kohshima, S., & Ohtani, S. (1997). A Community of Snow Algae on a Himalayan Glacier: Change of Algal Biomass and Community Structure with Altitude. *Arctic and Alpine Research*, *29*(1), 126–137. https://doi.org/10.1080/00040851.1997.12003222

Zwirn, M., Chen, C., Uher, B., & Schagerl, M. (2013). Induction of sexual reproduction in Spirogyra clones—Does an universal trigger exist? *Fottea*, *13*(1), 77–85. https://doi.org/10.5507/fot.2013.007
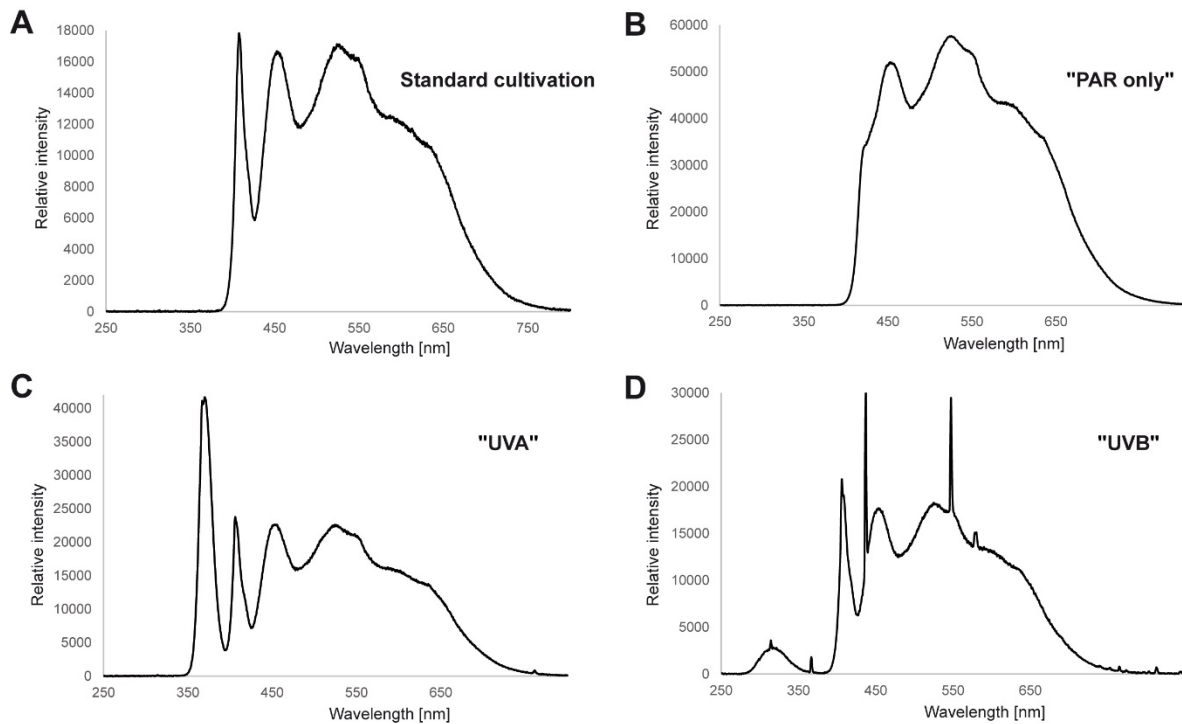
Figures:

Figure 1. Spectral emittance of the applied light sources. **(A)** Standard cultivation (LinearZ SunLike LEDs, 5,700 K). **(B)** "PAR only" treatment (SunLike high-power LED 5,000 K, 50 W). **(C)** "UVA" treatment (TL-D Blacklight Blue fluorescent tube lamp, 18 W + LinearZ SunLike LEDs, 5,700 K). **(D)** "UVB" treatment (UVB Broad Band TL, 20 W + LinearZ SunLike LEDs, 5,700 K).
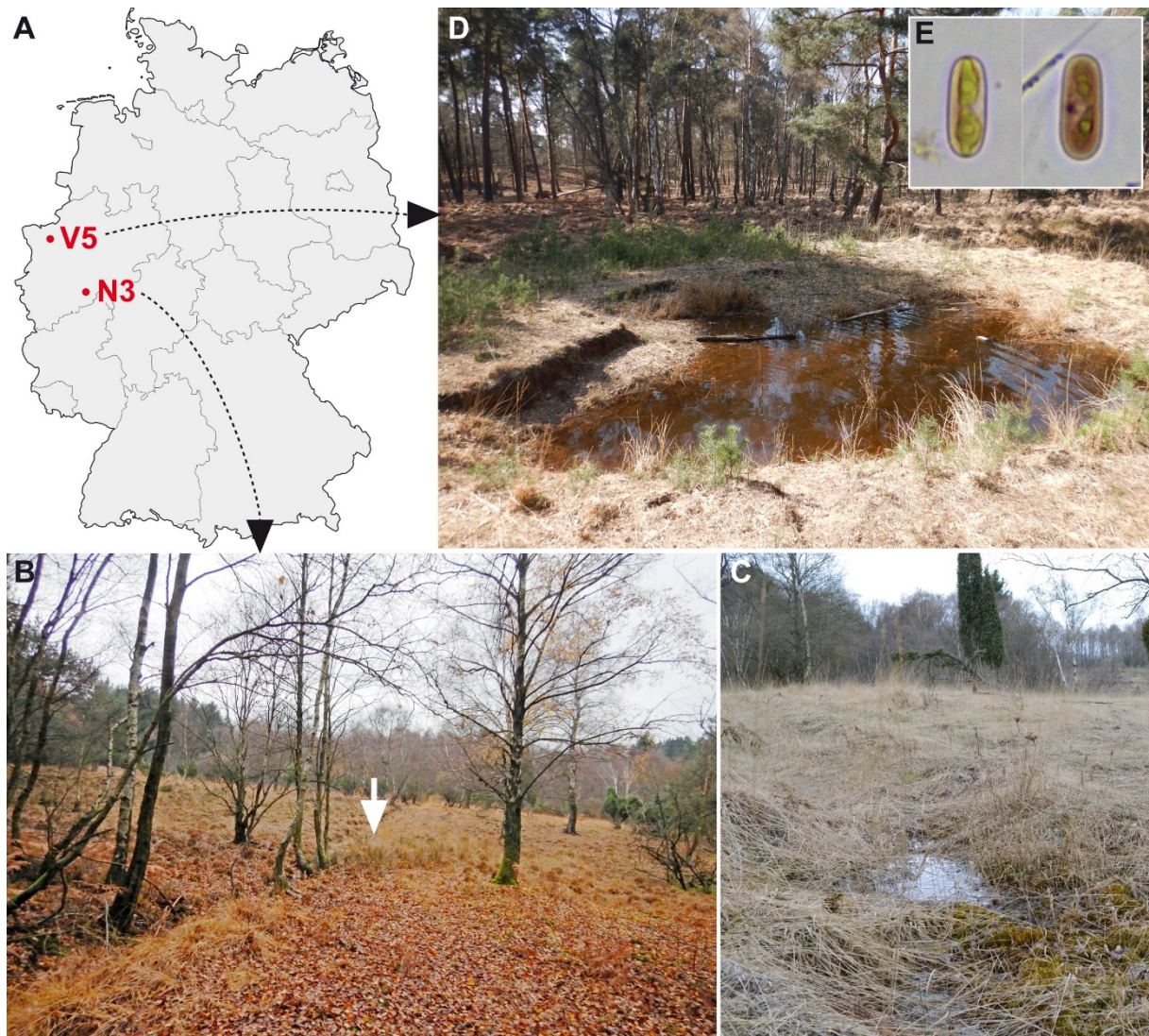
Figure 2. Collection sites of the studied *Ancylonema palustre* strains. **(A)** Map of Germany showing the two moorlands from which the algal strains (N3 and V5) were isolated. **(B, C)** Spring bog of Neuenhähnen, Germany. White arrow denotes waterlogged area with *Sphagnum* (shown in (C)), from which strain N3 was isolated. **(D)** Shallow bog pond with brownish water of the Großes Veen, Hamminkeln, Germany. Strain V5 was isolated from the oxygenated sediment. **(E)** Natural material of *A. palustre* from the pond shown in (D) with pronounced secondary pigmentation.
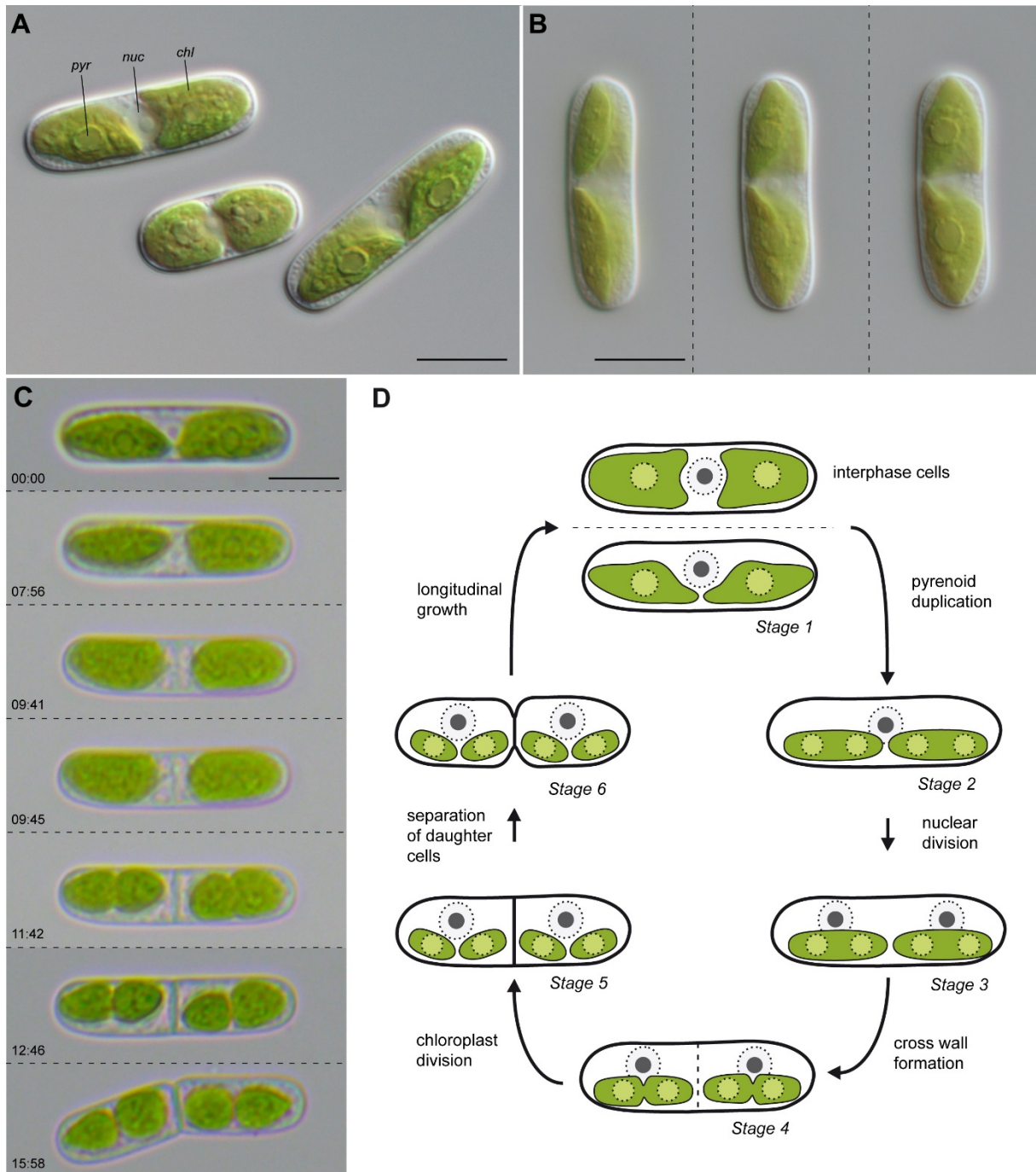
Figure 3. Morphology and cell division of *Ancylonema palustre*. **(A)** Cells of strain N3 under standard cultivation conditions. The nucleus (nuc) lies between two well-separated chloroplasts (chl), each of which contains a circular pyrenoid (pyr). **(B)** *A. palustre* cell (strain N3) shown in three focal planes. **(C)** Time series of cell division in strain N3 (time shown in mm:ss). **(D)** Generalized scheme of cell division in *A. palustre*. Scale bars: 10 μm.
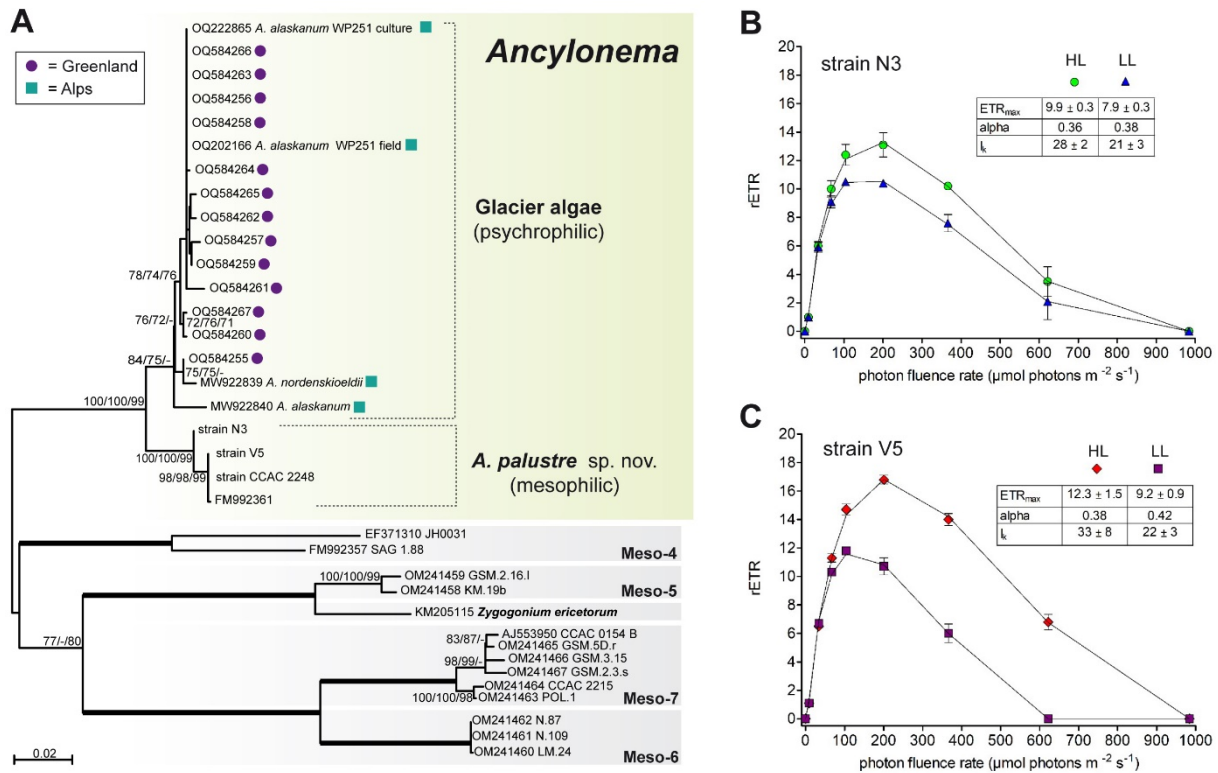
Figure 4. Phylogenetic position and photophysiology of *A. palustre*. **(A)** Maximum likelihood phylogeny of 35 zygnematophycean *rbc*L gene sequences displaying the relationships within the genus *Ancylonema*. Sequences from psychrophilic *Ancylonema* strains stem either from the Greenland ice sheet (violet circles) or the European Alps (blue squares). Support values > 70% from different analyses (ML/NJ/MP) are shown on the respective branches. Branches with maximum support (100/100/100) are bold. The scale bar represents 0.02 nucleotide substitutions per site. **(B, C)** Rapid light curves of *A. palustre* strains N3 (B) and V5 (C), and deduced parameters (rETR = relative electron transport rate, α = low light utilization efficiency, and I_k = light compensation point). Both strains were measured after acclimatization to "high light" (HL; green circles and red diamonds) and "low light" (LL; blue triangles and violet squares). Values are means of four replicate measurements and the datapoints were fitted to the photoinhibition model of Walsby (Walsby, 1997).
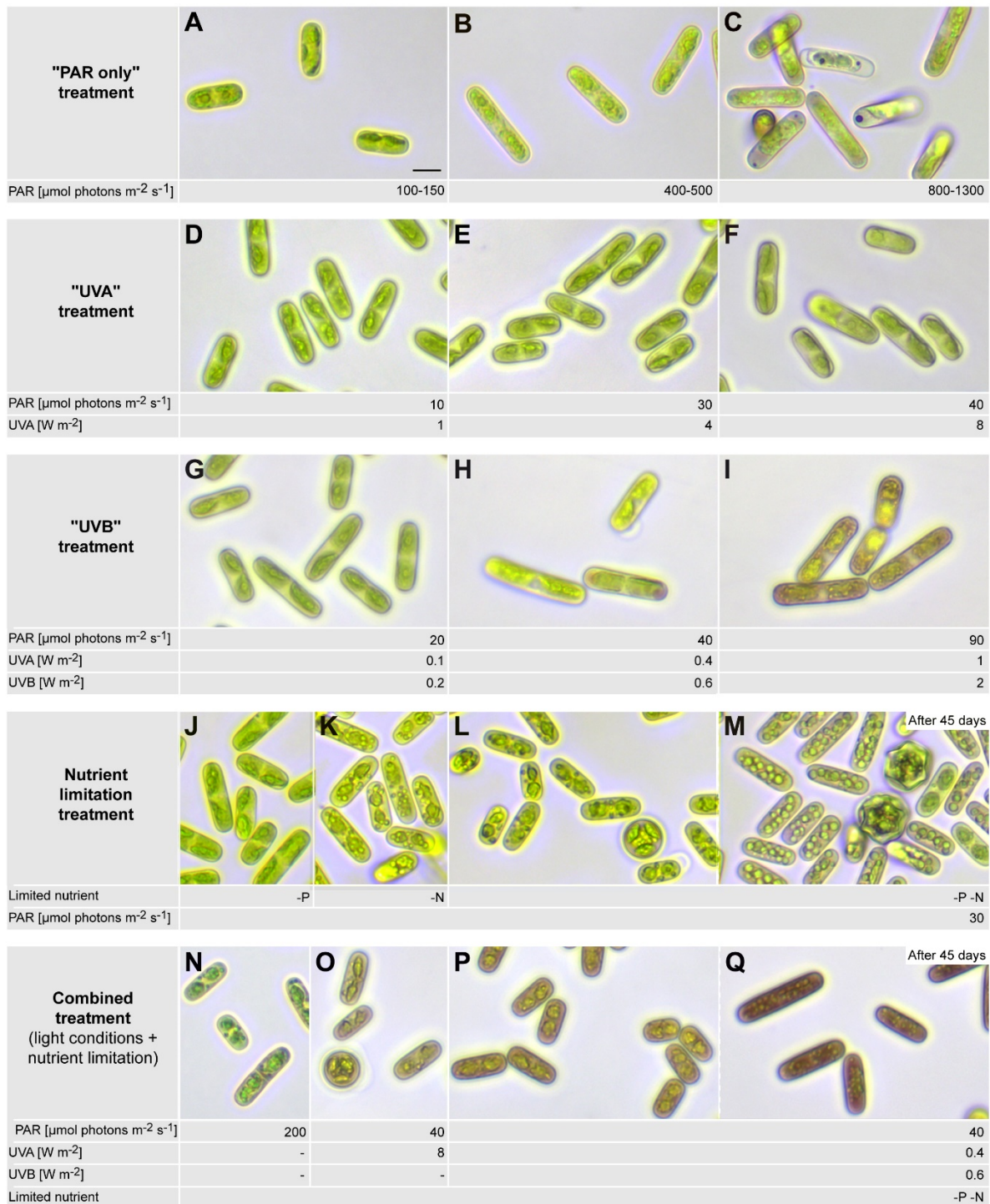
Figure 5. Phenotypic characteristics of *A. palustre* (strain N3) after ten days of incubation (if not stated differently) under different light regimes and nutrient conditions. **(A-C)** Three selected irradiance levels of the "PAR only" treatment. **(D-F)** Three selected irradiance levels of the "UVA" treatment. **(G-I)** Three selected irradiance levels of the "UVB" treatment. **(J)** KW medium without phosphate (-P). **(K)** KW medium without nitrate (-N). **(L, M)** KW medium without phosphate and nitrate (-P-N). **(N-Q)** -P-N limitation combined with "PAR only" (N), "UVA" (O), and "UVB" (P, Q) treatments. Scale bar: 10 μm.
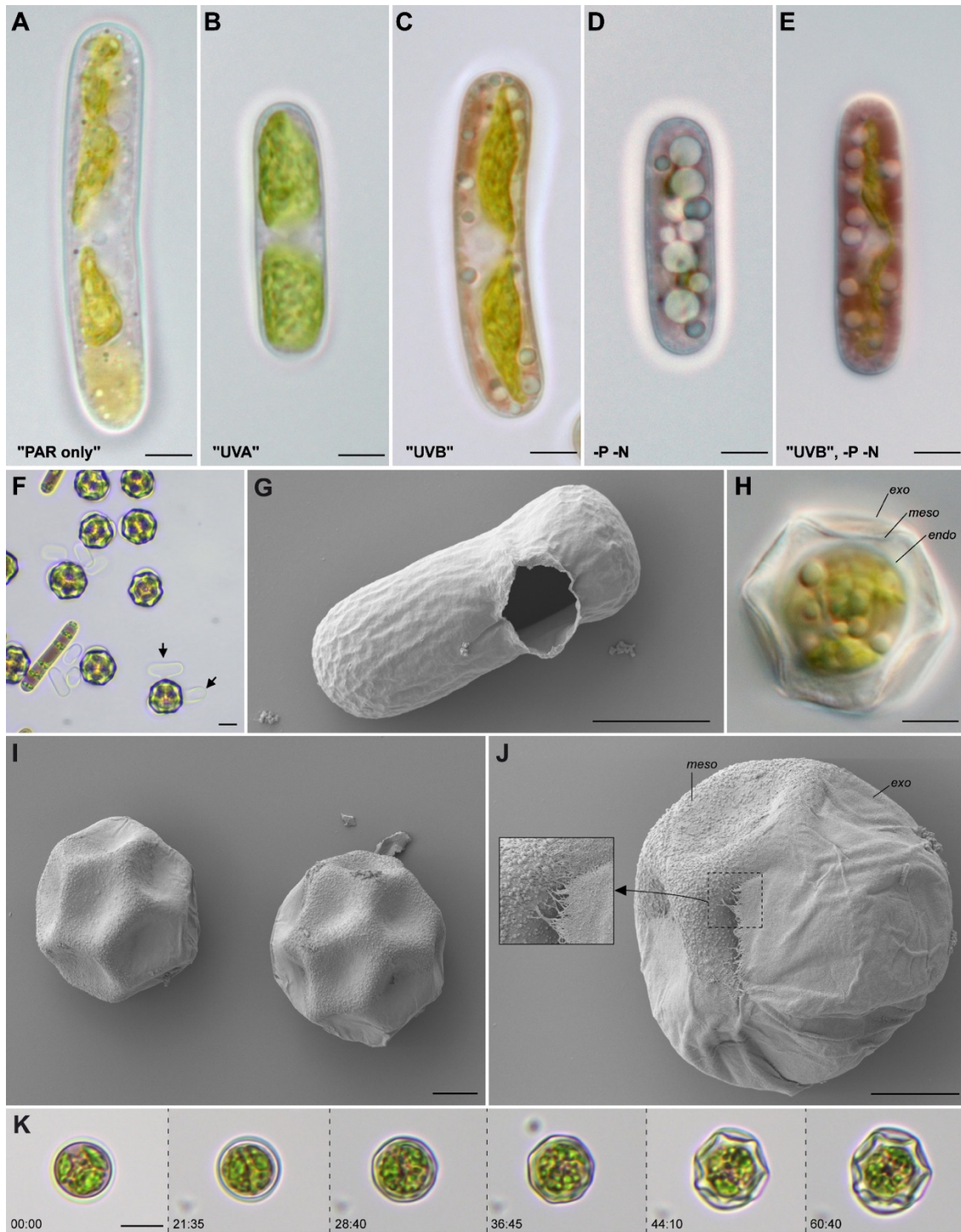
Figure 6. Phenotypes of *A. palustre* under different cultivation regimes and details of zygospore formation and structure. **(A-E)** Representative cells from cultures of strain N3 exposed to "PAR only" (see Figure 5C), "UVA" (see Figure 5F), "UVB" (see Figure 5I), -P-N limitation (see Figure 5M), and -P-N limitation combined with "UVB" (see Figure 5Q). **(F)** Mixed culture of strains N3 and V5 with mature zygospores, which are sometimes attached to empty parent cell walls (black arrows). **(G)** Scanning electron micrograph of an empty cell (strain V5) with a nearly circular hole after release of the gamete. **(H)** Mature zygospore (strain V5) with three distinctive cell walls, namely exospore (exo), mesospore (meso), and endospore (endo). **(I)** Scanning electron micrograph of two mature zygospores (strain V5) revealing the dodecahedron-like morphology. **(J)** Scanning electron micrograph of a zygospore (strain N3) with ruptured exospore (exo). **(K)** Time series of zygospore maturation in strain V5 (time shown in mm:ss). Scale bars: 5 μm in A-E, G-J; 10 μm in F, K.

Supplementary Data

A mesophilic relative of common glacier algae, *Ancylonema palustre* sp. nov., provides insights into the induction of vacuolar pigments in zygnematophytes

Anna Busch, Emilia Slominski, Daniel Remias, Lenka Procházková, Sebastian Hess

Table S1. Studied strains with sampling sites including coordinates, and sampling dates.

Strain	Location	Coordinates	Sampling date
V5	Pond, Großes Veen, Hamminkeln, Germany	51.712889, 6.560639	March 2021
N3	Wet *Sphagnum*, Neuenhähnen, Waldbröl, Germany	50.840533, 7.534120	November 2020

Table S2. Recipe of algal culture medium KW. One milliliter of each stock solution is added to one liter of demineralized water. The pH should be around 6. For the -P treatment, NaH_2PO_4 x H_2O and Na_2HPO_4 x 2 H_2O were omitted. For the -N treatment, KNO_3 was omitted. For the -P-N treatment, NaH_2PO_4 x H_2O, Na_2HPO_4 x 2 H_2O and KNO_3 were omitted.

Components	Stock solution
HEPES	238.1 g/l dH_2O
KNO_3	100 g/ l dH_2O
$MgSO_4$ x 7 H_2O	20 g/l dH_2O
NaH_2PO_4 x H_2O	0.69 g/50 ml
Na_2HPO_4 x 2 H_2O	0.89 g /50 ml
$CaCl_2$ x 2 H_2O	14.7 g/l dH_2O
P-II Metals stock solution EDTA (Titriplex III) H_3BO_3 $MnCl_2$ x 4 H_2O $ZnSO_4$ x 7 H_2O $CoCl_2$ x 6 H_2O	 3.00 g/l dH2O 1.14 g/l dH2O 144.00 mg/l dH2O 21.00 mg/l dH2O 4.00 mg/l dH2O
Fe-EDTA stock solution EDTA (Titriplex II) $FeSO_4$ x 7 H_2O 1N KOH	 5.22 g / l dH2O 4.98 g / l dH2O 54.00 ml / l dH2O

Table S3. Percentage of base differences between *rbcL* sequences of selected *Ancylonema* strains. All codon positions were included, ambiguous positions were not considered (pairwise deletion option).

	MW922839 *A. nordenskioeldii*	OQ222865 *A. alaskanum* WP251 strain	*A. palustre* V5	*A. palustre* 3N	FM992361 *A. palustre*
OQ222865 *A. alaskanum* WP251 strain	1,104417671				
A. palustre V5	2,985074627	2,911646586			
A. palustre 3N	2,885572139	2,81124498	0,385505012		
FM992361 *A. palustre*	2,985074627	2,911646586	0,077160494	0,537221796	
A. palustre CCAC2248	2,997002997	2,822580645	0	0,461538462	0,076982294

Figure S1. Boxplots showing the cell width (A) and cell lengths (B) of the two *A. palustre* strains N3 (blue) and V5 (orange); n = 100.
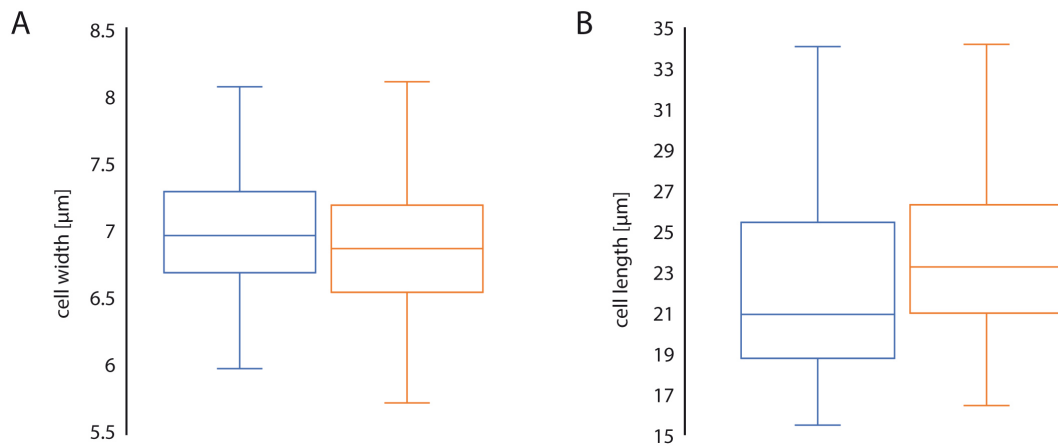
Figure S2. Maximum likelihood phylogeny of 15 zygnematophycean 18S rRNA gene sequences. Support values are shown on the respective branches (ML/NJ/MP) when > 40%. The scale bar represents 0.002 nucleotide substitutions per site.
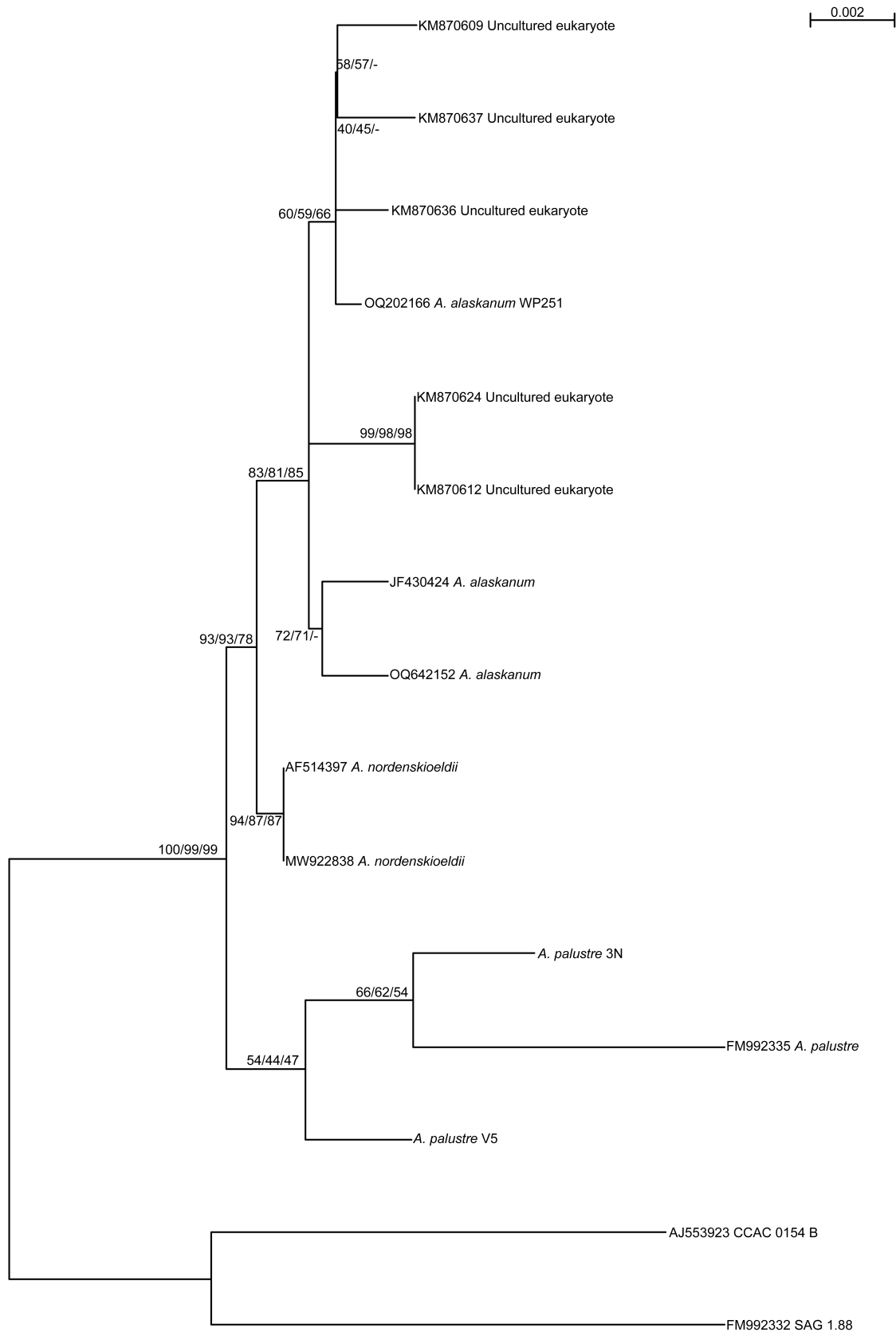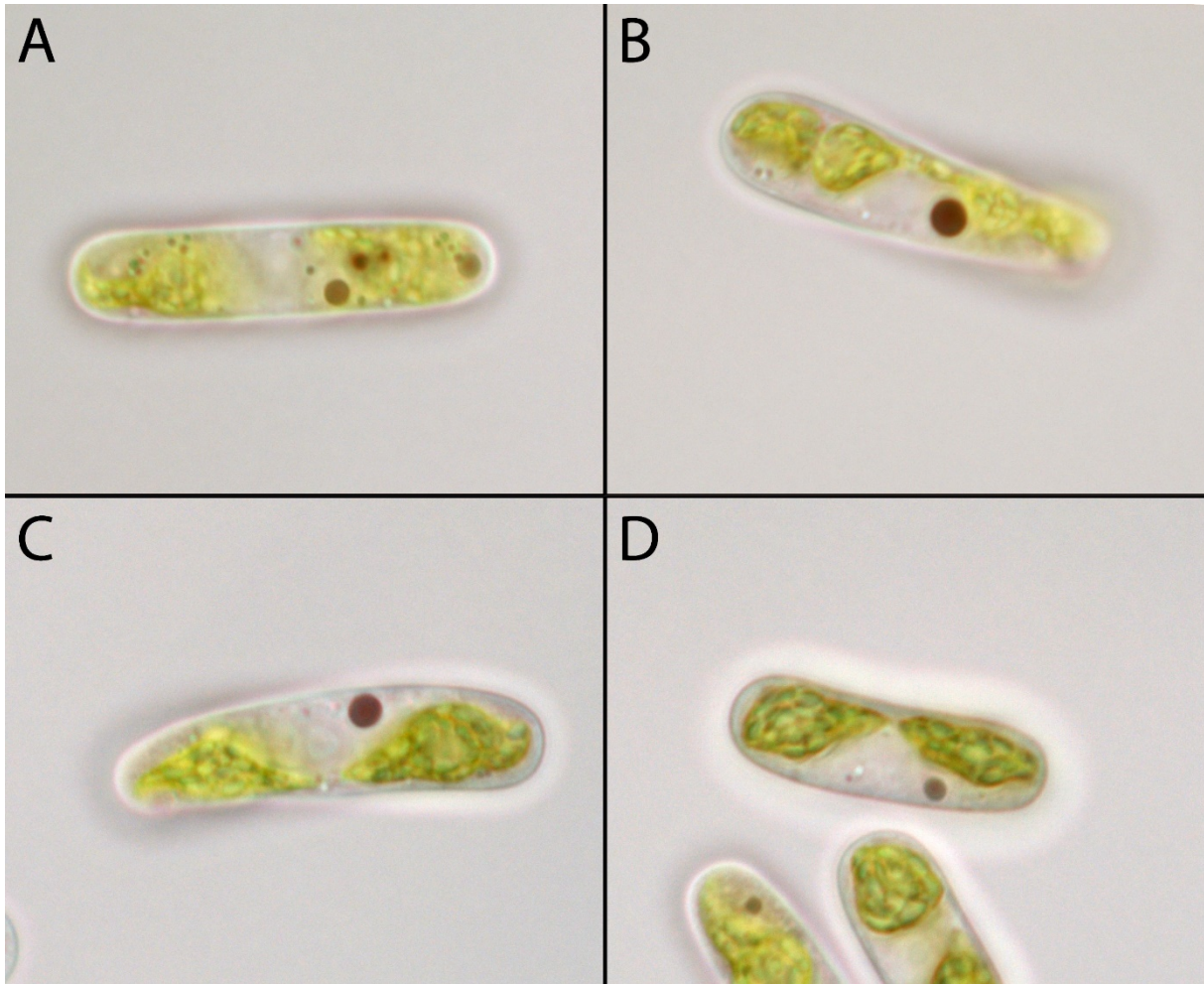
Figure S3. Cells (strain N3) with shrunken/deformed chloroplasts and pigment inclusions; brightfield. **(A, B)** High PAR treatment, > 500 µmol photons m^{-2} s^{-1}. **(C, D)** UVA treatment, > 8 W m^{-2}.

A phylogenomically informed five-order system for the closest relatives of land plants

Published in Current Biology

Chapter V

Current Biology

A phylogenomically informed five-order system for the closest relatives of land plants

Graphical abstract
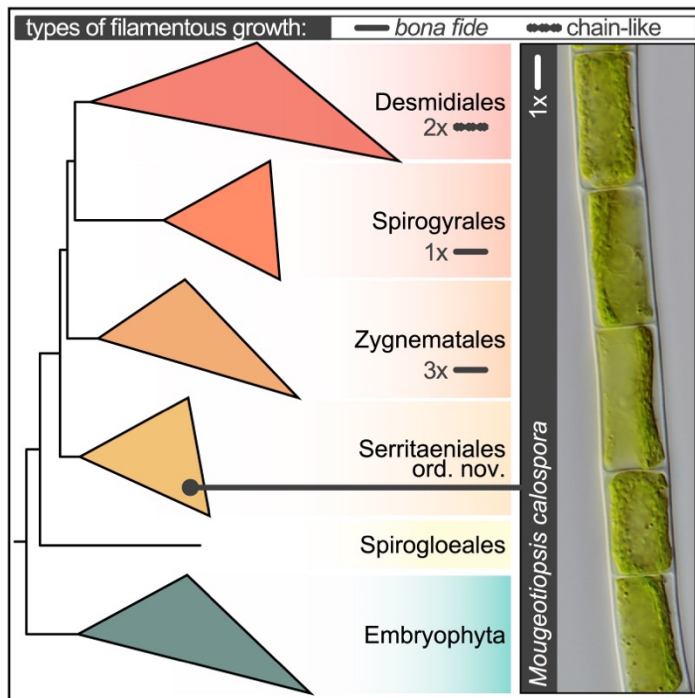
Authors

Sebastian Hess, Shelby K. Williams, Anna Busch, ..., Henrik Buschmann, Klaus von Schwartzenberg, Jan de Vries

Correspondence

sebastian.hess@uni-koeln.de (S.H.), devries.jan@uni-goettingen.de (J.d.V.)

In brief

Hess et al. use comprehensive phylogenomic analyses and present a five-order system for the Zygnematophyceae. They place the filamentous and pyrenoid-lacking *Mougeotiopsis* among unicellular zygnematophytes. Based on this framework, they propose at least five independent origins of true filamentous growth for the closest relatives of land plants.

Highlights

- Comprehensive phylogenomic analyses for 46 taxonomically diverse Zygnematophyceae

- Five-order system for the Zygnematophyceae, the closest relatives of land plants

- Filamentous and pyrenoid-lacking *Mougeotiopsis* sits in a deep clade of unicells

- Evidence for at least five independent origins of true filamentous growth

CellPress

Current Biology

CellPress
OPEN ACCESS

Report

A phylogenomically informed five-order system for the closest relatives of land plants

Sebastian Hess,[1,*] Shelby K. Williams,[2] Anna Busch,[1] Iker Irisarri,[3,4] Charles F. Delwiche,[5] Sophie de Vries,[3] Tatyana Darienko,[3] Andrew J. Roger,[2] John M. Archibald,[2] Henrik Buschmann,[6] Klaus von Schwartzenberg,[7] and Jan de Vries[3,4,8,9,*]

[1]Institute for Zoology, University of Cologne, Zülpicher Str. 47b, 50674 Cologne, Germany
[2]Department of Biochemistry and Molecular Biology, Dalhousie University, 5850 College St., Halifax NS B3H 4R2, Canada
[3]University of Goettingen, Institute for Microbiology and Genetics, Department of Applied Bioinformatics, Goldschmidtstr. 1, 37077 Goettingen, Germany
[4]University of Goettingen, Campus Institute Data Science (CIDAS), Goldschmidtstr. 1, 37077 Goettingen, Germany
[5]Cell Biology and Molecular Genetics, University of Maryland-College Park, College Park, MD, USA
[6]University of Applied Sciences Mittweida, Faculty of Applied Computer Sciences and Biosciences, Section Biotechnology and Chemistry, Molecular Biotechnology, Technikumplatz 17, 09648 Mittweida, Germany
[7]Universität Hamburg, Institute of Plant Science and Microbiology, Microalgae and Zygnematophyceae Collection Hamburg (MZCH) and Aquatic Ecophysiology and Phycology, Ohnhorststr. 18, 22609 Hamburg, Germany
[8]University of Goettingen, Goettingen Center for Molecular Biosciences (GZMB), Department of Applied Bioinformatics, Goldschmidtstr. 1, 37077 Goettingen, Germany
[9]Lead contact
*Correspondence: sebastian.hess@uni-koeln.de (S.H.), devries.jan@uni-goettingen.de (J.d.V.)
https://doi.org/10.1016/j.cub.2022.08.022

SUMMARY

The evolution of streptophytes had a profound impact on life on Earth. They brought forth those photosynthetic eukaryotes that today dominate the macroscopic flora: the land plants (Embryophyta).[1] There is convincing evidence that the unicellular/filamentous Zygnematophyceae—and not the morphologically more elaborate Coleochaetophyceae or Charophyceae—are the closest algal relatives of land plants.[2–6] Despite the species richness (>4,000), wide distribution, and key evolutionary position of the zygnematophytes, their internal phylogeny remains largely unresolved.[7,8] There are also putative zygnematophytes with interesting body plan modifications (e.g., filamentous growth) whose phylogenetic affiliations remain unknown. Here, we studied a filamentous green alga (strain MZCH580) from an Austrian peat bog with central or parietal chloroplasts that lack discernible pyrenoids. It represents *Mougeotiopsis calospora* PALLA, an enigmatic alga that was described more than 120 years ago[9] but never subjected to molecular analyses. We generated transcriptomic data of *M. calospora* strain MZCH580 and conducted comprehensive phylogenomic analyses (326 nuclear loci) for 46 taxonomically diverse zygnematophytes. Strain MZCH580 falls in a deep-branching zygnematophycean clade together with some unicellular species and thus represents a formerly unknown zygnematophycean lineage with filamentous growth. Our well-supported phylogenomic tree lets us propose a new five-order system for the Zygnematophyceae and provides evidence for at least five independent origins of true filamentous growth in the closest algal relatives of land plants. This phylogeny provides a robust and comprehensive framework for performing comparative analyses and inferring the evolution of cellular traits and body plans in the closest relatives of land plants.

RESULTS AND DISCUSSION

Morphology and phylogenetic position of a filamentous zygnematophyte without pyrenoids

Strain MZCH580 forms unbranched filaments with smooth cell walls and rounded tips (Figures 1A and 1B). Infolded cross walls ("replicate walls") or rhizoids known from some filamentous zygnematophytes[10] were not observed in our cultures. The filaments of strain MZCH580 tend to fragment as the cultures age, but cells divide and grow back into new filaments when fresh medium is added (Figures 1C and 1D). Interphase cells are 10–15 μm wide (mean = 12 μm, n = 40) and 12–55 μm long (mean =

22 μm, n = 80), and usually contain a single chloroplast. The chloroplast lacks visible pyrenoids and has a variable shape ranging from an off-center straight plate (Figure 1D) to a more parietal morphology, like a channel or half-pipe (Figures 1A and 1B). The 3D reconstruction of confocal fluorescence data reveals a common intermediate morphology (Figure 1E). The lateral sides of half-pipe-shaped chloroplasts display clear indentations, which are rare in filamentous green algae with chloroplasts of similar morphology (Figures 1A and 1B, arrows)—*Entransia fimbriata* (Klebsormidiophyceae), for example, has fimbriate or lobed chloroplasts, but of much more irregular morphology.[11] The nucleus is spherical (4–6 μm in diameter, n = 40) with a
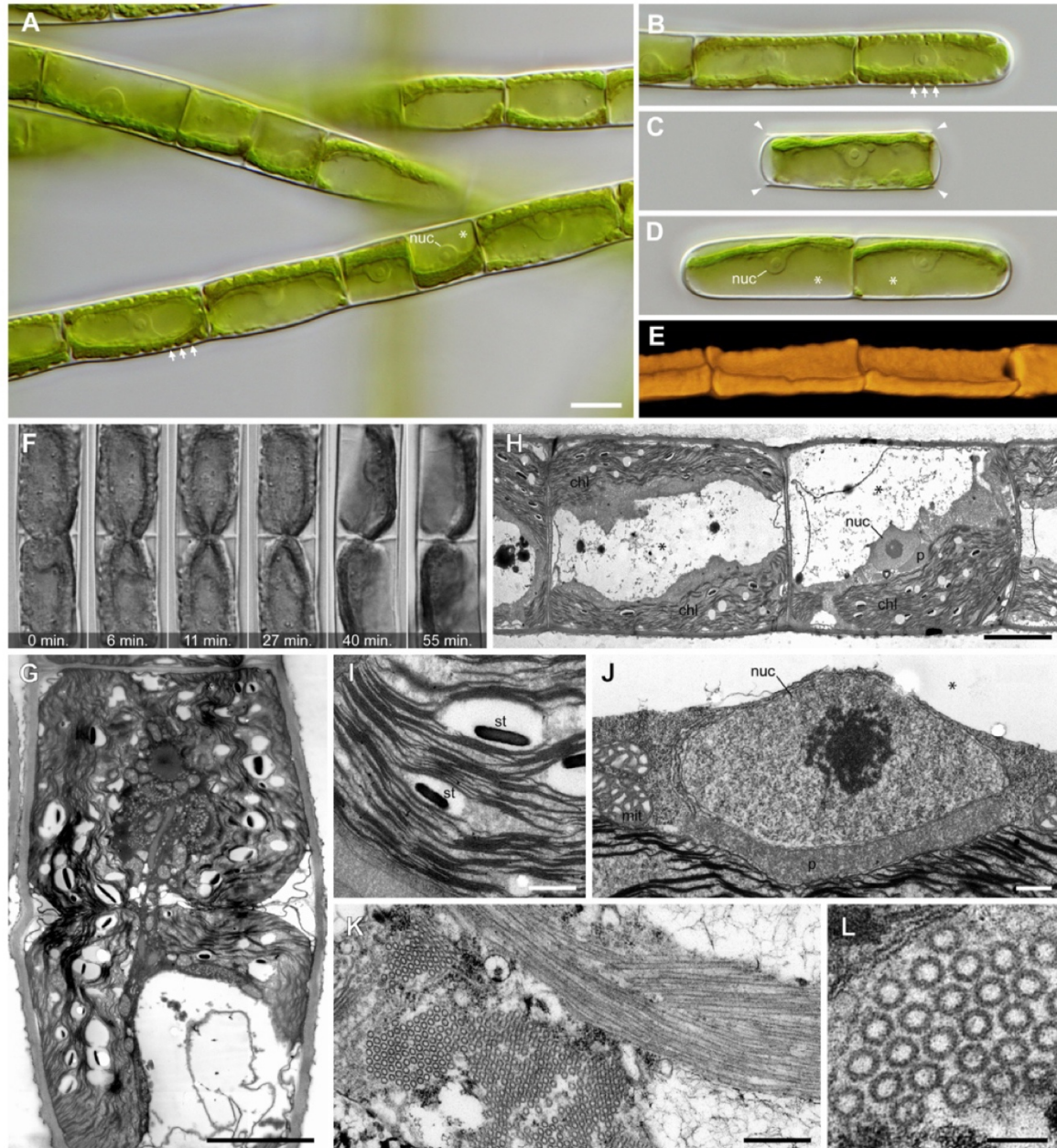
Figure 1. Morphology, cell division, and ultrastructure of *Mougeotiopsis calospora* strain MZCH580

(A) Filaments with cells of varying length; differential interference contrast (DIC). Note the indented chloroplast margins (arrows), the prominent nuclei (nuc) and the large vacuoles (asterisk).

(B) Filament with rounded tip; DIC.

(C) Single cell after fragmentation with cell wall remnants (arrowheads); DIC.

(D) Two-celled filament with smooth tips; DIC. Note the prominent nuclei (nuc) and the large vacuoles (asterisks).

(E) Three-dimensional reconstruction of the chloroplasts based on their autofluorescence; confocal microscopy.

(F) Time series of a dividing cell shows ingrowing cross wall; DIC.

(G) Ultrathin section through a dividing cell reveals the ingrowing cell wall (see plasma membrane) and the chloroplast in division.

(H) Ultrathin section through vegetative filament showing the position of the nucleus (nuc), peroxisome (p), chloroplasts (chl) and vacuoles (asterisks).

(I) Ultrathin section of starch grains (st) between the thylakoids of the chloroplast.

Current Biology
Report

CellPress
OPEN ACCESS

prominent central nucleolus (1–3 μm in diameter, n = 40), and always closely associated with the chloroplast (Figures 1A and 1D; nuc). Both chloroplast and nucleus are surrounded by a thin sheath of cytoplasm and opposed to or surrounded by a large vacuole (Figure 1D; asterisks).

Cell division is intercalary and involves the centripetal formation of a cross wall (Figure 1F; Videos S1 and S2). We did not observe any phragmoplast-like structure as known from many streptophyte algae.[12–14] Instead, ingrowing cell wall material seemed to pinch off the chloroplast (Figure 1F and Videos S1 and S2), which is corroborated on the ultrastructural level (Figure 1G). It appears that the chloroplast does not divide before the inset of cytokinesis, and that the cell division in strain MZCH580 largely depends on furrowing (cleavage, thus centripetal cell wall ingrowth). However, we cannot exclude the existence of a phragmoplast and our ultrastructural data of late stages of cytokinesis seem compatible with phragmoplast-like structures as known from many streptophyte algae, including other zygnematophytes (e.g., Spirogyra and Mougeotia[12,13]).

Our ultrastructural data confirm that the chloroplasts of strain MZCH580 lack pyrenoids but contain numerous lentiform starch grains (up to ~1 μm) interspersed between the thylakoids (Figures 1H and 1I). This is a very unusual chloroplast configuration. Pyrenoids are found in all other known zygnematophytes (and most green algae) and are considered important compartments for carbon concentration. That said, hornworts have frequently gained and lost pyrenoids—a phenomenon that does not correlate with atmospheric CO_2 concentration or lifestyle changes.[15] Mougeotiopsis appears to compensate for the lack of pyrenoid-based carbon concentration by an extremely high expression of homologs of ribulose-1,5-bisphosphate carboxylase/oxygenase small subunit 2 (rbcS2) and rubisco activase (rca); in fact, with transcripts per million (TPM) values of 44002 and 15238, they were, respectively, the highest and fourth highest expressed transcript in the whole transcriptome. In contrast, in the transcriptomes of the pyrenoid-bearing alga Mougeotia sp. MZCH240, rbcs and rca homologs never ranged among the top 100 most abundant transcripts (see de Vries et al.[16] and Fürst-Jansen et al.[17]). The ecophysiological consequences of the absence of pyrenoids in Mougeotiopsis are currently obscure.

Other noteworthy ultrastructural characteristics of strain MZCH580 are a giant peroxisome situated between the nucleus and the chloroplast (Figure 1J), and the occurrence of macrotubules (~44 nm in diameter; 44.02 nm ± 2.4 nm, n = 446) in cells with incomplete cytokinesis likely promoted by environmental factors (Figures 1K, 1L, and S1); the occurrence of macrotubules has been described in land plant tissues—for example, in cells of root tips but with a distinct mean diameter[18] (35 nm). A single peroxisome of similar localization was also reported for Klebsormidiophyceae such as Klebsormidium, Hormidiella, and Streptosarcina,[19–22] and the Zygnematophyceae Zygogonium,[23] suggesting that this is a rather widespread character in streptophyte algae. However, the filamentous zygnematophytes

Mougeotia, Spirogyra, and Zygnema contain numerous, much smaller peroxisomes, which do not exceed 1 μm in our TEM sections (Figure S2).

Based on taxonomic comparisons (see Table 1 and STAR Methods for details), we apply the name Mougeotiopsis calospora to strain MZCH580. However, as we did not observe any sexual processes (conjugation, flagellated gametes), zoospores, or aplanospores in our cultivated material, the suspected affinity to the zygnematophytes remained uncertain. While analysis of the rbcL gene (coding for the large chain of ribulose-1,5-bisphosphate carboxylase/oxygenase) placed strain MZCH580 within the streptophytes, a robust phylogenetic placement was not possible. To scrutinize the phylogenetic position of strain MZCH580, we generated RNA-seq data by Illumina sequencing and performed a de novo transcriptome assembly. The resulting transcriptome has a completeness of 96.3% (benchmarked universal 272 single-copy orthologs) and contains 52,188 predicted open reading frames (ORFs). We built a comprehensive multigene dataset of 326 conserved proteins (see STAR Methods) from streptophyte algae, land plants, and select chlorophyte algae as outgroup, with 84 taxa in total (see species and deposited data in STAR Methods). Our phylogenomic inferences with a sophisticated site-heterogeneous model of protein sequence evolution (LG+-PMSF(C60)+F+Γ) resulted in a well-supported phylogeny, whose overall topology is in line with current knowledge about streptophyte evolution (cf. Figure S3 and One Thousand Plant Transcriptomes Initiative[6]). To scrutinize this, we performed an approximately unbiased (AU) test under the best-fit model LG+C60+F+Γ with 10,000 multiscale bootstrap replicates. Our dataset rejected the topology of the One Thousand Plant Transcriptomes Initiative[6] (AU test p = 0.000). This, however, only concerned some relationships within Desmidiales, and neither their monophyletic arrangement nor any other aspect of the gross topology, thus also having no effect on any trait inferences below. Strain MZCH580 groups within the Zygnematophyceae with full nonparametric bootstrap support and forms a deep-branching lineage with the unicellular Serritaenia sp. (strain CCAC 0155) and "Mesotaenium endlicherianum" (strain SAG 12.97). Hence, strain MZCH580, referred to as Mougeotiopsis calospora hereafter, is clearly distinct from other filamentous genera (Mougeotia, Spirogyra, Zygnema, and Zygnemopsis), and represents a new lineage of zygnematophytes with filamentous growth.

Phylogenomics support a five-order taxonomy of the Zygnematophyceae

Previous phylogenies based on single (or few) marker genes have suggested that the traditional taxonomic separation into the two orders Desmidiales and Zygnematales does not reflect the evolutionary relationships of the Zygnematophyceae.[7,8] Yet, the taxonomy of this important algal class remains unresolved, in part due to the lack of robust phylogenetic data. Our multigene phylogeny clearly demonstrates that the Zygnematales as previously defined (all filamentous members plus

(J) Ultrathin section of the nucleus (nuc) with nucleolus, the large, elongate peroxisome (p), and mitochondria (mit). The vacuolar space is marked by the asterisk.
(K) Ultrathin section of bundled macrotubules in cross section (left) and longitudinal section (right).
(L) Detail of macrotubules in cross section.
Scale bars 10 μm in (A) (applies also for B–D); 5 μm in (G) and (H); 500 nm in (I)–(K); 100 nm in (L).
See also Figures S1, S2, and S4.

CelPress
OPEN ACCESS

Current Biology
Report

Table 1. Five-order taxonomy of the Zygnematophyceae

Order Serritaeniales

S.Hess & J.de Vries *ord. nov.*

Diagnosis: comprises unicells and filaments with smooth sidewalls, cells with axial or parietal chloroplasts, and simple cell walls (no pores and ornamentations), phylogenetically closely related to the type species (*Serritaenia testaceovaginata*; *rbc*L MW159377).

Type: Serritaeniaceae S.Hess & J.de Vries *fam. nov.*

Family Serritaeniaceae S.Hess & J.de Vries *fam. nov.*

Diagnosis: with characteristics of order Serritaeniales; unicells and filaments with smooth sidewalls, cells with axial or parietal chloroplasts, and simple cell walls (no pores and ornamentations), embedded or not in the mucilage.

Type: *Serritaenia* A.Busch & S.Hess 2021.

Comment: Currently the Serritaeniales includes a single family, the Serritaeniaceae with the genera *Serritaenia* and *Mougeotiopsis*.

Order Zygnematales

Bessey *emend.* S.Hess & J.de Vries

Emended description: Comprises unicells and unbranched and uniseriate filaments with smooth side walls, cells with stellate, plate- or ribbon-like chloroplasts and simple cell walls (no pores and ornamentations), phylogenetically closely related to strains SAG 698-1a (Genbank transcriptome shotgun assembly GFYA00000000).

Type: *Zygnema* C.Agardh, 1817, *nom. et typ. cons.*

Comment: Currently the Zygnematales includes a single family Zygnemataceae with the genera *Cylindrocystis, Mesotaenium* (current assumption, pending discovery of type species), *Mougeotia, Zygnema,* and *Zygnemopsis.* No culture is available from the type species of *Zygnema*.

Order Desmidiales

Bessey *emend.* S.Hess & J.de Vries

Emended description: Comprises unicells and chain-like filaments. Cell walls and morphologies of diverse complexity, including the "placoderm desmids" with cell wall pores, ornamentations and clear isthmus, and species with smooth cell walls and without isthmus. Phylogenetically closely related to strain *Desmidium aptogonum* (RNA-seq ERX2100155).

Type: *Desmidium* C.Agardh ex Ralfs, 1848.

Comment: Currently the Desmidiales includes a single family Desmidiaceae with the genera *Bambusina, Closterium, Cosmarium, Cosmocladium, Desmidium, Euastrum, Micrasterias, Netrium, Nucleotaenium, Onychonema, Penium, Phymatodocis, Planotaenium, Pleurotaenium, Staurastrum, Staurodesmus, Xanthidium,* and more. No culture is available from the type species of *Desmidium*.

Order Spirogyrales

Clements *emend.* S.Hess & J.de Vries

Emended description: Comprises filaments with smooth side walls, cells with one or more helical chloroplast and smooth cell walls without pores or ornamentation. Phylogenetically closely related to strain *Spirogyra pratensis* strain MZCH10213 (RNA-seq data: NCBI BioProject PRJNA543475, TSA GICF00000000).

Type: *Spirogyra* Link, 1820, *nom. cons.*

Comment: Currently the Spirogyrales includes only the genus *Spirogyra*. The closely related genus *Sirogonium* Kützing may also belong to this order, but this needs to be confirmed by phylogenomic studies. No culture is available from the type species of *Spirogyra*. The order Spirogyrales was originally validated by Clements (1909: 12); his description specified "Typically one-celled or filamentous algae, without zoospores; sexual reproduction by the conjugation of similar gametes; two fungous families." No fungi are currently included in this order.

unicells that are not placoderm desmids) are paraphyletic. Instead, the Zygnematophyceae comprise at least five deep-branching clades that we feel can be treated at the level of orders (Figure 2).

We introduce a new, phylogenomically informed five-order taxonomy of the Zygnematophyceae, by reinterpreting existing ordinal names and introducing a new order for *Mougeotiopsis* and its unicellular relatives (see Table 1). The Serritaeniales *ord. nov.* currently comprises the name-giving genus *Serritaenia* (unicells with a plate-like chloroplast and a mostly aerophytic life style[25]), the genome-sequenced strain SAG 12.97 (often referred to as "*Mesotaenium endlicherianum*"[26]; unicells with half-pipe-like chloroplasts and an aquatic lifestyle) and *Mougeotiopsis calospora,* strain MZCH580. Although these species differ markedly in growth form (unicells versus filaments), their chloroplasts are all characterized by indented or undulated margins[25,26] that are otherwise rare in zygnematophytes. Yet, *Mougeotiopsis calospora* is the only known zygnematophyte that lacks pyrenoids.

Our data corroborate the position of the Spirogloeales, consisting of the unicellular *Spirogloea muscicola* (formerly *Spirotaenia muscicola*), as sister lineage to all other Zygnematophyceae.[26] For the remaining part of the phylogenomic tree, we redefine three traditional orders. The Zygnematales are now limited to a morphologically diverse clade comprising unicellular zygnematophytes currently assigned to *Cylindrocystis* and *Mesotaenium*, plus three distinct branches of filamentous members (*Mougeotia, Zygnema,* and *Zygnemopsis*); the recovered topology demonstrates the polyphyly of the unicellular genera belonging to that order (*Cylindrocystis* and *Mesotaenium*), which require a taxonomic revision in the future. Chloroplasts of the Zygnematales are either stellate (*Cylindrocystis, Zygnema,* and *Zygnemopsis*) or ribbon/plate-like with smooth margins (*Mesotaenium* and *Mougeotia*).

The *Spirogyra* species with their characteristic helical chloroplasts form another, deep-branching clade, which is here defined as Spirogyrales Clements 1909 (Figure 2 and Table 1). This order was initially introduced to include algae of yellow-green appearance (including *Spirogyra*) and some fungal families.[27] We limit the concept of the Spirogyrales to those zygnematophycean algae that form the sister clade of the Desmidiales in our phylogeny. The latter order mainly comprises symmetric unicells with a

Current Biology
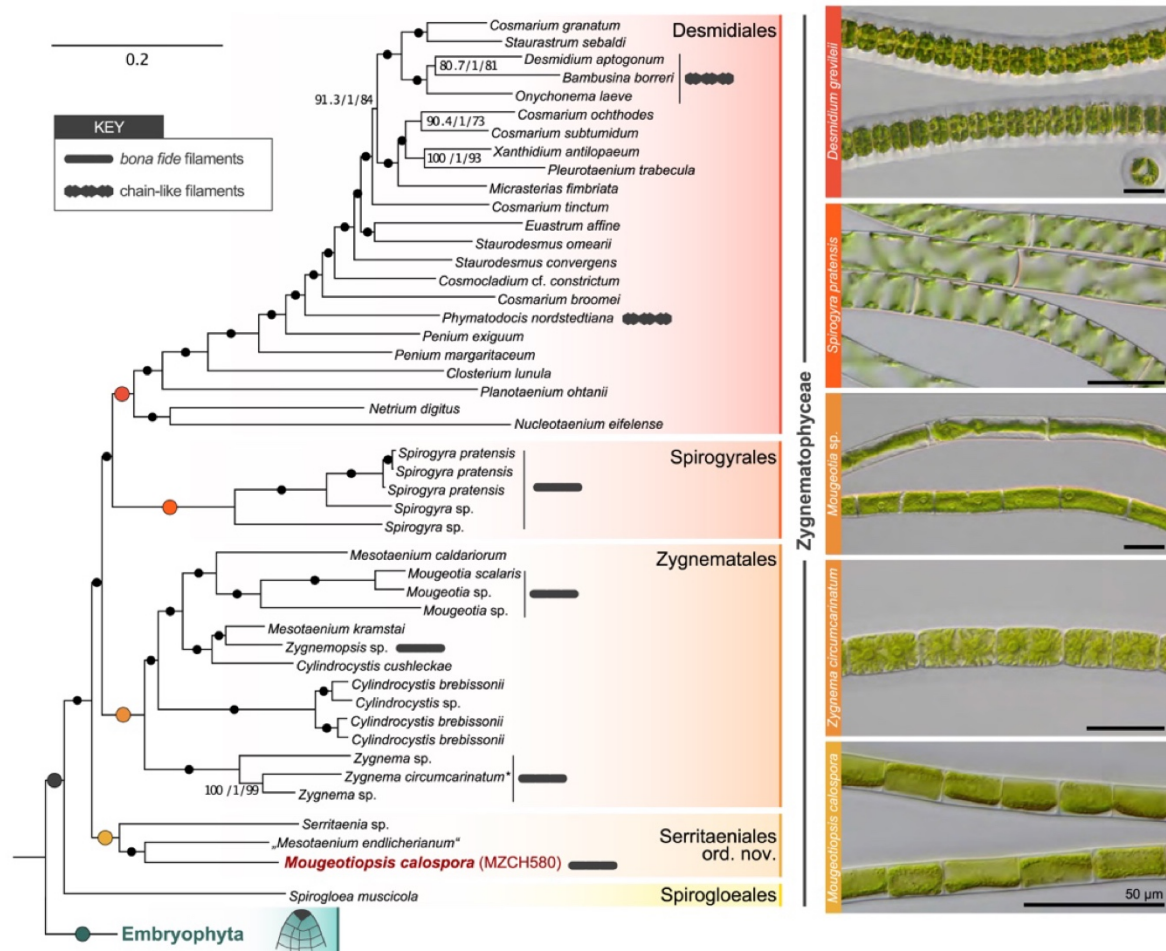### Report

CellPress
OPEN ACCESS

Figure 2. Position of strain MZCH580 in a well-resolved zygnematophycean phylogeny based on 326 genes

Section of the phylogenomic tree limited to zygnematophytes and embryophytes. Support values from three analyses (SH-aLRT/aBayes/nonparametric bootstrapping) are shown at the corresponding branches, except for branches with maximum support (marked by dots); large colored dots correspond to the (full) support recovered for the higher-order clades labeled on the right. The Zygnematophyceae comprise five deep-branching clades, which are here defined as orders. Gray symbols highlight zygnematophytes that form chain-like filaments (see micrograph of *Desmidium*) and *bona fide* filaments (see micrographs of *Spirogyra*, *Mougeotia*, *Zygnema*, and *Mougeotiopsis*); scale bars in all micrographs are 50 μm.

Scale bar for phylogeny is 0.2 expected substitutions per site. The entire phylogenomic tree with all streptophyte taxa is shown in Figure S3. Asterisk: a recent study by Feng et al.[24] found that SAG698-1a might be *Z. cylindricum* instead of *Z. circumcarinatum*.

pronounced central constriction (isthmus) and ornamented cell walls. However, at the base of the clade containing these typical placoderm desmids are three genera (*Netrium*, *Nucleotaenium*, and *Planotaenium*), which display a much simpler morphology (no cell wall ornamentations and no isthmus) and were formerly classified with the Zygnematales (in the family Mesotaeniaceae).[28] Interestingly, the same arrangement was previously recovered by combined analyses of three genes (nuclear SSU rRNA, *rbcL*, and chloroplast LSU rRNA),[29] and is here confirmed by phylogenomics. It appears that the desmids with elaborate cell shapes and complex cell walls (e.g., *Cosmarium*, *Penium*, *Micrasterias*, and *Xanthidium*) descended from unicellular ancestors with a simpler structure. Hence, the genera *Netrium*, *Nucleotaenium*, and

Planotaenium are here formally included in the order Desmidiales. The internal phylogeny and taxonomy of the Desmidiales, however, needs to be resolved by extended taxon sampling in the future, as many classically recognized desmid genera (e.g., *Cosmarium*, *Penium*, and *Staurodesmus*) are not monophyletic.

On the unicellularity of the ancestral zygnematophyte

Our robust phylogenetic framework of the zygnematophytes now enables comparisons of species in an evolutionary context; thus assessment of evolutionary scenarios with great confidence are feasible. It is remarkable that the majority of zygnematophycean species are unicellular,[30] as most of their streptophyte relatives (Embryophyta, Coleochaetophyceae, Charophyceae,

CelPress
OPEN ACCESS
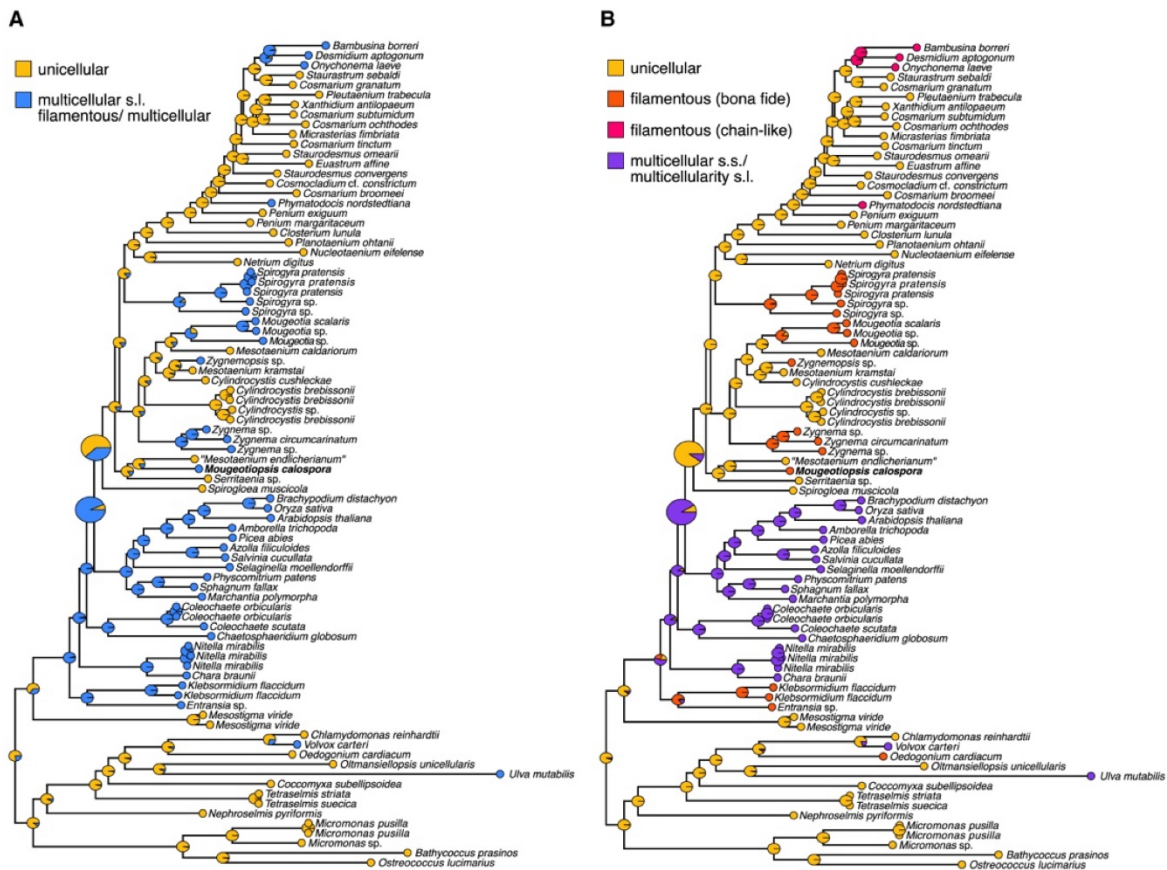
Current Biology
Report

Figure 3. Ancestral character state reconstruction for unicellular or multicellular (including filamentous) growth characters
(A and B) Growth types were coded as either a simplistic (A) two- and more nuanced (B) four- character state distributions to reflect different levels of complexity regarding the possibilities/hypotheses for the homology of growth types: yellow, unicellular; blue, multicellular *sensu lato* (including filamentous growth); orange, *bona fide* filamentous growth; pink, chain-like filaments (desmids); and purple, multicellular growth *sensu stricto*.

Klebsormidiophyceae, and Chlorokybophyceae) display some kind of multicellularity, from sarcinoids to three-dimensional tissues.[31] However, some zygnematophycean lineages exhibit more developmental complexity such as the formation of filaments, sometimes even with rhizoids or branched cells.[31,32] Traditionally these filamentous members have been bundled in the family Zygnemataceae,[28] but a close relationship of them was not recovered in previous phylogenies.[7,8]

Our fully supported phylogenomic tree reveals at least five separate lineages that contain true filaments, found in three orders (Figure 2): *Spirogyra* (Spirogyrales), *Mougeotia, Zygnema, Zygnemopsis* (all Zygnematales), and *Mougeotiopsis* (Serritaeniales). Other filamentous taxa (e.g., *Temnogametum iztacalense* and *Zygogonium ericetorum*) await genomic/transcriptomic sequencing and phylogenomic placement[33,34] The cells of all these filamentous species have straight and relatively simple cell walls, no central constrictions, and display an intimate cell-cell contact (i.e., typical cross walls)—yet without plasmodesmata.[35] At the same time, there are also filamentous desmids (e.g. *Desmidium, Bambusina, Onychonema*, and

Phymatodocis[36]), which differ markedly from the aforementioned lineages in their cellular details and filament morphology (see also Hall et al.[37]). The cells of *Desmidium, Bambusina, Onychonema*, and *Phymatodocis* display the typical characters of desmid cells (e.g., central constriction and cell wall ornamentation) and rather appear as cell chains. Together with the fact that the filamentous desmids are nested within the unicellular desmids, it is conceivable that there are distinct types of filamentous growth in the Zygnematophyceae, which evolved independently; we account for this possibility in our analyses (see Figure 3 and below). The Zygnematophyceae as a whole are nested within a clade of mostly multicellular streptophytes, the Phragmoplastophyta, with the most morphologically elaborate (the Embryophyta) as sister clade. Previous studies have therefore noted that the streamlined body plans of extant zygnematophytes—down to unicellularity—might have arisen by reductive evolution from a morphologically more complex ancestor.[5,38–41] Based on our current phylogeny, it seems most parsimonious that the last common ancestor of the zygnematophytes was unicellular—thus having already experienced a

Current Biology
Report

CellPress
OPEN ACCESS

reduction in its body plan. This scenario goes along with five independent origins of *bona fide* filaments; the alternative would require at least seven losses of multicellularity.

In an attempt to infer the body plan of the common ancestor of zygnematophytes, we performed ancestral character state reconstructions (ACSR) with various data coding strategies concerning the types of multicellularity (Figure 3). Irrespective of how the growth types were coded, a unicellular zygnematophyte ancestor was consistently inferred by our analyses, albeit with varying support (posterior probability [PP] = 0.58–0.93). Hence, we infer up to five tentative independent origins of true filamentous growth, and two additional independent origins of chain-like filaments (in the Desmidiales) (unicellular ancestors have PP = 0.80–1.00); under this scenario, the last common ancestor of the Zygnematophyceae and land plants was likely filamentous or multicellular (PP = 0.91–0.93), whereas the last common ancestor of Zygnematophyceae was likely unicellular (PP = 0.58–0.89). Given the effect of character coding in these analyses, we conclude that expanding our knowledge about the homology of the various types of multicellular and filamentous body plans in the green algae is essential.

Filamentous growth as observed in the Zygnematophyceae can be considered the least elaborate type of multicellularity.[42] Yet, the cellular and molecular traits underpinning this growth type remain obscure. The multiple growth type transitions in the zygnematophytes are consistent with parallel evolution from a common molecular machinery, but the relative simplicity of filamentous growth renders convergent evolution equally plausible. The hypothetical unicellular lynchpin at the base of the Zygnematophyceae is an attractive hypothesis: it could explain why zygnematophytes lack plasmodesmata (e.g., Brunkard and Zambryski[35]), why the cross walls often look distinct from other streptophytes, and perhaps even why the group as such returned to a cleavage-like cell division mechanism (see Buschmann and Zachgo[14]). Future research on the different filamentous lineages will need to establish a deeper understanding of the molecular machinery underpinning their common morphology.

In addition, recent culture-based efforts to explore terrestrial zygnematophytes indicated a high diversity of unicellular lineages,[43] which are not yet covered by genomic/transcriptomic sequencing and might change the evolutionary picture. Biased taxon sampling is indeed a serious problem for ACSR,[44,45] and thus genomic sequencing of further zygnematophytes is an important task for the future. The fossil record for Zygnematophyceae is sparse. Several of the ordinal lineages of Zygnematophyceae are potentially several hundreds of millions of years old (estimations based on molecular clock results presented in Morris et al.[46]). Hence, important information might be obscured by extinction events and new discoveries of living or fossil taxa could easily lead to new interpretations. For now, our phylogenomic data demonstrate that the zygnematophytes comprise multiple transitions of their body plan, and also enable the selection of relevant species for comparative cell biological research.

Conclusion

The identification of the Zygnematophyceae as the sister lineage to land plants was surprising, in part because of their relatively simple body plans. The study of zygnematophycean trait evolution is a challenge because of their species richness, diverse morphologies, and unresolved phylogeny. We have provided a phylogenomic backbone and a congruent classification system for the closest algal relatives of land plants. Looking at algal growth types through the lens of phylogenomics reveals dynamic emergence and formation of filamentous and unicellular growth among the Zygnematophyceae—traits whose evolutionary history might also feature reductive evolution from a more complex ancestor of Zygnematophyceae and land plants.

STAR★METHODS

Detailed methods are provided in the online version of this paper and include the following:

- KEY RESOURCES TABLE
- RESOURCE AVAILABILITY
  - ○ Lead contact
  - ○ Materials availability
  - ○ Data and code availability
- EXPERIMENTAL MODEL AND SUBJECT DETAILS
  - ○ Algal strains
- METHOD DETAILS
  - ○ Rationale for the application of the name *Mougeotiopsis calospora* to strain MZCH580
  - ○ Rationale for establishing a new order, Serritaeniales ord. nov.
  - ○ Light microscopy, time-lapse photography, and confocal imaging
  - ○ Transmission electron microscopy
  - ○ RNA isolation, sequencing and phylogenomics
  - ○ Ancestral character state reconstruction
- QUANTIFICATION AND STATISTICAL ANALYSIS

SUPPLEMENTAL INFORMATION

Supplemental information can be found online at https://doi.org/10.1016/j.cub.2022.08.022.

AUTHOR CONTRIBUTIONS

Conceptualization, S.H., J.d.V.; investigation, S.H., S.K.W., A.B., I.I., S.d.V., H.B., K.v.S., J.d.V.; writing – original draft, S.H., I.I., and J.d.V.; writing – review and editing, all authors; visualization, S.H., A.B., I.I., and J.d.V.; and funding acquisition, S.H. and J.d.V.

CellPress
OPEN ACCESS

Current Biology
Report

DECLARATION OF INTERESTS

The authors declare no competing interests.

REFERENCES

1. Bar-On, Y.M., Phillips, R., and Milo, R. (2018). The biomass distribution on Earth. Proc. Natl. Acad. Sci. USA 115, 6506–6511.

2. Wodniok, S., Brinkmann, H., Glöckner, G., Heidel, A.J., Philippe, H., Melkonian, M., and Becker, B. (2011). Origin of land plants: Do conjugating green algae hold the key? BMC Evol. Biol. 11, 104.

3. Timme, R.E., Bachvaroff, T.R., and Delwiche, C.F. (2012). Broad Phylogenomic Sampling and the Sister Lineage of Land Plants. PLoS One 7, e29696.

4. Ruhfel, B.R., Gitzendanner, M.A., Soltis, P.S., Soltis, D.E., and Burleigh, J.G. (2014). From algae to angiosperms-inferring the phylogeny of green plants (Viridiplantae) from 360 plastid genomes. BMC Evol. Biol. 14, 23.

5. Wickett, N.J., Mirarab, S., Nguyen, N., Warnow, T., Carpenter, E., Matasci, N., Ayyampalayam, S., Barker, M.S., Burleigh, J.G., Gitzendanner, M.A., et al. (2014). Phylotranscriptomic analysis of the origin and early diversification of land plants. Proc. Natl. Acad. Sci. USA 111, E4859–E4868.

6. One Thousand Plant Transcriptomes Initiative (2019). One thousand plant transcriptomes and the phylogenomics of green plants. Nature 574, 679–685.

7. Gontcharov, A.A. (2008). Phylogeny and classification of Zygnematophyceae (Streptophyta): current state of affairs. Fottea 8, 87–104.

8. Hall, J.D., Karol, K.G., McCourt, R.M., and Delwiche, C.F. (2008). Phylogeny of the conjugating green algae based on chloroplast and mitochondrial nucleotide sequence data. J. Phycol. 44, 467–477.

9. Palla, E. (1894). Ueber eine neue, pyrenoidlose Art und Gattung der Conjugaten. Ber. Deutsch. Bot. Ges. 12, 228–236.

10. Takano, T., Higuchi, S., Ikegaya, H., Matsuzaki, R., Kawachi, M., Takahashi, F., and Nozaki, H. (2019). Identification of 13 Spirogyra species (Zygnemataceae) by traits of sexual reproduction induced under laboratory culture conditions. Sci. Rep. 9, 7458.

11. Cook, M.E. (2004). Structure and asexual reproduction of the enigmatic charophycean green alga Entransia fimbriata (Klebsormidiales, Charophyceae). J. Phycol. 40, 424–431.

12. Fowke, L.C., and Pickett-Heaps, J.D. (1969). Cell division in Spirogyra. II. Cytokinesis. J. Phycol. 5, 273–281.

13. Pickett-Heaps, J.D., and Wetherbee, R. (1987). Spindle function in the green alga Mougeotia: absence of anaphase A correlates with postmitotic nuclear migration. Cell Motil Cytoskeleton 7, 68–77.

14. Buschmann, H., and Zachgo, S. (2016). The evolution of cell division: from streptophyte algae to land plants. Trends Plant Sci. 21, 872–883.

15. Villarreal, J.C., and Renner, S.S. (2012). Hornwort pyrenoids, carbon-concentrating structures, evolved and were lost at least five times during the last 100 million years. Proc. Natl. Acad. Sci. USA 109, 18873–18878.

16. de Vries, J., de Vries, S., Curtis, B.A., Zhou, H., Penny, S., Feussner, K., Pinto, D.M., Steinert, M., Cohen, A.M., von Schwartzenberg, K., and Archibald, J.M. (2020). Heat stress response in the closest algal relatives of land plants reveals conserved stress signaling circuits. Plant J. 103, 1025–1048.

17. Fürst-Jansen, J.M.R., de Vries, S., Lorenz, M., von Schwartzenberg, K., Archibald, J.M., and de Vries, J. (2022). Submergence of the filamentous Zygnematophyceae Mougeotia induces differential gene expression patterns associated with core metabolism and photosynthesis. Protoplasma 259, 1157–1174. https://doi.org/10.1007/s00709-021-01730-1.

18. Komis, G., Apostolakos, P., and Galatis, B. (2002). Hyperosmotic Stress Induces Formation of Tubulin Macrotubules in Root-Tip Cells of Triticum turgidum: Their Probable Involvement in Protoplast Volume Control. Plant Cell Physiol. 43, 911–922.

19. Stewart, K.D., Floyd, G.L., Mattox, K.R., and Davis, M.E. (1972). Cytochemical demonstration of a single peroxisome in a filamentous green alga. J. Cell Biol. 54, 431–434.

20. Honda, M., and Hashimoto, H. (2007). Close association of centrosomes to the distal ends of the microbody during its growth, division and partitioning in the green alga Klebsormidium flaccidum. Protoplasma 231, 127–135.

21. Holzinger, A., Lütz, C., and Karsten, U. (2011). Desiccation stress causes structural and ultrastructural alterations in the aeroterrestrial green alga Klebsormidium crenulatum (Klebsormidiophyceae, Streptophyta) isolated from an Alpine soil crust. J. Phycol. 47, 591–602.

22. Mikhailyuk, T., Lukešová, A., Glaser, K., Holzinger, A., Obwegeser, S., Nyporko, S., Friedl, T., and Karsten, U. (2018). New taxa of streptophyte algae (Streptophyta) from terrestrial habitats revealed using an integrative approach. Protist 169, 406–431.

23. Aigner, S., Remias, D., Karsten, U., and Holzinger, A. (2013). Unusual phenolic compounds contribute to ecophysiological performance in the purple-colored green alga Zygogonium ericetorum (Zygnematophyceae, Streptophyta) from a high-alpine habitat. J. Phycol. 49, 648–660.

24. Feng, X., Holzinger, A., Permann, C., Anderson, D., and Yin, Y. (2021). Characterization of two Zygnema strains (Zygnema circumcarinatum SAG 698-1a and SAG 698-1b) and a rapid method to estimate nuclear genome size of zygnematophycean green algae. Front. Plant Sci. 12, 610381.

25. Busch, A., and Hess, S. (2022). Sunscreen mucilage: a photoprotective adaptation found in terrestrial green algae (Zygnematophyceae). Eur. J. Phycol. 57, 107–124.

26. Cheng, S., Xian, W., Fu, Y., Marin, B., Keller, J., Wu, T., Sun, W., Li, X., Xu, Y., Zhang, Y., Wittek, S., Reder, T., Günther, G., Gontcharov, A., Wang, S., Li, L., Liu, X., Wang, J., Yang, H., Xu, X., Delaux, P.M., Melkonian, B., Wong, G.K.S., and Melkonian, M. (2019). Genomes of subaerial Zygnematophyceae provide insights into land plant evolution. Cell 179, 1057–1067.e14.

27. Clements, F.E. (1909). The genera of fungi (HW Wilson Company).

28. Guiry, M.D. (2013). Taxonomy and nomenclature of the Conjugatophyceae (= Zygnematophyceae). ALGAE 28, 1–29.

29. Gontcharov, A.A., and Melkonian, M. (2010). Molecular phylogeny and revision of the genus Netrium (Zygnematophyceae, Streptophyta): Nucleotaenium gen. nov. J. Phycol. 46, 346–362.

30. Hall, J.D., and McCourt, R.M. (2017). Zygnematophyceae. In Handbook of the protists, J.M. Archibald, A.G. Simpson, and C.H. Slamovits, eds. (Springer International Publishing), pp. 135–163.

31. Buschmann, H. (2020). Into another dimension: how streptophyte algae gained morphological complexity. J. Exp. Bot. 71, 3279–3286.

32. Ikegaya, H., Sonobe, S., Murakami, K., and Shimmen, T. (2008). Rhizoid differentiation of Spirogyra is regulated by substratum. J. Plant Res. 121, 571–579.

33. Garduño-Solórzano, G., Martínez-García, M., Scotta Hentschke, G., Lopes, G., Castelo Branco, R., Vasconcelos, V.M.O., Campos, J.E., López-Cano, R., and Quintanar-Zúñiga, R.E. (2021). The phylogenetic placement of Temnogametum (Zygnemataceae) and description of Temnogametum iztacalense sp. nov., from a tropical high mountain lake in Mexico. Eur. J. Phycol. 56, 159–173.

34. Stancheva, R., Hall, J.D., Herburger, K., Lewis, L.A., McCourt, R.M., Sheath, R.G., and Holzinger, A. (2014). Phylogenetic position of Zygogonium ericetorum (Zygnematophyceae, Charophyta) from a high alpine habitat and ultrastructural characterization of unusual aplanospores. J. Phycol. 50, 790–803.

Current Biology
Report

ɔ **CellPress**
OPEN ACCESS

35. Brunkard, J.O., and Zambryski, P.C. (2017). Plasmodesmata enable multicellularity: new insights into their evolution, biogenesis, and functions in development and immunity. Curr. Opin. Plant Biol. *35*, 76–83.

36. Andosch, A., Höftberger, M., Lütz, C., and Lütz-Meindl, U. (2015). Subcellular sequestration and impact of heavy metals on the ultrastructure and physiology of the multicellular freshwater alga *Desmidium swartzii*. Int. J. Mol. Sci. *16*, 10389–10410.

37. Hall, J.D., McCourt, R.M., and Delwiche, C.F. (2008). Patterns of cell division in the filamentous Desmidiaceae, close green algal relatives of land plants. Am. J. Bot. *95*, 643–654.

38. Harholt, J., Moestrup, Ø., and Ulvskov, P. (2016). Why Plants Were Terrestrial from the Beginning. Trends Plant Sci. *21*, 96–101.

39. Delwiche, C.F., and Cooper, E.D. (2015). The evolutionary origin of a terrestrial flora. Curr. Biol. *25*, R899–R910.

40. de Vries, J., and Archibald, J.M. (2018). Plant evolution: landmarks on the path to terrestrial life. New Phytol. *217*, 1428–1434.

41. Fürst-Jansen, J.M.R., de Vries, S., and de Vries, J. (2020). Evo-physio: on stress responses and the earliest land plants. J. Exp. Bot. *71*, 3254–3269.

42. Niklas, K.J., and Newman, S.A. (2013). The origins of multicellular organisms. Evol. Dev. *15*, 41–52.

43. Busch, A., and Hess, S. (2022). A diverse group of underappreciated zygnematophytes deserves in-depth exploration. Applied Phycology, 1–18. https://doi.org/10.1080/26388081.2022.2081819.

44. Heath, T.A., Hedtke, S.M., and Hillis, D.M. (2008). Taxon sampling and the accuracy of phylogenetic analyses. J. Syst. Evol. *46*, 239–257.

45. Litsios, G., and Salamin, N. (2012). Effects of Phylogenetic Signal on Ancestral State Reconstruction. Syst. Biol. *61*, 533–538.

46. Morris, J.L., Puttick, M.N., Clark, J.W., Edwards, D., Kenrick, P., Pressel, S., Wellman, C.H., Yang, Z., Schneider, H., and Donoghue, P.C.J. (2018). The timescale of early plant evolution. Proc. Natl. Acad. Sci. USA *115*, E2274–E2283.

47. Amborella Genome Project (2013). The *Amborella* genome and the evolution of flowering plants. Science *342*, 1241089.

48. Lamesch, P., Berardini, T.Z., Li, D., Swarbreck, D., Wilks, C., Sasidharan, R., Muller, R., Dreher, K., Alexander, D.L., Garcia-Hernandez, M., et al. (2012). The Arabidopsis Information Resource (TAIR): improved gene annotation and new tools. Nucleic Acids Res. *40*, D1202–D1210.

49. Li, F.-W., Brouwer, P., Carretero-Paulet, L., Cheng, S., de Vries, J., Delaux, P.-M., Eily, A., Koppers, N., Kuo, L.-Y., Li, Z., et al. (2018). Fern genomes elucidate land plant evolution and cyanobacterial symbioses. Nat. Plants *4*, 460–472.

50. Carpenter, E.J., Matasci, N., Ayyampalayam, S., Wu, S., Sun, J., Yu, J., Jimenez Vieira, F.R., Bowler, C., Dorrell, R.G., Gitzendanner, M.A., et al. (2019). Access to RNA-sequencing data from 1, 173 plant species: The 1000 Plant transcriptomes initiative (1KP). GigaScience *8*, giz126.

51. Moreau, H., Verhelst, B., Couloux, A., Derelle, E., Rombauts, S., Grimsley, N., Van Bel, M., Poulain, J., Katinka, M., Hohmann-Marriott, M.F., et al. (2012). Gene functionalities and genome structure in *Bathycoccus prasinos* reflect cellular specializations at the base of the green lineage. Genome Biol. *13*, R74.

52. The International Brachypodium Initiative (2010). Genome sequencing and analysis of the model grass *Brachypodium distachyon*. Nature *463*, 763–768.

53. Cooper, E., and Delwiche, C. (2016). Green algal transcriptomes for phylogenetics and comparative genomics. Figshare. https://doi.org/10.6084/m9.figshare.1604778.

54. Nishiyama, T., Sakayama, H., de Vries, J., Buschmann, H., Saint-Marcoux, D., Ullrich, K.K., Haas, F.B., Vanderstraeten, L., Becker, D., Lang, D., et al. (2018). The *Chara* genome: secondary complexity and implications for plant terrestrialization. Cell *174*, 448–464.e24.

55. Merchant, S.S., Prochnik, S.E., Vallon, O., Harris, E.H., Karpowicz, S.J., Witman, G.B., Terry, A., Salamov, A., Fritz-Laylin, L.K., Maréchal-Drouard, L., et al. (2007). The *Chlamydomonas* genome reveals the evolution of key animal and plant functions. Science *318*, 245–250.

56. Blaby, I.K., Blaby-Haas, C.E., Tourasse, N., Hom, E.F.Y., Lopez, D., Aksoy, M., Grossman, A., Umen, J., Dutcher, S., Porter, M., et al. (2014). The *Chlamydomonas* genome project: a decade on. Trends Plant Sci. *19*, 672–680.

57. Blanc, G., Agarkova, I., Grimwood, J., Kuo, A., Brueggeman, A., Dunigan, D.D., Gurnon, J., Ladunga, I., Lindquist, E., Lucas, S., et al. (2012). The genome of the polar eukaryotic microalga *Coccomyxa subellipsoidea* reveals traits of cold adaptation. Genome Biol. *13*, R39.

58. de Vries, J., Curtis, B.A., Gould, S.B., and Archibald, J.M. (2018). Embryophyte stress signaling evolved in the algal progenitors of land plants. Proc. Natl. Acad. Sci. USA *115*, E3471–E3480.

59. Ju, C., Van de Poel, B., Cooper, E.D., Thierer, J.H., Gibbons, T.R., Delwiche, C.F., and Chang, C. (2015). Conservation of ethylene as a plant hormone over 450 million years of evolution. Nat. Plants *1*, 14004.

60. Bowman, J.L., Kohchi, T., Yamato, K.T., Jenkins, J., Shu, S., Ishizaki, K., Yamaoka, S., Nishihama, R., Nakamura, Y., Berger, F., et al. (2017). Insights into Land Plant Evolution Garnered from the *Marchantia polymorpha* Genome. Cell *171*, 287–304.e15.

61. Worden, A.Z., Lee, J.H., Mock, T., Rouzé, P., Simmons, M.P., Aerts, A.L., Allen, A.E., Cuvelier, M.L., Derelle, E., Everett, M.V., et al. (2009). Green evolution and dynamic adaptations revealed by genomes of the marine picoeukaryotes *Micromonas*. Science *324*, 268–272.

62. Kawahara, Y., de la Bastide, M., Hamilton, J.P., Kanamori, H., McCombie, W.R., Ouyang, S., Schwartz, D.C., Tanaka, T., Wu, J., Zhou, S., et al. (2013). Improvement of the *Oryza sativa* Nipponbare reference genome using next generation sequence and optical map data. Rice *6*, 4.

63. Palenik, B., Grimwood, J., Aerts, A., Rouzé, P., Salamov, A., Putnam, N., Dupont, C., Jorgensen, R., Derelle, E., Rombauts, S., et al. (2007). The tiny eukaryote *Ostreococcus* provides genomic insights into the paradox of plankton speciation. Proc. Natl. Acad. Sci. USA *104*, 7705–7710.

64. Lang, D., Ullrich, K.K., Murat, F., Fuchs, J., Jenkins, J., Haas, F.B., Piednoel, M., Gundlach, H., Van Bel, M., Meyberg, R., et al. (2018). The *Physcomitrella patens* chromosome-scale assembly reveals moss genome structure and evolution. Plant J. *93*, 515–533.

65. Nystedt, B., Street, N.R., Wetterbom, A., Zuccolo, A., Lin, Y.-C., Scofield, D.G., Vezzi, F., Delhomme, N., Giacomello, S., Alexeyenko, A., et al. (2013). The Norway spruce genome sequence and conifer genome evolution. Nature *497*, 579–584.

66. Banks, J.A., Nishiyama, T., Hasebe, M., Bowman, J.L., Gribskov, M., DePamphilis, C., Albert, V.A., Aono, N., Aoyama, T., Ambrose, B.A., et al. (2011). The *Selaginella* genome identifies genetic changes associated with the evolution of vascular plants. Science *332*, 960–963.

67. De Clerck, O., Kao, S.-M., Bogaert, K.A., Blomme, J., Foflonker, F., Kwantes, M., Vancaester, E., Vanderstraeten, L., Aydogdu, E., Boesger, J., et al. (2018). Insights into the Evolution of Multicellularity from the Sea Lettuce Genome. Curr. Biol. *28*, 2921–2933.e5.

68. Prochnik, S.E., Umen, J., Nedelcu, A.M., Hallmann, A., Miller, S.M., Nishii, I., Ferris, P., Kuo, A., Mitros, T., Fritz-Laylin, L.K., et al. (2010). Genomic analysis of organismal complexity in the multicellular green alga *Volvox carteri*. Science *329*, 223–226.

69. Seppey, M., Manni, M., and Zdobnov, E.M. (2019). BUSCO: Assessing Genome Assembly and Annotation Completeness. Methods Mol. Biol. *1962*, 227–245. https://doi.org/10.1007/978-1-4939-9173-0_14.

70. Nguyen, L.-T., Schmidt, H.A., von Haeseler, A., and Minh, B.Q. (2015). IQ-TREE: A Fast and Effective Stochastic Algorithm for Estimating Maximum-Likelihood Phylogenies. Mol. Biol. Evol. *32*, 268–274.

71. Katoh, K., and Standley, D.M. (2013). MAFFT Multiple Sequence Alignment Software Version 7: Improvements in Performance and Usability. Mol. Biol. Evol. *30*, 772–780.

72. Revell, L.J. (2012). phytools: an R package for phylogenetic comparative biology (and other things): phytools: R package. Methods Ecol. Evol. *3*, 217–223.

CellPress
OPEN ACCESS

Current Biology
Report

73. Wang, H.-C., Minh, B.Q., Susko, E., and Roger, A.J. (2018). Modeling Site Heterogeneity with Posterior Mean Site Frequency Profiles Accelerates Accurate Phylogenomic Estimation. Syst. Biol. 67, 216–235.

74. Yang, Z., Kumar, S., and Nei, M. (1995). A new method of inference of ancestral nucleotide and amino acid sequences. Genetics 141, 1641–1650.

75. Capella-Gutiérrez, S., Silla-Martínez, J.M., and Gabaldón, T. (2009). trimAl: a tool for automated alignment trimming in large-scale phylogenetic analyses. Bioinformatics 25, 1972–1973.

76. Bolger, A.M., Lohse, M., and Usadel, B. (2014). Trimmomatic: a flexible trimmer for Illumina sequence data. Bioinformatics 30, 2114–2120.

77. von Schwartzenberg, K., Bornfleth, S., Lindner, A.-C., and Hanelt, D. (2013). The Microalgae and Zygnematophyceae Collection Hamburg (MZCH) – living cultures for research on rare streptophytic algae. Algol. Stud. 142, 77–107.

78. Zhou, H., and von Schwartzenberg, K. (2020). Zygnematophyceae: from living algae collections to the establishment of future models. J. Exp. Bot. 71, 3296–3304.

79. Nichols, H.W. (1973). Growth media – freshwater. In Handbook of Phycological Methods, J.R. Stein, ed. (London: Cambridge University Press), pp. 16–17.

80. McFadden, G.I., and Melkonian, M. (1986). Use of Hepes buffer for microalgal culture media and fixation for electron microscopy. Phycologia 25, 551–557.

81. Krieger, H., Kolkwitz, R., and Krieger, H. (1941). Zygnemales. In Kryptogamen-Flora von Deutschland und der Schweiz, 13, L. Rabenhorst, ed. (Leipzig: Becker & Erler), pp. 1–499.

82. Gontcharov, A.A., Marin, B.A., and Melkonian, M.A. (2003). Molecular phylogeny of conjugating green algae (Zygnemophyceae, Streptophyta) inferred from SSU rDNA sequence comparisons. J. Mol. Evol. 56, 89–104.

83. Gontcharov, A.A., Marin, B., and Melkonian, M. (2004). Are combined analyses better than single gene phylogenies? A case study using SSU rDNA and rbc L sequence comparisons in the Zygnematophyceae (Streptophyta). Mol. Biol. Evol. 21, 612–624.

84. Schindelin, J., Arganda-Carreras, I., Frise, E., Kaynig, V., Longair, M., Pietzsch, T., Preibisch, S., Rueden, C., Saalfeld, S., Schmid, B., et al. (2012). Fiji: an open-source platform for biological-image analysis. Nat. Methods 9, 676–682.

85. Spurr, A.R. (1969). A low-viscosity epoxy resin embedding medium for electron microscopy. J. Ultrastruct. Res. 26, 31–43.

86. Guillard, R.R.L. (1975). – Culture of phytoplankton for feeding marine invertebrates. In Culture of marine invertebrate animals, W.L. Smith, and M.H. Chanley, eds. (New York: Plenum Book Publ. Corp), pp. 29–60.

87. Haas, B.J., Papanicolaou, A., Yassour, M., Grabherr, M., Blood, P.D., Bowden, J., Couger, M.B., Eccles, D., Li, B., Lieber, M., et al. (2013). De novo transcript sequence reconstruction from RNA-seq using the Trinity platform for reference generation and analysis. Nat. Protoc. 8, 1494–1512.

88. Kang, S., Tice, A.K., Spiegel, F.W., Silberman, J.D., Pánek, T., Čepička, I., Kostka, M., Kosakyan, A., Alcântara, D.M.C., Roger, A.J., et al. (2017). Between a Pod and a Hard Test: The Deep Evolution of Amoebae. Mol. Biol. Evol. 34, 2258–2270.

89. Kalyaanamoorthy, S., Minh, B.Q., Wong, T.K.F., von Haeseler, A., and Jermiin, L.S. (2017). ModelFinder: fast model selection for accurate phylogenetic estimates. Nat. Methods 14, 587–589.

90. Shimodaira, H. (2002). An approximately unbiased test of phylogenetic tree selection. Syst. Biol. 51, 492–508.

Current Biology
Report

CellPress
OPEN ACCESS

STAR★METHODS

KEY RESOURCES TABLE

REAGENT or RESOURCE	SOURCE	IDENTIFIER
Critical commercial assays		
DNAse I	Thermo Fisher, Waltham, MA, USA	N/A
NEB mRNA stranded Library preparation kit	New England Biolabs, Beverly, MA, USA	N/A
Trizol	Thermo Fisher, Waltham, MA, USA	N/A
Deposited data		
Alignment	This study	https://doi.org/10.5281/zenodo.6805950
Amborella trichopoda genome	Amborella genome project[47]	https://phytozome.jgi.doe.gov/pz/portal.html#!info?alias=Org_Atrichopoda
Arabidopsis thaliana genome TAIR V10	TAIR[48]	http://www.arabidopsis.org
Azolla filiculoides genome	Li et al.[49]	https://www.fernbase.org
Bambusina borreri CCAC 0045 transcriptome, 1KP Code QWFV	Carpenter et al.[50]	http://www.onekp.com/public_data.html
Bathycoccus prasinos genome	Moreau et al.[51]	https://phycocosm.jgi.doe.gov/Batpra1/Batpra1.info.html
Brachypodium distachyon	The International Brachypodium Initiative[52]	https://phytozome-next.jgi.doe.gov/info/Bdistachyon_v3_1
Chaetophaeridium globosum SAG26.98 transcriptome	Cooper and Delwiche[53]	https://figshare.com/articles/dataset/Green_algal_transcriptomes_for_phylogenetics_and_comparative_genomics/1604778
Chara braunii S276 genome	Nishiyama et al.[54]	https://bioinformatics.psb.ugent.be/orcae/overview/Chbra
Chlamydomonas reinhardtii genome v5.5	Merchant et al.[55]; Blaby et al.[56]	https://phytozome.jgi.doe.gov/pz/portal.html#!info?alias=Org_Creinhardtii
Closterium lunula M2156 transcriptome, 1KP Code DRFX	Carpenter et al.[50]	http://www.onekp.com/public_data.html
Coccomyxa subellipsoidea genome v2.0	Blanc et al.[57]	https://phytozome.jgi.doe.gov/pz/portal.html#!info?alias=Org_CsubellipsoideaC_169
Coleochaete scutata SAG50.90 transcriptome	de Vries et al.[58]	https://www.ncbi.nlm.nih.gov/Traces/wgs/wgsviewer.cgi?val=GFXZ00000000
Coleochaete orbicularis transcriptome	Ju et al.[59]	https://www.ncbi.nlm.nih.gov/Traces/wgs/wgsviewer.cgi?val=GBSL01&search=GBSL01000000&display=scaffolds
Coleochaete orbicularis transcriptome	Cooper and Delwiche[53]	https://figshare.com/articles/dataset/Green_algal_transcriptomes_for_phylogenetics_and_comparative_genomics/1604778
Cosmarium broomei CCAC 0143 transcriptome, 1KP Code HIDG	Carpenter et al.[50]	http://www.onekp.com/public_data.html
Cosmarium granatum CCAC 0137 transcriptome, 1KP Code MNNM	Carpenter et al.[50]	http://www.onekp.com/public_data.html
Cosmarium ochthodes M1384 transcriptome, 1KP Code HJVM	Carpenter et al.[50]	http://www.onekp.com/public_data.html
Cosmarium subtumidum M3067 transcriptome, 1KP Code WDGV	Carpenter et al.[50]	http://www.onekp.com/public_data.html

(Continued on next page)

CellPress
OPEN ACCESS

Current Biology
Report

Continued

REAGENT or RESOURCE	SOURCE	IDENTIFIER
Cosmarium tinctum M2301 transcriptome, 1KP Code BHBK	Carpenter et al.[50]	http://www.onekp.com/public_data.html
Cosmocladium cf. *constrictum* ASW 07118 transcriptome, 1KP Code RQFE	Carpenter et al.[50]	http://www.onekp.com/public_data.html
Cylindrocystis brebissonii M2213 transcriptome, 1KP Code YOXI	Carpenter et al.[50]	http://www.onekp.com/public_data.html
Cylindrocystis brebissonii M2853/M2213 transcriptome, 1KP Code YLBK	Carpenter et al.[50]	http://www.onekp.com/public_data.html
Cylindrocystis brebissonii M2853 transcriptome, 1KP Code RPGL	Carpenter et al.[50]	http://www.onekp.com/public_data.html
Cylindrocystis cushleckae M2158 transcriptome, 1KP Code JOJQ	Carpenter et al.[50]	http://www.onekp.com/public_data.html
Cylindrocystis sp. M3015 transcriptome, 1KP Code VAZE	Carpenter et al.[50]	http://www.onekp.com/public_data.html
Desmidium aptogonum ASW 07112 transcriptome, 1KP Code DFDS	Carpenter et al.[50]	http://www.onekp.com/public_data.html
Entransia sp. transcriptome	Cooper and Delwiche[53]	https://figshare.com/articles/dataset/Green_algal_transcriptomes_for_phylogenetics_and_comparative_genomics/1604778
Euastrum affine ASW 07012 transcriptome, 1KP Code GYRP	Carpenter et al.[50]	http://www.onekp.com/public_data.html
Klebsormidium flaccidum UTEX 321 transcriptome	Cooper and Delwiche[53]	https://figshare.com/articles/dataset/Green_algal_transcriptomes_for_phylogenetics_and_comparative_genomics/1604778
Klebsormidium flaccidum SAG2307 transcriptome	de Vries et al.[58]	https://www.ncbi.nlm.nih.gov/Traces/wgs/wgsviewer.cgi?val=GFXY00000000
Marchantia polymorpha genome v3.1	Bowman et al.[60]	https://phytozome.jgi.doe.gov/pz/portal.html#!info?alias=Org_Mpolymorpha
Mesotaenium braunii (*Serritaenia* sp.) M2214 transcriptome, 1KP Code WSJO	Carpenter et al.[50]	http://www.onekp.com/public_data.html
Mesotaenium caldariorum SAG 648-1 transcriptome, 1KP Code HKZW	Carpenter et al.[50]	http://www.onekp.com/public_data.html
Mesotaenium kramstei UTEX LB 1025 transcriptome, 1KP Code NBYP	Carpenter et al.[50]	http://www.onekp.com/public_data.html
"*Mesotaenium endlicherianum*" SAG12.97 transcriptome, 1KP Code WDCW	Carpenter et al.[50]	http://www.onekp.com/public_data.html
Mesostigma viride CCAC 1140 transcriptome	Ju et al.[59]	https://www.ncbi.nlm.nih.gov/Traces/wgs/wgsviewer.cgi?val=GBSK00000000
Mesostigma viride NIES995 transcriptome	de Vries et al.[58]	https://www.ncbi.nlm.nih.gov/Traces/wgs/wgsviewer.cgi?val=GFXX00000000
Micrasterias fimbriata ASW 07026 transcriptome, 1KP Code MCHJ	Carpenter et al.[50]	http://www.onekp.com/public_data.html
Micromonas pusilla genome v3.0	Worden et al.[61]	https://phytozome.jgi.doe.gov/pz/portal.html#!info?alias=Org_MpusillaCCMP1545
Micromonas sp. RCC299 genome v3.0	Worden et al.[61]	https://phytozome.jgi.doe.gov/pz/portal.html#!info?alias=Org_MspRCC299
Mougeotia scalaris SAG164.80 transcriptome	Cooper and Delwiche[53]	https://figshare.com/articles/dataset/Green_algal_transcriptomes_for_phylogenetics_and_comparative_genomics/1604778
Mougeotia sp. MZCH240 transcriptome	de Vries et al.[16]; Fürst-Jansen et al.[17]	https://www.ncbi.nlm.nih.gov/Traces/wgs/wgsviewer.cgi?val=GHUK00000000.

(Continued on next page)

Current Biology
Report

CellPress
OPEN ACCESS

Continued

REAGENT or RESOURCE	SOURCE	IDENTIFIER
Mougeotiopsis calospora transcriptome assembly	This study	GenBank: GJZN00000000.1
Mougeotiopsis calospora transcriptome reads	This study	Sequence Read Archive: SRR19751296
Nephroselmis pyriformis CCMP 717 transcriptome	Cooper and Delwiche[53]	https://figshare.com/articles/dataset/Green_algal_transcriptomes_for_phylogenetics_and_comparative_genomics/1604778
Netrium digitus CCAC 0148 transcriptome, 1KP Code FFGR	Carpenter et al.[50]	http://www.onekp.com/public_data.html
Nitella mirabilis transcriptome	Ju et al.[59]	https://www.ncbi.nlm.nih.gov/Traces/wgs/wgsviewer.cgi?val=GBST01&search=GBST01000000&display=scaffolds
Nitella mirabilis transcriptomes of lower and upper tissues	Cooper and Delwiche[53]	https://figshare.com/articles/dataset/Green_algal_transcriptomes_for_phylogenetics_and_comparative_genomics/1604778
Nucleotaenium eifelense M3006 transcriptome, 1KP Code KMNX	Carpenter et al.[50]	http://www.onekp.com/public_data.html
Oedogonium cardiacum UTEX LB40 transcriptome	Cooper and Delwiche[53]	https://figshare.com/articles/dataset/Green_algal_transcriptomes_for_phylogenetics_and_comparative_genomics/1604778
Oltmansiellopsis unicellularis SCCAP K-0250 transcriptome	Cooper and Delwiche[53]	https://figshare.com/articles/dataset/Green_algal_transcriptomes_for_phylogenetics_and_comparative_genomics/1604778
Onychonema laeve CCAC 0151 transcriptome, 1KP Code GGWH	Carpenter et al.[50]	http://www.onekp.com/public_data.html
Oryza sativa Nipponbare genome v7.0	Kawahara et al.[62]	https://phytozome.jgi.doe.gov/pz/portal.html#!info?alias=Org_Osativa
Ostreococcus lucimarinus genome v2.0	Palenik et al.[63]	https://phytozome.jgi.doe.gov/pz/portal.html#!info?alias=Org_Olucimarinus
Penium exiguum CCAC 0142 transcriptome, 1KP Code YSQT	Carpenter et al.[50]	http://www.onekp.com/public_data.html
Penium margaritaceum SAG22.82 transcriptome	Cooper and Delwiche[53]	https://figshare.com/articles/dataset/Green_algal_transcriptomes_for_phylogenetics_and_comparative_genomics/1604778
Phymatodocis nordstedtiana SVCK 327 transcriptome, 1KP Code RPQV	Carpenter et al.[50]	http://www.onekp.com/public_data.html
Physcomitrium patens genome v3.3	Lang et al.[64]	https://phytozome.jgi.doe.gov/pz/portal.html#!info?alias=Org_Ppatens
Picea abies genome	Nystedt et al.[65]	https://plantgenie.org/FTP?dir=Data%2FConGenIE%2FPicea_abies%2Fv1.0
Planotaenium ohtanii M2697 transcriptome, 1KP Code SNOX	Carpenter et al.[50]	http://www.onekp.com/public_data.html
Pleurotaenium trabecula CCAC 0163 transcriptome, 1KP Code MOYY	Carpenter et al.[50]	http://www.onekp.com/public_data.html
Salvinia cucullata genome	Li et al.[49]	https://www.fernbase.org
Selaginella moellendorffii genome	Banks et al.[66]	https://phytozome-next.jgi.doe.gov/info/Smoellendorffii_v1_0
Sphagnum fallax v0.5 genome	Obtained from Phytozome with permission	https://phytozome-next.jgi.doe.gov/info/Sfallax_v0_5
Spirogloea muscicola CCAC 0214 transcriptome, 1KP Code TPHT	Carpenter et al.[50]	http://www.onekp.com/public_data.html

(Continued on next page)

CelPress
OPEN ACCESS

Current Biology
Report

Continued

REAGENT or RESOURCE	SOURCE	IDENTIFIER
Spirogyra pratensis MZCH10213 transcriptome	de Vries et al.[16]	https://www.ncbi.nlm.nih.gov/Traces/wgs/wgsviewer.cgi?val=GICF00000000.
Spirogyra pratensis UTEX 921 transcriptome	Cooper and Delwiche[53]	https://figshare.com/articles/dataset/Green_algal_transcriptomes_for_phylogenetics_and_comparative_genomics/1604778
Spirogyra pratensis UTEX 928 transcriptome	Ju et al.[59]	https://www.ncbi.nlm.nih.gov/Traces/wgs/wgsviewer.cgi?val=GBSM01000000
Spirogyra sp. M1810 transcriptome, 1KP Code HAOX	Carpenter et al.[50]	http://www.onekp.com/public_data.html
Spirogyra sp. Transcriptome Au1	Cooper and Delwiche[53]	https://figshare.com/articles/dataset/Green_algal_transcriptomes_for_phylogenetics_and_comparative_genomics/1604778
Staurastrum sebaldi M1129 transcriptome, 1KP Code ISHC	Carpenter et al.[50]	http://www.onekp.com/public_data.html
Staurodesmus convergens M2558 transcriptome, 1KP Code WCQU	Carpenter et al.[50]	http://www.onekp.com/public_data.html
Staurodesmus omearii M0751 transcriptome, 1KP Code RPRU	Carpenter et al.[50]	http://www.onekp.com/public_data.html
Tetraselmis striata transcriptome	Cooper and Delwiche[53]	https://figshare.com/articles/dataset/Green_algal_transcriptomes_for_phylogenetics_and_comparative_genomics/1604778
Tetraselmis suecica transcriptome	Cooper and Delwiche[53]	https://figshare.com/articles/dataset/Green_algal_transcriptomes_for_phylogenetics_and_comparative_genomics/1604778
Ulva mutabilis genome	De Clerck et al.[67]	https://bioinformatics.psb.ugent.be/orcae/overview/Ulvmu
Volvox carteri genome v2.1	Prochnik et al.[68]	https://phytozome.jgi.doe.gov/pz/portal.html#!info?alias=Org_Vcarteri
Xanthidium antilopaeum M1229 transcriptome, 1KP Code GBGT	Carpenter et al.[50]	http://www.onekp.com/public_data.html
Zygnema circumcarinatum SAG698-1a transcriptome	de Vries et al.[58]	https://www.ncbi.nlm.nih.gov/Traces/wgs/wgsviewer.cgi?val=GFYA00000000
Zygnema sp.-B M1384 transcriptome 1KP Code WGMD	Carpenter et al.[50]	http://www.onekp.com/public_data.html
Zygnema sp. transcriptome 1KP Code FMRU	Carpenter et al.[50]	http://www.onekp.com/public_data.html
Zygnemopsis sp. CCAP 699/1 transcriptome 1KP Code MFZO	Carpenter et al.[50]	http://www.onekp.com/public_data.html
Experimental models: Organisms/strains		
Mougeotiopsis calospora MZCH580	Obtained from Microalgae and Zygnematophyceae Collection Hamburg (MZCH)	maintained at Microalgae and Zygnematophyceae Collection Hamburg (MZCH)
Mougeotia sp. MZCH240	Obtained from Microalgae and Zygnematophyceae Collection Hamburg (MZCH)	maintained at Microalgae and Zygnematophyceae Collection Hamburg (MZCH)
Spirogyra pratensis MZCH10213	Obtained from Microalgae and Zygnematophyceae Collection Hamburg (MZCH)	maintained at Microalgae and Zygnematophyceae Collection Hamburg (MZCH)
Zygnema circumcarinatum MZCH10230	Obtained from Microalgae and Zygnematophyceae Collection Hamburg (MZCH)	maintained at Microalgae and Zygnematophyceae Collection Hamburg (MZCH)

(Continued on next page)

Current Biology
Report

CellPress
OPEN ACCESS

Continued

REAGENT or RESOURCE	SOURCE	IDENTIFIER
Software and algorithms		
BUSCO v.5.0.0	Seppey et al.[69]	https://busco.ezlab.org
FASTQC	Babraham Institute	www.bioinformatics.babraham.ac.uk/projects/fastqc
IQ-Tree v1.5.5 and v1.6.12	Nguyen et al.[70]	http://www.iqtree.org
MAFFT v7.310	Katoh and Standley[71]	https://mafft.cbrc.jp/alignment/software/
Phytools	Revell[72]	https://cran.r-project.org/web/packages/phytools/index.html
Posterior Mean Site Frequency Profiles	Wang et al.[73]	Implemented in IQ-Tree http://www.iqtree.org
Re-routing method according to Yang 1995	Yang[74]	N/A
Trimal v1.4.rev15	Capella-Gutierrez et al.[75]	http://trimal.cgenomics.org
Transcdecoder v.5.5.0	Brian J. Haas	https://github.com/TransDecoder/TransDecoder/releases
Trimmomatic v0.36	Bolger et al.[76]	http://www.usadellab.org/cms/?page=trimmomatic

RESOURCE AVAILABILITY

Lead contact

Further information and requests for resources and reagents should be directed to and will be fulfilled by the lead contact, Jan de Vries (devries.jan@uni-goettingen.de).

Materials availability

This study did not generate new unique reagents.

Data and code availability

- RNA-seq data have been deposited at the NCBI under the BioProject accession PRJNA849386 and the Sequence Read Archive (SRA) under the accession SRR19751296; all data are publicly available as of the date of publication. Accession numbers are additionally listed in the key resources table.
- A transcriptome assembly has been deposited at NCBI Transcriptome Shotgun Assembly Sequence Database (TSA) under the accession GJZN00000000. The version described in this paper is the first version, GJZN01000000. The assembly is publicly available as of the date of publication. The accession number is additionally listed in the key resources table. The alignment has been uploaded to Zenodo: https://doi.org/10.5281/zenodo.6805950
- No original code was used; all computational analyses were performed with published tools and are cited in the STAR Methods section.

EXPERIMENTAL MODEL AND SUBJECT DETAILS

Algal strains

Mougeotiopsis calospora (strain MZCH580), *Mougeotia* sp. (MZCH240), *Spirogyra pratensis* (strain MZCH20213) and *Zygnema circumcarinatum* (MZCH10230) were obtained from the Microalgae and Zygnematophyceae Collection Hamburg (MZCH)[77,78] and grown in WHM medium[79] or Waris-H medium[80] at 20°C and under full-spectrum fluorescent lamps or white LEDs (30-50 µmol photons m^{-2} s^{-1}; 16h:8h light-dark cycle), if not stated otherwise in the experimental details (see below).

METHOD DETAILS

Rationale for the application of the name *Mougeotiopsis calospora* to strain MZCH580

In terms of its gross morphology, strain MZCH580 resembles members of the genera *Klebsormidium* (Klebsormidiophyceae), *Ulothrix* (Ulvophyceae) and *Mougeotia* (Zygnematophyceae), all of which form unbranched filaments and have plate-like or parietal plastids. However, the absence of pyrenoids in strain MZCH580 is a major distinguishing character, as algae from the three mentioned genera (and classes) typically have prominent pyrenoids surrounded by a sheath of starch grains. There are, however, two historical descriptions from the late 19th century that describe pyrenoid-lacking, filamentous green algae with plate like chloroplasts:

CellPress
OPEN ACCESS

Current Biology
Report

Mougeotiopsis calospora Palla, 1894 and *Mesogerron fluitans* Brand, 1899. *Mougeotiopsis* is a putative zygnematophyte, as scalariform conjugation and the formation of zygospores was clearly documented.[9] Instead, *Mesogerron* was only described on the basis of vegetative material, and first suspected to be related to *Ulothrix* (Ulvophyceae, Chlorophyta). Based on the marked resemblance in their vegetative characters (filament width of 15–18 μm, cell architecture, and chloroplast morphology), *Mougeotiopsis* and *Mesogerron* were later treated as heterotypic synonyms (Krieger, 1941[81]). Strain MZCH580 matches both descriptions concerning the varying cell length (including cells that are shorter than wide), cell architecture (plastid-associated nucleus) and chloroplast morphology (plate-like to parietal with pronounced lateral indentations), but it has somewhat smaller cells (filament width of 10–15 μm). The morphological similarity, however, is compelling, and variation in filament width is known for many closely related strains or species of green algae. We were unable to locate the type material of *Mougeotiopsis calospora*, but studied original material of *Mesogerron fluitans* (collected by F. Brand in 1899 and provided by the Herbarium of the Academy of Natural Sciences of Philadelphia). The dried filaments of that species were morphologically similar to those of strain MZCH580, especially in the marked variation in cell length observed in the filaments (Figure S4). Amplification of genetic material from this sample did not work.

Rationale for establishing a new order, Serritaeniales ord. nov.

In our phylogeny, the branch in question comprises three distinct groups of organisms: *Mougeotiopsis calospora* (one strain known), the genus *Serritaenia* (several strains known[25]), and strain SAG 12.97, a unicellular zygnematophyte that is often referred to as "*Mesotaenium endlicherianum*". Currently, there is only one existent ordinal name that is based on the mentioned taxon names, namely Mesotaeniales Fritsch. However, the phylogenetic position of the genus *Mesotaenium* is still uncertain, as the designation of strain SAG 12.97 is potentially based on misidentification. In the opinion of some authors (S.H. and A.B.), the morphology of SAG 12.97 does not conform with the description of the type species *M. endlicherianum* Nägeli. This problem was already recognized by other specialists for zygnematophycean algae who studied strain SAG 12.97.[82,83] Hence, we are hesitant to reuse the name Mesotaeniales and instead introduce a new ordinal name based on the well-studied and credible genus *Serritaenia*. Descriptions of the zygnematophycean orders defined in this study are provided in Table 1.

Light microscopy, time-lapse photography, and confocal imaging

High-resolution imaging of *Mougeotiopsis calospora* was done with the Zeiss IM35 inverted microscope (Carl Zeiss, Oberkochen, Germany) equipped with the objective lens Planapochromat 63×/1.4, electronic flash, and the Canon EOS 6D digital single-lens reflex camera (Canon, Tokyo, Japan). Time lapse imaging was performed on a Leica DM5000B microscope (Leica Microsystems Wetzlar GmbH, Wetzlar, Germany) controlled by the Micromanager software at six frames per minute, shown as 10 FPS. Color balance and contrast of micrographs were adjusted with Photoshop CS4 (Adobe Inc., CA, USA). Confocal laser scanning microscopy was done with a Leica TCS SPE system (SP5) and the Leica LCS software (Leica Microsystems Wetzlar GmbH, Wetzlar, Germany). Chlorophyll was excited with a wavelength of 635 nm and the emission of 646–782 nm was recorded. Confocal z stacks were processed and converted to three-dimensional data with the image processing package Fiji.[84]

Transmission electron microscopy

Algal filaments were fixed with 2 % glutaraldehyde in 75 mM cacodylate buffer (pH 7.0) for 1 h at RT, rinsed with 75 mM cacodylate buffer, and postfixed with 1 % osmium tetroxide in 75 mM cacodylate buffer overnight at 4 °C. After rinsing in cacodylate buffer, the samples were dehydrated in a graded acetone series and embedded according to Spurr.[85] The resulting TEM blocks were sectioned on an Ultracut E ultramicrotome (Leica-Reichert-Jung, Vienna, AU), stained with 2 % uranyl acetate and 2 % lead citrate. Sections were then examined with the LEO 906E transmission electron microscope (LEO, Oberkochen, Germany) and imaged with a MultiScan Typ 794 CCD camera and the Digital Micrograph 3.4.4 software (both Gatan Inc., Pleasanton, USA).

RNA isolation, sequencing and phylogenomics

For the isolation of total RNA, *Mougeotiopsis calospora* was grown on a modified freshwater F/2 medium[86] with 1% agar at 22°C. An LED light source provided photosynthetically active radiance at 120 μmol photons*m^{-2}*s^{-1} under a 12:12 h light/dark photocycle. Harvesting, RNA extraction and transcriptome sequencing was carried out as described by de Vries et al.[16] In brief, filaments of a growing algal culture were harvested and directly transferred into Trizol (Thermo Fisher, Waltham, MA, USA). The algal sample was homogenized using a Tenbroek tissue homogenizer and all following steps were performed in accordance to the manufacturer's instructions. To remove possible residual DNA, RNA samples were treated with DNAse I (Thermo Fisher). Adequate RNA quality was verified using a formamide agarose gel. Samples were shipped on dry ice to Genome Québec (Montreal, Canada), where additional RNA quantification and quality assessments were performed using a Bioanalyzer (Agilent Technologies Inc., Santa Clara, CA, USA). Library construction was performed using the NEB mRNA stranded Library preparation kit (New England Biolabs, Beverly, MA, USA). Sequencing of the libraries was carried out on the NovaSeq 6000 (Illumina), yielding 28188133 paired end reads of 101 base pairs in length. Quality of the reads was assessed using FastQC version 0.11.7. Reads were trimmed using Trimmomatic version 0.36[76], applying settings for quality trimming and adapter removal (ILLUMINACLIP:Adapters.fa:2:30:10:2:TRUE HEADCROP:10 TRAILING:3 SLIDINGWINDOW:4:20 MINLEN:36). The transcriptome was assembled de novo with Trinity.[87] Transcriptome completeness was assessed with BUSCO v.5.0.0[69] using the viridiplantae_odb10 database in the transcriptome mode. Open reading frames (ORFs) were predicted with Transdecoder v.5.5.0.

Current Biology
Report

CellPress
OPEN ACCESS

We downloaded 83 transcriptomes and genomes of Streptophyta and Chlorophyta (see key resources table). Using a previously constructed phylogenomic dataset, we searched the selected sequencing data for orthologs of the 351 highly conserved proteins.[88] After alignment and trimming using MAFFT v7.310[71] and trimal v1.4.rev15,[75] careful inspection of single-protein phylogenies estimated with IQ-TREE v1.5.5 under the LG4X model was undertaken to remove contaminants and paralogs. Once the data set was refined, orthologs that were missing in over 50% of taxa were removed; that said, we retained all orthologs that were present in *Mougeotiopsis* (overwriting the aforementioned 50% filtering). We estimated a maximum likelihood phylogeny based on the concatenated alignment of a final set of 326 translated proteins (cumulative maximum of 115,424 sites; see alignment on Zenodo, https://doi.org/10.5281/zenodo.6805950;) the final set of proteins/protein-coding genes was: AAP, ABHD13, Actin, ADK2, AGB1, AGX, AKTIP, ALG11, ALIS1, AMP2B, AOAH, AP1S2, AP3M1, AP3S1, AP4M, AP4S1, APBLC, ar21, arf3, ARL6, ARP2, ARP3, arpc1, ARPC4, ATEHD2, ATG2, atp6, ATP6V0A1, ATP6V0D1, ATPDIL14, ATSAR2, Atub, BAT1, Btub, C16orf80, C22orf28, C3H4, calr, capz, CC1, CCDC113, CCDC37, CCDC40, CCDC65, cct-A, cct-B, cct-D, cct-E, cct-G, cct-N, cct-T, cct-Z, CDK5, CLAT, COP-beta, COPE, COPG2, COPS2, COPS6, COQ4-mito, CORO1C, crfg, CRNL1, CS, CTP, D2HGDH-mito, DCAF13, DHSA1, DHSB3, DHYS, DIMT1L, DNAI2, DNAJ, DNAL1, DNM, DPP3, DRG2, ECHM, EF2, EFG-mito, EFTUD1, EIF3B, EIF3C, EIF3I, EIF4A3, EIF4E, ERLIN1, ETFA, FA2H, FAH, FAM18B, FAM96B, FAM, fh, fibri, FOLD, fpps, FTSJ1, GAS8, GCST, gdi2, GDI, glcn, GLGB2, GMPP3, gnb2l, gnbpa, GNL2, grc5, GRWD1, GSS, Gtub, H2A, H2B, h3, h4, HDDC2, HGO, HM13, hmt1, HSP70C, hsp70mt, HSP90, HYOU1, if2b, if2g, if2p, if6, IFT46, IFT57, IFT88, IMB1, IMP4, ino1, IP5PD, IPO4, IPO5, KARS, KDELR2, l10a, l12e-D, LRRC48, mat, mcm-A, mcm-B, mcm-C, mcm-D, mcm-E, metap2, METTL1, MLST8, MMAA-mito, mra1, MTHFR, MTLPD2, MYG1, NAA15, NAE1, NAPA, ndf1, NDUFV2-mito, NFS1-mito, NMD3, NMT1, NOP5A, NSA2, nsf1-C, nsf1-E, nsf1-G, nsf1-H, nsf1-I, nsf1-J, nsf1-K, nsf1-L, nsf1-M, nsf2-A, nsf2-F, ODB2, ODBA, ODBB, ODO2A, ODPA2, ODPB, oplah, orf2, osgep, PABPC4, pace2-A, pace2B, Pace2C, pace5, PCY2, PELO, PGM2, PIK3C3, PLS3, PMM2, PMPCB, PPP2R3, PPP2R5C, PPX2, PR19A, PSD11, PSD7, psma-A, psma-B, psma-C, psma-E, psma-F, psma-G, psma-H, psma-J, psmb-K, psmb-L, psmb-M, psmb-N, PSMD12, PSMD6, psmd, PURA, PYGB, rac, rad23, Rad51A, ran, RBX1, rf1, rla2a, rla2b, RPAC1, RPF1, rpl11, rpl12, Rpl13A, Rpl13e, Rpl14e, Rpl15, rpl17, Rpl18, rpl19, rpl20, rpl21, RPL24A, rpl26, rpl27, Rpl2, rpl30, rpl31, rpl32, rpl33, rpl35, Rpl3, rpl43, rpl44, Rpl4b, Rpl5, rpl6, Rpl7a, rpl9, RPN1B, rpo-A, rpo-B, rpo-C, RPPK, rppO, rps10, rps11, rps12, rps14, rps15, rps16, rps17, rps18, rps20, rps23, rps26, rps27, rps2, rps3, rps4, rps5, rps6, rps8, RPTOR, RRAGD, RRM1, s15a, s15p, sap40, SCO1-mito, SCSB, SEC23, SF3B2, SND1, SPTLC1, sra, srp54, STXBP1, suca, SYGM1, SYNJ, tfiid, TM9SF1, TMS, topo1, trs, UBA3, ubc, UBE12, UBE2J2, Ubq, VAPA, VARS, vata, vatb, vatc, vate, VBP1, VPS18, VPS26B, WBSCR22, WD66, wd, wrs, xpb, YKT6. This tree was used as a guide to infer the final phylogeny under the LG+PMSF(C60)+F+Γ model[73] of evolution; this is in line with the results of ModelFinder,[89] which determined from 144 protein models LG+F+I+G4 as best-fit model according to Bayesian Information Criterion. Bootstrap analysis was conducted with 100 nonparametric bootstrap replicates using this model.

Ancestral character state reconstruction

Ancestral character state reconstruction was performed with Phytools (Revell[72]), which implements Yang's[74] re-rooting method to infer marginal ancestral state estimates for the internal nodes in the tree (Figure 3). We performed two independent analyses assuming 2-, and 4-character states in order to understand the effect of character coding on the inferred ancestral character states. The 2-state model used (1) unicellular and (2) multicellular *sensu lato* (filamentous or multicellular); the 4-state model differentiated between (2) *bona fide* filamentous algae excluding desmids, (3) chain-like filamentous desmids, and (4) multicellular *sensu stricto* (embryophytes, Coleochaetophyceae, Charophyceae, *Volvox, Ulva*). All models assumed unordered states (equal rates of change).

QUANTIFICATION AND STATISTICAL ANALYSIS

For the quantification of the average diameter of macrotubules, 446 sections of macrotubules were examined with the LEO 906E transmission electron microscope (LEO, Oberkochen, Germany) and imaged with a MultiScan Typ 794 CCD camera; all 446 counts of the diameter were obtained with the Digital Micrograph 3.4.4 software (both Gatan Inc., Pleasanton, USA).

After inspection of single-protein phylogenies estimated with IQ-TREE v1.5.5 under the LG4X to remove contaminants and paralogs, the data set was refined: orthologs that were missing in over 50% of taxa were removed; that said, we retained all orthologs that were present in *Mougeotiopsis* (overwriting the 50% filtering). The final phylogeny was inferred under the LG+PMSF(C60)+F+Γ model[73] of evolution; this is in line with the results of ModelFinder,[89] which determined from 144 protein models LG+F+I+G4 as best-fit model according to Bayesian Information Criterion. Bootstrap analysis was conducted with 100 nonparametric bootstrap replicates using this model; approximate likelihood ratio test (SH-aLRT) was carried out with 1000 replicates and additionally approximate Bayes (aBayes) test was carried out.

For the Approximately Unbiased test of the phylogenetic tree, we compared our phylogenomic hypothesis with that previously proposed by the One Thousand Plant Transcriptomes Initiative[6] (main ASTRAL tree in Figure 2 based on 410 loci), which differed with ours in the relative position of a few species within Desmidiales. We performed an Approximately Unbiased test (AU test)[90] under best-fit LG+C60+F+Γ model with 10,000 multiscale bootstrap replicates using IQ-TREE v.1.6.12.

Supplemental Information

A phylogenomically informed five-order

system for the closest relatives of land plants

Sebastian Hess, Shelby K. Williams, Anna Busch, Iker Irisarri, Charles F. Delwiche, Sophie de Vries, Tatyana Darienko, Andrew J. Roger, John M. Archibald, Henrik Buschmann, Klaus von Schwartzenberg, and Jan de Vries
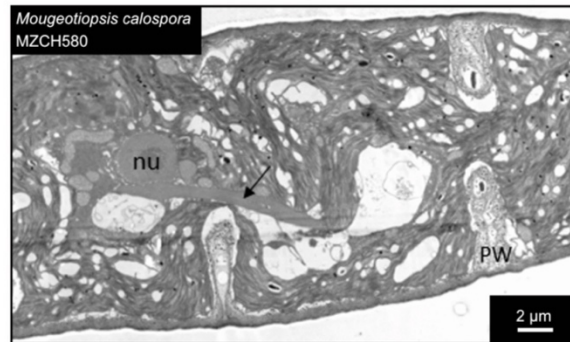
Figure S1: Macrotubule formation as detected in TEM sections of *Mougeotiopsis calospora* cells with incomplete cytokinesis, related to Figure 1. Overview showing three cells with incomplete cytokinesis and partial cross walls. Arrow indicates bundle of macrotubules.
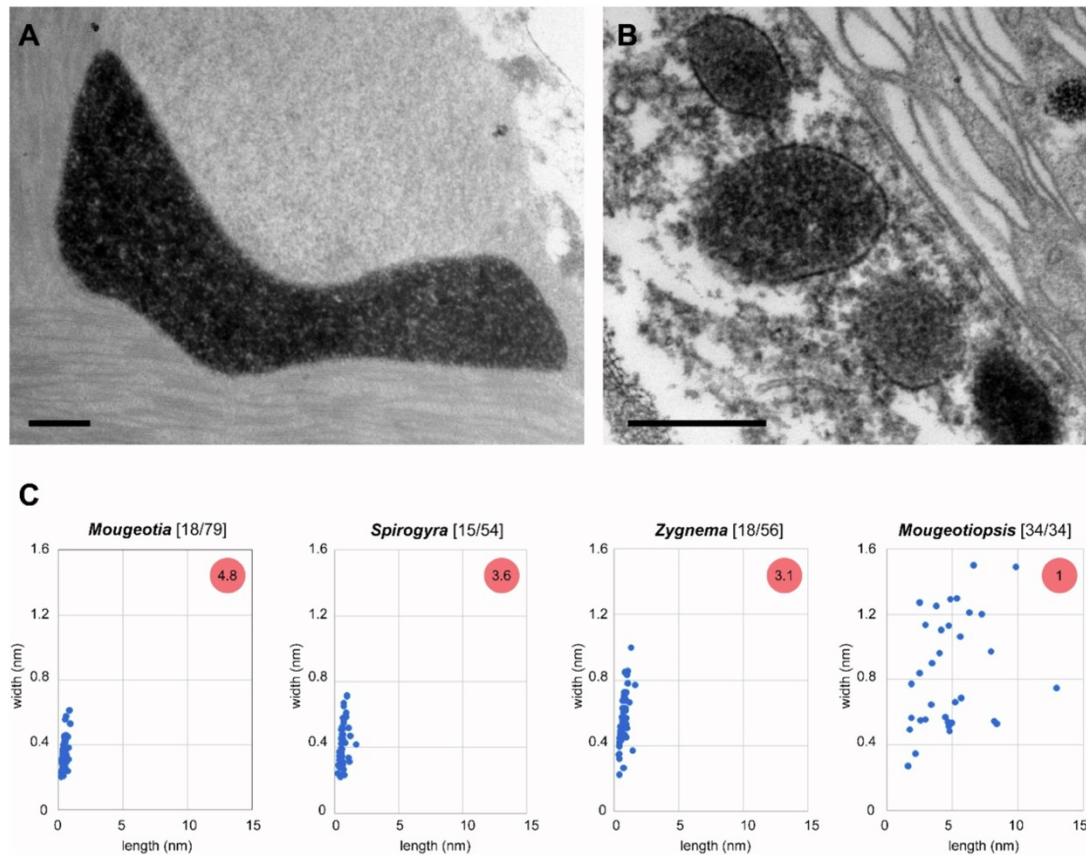
Figure S2: Peroxisomes of filamentous zygnematophytes, related to Figure 1. A: Transmission electron micrograph of a DAB-stained peroxisome of *Mougeotiopsis calospora*, strain MZCH580. **B:** Transmission electron micrograph of DAB-stained peroxisomes of *Mougeotia* sp., strain MZCH240. **C:** Sizes of peroxisome sections of four filamentous zygnematophytes as measured in transmission electron micrographs. The number of analysed cells/peroxisomes are shown in square brackets, and the average number of peroxisome cross sections per cell in the red circles. Scale bars, 0.5 µm.
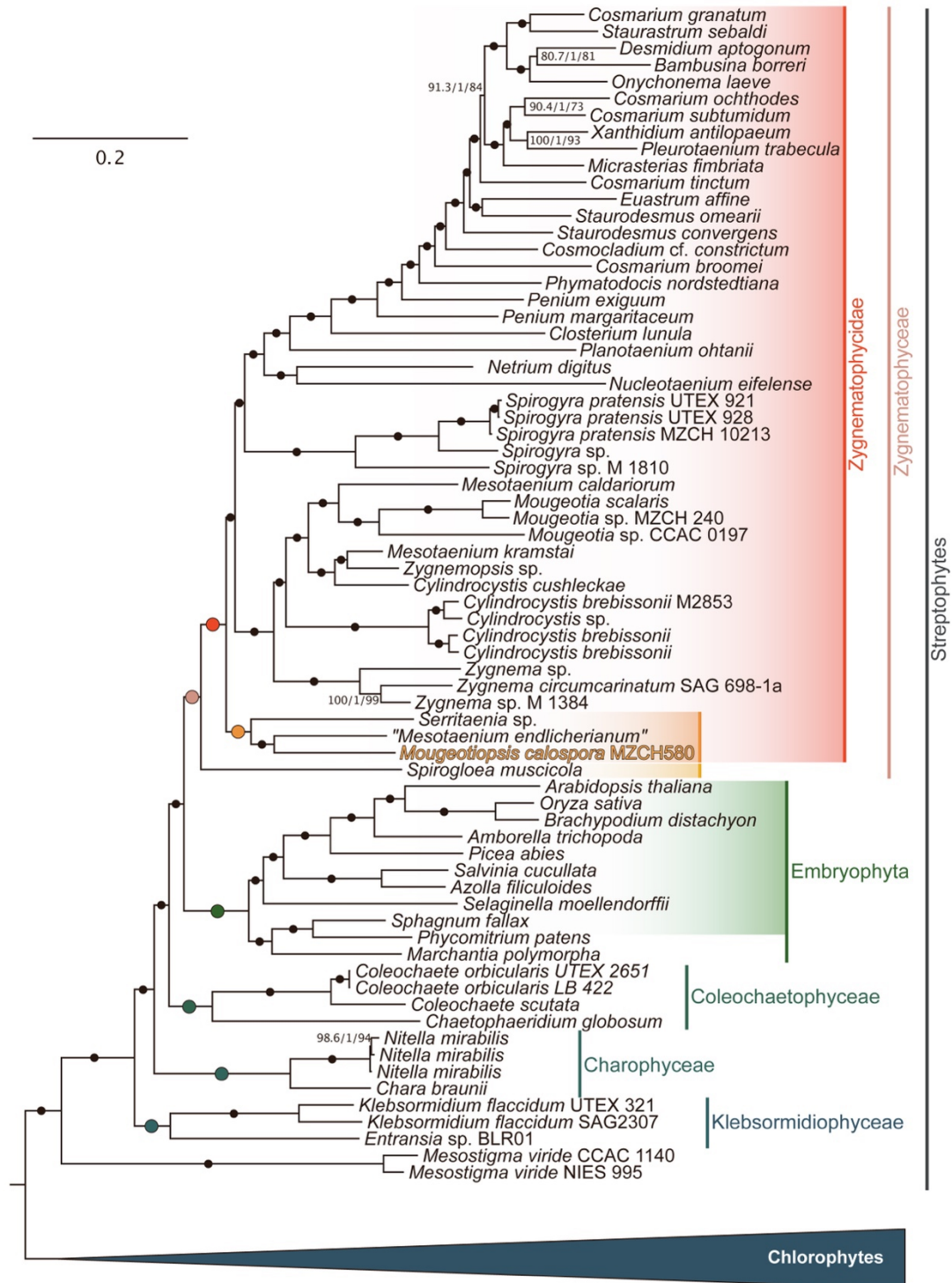
Figure S3: Multigene phylogeny of 84 Viridiplantae, related to Figure 2. Phylogenomic tree that shows the relationship of all streptophyte species analysed; the tree was rooted with the clade of chlorophytes. Scale bar, 0.2 substitutions per site. Support values from three analyses (SH-aLRT/aBayes/nonparametric bootstrapping) are shown at the corresponding branches, except for branches with maximum support (marked by dots); colored dots correspond to the (full) support recovered for the higher-order clades labeled on the right.
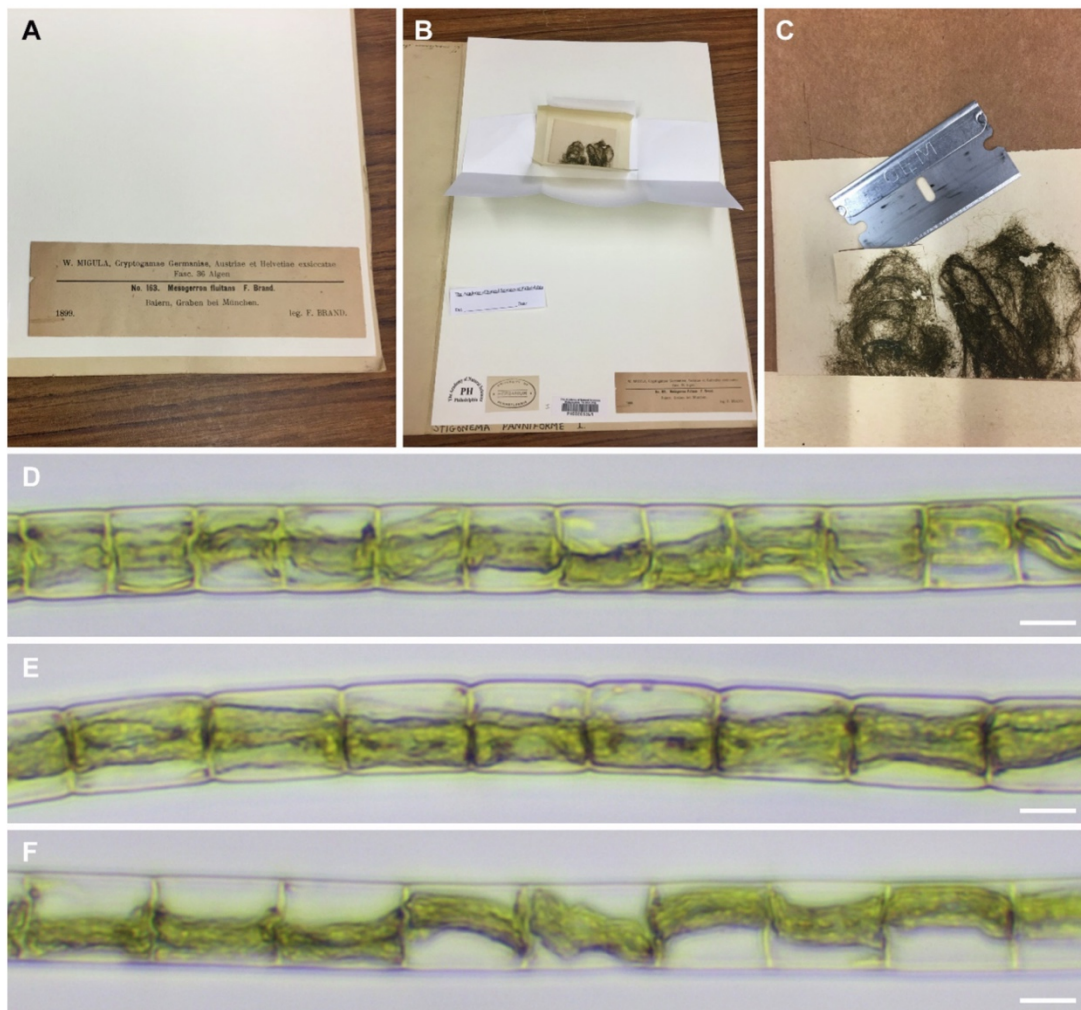
Figure S4: Destructive sampling of *Mesogerron fluitans* collected by Brand and morphological characteristics of the material, related to Figure 1. A and B: Specimen in the Herbarium of the Academy of Natural Sciences of Philadelphia (PH). **C:** Removal of dried algal material. **D–F:** Rehydrated algal filaments of the sample. Note the varying cell length and the chloroplast morphology resembling that of strain MZCH580. Images in A–C: courtesy of Richard McCourt. Scale bars, 10 μm.

- Perspectives for understanding the diversity of saccoderm desmids

- Deciphering the molecular background of a new photoprotective strategy in zygnematophytes

- Biodiversity meets functional characterization: new avenues to explore

Summarizing discussion

Perspectives for understanding the diversity of saccoderm desmids

The Zygnematophyceae have received considerable attention due to their ubiquity in freshwater ecosystems, their interesting evolutionary position, and the beauty of the placoderm desmids (e.g Gerrath, 1993; Brook & Williamson, 2010; de Vries *et al.*, 2017, 2018, 2020). Yet, their internal relationships and their taxonomy have not been appropriately clarified. The delimitation of species within the zygnematophytes is challenging, and despite a long history of research, a stable taxonomic system of the major groups which reflects their phylogeny was lacking (Cheng et al., 2019; Gontcharov et al., 2004; Gontcharov & Melkonian, 2008, 2011; Hall et al., 2008). Numerous species concepts have been proposed to define species boundaries (e.g. biological, morphological, phylogenetic, ecological species concepts) (Novarino, 2012). However, when considered in isolation, each of these concepts has certain limitations, and the extent to which they can be applied to different organisms varies considerably (Guiry, 2012). For example, the biological species concept relies on reproductive isolation as a defining character. In microorganisms, however, not all groups mate and mating experiments are difficult to perform (Caron & Hu, 2019; Schlegel & Meisterfeld, 2003). Hence, the biological species concept alone cannot be applied to many microorganisms.

In this thesis, an integrative taxonomic approach was used to delimit taxonomic units within the Zygnematophyceae. Integrative taxonomy is a method of species delimitation that combines a variety of data, including molecular, phenotypic, behavioral and ecological data, in order to provide a comprehensive understanding of the diversity within a given group (Cicero et al., 2021). In this thesis, a combination of molecular, phenotypic and ecological data was used. Phylogenetic inferences were based on *rbc*L and 18S rRNA gene sequences. In the Zygnematophyceae, the 18S rRNA gene turned out to be too conserved to draw evolutionary conclusions at the genus and species level. The rbcL gene-based phylogenies, in contrast, resolved genus-level clades well and can differentiate intra-genus diversity. Furthermore, the *rbc*L gene is the most commonly used genetic marker for the Zygnematophyceae, resulting in the best possible coverage of different zygnematophyte taxa in molecular analyses (Busch & Hess, 2022b, 2022a). Nevertheless, based on the *rbc*L gene phylogenies, the distinction between species is not entirely clear in all genera. For example, certain strains of the genus *Serritaenia* showed marked differences in cell morphology besides identical *rbc*L gene sequences (Busch & Hess, 2022b). In the future, a detailed taxonomy of species (e.g. in the genus *Serritaenia*) could be based on more variable genetic markers, such as the internal transcribed spacers (ITS-1 and ITS-2) of the rRNA operon. This approach has been successfully employed in other streptophyte green algal groups (Mikhailyuk et al., 2008, 2018; Remias et al., 2023).

The phylogenetic analyses were combined with morphological studies based on axenic cultures. The comparability of the morphological studies was ensured by well-defined culture conditions (e.g. light regime, nutrient composition of the culture medium, and temperature), which turned out to be very important due to phenotypic plasticity within the Zygnematophyceae. Based on my own observations in the saccoderm desmids, phenotypic plasticity can relate to chloroplast morphology, growth form and

the presence of colored specialized compounds (Busch & Hess, 2022b). Furthermore, in certain placoderm desmids (e.g. *Micrasterias*, *Staurastrum*) the cell shape and size was shown to change in relation to the pH and temperature (Černá & Neustupa, 2010; Neustupa & Woodard, 2024). The selected methodology led to the identification of taxonomically valuable characters, which are suited to distinguish several of the twelve lineages of *Mesotaenium*-like algae. These morphological characteristics include the cell shape, chloroplast shape and number during interphase, pyrenoid shape as well as nucleus position (Busch & Hess, 2022a). Moreover, the cell width turned out to be a valuable character to distinguish between genotypes (possible species) of a given lineage of saccoderm desmids, as for example shown in the genera *Serritaenia* (Busch & Hess, 2022b), *Ancylonema* (Chapter IV: Busch et al., under review), and *Cylindrocystis* (Barcytė et al., 2020). Moreover, the full vegetative life history (incl. cell division) and zygospore development was studied with time-lapse microscopy. The full reconstruction of the vegetative life history allowed an optimal evaluation of cell morphological characters, since chloroplast number and shape as well as the cell length vary during the different life history stages (Chapter IV: Busch et al., under review). In addition, the morphology of the zygospore is valuable for the identification of species in the Zygnematophyceae. The zygospores of the different zygnematophyte taxa exhibit considerable variation in morphology, and have been used traditionally to differentiate species of placoderm desmids and filamentous zygnematophytes (Brook, 1981; Brook & Williamson, 2010; Permann et al., 2021; Takano et al., 2019). However, conjugation and zygospore formation cannot be always observed in natural material. In the laboratory, these processes have been successfully induced in a few cases, e.g. *Spirogyra* species (El-Sheekh et al., 2017), *Closterium peracerosum-strigosum-littorale* complex (Tsuchikane et al., 2012), and *Mesotaenium kramstai* (Tiflickjian & Raybum, 1986). The successful induction of conjugation in *A. palustre* by nutrient limitation now encourages to test other new zygnematophyte strains as well. If successful, this can add another layer of taxonomically valuable information for the future delimitation of saccoderm desmids. With respect to the ecological versatility of the group, an ecological characterization should be part of an integrative approach as well. The optimal growth temperature as well as photophysiological parameters varies between strains, and is certainly related to their evolution and natural distribution. Members of the genus *Ancylonema* for example show clear differences in growth temperature as well photosynthetic capacity (Chapter IV: Busch et al., under review). Extended information on the ecophysiology of the described species might help us to understand the remarkable pseudo-cryptic diversity observed within certain genera (e.g. *Serritaenia*) and the ecological niches these algae occupy.

While standard genetic markers such as the *rbc*L gene are well suited to resolve recent evolutionary splits, the deep nodes of the zygnematophycean phylogeny cannot be resolved (Busch & Hess, 2022a; Gontcharov et al., 2004). However, this is important to understand the evolution of characters within the group. The zygnematophytes comprise filamentous forms, rather simple rod-shaped cells as well as the symmetric placoderm desmids (Busch & Hess, 2022a). Placoderm desmids, for example, exhibit a diversity of cell wall ornamentations (spines, pores, warts), whose biological

functions are so far unknown (Kouwets, 2008). Furthermore, it was unknown how the filamentous forms (e.g. *Spirogyra*, *Mougeotia*, *Zygnema*) are related to each other and how the trait of simple multicellularity arose during evolution (Cheng et al., 2019; Gontcharov, 2008; Gontcharov et al., 2004; Hall et al., 2008). A modern approach to resolve such questions is phylogenomics. In a collaborative approach, we inferred a multigene phylogeny of the Zygnematophyceae with 326 nuclear loci. Based on this well-supported phylogenomic tree, we could resolve the major zygnematophycean groups very well, and established a new five-order system of the Zygnematophyceae. Furthermore, the phylogenomic tree revealed that filamentous growth evolved at least five times independently within the zygnematophytes (Hess et al., 2022). However, the tree only captured a fraction of the existent zygnematophyte diversity and many of the saccoderm desmids studied in this thesis were not available at the time. In fact, my single gene trees reveal a much greater diversity of these morphologically plain zygnematophytes, which is currently not reflected in multigene phylogenies and higher-level systematics (Busch & Hess, 2022a). In the future, I aim to include these lineages in new phylogenomic studies and to further develop the taxonomy of zygnematophytes, in particular of the polyphyletic genera *Mesotaenium* and *Cylindrocystis*.

Deciphering the molecular background of a new photoprotective strategy in zygnematophytes

Although many members of the Zygnematophyceae live in high-light habitats, not much is known about their photoprotective mechanisms (Fucikova et al., 2008; Pichrtová et al., 2016; Remias, Holzinger, et al., 2012). Given that these algae are the closest relatives of land plants, it is reasonable to assume that their adaptive strategies are similar to those of plants (Cheng et al., 2019; de Vries et al., 2017, 2018; De Vries & Archibald, 2018). Many plants synthesize specialized compounds of the flavonoid family in response to various abiotic stressors, including UVB radiation (Ferreyra et al., 2021). For example, the well-known anthocyanins, water-soluble compounds of red to blue color that accumulate in vacuoles, originate from the flavonoid biosynthetic pathway (Barceló et al., 1994; Davies et al., 2022). Furthermore, auronidins and sphagnorubins, which derive from the same pathway, are known from bryophytes of sun-exposed habitats. These reddish to violet pigments accumulate in the plant cell wall (Berland et al., 2019; Davies et al., 2022; Rudolph et al., 1981; Rudolph & Vowinkel, 1969). Earlier studies already indicated that the prominent secondary pigments of some zygnematophytes differ markedly from those of land plants. In members of the two genera *Ancylonema* and *Zygogonium,* the intracellular, reddish compounds were identified as purpurogallin derivatives and gallic acid polymers, respectively (Newsome & van Breemen, 2012; Remias et al., 2012). These compounds are thought to originate directly from the shikimate biosynthetic pathway, and, hence, stem from a metabolic route different to those of the mentioned plant sunscreens.

In this thesis, I studied a group of saccoderm desmids which exhibit an unusual pigmentation of their extracellular mucilage. This phenomenon was documented more than 150 years ago in a species named *Mesotaenium braunii* (de Bary, 1858), and more recently in *Mesotaenium testaceovaginatum* (Fucikova et al., 2008) - both now belong to the new genus *Serritaenia* introduced during my doctoral studies (Busch & Hess, 2022b). However, the formation and ecological function of the extracellular pigments in these algae remained unknown. In my work, I established axenic cultures and developed an experimental setup to trigger the pigment biosynthesis in the laboratory. This was the basis for providing the evidence that the extracellular pigments have a sunscreen function, and for identifying some relevant molecular components through comparative transcriptomics (Busch et al., 2024; Busch & Hess, 2022b). To qualify as a microbial ultraviolet sunscreen, a compound has to meet certain criteria: 1) The compound must exhibit a high absorption coefficient in the UV range. 2) The natural concentration of the compound must be sufficient to cause a significant reduction in the UV dose received. 3) The compound should be produced specifically during sensitive life cycle stages and/or in response to UV exposure. 4) The compound should be deposited in a conformation that is optimal for screening (e.g. in tegumentary layers) (Gao & Garcia-Pichel, 2011). The pigmented mucilage of *Serritaenia* fulfills all of the aforementioned criteria and has been demonstrated to block up to 60% of the incident UVB radiation, which compares to the estimated UVB screening factors of cyanobacterial mycosporine-like amino acids (Busch & Hess, 2022b; Garcia-Pichel & Castenholz, 1993). Overall, the "sunscreen mucilage" of *Serritaenia* clearly represents a photoprotective strategy, which is unique among the known zygnematophytes – maybe even among all green algae.

The closest analogies of *Serritaenia*'s sunscreen mucilage can be found in the world of prokaryotes (**Fig. 4**). Cyanobacteria accumulate photoprotective pigments in their gelatinous sheaths or capsules. Two compounds have been identified, namely scytonemin (e.g. in *Scytonema* species; yellow color) (Garcia-Pichel & Castenholz, 1991; Proteau et al., 1993) and gloeocapsin (e.g. in *Gloeocapsa* species; red color) (Storme et al., 2015). The synthesis of scytonemin begins in the cytoplasm, later reactions likely occur in the periplasm (cyanobacteria are gram-negative), yielding scytonemin, which then accumulates in the extracellular sheath (Gao & Garcia-Pichel, 2011; Soule et al., 2009). However, as shown in this thesis, the compounds in the sunscreen mucilage of prokaryotic and eukaryotic algae are different. While scytonemin absorbs light with a maximum in the UVA waveband (Garcia-Pichel & Castenholz, 1991), *Serritaenia*'s sunscreen mucilage has its
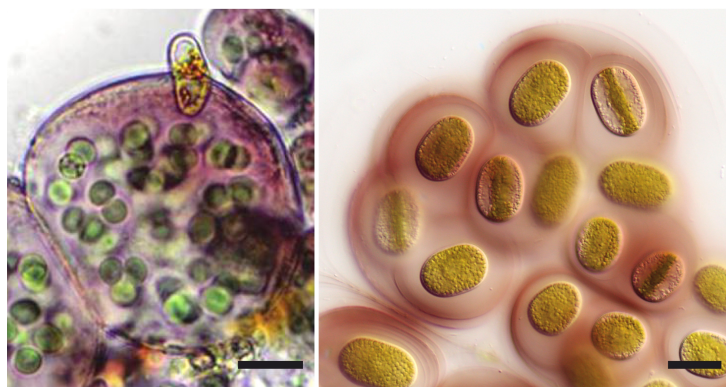

Fig. 4: *Gloeocapsa* sp. (left) and *Serritaenia* sp. (right) with pigmented extracellular mucilage; from Storme et al., 2015 and Busch & Hess, 2022a, modified. Scale bars 10 µm (left) and 20 µm (right). Left: The publisher for this copyrighted material is Mary Ann Liebert, Inc. publishers.

absorbance maximum in the UVB waveband (Busch & Hess, 2022b). Furthermore, the cyanobacterial sheath pigments can be readily extracted with methanol/ethyl acetate mixtures or acetone (Garcia-Pichel & Castenholz, 1991). In contrast, *Serritaenia*'s sunscreen pigment is resistant to a variety of solvents as well as harsh acid hydrolysis, and so far, was not accessible to standard chemical analyses such as chromatographic methods coupled with mass spectrometry (Busch & Hess, 2022b). Given all these differences and the considerable evolutionary divergence between *Serritaenia* and Cyanobacteria, it is unlikely that the pigmentation observed in *Serritaenia* corresponds to that of cyanobacteria. It is likely to be a sunscreen compound new to science.

In order to approach the question of its chemical nature from a different perspective, I have explored the metabolic pathways that are induced during the synthesis of *Serritaenia*'s sunscreen mucilage with comparative transcriptomics. For most general cellular processes, including the perception of UV radiation, I identified clear homologues from land plant model systems. The finding of a relatively complete and conserved UVR8 receptor system, which senses UVB radiation in higher plants, was very interesting (Busch et al., 2024). This suggests that the perception systems for ubiquitous terrestrial stressors are likely old and conserved in the green lineage (Tilbrook et al., 2016; Zhang et al., 2022). In contrast, the specialized metabolite pathways of *Serritaenia* diverged notably from those of plant model systems. While the enzyme repertoire of the shikimate pathway was complete, the phenylpropanoid biosynthesis was only fragmentarily recovered, and the flavonoid biosynthesis pathways (including anthocyanin biosynthesis) seemed not functional in *Serritaenia* (Busch et al., 2024). However, there are reports of phenolic compounds and flavonoids, detected by mass spectrometry, in members of the Zygnematophyceae (Holzinger et al., 2018; Jiao et al., 2020). Furthermore, phenolic polymers, that were referred to as "lignin-like substances", have been detected in other streptophyte green algae, namely *Coleochaete* and *Nitella* (Delwiche et al., 1989; Ligrone et al., 2008). As the known biosynthetic pathways for polyphenols and flavonoids are fragmentary in zygnematophytes, the presence of such substances may be explained by novel enzymes that currently cannot be annotated, cryptic activities of known enzymes, or alternative biosynthetic routes that are yet to be explored.

Despite these knowledge gaps, *Serritaenia*'s response to UV radiation points to the regulation of enzymes, which are part of the plant phenylpropanoid pathway. In addition, the data revealed some enzymes with exciting functionalities, which are highly upregulated under UV exposure. This includes extracellular oxidative enzymes, such as a class III peroxidase and multicopper oxidases, as well as ABCG transporters (Busch et al., 2024). In plants, ABCG transporters were shown to transport phenolics across the plasma membrane (Alejandro et al., 2012; Takeuchi et al., 2018). Class III peroxidases and multicopper oxidases subsequently facilitate the polymerization of such phenolic moieties, resulting in the formation of phenolic polymers within the apoplast (McCaig et al., 2005; Ostergaard et al., 2000; Sakharov et al., 2001). Altogether the results gained with comparative transcriptomics point to a

polyphenolic nature of *Serritaenia*'s sunscreen pigment, whose synthesis might be extracellular and oxidative.

This hypothesis aligns very well with the observations made during the attempts to purify *Serritaenia*'s sunscreen pigment. The precipitation under acidic conditions and the destruction under strong alkaline treatment are typical for other, well-known phenolic polymers (Butler & Day, 1998; de Ascensao & Dubery, 2003; García et al., 2009). In fact, phenolic polymers are common in phylogenetically diverse organisms, where they have various biological functions. For example, lignins are a class of phenolic polymers of vascular plants (tracheophytes) with the main building blocks: coniferyl alcohol, sinapyl alcohol, and p-coumaryl alcohol. Lignins are formed by monolignol polymerization via free radical coupling in the plant cell wall, where they enhance the hydrophobic properties and rigidity (Vanholme et al., 2019). Melanins constitute another group of polyphenols, which are well-known as sunscreens in animals (incl. humans). These brown to black pigments have been found in members from various higher-level taxa in the prokaryotes and eukaryotes (Plonka & Grabacka, 2006). In fungi, melanins are localized in the cell wall and supply protection against high radiation, drought and extreme temperatures (Butler & Day, 1998). However, the defined composition of lignins, which are primarily composed of the three aforementioned monolignols, and the black to brown color of melanins (independent of the pH value) make it unlikely that the sunscreen pigment of *Serritaenia* belongs to one of these organic compounds. In the future, the sequence data generated (transcriptomics) will be complemented by analytical data (metabolomics) in order to decipher the precursor molecules and monomers from which the sunscreen is made. In addition, mass spectrometry imaging (MSI) may offer a potential solution to circumvent the purification hurdle. The technique could be used to identify specialized compounds and proteins enriched in the pigmented mucilage of *Serritaenia*.

The present studies have paved the way for a detailed characterization of interesting proteins in *Serritaenia*, whose plant homologues have important functions in the transport and synthesis of specialized compounds. So far, the function of these proteins in the Zygnematophyceae remained completely unknown. In the future, interesting protein candidates identified in the *Serritaenia* transcriptome can be expressed in heterologous expression systems, e.g. in the yeast *Pichia pastoris*. The class III peroxidase and multicopperoxidases of *Serritaenia*, for example, could be tested for their activity on phenolic compounds. Vesicles from yeast expressing *Serriatenia*'s ATP-binding cassette transporters, could be isolated and tested for their transport activity on different compounds (as done for the monolignol transporter AtABCG29 from *A. thaliana*). Another approach is to use plant knockout mutants for rescue experiments. Here, homologs identified in *Serritaenia* (e.g. the ABCG transporters) can be tested for phenotype rescue in corresponding knockout lines, e.g. the AtABCG29 knockout mutant in *A. thaliana* (Alejandro et al., 2012). By establishing the actual activities of *Serritaenia*'s extracellular oxidative enzymes and ATP-binding cassette transporters, we will be able to further

uncover the cellular processes that protect Zygnematophytes in high-light habitats. Overall, such studies will broaden our view, which was long focused on model plants.

Biodiversity meets functional characterization: new avenues to explore

Over the last decade, genomes and transcriptomes have become increasingly available from a wide range of organisms, including over 200 assembled algal genomes. (Hanschen & Starkenburg, 2020). The application of "omics"-techniques (i.e. genomics and transcriptomics) find wide applications in different biological disciplines. This includes cell biology, ranging from physiology and metabolism to development and life cycles to questions of evolutionary biology (Anderson, 2022). The application of phylogenomics, for instance, contributes to the understanding of evolutionary trends and significant evolutionary processes, including terrestrialization, primary endosymbiosis events, and the origin of eukaryotic life on earth (Burki et al., 2020; De Vries & Archibald, 2018; Eme et al., 2011; Irisarri et al., 2022). Another powerful tool is the application of comparative transcriptomics to get a global snapshot of expressed genes under defined conditions in an organism. Most importantly, *de novo* transcriptome assemblies offer the potential to study cellular behavior on a molecular scale in non-model organisms, which lack genome data and an established transformation system. This approach enables the transfer of knowledge from reference organisms to less well-characterized systems (Blaby-Haas & Merchant, 2019; Cordoba et al., 2021; Geng et al., 2021). The method, however, also has its limitations as functional annotations rely heavily on the available data from model organisms in the databases. In *S. testaceovaginata*, for example, 20 of the 50 most upregulated genes could not be functionally annotated using the NCBI RefSeq database (National Library of Medicine reference sequences database) (Busch et al. 2024). Whole genome assemblies of other algal groups contain a similarly high proportion of genes that cannot be functionally annotated. For instance, over 30% of the predicted proteins in the genome of the streptophyte green alga *Klebsormidium nitens* lacked a Pfam domain and could not be assigned to any of the nearly 1.2 million orthologous groups defined in the EggNOG database (Blaby-Haas & Merchant, 2019). This illustrates the extent of the genes and functional capabilities of non-model organisms that remain to be discovered.

Streptophyte green algae are poorly characterized on the genetic level. The majority of protein functional annotations are derived from sequence similarity searches against one or more databases. In contrast, in *A. thaliana*, the most extensively studied photosynthetic eukaryote, 30% of functional annotations are associated with experimental evidence (Blaby-Haas & Merchant, 2019; Hanschen & Starkenburg, 2020). Due to the relatively close relationship of zygnematophytes and land plants, most predicted proteins in *Serritaenia* were functionally annotated with potential homologs from the model plant *A. thaliana*. However, these annotations must be interpreted with caution. Although the Zygnematophyceae are the sister clade of land plants, it is important to note that there is still a significant evolutionary distance between these algae and the well-studied flowering plants. Hence, predicted

homologs do not necessarily have the same function. To further evaluate a putative homology of certain proteins and their function, protein phylogenetics are a powerful tool. This also applies to the *in silico* analysis of protein domains and protein structure predictions (Busch et al., 2024). However, the available bioinformatic tools for functional annotation cannot fully replace wet-lab studies on proteins. In the future, it will be necessary to conduct experimental research on enzymes and molecular factors of underrepresented organisms. This will help us to make much more accurate functional predictions on the basis of genetic data.

Biodiversity exploration and functional studies on the cellular level have long been separate disciplines in biology. My doctoral study on a poorly-known subgroup of zygnematophyte algae combines both. It illustrates how this combination leads to an understanding of the cellular functions and ecology of a group of organisms, and provides evolutionary insights as well. In this approach, genomes and transcriptomes are valuable resources as they provide a window into the functional potential of non-model organisms. Especially protist research profits enormously from "omics"-techniques. We now gain a much deeper understanding of the molecular basis of biological phenomena – from the cellular to ecosystem level (Anderson, 2022). In the future, the combination of biodiversity and functional research will extend the databases with phylogenetically diverse datasets. Furthermore, the *in vitro* characterization of non-model factors will likely reveal novel metabolic routes, and deepen our understanding of speciation and ecosystem functioning.

Additional references

(for Introduction and Summarizing discussion)

Aigner, S., Remias, D., Karsten, U., & Holzinger, A. (2013). Unusual phenolic compounds contribute to ecophysiological performance in the purple-colored green alga *Zygogonium ericetorum* (Zygnematophyceae, Streptophyta) from a high-alpine habitat. *Journal of Phycology*, *49*(4), 648-660.

Alejandro, S., Lee, Y., Tohge, T., Sudre, D., Osorio, S., Park, J., Bovet, L., Lee, Y., Geldner, N., Fernie, A. R., & Martinoia, E. (2012). AtABCG29 Is a monolignol transporter involved in lignin biosynthesis. *Current Biology*, *22*(13), 1207–1212.

Anderson, O. R. (2022). Recent advances in application of transcriptomics: Research on heterotrophic and autotrophic protists. *Acta Protozoologica*, *61*.

Ashley, J., Rushforth, S. R., & Johansen, J. R. (1985). Soil algae of cryptogamic crusts from the Uintah Basin, Utah, USA. *The Great Basin Naturalist*, 432–442.

Barceló, A. R., Calderón, A. A., Zapata, J. M., & Muñoz, R. (1994). The histochemical localization of anthocyanins in seeded and seedless grapes (*Vitis vinifera*). *Scientia Horticulturae*, *57*(3), 265–268.

Barcytė, D., Pilátová, J., Mojzeš, P., & Nedbalová, L. (2020). The arctic *Cylindrocystis* (Zygnematophyceae, Streptophyta) green algae are genetically and morphologically diverse and exhibit effective accumulation of polyphosphate. *Journal of Phycology*, *56*(1), 217-232.

Baumann, K., Jung, P., Samolov, E., Lehnert, L. W., Büdel, B., Karsten, U., Bendix, J., Achilles, S., Schermer, M., Matus, F., Oses, R., Osses, P., Morshedizad, M., Oehlschläger, C., Hu, Y., Klysubun, W., & Leinweber, P. (2018). Biological soil crusts along a climatic gradient in Chile: Richness and imprints of phototrophic microorganisms in phosphorus biogeochemical cycling. *Soil Biology and Biochemistry*, *127*, 286–300.

Becker, B., & Marin, B. (2009). Streptophyte algae and the origin of embryophytes. *Annals of Botany*, *103*(7), 999–1004.

Benton, M. J., Wilf, P., & Sauquet, H. (2022). The angiosperm terrestrial revolution and the origins of modern biodiversity. *New Phytologist*, *233*(5), 2017–2035.

Berland, H., Albert, N. W., Stavland, A., Jordheim, M., McGhie, T. K., Zhou, Y., Zhang, H., Deroles, S. C., Schwinn, K. E., Jordan, B. R., Davies, K. M., & Andersen, Ø. M. (2019). Auronidins are a previously unreported class of flavonoid pigments that challenges when anthocyanin biosynthesis evolved in plants. *Proceedings of the National Academy of Sciences*, *116*(40), 20232–20239.

Besendahl, A., & Bhattacharya, D. (1999). Evolutionary analyses of small-subunit rDNA coding regions and the 1506 group I introns of the Zygnematales (Charophyceae, Streptophyta). *Journal of Phycology*, *35*(3), 560–569.

Bhattacharya, D., & Medlin, L. (1998). Algal phylogeny and the origin of land plants. *Plant Physiology*, *116*(1), 9–15.

Bhattacharya, D., & Medlin, L. (1995). The phylogeny of plastids: A review based on comparisons of small-subunit ribosomal RNA coding regions. *Journal of Phycology*, *31*(4), 489–498.

Bidigare, R. R., Ondrusek, M. E., Kennicutt, M. C., Iturriaga, R., Harvey, H. R., Hoham, R. W., & Macko, S. A. (1993). Evidence a photoprotective for secondary carotenoids of snow algae. *Journal of Phycology*, *29*(4), Article 4.

Bierenbroodspot, M. J., Darienko, T., de Vries, S., Fürst-Jansen, J. M. R., Buschmann, H., Pröschold, T., Irisarri, I., & de Vries, J. (2024). Phylogenomic insights into the first multicellular streptophyte. *Current Biology*, *34*(3), 670-681.e7.

Blaby-Haas, C. E., & Merchant, S. S. (2019). Comparative and Functional Algal Genomics. *Annual Review of Plant Biology*, *70*, 605–638.

Broady, P. A. (1979). Qualitative and quantitative observations on green and yellow-green algae in some English soils. *British Phycological Journal*, *14*(2), 151–160.

Brook, A. J. (1981). *The biology of desmids* (Vol. 16). University of California Press.

Brook, A. J., & Williamson, D. B. (2010). A monograph on some British desmids. *The Ray Society. London: UK*, 364.

Büdel, B., Dulić, T., Darienko, T., Rybalka, N., & Friedl, T. (2016). Cyanobacteria and algae of biological soil crusts. In B. Weber, B. Büdel, & J. Belnap (Eds.), *Biological Soil Crusts: An Organizing Principle in Drylands* (Vol. 226, pp. 55–80). Springer International Publishing.

Burki, F., Roger, A. J., Brown, M. W., & Simpson, A. G. B. (2020). The new tree of eukaryotes. *Trends in Ecology & Evolution*, *35*(1), 43–55.

Busch, A., Gerbracht, J. V., Davies, K., Hoecker, U., & Hess, S. (2024). Comparative transcriptomics elucidates the cellular responses of an aeroterrestrial zygnematophyte to UV radiation. *Journal of Experimental Botany*, erae131.

Busch, A., & Hess, S. (2022a). A diverse group of underappreciated zygnematophytes deserves in-depth exploration. *Applied Phycology*, *3*(1), 206-323

Busch, A., & Hess, S. (2022b). Sunscreen mucilage: A photoprotective adaptation found in terrestrial green algae (Zygnematophyceae). *European Journal of Phycology*, *57*(1), 107–124.

Butler, M. J., & Day, A. W. (1998). Fungal melanins: A review. *Canadian Journal of Microbiology*, *44*(12), 1115–1136.

Caron, D. A., & Hu, S. K. (2019). Are we overestimating protistan diversity in nature? *Trends in Microbiology*, *27*(3), 197–205.

Cavalier-Smith, T. (2000). Membrane heredity and early chloroplast evolution. *Trends in Plant Science*, *5*(4), 174–182.

Černá, K., & Neustupa, J. (2010). The pH-related morphological variations of two acidophilic species of Desmidiales (Viridiplantae) isolated from a lowland peat bog, Czech Republic. *Aquatic Ecology*, *44*(2), 409-419.

Cheng, S., Xian, W., Fu, Y., Marin, B., Keller, J., Wu, T., Sun, W., Li, X., Xu, Y., & Zhang, Y. (2019). Genomes of subaerial Zygnematophyceae provide insights into land plant evolution. *Cell*, *179*(5), 1057-1067.

Chia, M. A., Chimdirim, P. K., & Japhet, W. S. (2015). Lead induced antioxidant response and phenotypic plasticity of *Scenedesmus quadricauda* (Turp.) de Brébisson under different nitrogen concentrations. *Journal of Applied Phycology*, *27*(1), 293–302.

Cicero, C., Mason, N. A., Jiménez, R. A., Wait, D. R., Wang-Claypool, C. Y., & Bowie, R. C. K. (2021). Integrative taxonomy and geographic sampling underlie successful species delimitation. *Ornithology*, *138*(2), ukab009.

Cordoba, J., Perez, E., Van Vlierberghe, M., Bertrand, A. R., Lupo, V., Cardol, P., & Baurain, D. (2021). De novo transcriptome meta-assembly of the mixotrophic freshwater microalga *Euglena gracilis*. *Genes*, *12*(6), 842

Dadras, A., Fürst-Jansen, J. M. R., Darienko, T., Krone, D., Scholz, P., Sun, S., Herrfurth, C., Rieseberg, T. P., Irisarri, I., Steinkamp, R., Hansen, M., Buschmann, H., Valerius, O., Braus, G. H., Hoecker, U., Feussner, I., Mutwil, M., Ischebeck, T., de Vries, S. et al. (2023). Environmental gradients reveal stress hubs pre-dating plant terrestrialization. *Nature Plants*, *9*(9), 1419–1438.

Davies, K. M., Landi, M., van Klink, J. W., Schwinn, K. E., Brummell, D. A., Albert, N. W., Chagné, D., Jibran, R., Kulshrestha, S., Zhou, Y., & Bowman, J. L. (2022). Evolution and function of red pigmentation in land plants. *Annals of Botany*, *130*(5), 613–636.

de Ascensao, A. R. F. D. C., & Dubery, I. A. (2003). Soluble and wall-bound phenolics and phenolic polymers in *Musa acuminata* roots exposed to elicitors from *Fusarium oxysporum* f.sp. Cubense. *Phytochemistry*, *63*(6), 679–686.

de Bary, A. (1858). *Untersuchungen über die Familie der Conjugaten (Zygnemeen und Desmidieen): Ein Beitrag zur physiologischen und beschreibenden Botanik.* A. Förstnersche Buchhandlung.

De Vries, J., & Archibald, J. M. (2018). Plant evolution: Landmarks on the path to terrestrial life. *New Phytologist*, *217*(4), 1428–1434.

de Vries, J., Curtis, B. A., Gould, S. B., & Archibald, J. M. (2018). Embryophyte stress signaling evolved in the algal progenitors of land plants. *Proceedings of the National Academy of Sciences*, *115*(15), E3417-E3480.

de Vries, J., de Vries, S., Curtis, B. A., Zhou, H., Penny, S., Feussner, K., Pinto, D. M., Steinert, M., Cohen, A. M., von Schwartzenberg, K., & Archibald, J. M. (2020). Heat stress response in the closest algal relatives of land plants reveals conserved stress signaling circuits. *The Plant Journal*, *103*(3), 1025-1048.

de Vries, J., de Vries, S., Slamovits, C. H., Rose, L. E., & Archibald, J. M. (2017). How embryophytic is the biosynthesis of phenylpropanoids and their derivatives in streptophyte algae? *Plant and Cell Physiology*, *58*(5), 934–945.

Delaux, P.-M., Nanda, A. K., Mathé, C., Sejalon-Delmas, N., & Dunand, C. (2012). Molecular and biochemical aspects of plant terrestrialization. *Perspectives in Plant Ecology, Evolution and Systematics*, *14*(1), 49–59.

Delwiche, C. F., & Cooper, E. D. (2015). The evolutionary origin of a terrestrial flora. *Current Biology*, *25*(19), R899–R910.

Delwiche, C. F., Graham, L. E., & Thomson, N. (1989). Lignin-like compounds and sporopollen in *Coleochaete*, an algal model for land plant ancestry. *Science*, *245*(4916), 399–401.

Di Mauro, B., Garzonio, R., Baccolo, G., Franzetti, A., Pittino, F., Leoni, B., Remias, D., Colombo, R., & Rossini, M. (2020). Glacier algae foster ice-albedo feedback in the European Alps. *Scientific Reports*, *10*(1), 4739.

Domozych, D. S., & Domozych, C. R. (2008). Desmids and biofilms of freshwater wetlands: Development and microarchitecture. *Microbial Ecology*, *55*(1), 81–93.

Domozych, D. S., Kozel, L., & Palacio-Lopez, K. (2021). The effects of osmotic stress on the cell wall-plasma membrane domains of the unicellular streptophyte, *Penium margaritaceum*. *Protoplasma*, *258*(6), 1231–1249.

El-Sheekh, M. M., Schagerl, M., Gharieb, M., & Elsoud, G. A. (2017). Induction of sexual reproduction and zygospore patterns in the filamentous green alga *Spirogyra* (Conjugatophyceae: Zygnematales). *Journal of BioScience and Biotechnology*, *6*(2), 147-154.

Eme, L., Trilles, A., Moreira, D., & Brochier-Armanet, C. (2011). The phylogenomic analysis of the anaphase promoting complex and its targets points to complex and modern-like control of the cell cycle in the last common ancestor of eukaryotes. *BMC Evolutionary Biology*, *11*(1), 265.

Feng, X., Zheng, J., Irisarri, I., Yu, H., Zheng, B., Ali, Z., de Vries, S., Keller, J., Fürst-Jansen, J. M. R., Dadras, A., Zegers, J. M. S., Rieseberg, T. P., Dhabalia Ashok, A., Darienko, T., Bierenbroodspot, M. J., Gramzow, L., Petroll, R., Haas, F. B., Fernandez-Pozo, N. et al. (2024). Genomes of multicellular algal sisters to land plants illuminate signaling network evolution—Nature Genetics. *Nature Genetics*. 1-14.

Ferreyra, M. L. F., Serra, P., & Casati, P. (2021). Recent advances on the roles of flavonoids as plant protective molecules after UV and high light exposure. *Physiologia Plantarum*, *173*(3), 736–749.

Foets, J., Stanek-Tarkowska, J., Teuling, A. J., Van de Vijver, B., Wetzel, C. E., & Pfister, L. (2021). Autecology of terrestrial diatoms under anthropic disturbance and across climate zones. *Ecological Indicators*, *122*, 107248.

Fucikova, K., Hall, J. D., Johansen, J. R., & Lowe, R. (2009). Desmid flora of the Great Smoky Mountains National Park, USA. *Acta Botanica Hungarica*, *51*, 1-2.

Fuller, C. L. (2013*). Examining morphological and physiological changes in* Zygnema irregulare *during a desiccation and recovery period* [master thesis].

Fürst-Jansen, J. M. R., de Vries, S., Lorenz, M., von Schwartzenberg, K., Archibald, J. M., & de Vries, J. (2021). Submergence of the filamentous Zygnematophyceae Mougeotia induces differential gene expression patterns associated with core metabolism and photosynthesis. *Protoplasma*.

Gao, Q., & Garcia-Pichel, F. (2011). Microbial ultraviolet sunscreens. *Nature Reviews Microbiology*, *9*(11), 791-802.

García, A., Toledano, A., Serrano, L., Egüés, I., González, M., Marín, F., & Labidi, J. (2009). Characterization of lignins obtained by selective precipitation. *Separation and Purification Technology*, *68*(2), 193–198.

Garcia-Pichel, F., & Castenholz, R. W. (1991). Characterization and biological implications of scytonemin, a cyanobacterial sheath pigment. *Journal of Phycology*, *27*(3), 395-409.

Garcia-Pichel, F., & Castenholz, R. W. (1993). Occurrence of UV-absorbing, mycosporine-like compounds among cyanobacterial isolates and an estimate of their screening capacity. *Applied and Environmental Microbiology*, *59*(1), 163-169.

Garduño-Solórzano, G., Martínez-García, M., Scotta Hentschke, G., Lopes, G., Castelo Branco, R., Vasconcelos, V. M. O., Campos, J. E., López-Cano, R., & Quintanar-Zúñiga, R. E.

(2021). The phylogenetic placement of *Temnogametum* (Zygnemataceae) and description of *Temnogametum iztacalense* sp. Nov., from a tropical high mountain lake in Mexico. *European Journal of Phycology*, *56*(2), 159-173.

Gaysina, L. A., Bohunická, M., Hazuková, V., & Johansen, J. R. (2018). Biodiversity of Terrestrial Cyanobacteria of the South Ural Region. *Cryptogamie, Algologie*, *39*(2), 167–198.

Geng, Y., Cai, C., McAdam, S. A. M., Banks, J. A., Wisecaver, J. H., & Zhou, Y. (2021). A de novo transcriptome assembly of *Ceratopteris richardii* provides insights into the evolutionary dynamics of complex gene families in land plants. *Genome Biology and Evolution*, *13*(3), evab042.

Gerrath, J. F. (1993). The biology of desmids: A decade of progress. *Progress in Phycological Research*, *9*, 79–192.

Gitzendanner, M. A., Soltis, P. S., Wong, G. K.-S., Ruhfel, B. R., & Soltis, D. E. (2018). Plastid phylogenomic analysis of green plants: A billion years of evolutionary history. *American Journal of Botany*, *105*(3), 291-301.

Gontcharov, A. A. (2008). Phylogeny and classification of Zygnematophyceae (Streptophyta): Current state of affairs. *Fottea*, *8*(2), 87-104.

Gontcharov, A. A., Marin, B., & Melkonian, M. (2003). Molecular Phylogeny of Conjugating Green Algae (Zygnemophyceae, Streptophyta) Inferred from SSU rDNA Sequence Comparisons. *Journal of Molecular Evolution*, *56*(1), 89-104.

Gontcharov, A. A., Marin, B., & Melkonian, M. (2004). Are combined analyses better than single gene phylogenies? A case study using SSU rDNA and rbc L sequence comparisons in the Zygnematophyceae (Streptophyta). *Molecular Biology and Evolution*, *21*(3), 612-624.

Gontcharov, A. A., & Melkonian, M. (2008). In search of monophyletic taxa in the family Desmidiaceae (Zygnematophyceae, Viridiplantae): The genus *Cosmarium*. *American Journal of Botany*, *95*(9), 1079-1095.

Gontcharov, A. A., & Melkonian, M. (2011). A study of conflict between molecular phylogeny and taxonomy in the Desmidiaceae (Streptophyta, Viridiplantae): Analyses of 291 *rbc*L sequences. *Protist*, *162*(2), 253–267.

Graham, L. E., Cook, M. E., & Busse, J. S. (2000). The origin of plants: Body plan changes contributing to a major evolutionary radiation. *Proceedings of the National Academy of Sciences*, *97*(9), 4535–4540.

Guiry, M. D. (2012). How many species of algae are there? *Journal of Phycology*, *48*(5), 1057–1063.

Hall, J. D., Karol, K. G., McCourt, R. M., & Delwiche, C. F. (2008). Phylogeny of the conjugating green algae based on chloroplast and mitochondrial nucleotide sequence data. *Journal of Phycology*, *44*(2), 467-477.

Hall, J. D., & McCourt, R. (2017). Zygnematophyta. In J. M. Archibald, A. G. B. Simpson & C. H. Slamovits (Eds.), *Handbook of the Protists* (Vol. 2, pp 135-163). Springer International Publishing AG.

Halliwell, B. (1987). Oxidants and human disease: Some new concepts. *The FASEB Journal*, *1*(5), 358–364.

Hanschen, E. R., & Starkenburg, S. R. (2020). The state of algal genome quality and diversity. *Algal Research*, *50*, 101968.

Hargreaves, A., Taiwo, F. A., Duggan, O., Kirk, S. H., & Ahmad, S. I. (2007). Near-ultraviolet photolysis of β-phenylpyruvic acid generates free radicals and results in DNA damage. *Journal of Photochemistry and Photobiology B: Biology*, *89*(2–3), 110-116.

Hartmann, A., Glaser, K., Holzinger, A., Ganzera, M., & Karsten, U. (2020). Klebsormidin A and B, two new UV-sunscreen compounds in green microalgal *Interfilum* and *Klebsormidium* species (Streptophyta) from terrestrial habitats. *Frontiers in Microbiology*, *11*, 499.

Hawes, I. (1990). Effects of freezing and thawing on a species of *Zygnema* (Chlorophyta) from the Antarctic. *Phycologia*, *29*(3), 326–331.

Herburger, K., Xin, A., & Holzinger, A. (2019). Homogalacturonan accumulation in cell walls of the green alga *Zygnema* sp. (Charophyta) increases desiccation resistance. *Frontiers in Plant Science*, *10*, 540.

Hess, S., Williams, S. K., Busch, A., Irisarri, I., Delwiche, C. F., De Vries, S., Darienko, T., Roger, A. J., Archibald, J. M., Buschmann, H., Von Schwartzenberg, K., & De Vries, J.

(2022). A phylogenomically informed five-order system for the closest relatives of land plants. *Current Biology*, *32*(20), 4473-4482.

Hodač, L., Hallmann, C., Rosenkranz, H., Faßhauer, F., & Friedl, T. (2012). Molecular evidence for the wide distribution of two lineages of terrestrial green algae (Chlorophyta) over tropics to temperate zone. *International Scholarly Research Notices*, *2012*, e795924.

Hodač, L., Hallmann, C., Spitzer, K., Elster, J., Faßhauer, F., Brinkmann, N., Lepka, D., Diwan, V., & Friedl, T. (2016). Widespread green algae *Chlorella* and *Stichococcus* exhibit polar-temperate and tropical-temperate biogeography. *FEMS Microbiology Ecology*, *92*(8), fiw122.

Holzinger, A., Albert, A., Aigner, S., Uhl, J., Schmitt-Kopplin, P., Trumhová, K., & Pichrtová, M. (2018). Arctic, Antarctic, and temperate green algae *Zygnema* spp. under UV-B stress: Vegetative cells perform better than pre-akinetes. *Protoplasma*, *255*(4), 1239-1252.

Holzinger, A., Kaplan, F., Blaas, K., Zechmann, B., Komsic-Buchmann, K., & Becker, B. (2014). Transcriptomics of desiccation tolerance in the streptophyte green alga *Klebsormidium* reveal a land plant-like defense reaction. *PLOS ONE*, *9*(10), e110630.

Holzinger, A., & Karsten, U. (2013). Desiccation stress and tolerance in green algae: Consequences for ultrastructure, physiological and molecular mechanisms. *Frontiers in Plant Science*, *4*, 58296.

Honegger, R. (2009). Lichen-forming fungi and their photobionts. *Plant Relationships*, 307–333.

Irisarri, I., Darienko, T., Pröschold, T., Fürst-Jansen, J. M. R., Jamy, M., & de Vries, J. (2021). Unexpected cryptic species among streptophyte algae most distant to land plants. *Proceedings of the Royal Society B: Biological Sciences*, *288*(1963), 20212168.

Irisarri, I., Strassert, J. F. H., & Burki, F. (2022). Phylogenomic Insights into the Origin of Primary Plastids. *Systematic Biology*, *71*(1), 105–120.

Jiao, C., Sørensen, I., Sun, X., Sun, H., Behar, H., Alseekh, S., Philippe, G., Palacio Lopez, K., Sun, L., Reed, R., Jeon, S., Kiyonami, R., Zhang, S., Fernie, A. R., Brumer, H., Domozych, D. S., Fei, Z., & Rose, J. K. C. (2020). The *Penium margaritaceum* genome: Hallmarks of the origins of land plants. *Cell*, *181*(5), 1097-1111.

Jung, P., Schermer, M., Briegel-Williams, L., Baumann, K., Leinweber, P., Karsten, U., Lehnert, L., Achilles, S., Bendix, J., & Büdel, B. (2019). Water availability shapes edaphic and lithic cyanobacterial communities in the Atacama Desert. *Journal of Phycology*, *55*(6), 1306–1318.

Kadlubowska, J. Z. (1984). *Süsswasserflora von Mitteleuropa, Band 16: Chlorophyta VIII, Conjugatophyceae I: Zygnemales.* Gustav Fischer Verlag.

Karol, K. G., McCourt, R. M., Cimino, M. T., & Delwiche, C. F. (2001). The closest living relatives of land plants. *Science*, *294*(5550), 2351–2353.

Karsten, U., & Holzinger, A. (2014). Green algae in alpine biological soil crust communities: Acclimation strategies against ultraviolet radiation and dehydration. *Biodiversity and Conservation*, *23*(7), 1845-1858.

Karsten, U., Schumann, R., & Mostaert, A. (2007). Aeroterrestrial algae growing on man-made surfaces. In J. Seckbach (Ed.), *Algae and Cyanobacteria in Extreme Environments* (pp. 583–597). Springer Netherlands.

Kiemle, S. N., Domozych, D. S., & Gretz, M. R. (2007). The extracellular polymeric substances of desmids (Conjugatophyceae, Streptophyta): Chemistry, structural analyses and implications in wetland biofilms. *Phycologia*, *46*(6), 617-627.

Kitzing, C., & Karsten, U. (2015). Effects of UV radiation on optimum quantum yield and sunscreen contents in members of the genera *Interfilum*, *Klebsormidium*, *Hormidiella* and *Entransia* (Klebsormidiophyceae, Streptophyta). *European Journal of Phycology*, *50*(3), 279-287.

Kouwets, F. (2008). The species concept in desmids: The problem of variability, infraspecific taxa and the monothetic species definition. *Biologia*, *63*(6), 881-887.

Kranner, I., & Birtić, S. (2005). A modulating role for antioxidants in desiccation tolerance. *Integrative and Comparative Biology*, *45*(5), 734–740.

Kranz, H. D., Mikš, D., Siegler, M.-L., Capesius, I., Sensen, C. W., & Huss, V. A. R. (1995). The origin of land plants: Phylogenetic relationships among charophytes, bryophytes, and vascular plants inferred from complete small-subunit ribosomal RNA gene sequences. *Journal of Molecular Evolution*, *41*(1), 74–84.

Kutovaya, O. V., Vasilenko, E. S., & Lebedeva, M. P. (2012). Microbiological and micromorphological characteristics of extremely arid desert soils in the Ili Depression (Kazakhstan). *Eurasian Soil Science*, *45*(12), 1147–1158.

Kützing, F. T. (1843). *Phycologia generalis oder Anatomie, Physiologie und Systemkunde der Tange*. Brockhaus.

Leliaert, F., Smith, D. R., Moreau, H., Herron, M. D., Verbruggen, H., Delwiche, C. F., & Clerck, O. D. (2012). Phylogeny and molecular evolution of the green algae. *Critical Reviews in Plant Sciences*, *31*(1), 1–46.

Lemieux, C., Otis, C., & Turmel, M. (2007). A clade uniting the green algae *Mesostigma viride* and *Chlorokybus atmophyticus* represents the deepest branch of the Streptophyta in chloroplast genome-based phylogenies. *BMC Biology*, *5*(1), 2.

Lemoine, Y., & Schoefs, B. (2010). Secondary ketocarotenoid astaxanthin biosynthesis in algae: A multifunctional response to stress. *Photosynthesis Research*, *106*(1), 155–177.

Lepock, J. R., Frey, H. E., & Ritchie, K. P. (1993). Protein denaturation in intact hepatocytes and isolated cellular organelles during heat shock. *The Journal of Cell Biology*, *122*(6), 1267–1276.

Ligrone, R., Carafa, A., Duckett, J. G., Renzaglia, K. S., & Ruel, K. (2008). Immunocytochemical detection of lignin-related epitopes in cell walls in bryophytes and the charalean alga *Nitella*. *Plant Systematics and Evolution*, *270*(3), 257–272.

Lin, C.-S., Chou, T.-L., & Wu, J.-T. (2013). Biodiversity of soil algae in the farmlands of mid-Taiwan. *Botanical Studies*, *54*(1), 41.

Lípová, L., Krchňák, P., Komenda, J., & Ilík, P. (2010). Heat-induced disassembly and degradation of chlorophyll-containing protein complexes in vivo. *Biochimica et Biophysica Acta (BBA) - Bioenergetics*, *1797*(1), 63–70.

Liu, G., Zhang, Q., Zhu, H., & Hu, Z. (2012). Massive *Trentepohlia*-bloom in a Gglacier valley of Mt. Gongga, China, and a new variety of *Trentepohlia* (Chlorophyta). *PLOS ONE*, *7*(7), e37725.

Lüttge, U., Beck, E., & Bartels, D. (2011). *Plant desiccation tolerance*. Springer.

Lütz, C., Seidlitz, H. K., & Meindl, U. (1997). Physiological and structural changes in the chloroplast of the green alga *Micrasterias denticulata* induced by UV-B simulation. In J. Rozema, W. W. C. Gieskes, S. C. Van De Geijn, C. Nolan, & H. De Boois (Eds.), *UV-B and Biosphere* (pp. 54–64). Springer Netherlands.

Lutz, S., Anesio, A. M., Jorge Villar, S. E., & Benning, L. G. (2014). Variations of algal communities cause darkening of a Greenland glacier. *FEMS Microbiology Ecology*, *89*(2), 402–414.

McCaig, B. C., Meagher, R. B., & Dean, J. F. D. (2005). Gene structure and molecular analysis of the laccase-like multicopper oxidase (LMCO) gene family in Arabidopsis thaliana. *Planta*, *221*(5), 619–636.

McCourt, R. M., Karol, K. G., Bell, J., Helm-Bychowski, K. M., Grajewska, A., Wojciechowski, M. F., & Hoshaw, R. W. (2000). Phylogeny of the conjugating green algae (Zygnemophyceae) based on rbc L sequences. *Journal of Phycology*, *36*(4), 747-758.

McFadden, G. I., & van Dooren, G. G. (2004). Evolution: Red algal genome affirms a common origin of all plastids. *Current Biology*, *14*(13), R514–R516.

McKernan, P., & Juliano, S. (2001). Effects of nutrient enrichment on the growth of the green alga *Spirogyra* in Conesus Lake, N.Y. *Journal of Science and Mathematics*, *2*(1), 19-25.

Mikhailyuk, T., Glaser, K., Holzinger, A., & Karsten, U. (2015). Biodiversity of *Klebsormidium* (Streptophyta) from alpine biological soil crusts (Alps, Tyrol, Austria, and Italy). *Journal of Phycology*, *51*(4), 750–767.

Mikhailyuk, T. I., Sluiman, H. J., Massalski, A., Mudimu, O., Demchenko, E. M., Kondratyuk, S. Ya., & Friedl, T. (2008). New streptophyte green algae from terrestrial habitats and an assessment of the genus *Interfilum* (Klebsormidiophyceae, Streptophyta). *Journal of Phycology*, *44*(6), 1586–1603.

Mikhailyuk, T., Lukešová, A., Glaser, K., Holzinger, A., Obwegeser, S., Nyporko, S., Friedl, T., & Karsten, U. (2018). New taxa of streptophyte algae (Streptophyta) from terrestrial habitats revealed using an integrative approach. *Protist*, *169*(3), 406–431.

Mix, M. (1972). Die Feinstruktur der Zellwände bei Mesotaeniaceae und Gonatozygaceae mit einer vergleichenden Betrachtung der verschiedenen Wandtypen der Conjugatophyceae und über deren systematischen Wert. *Archiv für Mikrobiologie*, *81*(3), 197–220.

Morris, J. L., Puttick, M. N., Clark, J. W., Edwards, D., Kenrick, P., Pressel, S., Wellman, C. H., Yang, Z., Schneider, H., & Donoghue, P. C. J. (2018). The timescale of early land plant evolution. *Proceedings of the National Academy of Sciences*, *115*(10).

Nagao, M., Matsui, K., & Uemura, M. (2008). *Klebsormidium flaccidum*, a charophycean green alga, exhibits cold acclimation that is closely associated with compatible solute accumulation and ultrastructural changes. *Plant, Cell & Environment*, *31*(6), 872–885.

Nedbalová, L., & Sklenár, P. (2008). New records of snow algae from the Andes of Ecuador. *Arnaldoa*, *15*, 17–20.

Nemjová, K., Neustupa, J., Šťastnỳ, J., Škaloud, P., & Veselá, J. (2011). Species concept and morphological differentiation of strains traditionally assigned to *Micrasterias truncata*. *Phycological Research*, *59*(3), Article 3.

Neustupa, J., & Némcová, Y. (2001). Morphological and taxonomic study of three terrestrial eustigmatophycean species. *Nova Hedwigia Beiheft*, *123*, 373–386.

Neustupa, J., St'astny, J., & Hodac, L. (2008). Temperature-related phenotypic plasticity in the green microalga *Micrasterias rotata*. *Aquatic Microbial Ecology*, *51*(1), 77-86.

Neustupa, J., Stastny, J., & Woodard, K. (2023). Ecological monitoring of disturbed mountain peatlands: An analysis based on desmids. *Biodiversity and Conservation*, *32*(8), 2671–2691.

Neustupa, J., & Woodard, K. (2024). The effects of temperature on plasticity, shape symmetry and seasonal variation in the freshwater benthic green microalga *Micrasterias thomasiana*. *Aquatic Ecology*.

Newsome, A. G., & van Breemen, R. (2012). Characterization of the purple vacuolar pigment of *Zygogonium ericetorum* alga. *Planta Medica*, *78*(11), 1253-1253.

Nishiyama, T., Sakayama, H., de Vries, J., Buschmann, H., Saint-Marcoux, D., Ullrich, K. K., Haas, F. B., Vanderstraeten, L., Becker, D., Lang, D., Vosolsobě, S., Rombauts, S., Wilhelmsson, P. K. I., Janitza, P., Kern, R., Heyl, A., Rümpler, F., Villalobos, L. I. A. C., Clay, J. M. et al. (2018). The *Chara* Genome: Secondary complexity and implications for plant terrestrialization. *Cell*, *174*(2), 448-464.e24

Novarino, G. (2012). Cryptomonad taxonomy in the 21st century: The first two hundred years. *Phycological Reports: Current advances in algal taxonomy and its applications: Phylogenetic, ecological and applied perspective. Institute of Botany, Polish Academy of Sciences, Kraków*, 19–52.

Oren, A., Kühl, M., & Karsten, U. (1995). An endoevaporitic microbial mat within a gypsum crust:zonation of phototrophs, photopigments, and light penetration. *Marine Ecology Progress Series*, *128*, 151–159.

Ostergaard, L., Teilum, K., Mirza, O., Mattsson, O., Petersen, M., Welinder, K. G., Mundy, J., Gajhede, M., & Henriksen, A. (2000). Arabidopsis ATP A2 peroxidase. Expression and high-resolution structure of a plant peroxidase with implications for lignification. *Plant Molecular Biology*, *44*(2), 231-243.

Palacio-López, K., Tinaz, B., Holzinger, A., & Domozych, D. S. (2019). Arabinogalactan Proteins and the Extracellular Matrix of Charophytes: A Sticky Business. *Frontiers in Plant Science*, *10*.

Pattison, D. I., & Davies, M. J. (2006). Actions of ultraviolet light on cellular structures. In L.P. Bignold (Ed.), *Cancer: Cell structures, carcinogens and genomic instability* (pp. 131–157). Birkhäuser.

Paulsen, B. S., Vieira, A. A. H., & Klaveness, D. (1992). Structure of extracellular polysaccharides produced by *Cryptomonas* sp. (Cryptophyceae). *Journal of Phycology*, *28*(1), 61–63.

Permann, C., Becker, B., & Holzinger, A. (2022). Temperature- and light stress adaptations in Zygnematophyceae: The challenges of a semi-terrestrial lifestyle. *Frontiers in Plant Science*, *13*, 945394.

Permann, C., Gierlinger, N., & Holzinger, A. (2022). Zygospores of the green alga *Spirogyra*: New insights from structural and chemical imaging. *Frontiers in Plant Science*, *13*.

Permann, C., Herburger, K., Niedermeier, M., Felhofer, M., Gierlinger, N., & Holzinger, A. (2021). Cell wall characteristics during sexual reproduction of *Mougeotia* sp.

(Zygnematophyceae) revealed by electron microscopy, glycan microarrays and RAMAN spectroscopy. *Protoplasma*, *258*(6), 1261–1275.

Pichrtová, M. (2015). *Stress resistance of polar hydro-terrestrial algae Zygnema spp. (Zygnematophyceae, Streptophyta)* [doctoral thesis].

Pichrtová, M., Hájek, T., & Elster, J. (2014). Osmotic stress and recovery in field populations of *Zygnema* sp. (Zygnematophyceae, Streptophyta) on Svalbard (High Arctic) subjected to natural desiccation. *FEMS Microbiology Ecology*, *89*(2), 270–280.

Pichrtová, M., Hájek, T., & Elster, J. (2016). Annual development of mat-forming conjugating green algae *Zygnema* spp. In hydro-terrestrial habitats in the Arctic. *Polar Biology*, *39*(9), 1653-1662.

Pichrtová, M., Remias, D., Lewis, L. A., & Holzinger, A. (2013). Changes in phenolic compounds and cellular ultrastructure of Arctic and Antarctic strains of *Zygnema* (Zygnematophyceae, Streptophyta) after exposure to experimentally enhanced UV to PAR ratio. *Microbial Ecology*, *65*(1), 68-83.

Pickett-Heaps, J. D., & Fowke, L. C. (1971). Conjugation in the desmid *Closterium littorale*. *Journal of Phycology*, *7*(1), 37–50.

Pimm, S. L., & Joppa, L. N. (2015). How many plant species are there, where are they, and at what rate are they going extinct? *Annals of the Missouri Botanical Garden*, *100*(3), 170–176.

Plonka, P. M., & Grabacka, M. (2006). Melanin synthesis in microorganisms—Biotechnological and medical aspects. *Acta Biochimica Polonica*, *53*(3), 429–443.

Prescott, G. W. (1972). *A Synopsis of North American Desmids: Sect. 1-Desmidiaceae, Placodermae*. University of Nebraska press.

Procházková, L., Remias, D., Nedbalová, L., & Raymond, J. A. (2024). A DUF3494 ice-binding protein with a root cap domain in a streptophyte glacier ice alga. *Frontiers in Plant Science*, *14*.

Procházková, L., Řezanka, T., Nedbalová, L., & Remias, D. (2021). Unicellular versus filamentous: The glacial alga *Ancylonema alaskana* comb. et stat. nov. and its ecophysiological relatedness to *Ancylonema nordenskioeldii* (Zygnematophyceae, Streptophyta). *Microorganisms*, *9*(5), 1103.

Proteau, P. J., Gerwick, W. H., Garcia-Pichel, F., & Castenholz, R. (1993). The structure of scytonemin, an ultraviolet sunscreen pigment from the sheaths of cyanobacteria. *Experientia*, *49*(9), 825-829.

Queiroz, C. G. S., Alonso, A., Mares-Guia, M., & Magalhães, A. C. (1998). Chilling-induced changes in membrane fluidity and antioxidant enzyme activities in *Coffea arabica* L. roots. *Biologia Plantarum*, *41*(3), 403–413.

Remias, D., Holzinger, A., Aigner, S., & Lütz, C. (2012). Ecophysiology and ultrastructure of Ancylonema nordenskiöldii (Zygnematales, Streptophyta), causing brown ice on glaciers in Svalbard (high arctic). *Polar Biology*, *35*(6), 899-908.

Remias, D., Holzinger, A., & Lütz, C. (2009). Physiology, ultrastructure and habitat of the ice alga *Mesotaenium berggrenii* (Zygnemaphyceae, Chlorophyta) from glaciers in the European Alps. *Phycologia*, *48*(4), 302-312

Remias, D., & Procházková, L. (2023). The first cultivation of the glacier ice alga *Ancylonema alaskanum* (Zygnematophyceae, Streptophyta): Differences in morphology and photophysiology of field vs laboratory strain cells. *Journal of Glaciology*, *69*(276), 1080-1084.

Remias, D., Procházková, L., Nedbalová, L., Benning, L. G., & Lutz, S. (2023). Novel insights in cryptic diversity of snow and glacier ice algae communities combining 18S rRNA gene and ITS2 amplicon sequencing. *FEMS Microbiology Ecology*, *99*(12), fiad134.

Remias, D., Schwaiger, S., Aigner, S., Leya, T., Stuppner, H., & Lütz, C. (2012). Characterization of an UV-and VIS-absorbing, purpurogallin-derived secondary pigment new to algae and highly abundant in M esotaenium berggrenii (Z ygnematophyceae, Chlorophyta), an extremophyte living on glaciers. *FEMS Microbiology Ecology*, *79*(3), 638-648.

Rensing, S. A., Lang, D., Zimmer, A. D., Terry, A., Salamov, A., Shapiro, H., Nishiyama, T., Perroud, P.-F., Lindquist, E. A., Kamisugi, Y., Tanahashi, T., Sakakibara, K., Fujita, T., Oishi, K., Shin-I, T., Kuroki, Y., Toyoda, A., Suzuki, Y., Hashimoto, S., et al. (2008). The

Physcomitrella genome reveals evolutionary insights into the conquest of land by plants. *Science*, *319*(5859), 64–69.

Rice, S. A., & Doty, P. (1957). The Thermal Denaturation of Desoxyribose Nucleic Acid. *Journal of the American Chemical Society*, *79*(15), 3937–3947.

Rieseberg, T. P., Dadras, A., Bergschmidt, L. I. N., Bierenbroodspot, M. J., Fürst-Jansen, J. M. R., Irisarri, I., de Vries, S., Darienko, T., & de Vries, J. (2023). Divergent responses in desiccation experiments in two ecophysiologically different Zygnematophyceae. *Physiologia Plantarum*, *175*(6), e14056.

Rindi, F., Allali, H. A., Lam, D. W., & López-Bautista, J. M. (2009). An overview of the biodiversity and biogeography of terrestrial green algae. *Biodiversity Hotspots*, *125*.

Rippin, M., Becker, B., & Holzinger, A. (2017). Enhanced desiccation tolerance in mature cultures of the streptophytic green alga *Zygnema circumcarinatum* revealed by transcriptomics. *Plant and Cell Physiology*, *58*(12), 2067–2084.

Roos, J. C., & Vincent, W. F. (1998). Temperature dependence of UV radiation effects on Antarctic cyanobacteria. *Journal of Phycology*, *34*(1), 118–125.

Rothschild, L. J., & Mancinelli, R. L. (2001). Life in extreme environments. *Nature*, *409*(6823), 1092–1101.

Rudolph, H., Krause, H.-J., Blaicher, M., & Herms, E. (1981). Investigations of the shikimic acid metabolism in *Sphagnum magellanicum* during synthesis of sphagnorubin induced by chilling. *Biochemie Und Physiologie Der Pflanzen*, *176*(8), 728–736.

Rudolph, H., & Vowinkel, E. (1969). Notizen: Sphagnorubin, ein kristallines Membranochrom aus *Sphagnum magellanicum*. *Zeitschrift Für Naturforschung B*, *24*(9), 1211–1212.

Rybalka, N., Blanke, M., Tzvetkova, A., Noll, A., Roos, C., Boy, J., Boy, D., Nimptsch, D., Godoy, R., & Friedl, T. (2023). Unrecognized diversity and distribution of soil algae from Maritime Antarctica (Fildes Peninsula, King George Island). *Frontiers in Microbiology*, *14*.

Rybalka, N., Mikhailyuk, T., Darienko, T., Dultz, S., Blanke, M., & Friedl, T. (2020). Genotypic and phylogenetic diversity of new isolates of terrestrial Xanthophyceae (Stramenopiles) from maritime sandy habitats. *Phycologia*, *59*(6), 506–514.

Sakharov, I. Yu., Vesgac B, M. K., Galaev, I. Yu., Sakharova, I. V., & Pletjushkina, O. Yu. (2001). Peroxidase from leaves of royal palm tree *Roystonea regia*: Purification and some properties. *Plant Science*, *161*(5), 853–860.

Schiwitza, S., & Nitsche, F. (2021). A needle in the haystack – Mapping sequences to morphology exemplified by the loricate choanoflagellate *Enibas thessalia* sp. nov. (Acanthoecida, Acanthoecidae). *Protist*, *172*(1), 125782.

Schlegel, M., & Meisterfeld, R. (2003). The species problem in protozoa revisited. *European Journal of Protistology*, *39*(4), 349–355.

Sekimoto, H. (2000). Intercellular communication during sexual reproduction of *Closterium* (Conjugatophyceae). *Journal of Plant Research*, *113*(3), 343–352.

Smirnoff, N. (1993). The Role of Active Oxygen in the Response of Plants to Water Deficit and Desiccation. *The New Phytologist*, *125*(1), 27–58.

Soule, T., Palmer, K., Gao, Q., Potrafka, R. M., Stout, V., & Garcia-Pichel, F. (2009). A comparative genomics approach to understanding the biosynthesis of the sunscreen scytonemin in cyanobacteria. *BMC Genomics*, *10*(1), 336.

Stancheva, R., Hall, J. D., Herburger, K., Lewis, L. A., McCourt, R. M., Sheath, R. G., & Holzinger, A. (2014). Phylogenetic position of *Zygogonium ericetorum* (Zygnematophyceae, Charophyta) from a high alpine habitat and ultrastructural characterization of unusual aplanospores. *Journal of Phycology*, *50*(5), 790–803.

Steponkus, P. L., & Lynch, D. V. (1989). Freeze/thaw-induced destabilization of the plasma membrane and the effects of cold acclimation. *Journal of Bioenergetics and Biomembranes*, *21*(1), 21–41.

Storme, J.-Y., Golubic, S., Wilmotte, A., Kleinteich, J., Velázquez, D., & Javaux, E. J. (2015). Raman characterization of the UV-protective pigment gloeocapsin and its role in the survival of cyanobacteria. *Astrobiology*, *15*(10), 843-857.

Sun, Y., Harpazi, B., Wijerathna-Yapa, A., Merilo, E., Vries, J. de, Michaeli, D., Gal, M., Cuming, A. C., Kollist, H., & Mosquna, A. (2019). A ligand-independent origin of abscisic acid perception. *Proceedings of the National Academy of Sciences*, *116*(49), 24892–24899.

Takano, T., Higuchi, S., Ikegaya, H., Matsuzaki, R., Kawachi, M., Takahashi, F., & Nozaki, H. (2019). Identification of 13 *Spirogyra* species (Zygnemataceae) by traits of sexual reproduction induced under laboratory culture conditions. *Scientific Reports*, *9*(1), 7458.

Takeuchi, M., Kegasa, T., Watanabe, A., Tamura, M., & Tsutsumi, Y. (2018). Expression analysis of transporter genes for screening candidate monolignol transporters using Arabidopsis thaliana cell suspensions during tracheary element differentiation. *Journal of Plant Research*, *131*(2), 297-305.

Tan, M., Mei, J., & Xie, J. (2021). The formation and control of ice crystal and its impact on the quality of frozen aquatic products: A Review. *Crystals*, *11*(1), 68.

Tiflickjian, J. D., & Raybum, W. R. (1986). Nutritional requirements for sexual reproduction in *Mesotaenium kramstai* (chlorophyta). *Journal of Phycology*, *22*(1), 1–8.

Tilbrook, K., Dubois, M., Crocco, C. D., Yin, R., Chappuis, R., Allorent, G., Schmid-Siegert, E., Goldschmidt-Clermont, M., & Ulm, R. (2016). UV-B Perception and Acclimation in Chlamydomonas reinhardtii. *The Plant Cell*, *28*(4), 966–983.

Timme, R. E., Bachvaroff, T. R., & Delwiche, C. F. (2012). Broad phylogenomic sampling and the sister lineage of land plants. *PLoS One*, *7*(1), e29696.

Tsuchikane, Y., & Sekimoto, H. (2019). The genus *Closterium*, a new model organism to study sexual reproduction in streptophytes. *New Phytologist*, *221*(1), 99–104.

Tsuchikane, Y., Tsuchiya, M., Hindák, F., Nozaki, H., & Sekimoto, H. (2012). Zygospore formation between homothallic and heterothallic strains of *Closterium*. *Sexual Plant Reproduction*, *25*(1), 1–9.

Turmel, M., Otis, C., & Lemieux, C. (2006). The chloroplast genome sequence of *Chara vulgaris* sheds new light into the closest green algal relatives of land plants. *Molecular Biology and Evolution*, *23*(6), 1324–1338.

Vanholme, R., De Meester, B., Ralph, J., & Boerjan, W. (2019). Lignin biosynthesis and its integration into metabolism. *Current Opinion in Biotechnology*, *56*, 230–239.

Vincent, W. F., & Neale, P. J. (2000). Mechanisms of UV damage to aquatic organisms. *The Effects of UV Radiation in the Marine Environment*, 149–176.

Wickett, N. J., Mirarab, S., Nguyen, N., Warnow, T., Carpenter, E., Matasci, N., Ayyampalayam, S., Barker, M. S., Burleigh, J. G., & Gitzendanner, M. A. (2014). Phylotranscriptomic analysis of the origin and early diversification of land plants. *Proceedings of the National Academy of Sciences*, *111*(45), E4859-E4868.

Williamson, C. J., Anesio, A. M., Cook, J., Tedstone, A., Poniecka, E., Holland, A., Fagan, D., Tranter, M., & Yallop, M. L. (2018). Ice algal bloom development on the surface of the Greenland Ice Sheet. *FEMS Microbiology Ecology*, *94*(3), fiy025.

Wodniok, S., Brinkmann, H., Glöckner, G., Heidel, A. J., Philippe, H., Melkonian, M., & Becker, B. (2011). Origin of land plants: Do conjugating green algae hold the key? *BMC Evolutionary Biology*, *11*(1), 1-10.

Zhang, Z., Xu, C., Zhang, S., Shi, C., Cheng, H., Liu, H., & Zhong, B. (2022). Origin and adaptive evolution of UV RESISTANCE LOCUS 8-mediated signaling during plant terrestrialization. *Plant Physiology*, *188*(1), 332-346.

Zhao, Y., Yi, Z., Gentekaki, E., Zhan, A., Al-Farraj, S. A., & Song, W. (2016). Utility of combining morphological characters, nuclear and mitochondrial genes: An attempt to resolve the conflicts of species identification for ciliated protists. *Molecular Phylogenetics and Evolution*, *94*, 718–729.

Zohary, T., Alster, A., Hadas, O., & Obertegger, U. (2019). There to stay: Invasive filamentous green alga *Mougeotia* in Lake Kinneret, Israel. *Hydrobiologia*, *831*(1), 87–100.

Acknowledgements

I would like to express my gratitude to the following individuals and organizations for their support during the completion of my doctoral thesis:

Erklärung gemäß § 7 Absatz 8

„Hiermit versichere ich an Eides statt, dass ich die vorliegende Dissertation selbstständig und ohne die Benutzung anderer als der angegebenen Hilfsmittel und Literatur angefertigt habe. Alle Stellen, die wörtlich oder sinngemäß aus veröffentlichten und nicht veröffentlichten Werken dem Wortlaut oder dem Sinn nach entnommen wurden, sind als solche kenntlich gemacht. Ich versichere an Eides statt, dass diese Dissertation noch keiner anderen Fakultät oder Universität zur Prüfung vorgelegen hat; dass sie - abgesehen von unten angegebenen Teilpublikationen und eingebundenen Artikeln und Manuskripten - noch nicht veröffentlicht worden ist sowie, dass ich eine Veröffentlichung der Dissertation vor Abschluss der Promotion nicht ohne Genehmigung des Promotionsausschusses vornehmen werde. Die Bestimmungen dieser Ordnung sind mir bekannt. Darüber hinaus erkläre ich hiermit, dass ich die Ordnung zur Sicherung guter wissenschaftlicher Praxis und zum Umgang mit wissenschaftlichem Fehlverhalten der Universität zu Köln gelesen und sie bei der Durchführung der Dissertation zugrundeliegenden Arbeiten und der schriftlich verfassten Dissertation beachtet habe und verpflichte mich hiermit, die dort genannten Vorgaben bei allen wissenschaftlichen Tätigkeiten zu beachten und umzusetzen. Ich versichere, dass die eingereichte elektronische Fassung der eingereichten Druckfassung vollständig entspricht."

Teilpublikationen:

Busch A., Slominski E., Remias D., Procházková L., Hess S. (2024). A mesophilic relative of common glacier algae, *Ancylonema palustre* sp. nov., provides insights into the induction of vacuolar pigments in zygnematophytes. *Environmental Microbiology* 26(8), e16680. https://doi.org/10.1111/1462-2920.16680

Busch A., Gerbracht J. V., Davies K., Hoecker U., Hess S. (2024). Comparative transcriptomics elucidates the cellular responses of an aeroterrestrial zygnematophyte to UV radiation. *Journal of Experimental Botany*: erae131. https://doi.org/10.1093/jxb/erae131

Hess S., Williams,S. K., **Busch A.**, Irisarri I., Delwiche,C. F., de Vries S., Darienko T., Roger A. J., Archibald J. M., Buschmann,H., von Schwartzenberg,K., de Vries J. (2022): A phylogenomically informed five-order system for the closest relatives of land plants. *Current Biology* 32: 4473-4482. https://doi.org/10.1016/j.cub.2022.08.022

Busch A., Hess S. (2022): A diverse group of underappreciated zygnematophytes deserves in-depth exploration. *Applied Phycology* 3: 306-323. https://doi.org/10.1080/26388081.2022.2081819

Busch A., Hess S. (2022): Sunscreen mucilage: a photoprotective adaptation found in terrestrial green algae (Zygnematophyceae). *European Journal of Phycology* 57: 107-124. https://doi.org/10.1080/09670262.2021.1898677